

**THE INFLUENCE OF WEAK INTERACTIONS
ON PHASE TRANSFORMATIONS AND
POLYMORPHISM IN DISUBSTITUTED
N-ARYL -FORMAMIDES AND -THIOAMIDES**

BERNARD OMONDI



“A thesis submitted to the Faculty of Science, University of the Witwatersrand,
Johannesburg, in fulfillment of the requirements of the degree of Doctor of
Philosophy.”

Johannesburg, 2006

DECLARATION

I declare that this thesis is my own, unaided work. It is being submitted for the Degree of Doctor of Philosophy in the University of the Witwatersrand, Johannesburg. It has not been submitted before for any degree or examination in any other University.

Bernard Omondi

On this _____ day of _____ 20 _____.

Abstract

A series of arylformamides and arylthioamides has been synthesized and analyzed using nuclear magnetic resonance spectroscopy (NMR), differential scanning calorimetry (DSC), powder and single crystal X-ray diffraction. The work involved the study of hydrogen bonding, weak intermolecular interactions, phase changes and co-crystallization in aryl - formamides and -thioamides resulting in the structure determination of twenty four crystals.

Three sets of isomorphous compounds were identified from the 24 solid state structures: set one; 2,6-difluorophenylformamide (**1a**), 2,6-dichlorophenylformamide (**2a**) and 2-chloro-6-methylphenylformamide (**4a**); set two; 2,6-dimethylphenylthioamide (**17**) and 2-chloro-6-methylphenylthioamide (**18**) and set three; 2,6-diisopropylphenylformamide (**6**) and 2,6-diisopropylphenylthioamide (**20**). In the first two sets, **1a**, **2a** and **4a**, and **17** and **18**, there are similar regions of halogen interactions and hydrocarbon interactions with disorder in the chloro-methyl substituents in structures **4a** and **18**. As for compounds **6** and **20**, both the chemical and geometrical effects (size and volume of the isopropyl substituents) play a role in their isomorphism.

A mixture of 2,6-dichlorophenylformamide (**2a**) and 2,6-dimethylphenylformamide (**3**) yielded a co-crystal **22** in which there was one molecule in the asymmetric unit, same as co-crystal **23** [derived from 2,6-dichlorophenylthioamide (**17**) and 2,6-dimethylphenylthioamide (**18**)]. The molecules of the two co-crystals displayed disorder in the substituents on the 2 and 6 positions of the aryl ring as a result of the occurrence of chlorine and methyl groups in the same crystallographic sites. Co-crystal **22** adopted the structure of 2,6-dichlorophenylformamide **2a**. Co-crystal **23** also had a

structure similar to that of **2a** and co-crystal **22**. Co-crystal **24** derived from a mixture of 2,6-diisopropylphenylformamide (**6**) and 2,6-diisopropylphenylthioamide (**20**), and also had one molecule in the asymmetric unit which showed disorder in the position occupied by oxygen and sulfur atoms.

The 24 structures studied exhibited a variety of motifs formed from weak intermolecular interactions. Investigation of these weak intermolecular interactions revealed four different categories¹ for the arylformamides and only one category for the arylthioamides. The categories were different in their formation of N-H...O/S hydrogen bonds (in which adjacent molecules are related by 2_1 -screw axes, glide planes or by translation) forming chains (as in category 1, 2 and 5), sheets (as in Category 3) or dimers and tetramers (as in category 4). The chains in categories 1, 2 and 5 are in the form of spirals (molecules along the chain are related by 2_1 -screw axes or glide planes) or stacks (molecules along the chains are related by translation).

Compounds from the different categories had certain interactions that contributed most to the stabilizations of their crystals. Apart from the N-H...O/S hydrogen bonds, π ... π , C-H... π , C-F... π , C-H...F, C-H...Cl, C-H...O, Cl...Cl, Br...Br, Cl...O and Br...O interactions also had a role to play in the stabilization of the different structures. Lattice energies and the energies relating to different molecular arrangements were calculated using Gavezzottis' OPIX program suit. This showed that the N-H...O/S hydrogen bonds and π ... π interactions were the most important interactions amongst the 24 structures discussed in this work.

The crystal structures, thermal behaviour and phase transformations of all arylformamides and arylthioamides have shown that a phase

¹ Category = different types of hydrogen bonding patterns formed by disubstituted phenyl-formamides and -thioamides discussed in this thesis.

transformation was only observed when a halogen atom was one of the substituents and only for some of the formamides. 2,6-dichlorophenylformamide **2a** and 2-chloro-6-methylphenylformamide **4a** transform to a high-temperature form at 155 and 106 °C, respectively. The high-temperature forms **2b** and **4b** (grown by sublimation) are both monoclinic but not isomorphous, with one short axis of about 4.3 Å, and consist of chains of N–H...O hydrogen-bonded molecules stacked along the short axis, related by translation. **1a** and **1b** are related to the above polymorphs in their formation of N–H...O hydrogen bonding patterns.

Finally, this contribution has analyzed the role of weak interactions on the structural and thermal properties of the compounds studied. In addition, a mechanism for the phase change in 2,6-dichlorophenylformamide has been proposed and rationalized through the examination of the structures themselves together with lattice energy calculations.

Dedication

To
Audrey
Annette
And
Dorine

Acknowledgements

First and foremost to the almighty God for keeping me and my family (my daughter Audrey, and my wife Annette) through the difficult time of writing up this thesis, we give you thanks.

Secondly with lots of pleasure I express my deepest gratitude to Prof. Demi C. Levendis, Prof. Marcus Layh, Dr. Manuel A. Fernandes and Dr. David G. Billing for their great help, kindness, support and optimistic approach throughout my Ph.D. program.

I also appreciate the kind and valuable help of Dr. M. Bala for agreeing to read my thesis (even though he had to leave for Durban before he could read it), Mr. Mampa for valuable contribution regarding NMR studies, and my office mate Andy "Ivory" for the occasional chat about life.

I would like to thank dear friends Asheena Budhai, Mabel Elena Coyanis, Messai Mamo, Patricia Gitari and Simon Molele for their continuous encouragement and support throughout the project not forgetting the Head of the Department, Prof. H. M. Marques, and all present and past members of the Chemistry Department.

I thank the National Research Foundation (NRF), the International Union of Crystallography (IUCr) and the University of Witwatersrand for funding the project and myself for the entire four years.

Finally to all my brothers (Gee and Deno) and sisters Edwina, Millicent, Emily and Evelyn, and the late Joyce and Rose [God rest their souls in peace] and to my beloved parents, Toby and Dorina thanks for your patience and support.

Table of Contents	Page number
DECLARATION	i
ABSTRACT	ii
DEDICATION	v
ACKNOWLEDGEMENTS	vi
TABLE OF CONTENTS	vii
LIST OF FIGURES	xiii
LIST OF TABLES	xviii
LIST OF SCHEMES	xx
LIST OF SYMBOLS	xxi
ABBREVIATIONS	xxii
CHAPTER 1	
1. Introduction and Literature background	1
1.1 Introduction	1
1.1.1 Relevance of formamides and thioamides	6
1.2 Aims of the project	10
1.3 Literature background	12
1.3.1 Hydrogen bonding and weak intermolecular Interactions	13
1.3.2 The nature and properties of hydrogen bonds	15
1.3.3 Examples of hydrogen bonds and intermolecular interactions in molecular crystals of arylformamides and thioamides	18
1.3.3.1 N-H...O=C hydrogen bonds	19
1.3.3.2 N-H...S=C hydrogen bond	21
1.3.3.3 The C-H...O and C-H...S hydrogen bonds	23
1.3.3.4 Halogen-H bonding and other related Halogen generated weak intermolecular interactions	29
1.3.3.5 C-H...π and π...π interactions	34
1.3.4 N-H...O=C hydrogen bonding motifs in phenyl amides	37
1.3.5 Use of graph-set notation and packing patterns to characterize hydrogen-bonding networks	49
1.3.6 Isomorphism	52

1.3.7	Cocrystallization	55
1.3.7.1	Hydrogen bonding directed Cocrystallization	58
1.3.7.2	Chloro-methyl exchange directed co- crystallization	58
1.3.8	Polymorphism and phase transitions	60
1.3.8.1	Thermodynamics of transformations in molecular structures	64
1.3.9	Evaluation of intermolecular interactions via lattice energy calculations	65
1.3.10	Nuclear Magnetic resonance studies of Arylformamides, acetanilides and thioamides	69

CHAPTER 2

2.	Experimental Methods	72
2.1	Synthesis of arylformamides (compounds 1 – 14)	72
2.2	Synthesis of arylthioamides (compounds 15 – 20)	76
2.3	Crystal growth	78
2.4	Synthesis of co-crystals of compounds 2 and 3/ 15 and 16 and 6 and 20	79
2.5	Single crystal X-ray diffraction	79
2.6	Powder X-ray diffraction	81
2.7	DSC measurements	81
2.8	Lattice energy calculations	82

CHAPTER 3

3.	Structural analyses of disubstituted arylformamides and arylthioamides	85
3.1	2,6-disubstituted arylformamides	86
3.1.1	Introduction	86
3.1.2	Molecular structures of 2,6 disubstituted aryl- Formamides	87
3.1.3	Crystal packing and intermolecular interactions in 2,6 disubstituted arylformamides	94
3.1.4	Discussion of crystal packing and intermolecular interactions in 2,6 disubstituted arylformamides	108
3.2	Disubstituted formamides with substituents in positions other than 2,6	109

3.2.1	Introduction	109
3.2.2	Molecular structures of compounds 7 – 14	111
3.2.3	Crystal packing and intermolecular interactions	114
3.2.3.1	2,4-dichloro- and 2,4-dibromo-arylformamides	116
3.2.3.2	2,5-dichlorophenylformamide, 2,5-dibromophenylformamide and 5-chloro-2-methylphenylformamide	121
3.2.3.3	3,4-dichlorophenylformamide and 3,5-dichlorophenyl formamide	127
3.2.4	Discussion of crystal packing and intermolecular interactions in compounds 7 – 14	132
3.3	2,6-disubstituted arylthioamides	133
3.3.1	Introduction	133
3.3.2	Molecular structures of compounds 2,6-disubstituted arylthioamides	134
3.3.3	Crystal packing and intermolecular interactions	138
3.3.4	Discussion of crystal packing and intermolecular interactions in compounds 15 – 20	151
3.4	Phenylformamide	152
3.4.1	Introduction	152
3.4.2	NMR spectroscopic studies of compound 21	153
3.4.3	Molecular structure of phenylformamide	154
3.4.4	Crystal packing and intermolecular interactions in phenylformamide	156
3.4.5	Discussion	159
3.5	Co-crystals of aryl -formamides and -thioamides	161
3.5.1	Introduction	161
3.5.2	Molecular structures of co-crystal 22, 23 and 24 .	161
3.5.3	Crystal structure of co-crystal 22 .	163
3.5.4	Crystal structure of co-crystal 23 .	164
3.5.5	Crystal structure of co-crystal 24 .	166

CHAPTER 4

4.	Polymorphism and phase changes in compounds 2,6-difluoro-, 2,6-dichloro- and 2-chloro-6-methyl- phenylformamides	168
4.1	Introduction	168
4.2	Polymorphism in 2,6-dichloro- and 2-chloro-6-methyl-phenylformamides	169

4.2.1	Thermal Analysis	170
4.2.2	Powder X-ray diffraction	171
4.2.3	Molecular structure of compounds 2a , 2b , 4a and 4b .	174
4.2.4	Crystal packing, hydrogen bonding and intermolecular interactions	179
4.2.5	Proposed mechanism for the phase change of 2a to 2b	185
4.3	Polymorphism in 2,6-difluorophenylformamide	191
4.3.1	Molecular structure of 2,6-difluorophenylformamide (1a and 1b).	192
4.3.2	Crystal packing, hydrogen bonding and intermolecular interactions.	195
4.3.3	Results from lattice energy calculations	199

CHAPTER 5

5.	Isomorphism and Co-crystallization of some aryl -formamides and -thioamides.	203
5.1	Introduction	203
5.2	Isomorphism and co-crystallization in 2,6 disubstituted arylformamides.	205
5.2.1	Isomorphism	205
5.2.2	Co-crystallization of 2,6-dichlorophenylformamide (2a) and 2,6-dimethylphenylformamide (3).	209
5.2.2.1	Powder X-ray diffraction analysis.	211
5.3	Isomorphism and co-crystallization in 2,6 disubstituted arylthioamides.	214
5.3.1	Isomorphism	214
5.3.2	Co-crystallization of 2,6-dimethylphenylthioamide 16 and 2-chloro-6-methylphenylthioamide 17 .	215
5.3.2.1	Powder X-ray diffraction analysis.	217
5.4	Isomorphism and co-crystallization in 2,6-diisopropylphenylformamide and 2,6-diisopropylphenylthioamide.	219
5.4.1	Isomorphism	219
5.4.2	Co-crystallization in 2,6-diisopropylphenylformamide and 2,6-diisopropylphenylthioamide.	221
5.4.2.1	Powder X-ray diffraction analysis.	223
5.5	Discussion of isomorphism and co-crystallization in aryl formamides and -thioamides.	-
5.5.1	Isomorphism	225
5.5.2	Co-crystallization	229

CHAPTER 6

6.	An in-depth look at the nature of hydrogen bonds and weak intermolecular interactions in compounds 1 – 21	232
6.1	Introduction	232
6.2	N-H...O hydrogen bonds in phenylformamides	233
6.2.1	The main packing modes and motifs formed by the N-H...O hydrogen bond in compounds 1 – 14	234
6.2.2	Factors determining the molecular packing modes of compounds 1 – 14	237
6.3	The N-H...S hydrogen bond	242
6.3.1	Molecular packing mode and the hydrogen bond geometry of compounds 15 – 20	242
6.4	The C-H...O and C-H...S hydrogen bonds in compounds 1 – 20	245
6.5	Halogen bonding in compounds 1 – 20	253
6.5.1	Geometry of X...X interactions in compounds 1 – 20	254
6.6	Influence of C-H... π and π ... π interactions in compounds 1 – 21	257
6.6.1	C-H... π and C-F... π	257
6.6.2	π ... π interactions	260
6.7	Discussion	262
6.8	Results from lattice energy calculations	264
6.8.1	Category 1: [C(4) chains in Figure 6.1a]	265
6.8.2	Category 2: [C(4) stacks in Figure 6.1b]	268
6.8.3	Comparison of compounds 1, 2 and 4- a and b	272
6.8.4	Categories 3 and 4: [Sheets, dimers and tetramers]	273
6.8.5	Arylthioamides 15 – 20 [Category 5]	277
6.9	Conclusion	280

CHAPTER 7

7.	Conclusions	282
7.1	Introduction	282
7.2	Conformations and hydrogen bonding patterns	283
7.3	Major interactions in the crystal structures of the formamides and thioamides	285
7.4	Isomorphism	288
7.5	Cocrystallization	290
7.6	Polymorphism and phase transitions	292

REFERENCES

294

APPENDICES

- A** Full experimental details for structures **1 - 24**
- B** ORTEP diagrams for compounds **1 - 24**
- C** Selected NMR spectra
- D** Diagrams not included in the text
- E** CD – CIF files for compounds 1 - 24

List of Figures	Page number
Figure 1.1	Hydrogen bonding (dashed blue line) between two peptide links 21
Figure 1.2	The main hydrogen bonding motifs in aryl thioamides 23
Figure 1.3	A general representation of the C-H...O hydrogen bond showing the relevant notation as used in this discussion 25
Figure 1.4	Two common motifs formed by the C-H...O hydrogen bond in aryl formamides and acetanilides from literature 27
Figure 1.5	Dimers of C-H...S hydrogen bonded formamides 29
Figure 1.6a	A simplified representation of the electrostatic potential on a halo-benzene 32
Figure 1.6b	An illustration of the two types of Cl...Cl interactions 33
Figure 1.7	Representations of the two types of aromatic interactions with red lines showing the relative orientations of the interacting rings 36
Figure 1.8	The three general motifs that are noticed in secondary and primary amides 39
Figure 1.9	Hydrogen bonding pattern of 2,6-dichloroacetanilide. 42
Figure 1.10	Stereo view of Trans-2,2'6,6'-tetramethylbenzanilide. 43
Figure 1.11	N-H...O hydrogen bonded chains in <i>N</i> -(2,6-Di-isopropylphenyl) <i>p</i> -t-butylbenzamide and in 2-Vinyl- <i>N</i> -(2,6-dimethylphenyl)benzamide. 45
Figure 1.12	N-H...O hydrogen bonded chains of <i>N</i> -Acetyl-4-bromo-2,6-dichloroaniline and <i>N</i> -Formyl-4-bromo-2,6-difluoroaniline 47
Figure 1.13	Sheets of hydrogen bonded chains in acetanilide (ACANIL) and <i>P</i> -hydroxyphenylformamide (HXACAN). 48
Figure 1.14	Examples of graph-set assignments for common hydrogen-bond motifs. 50
Figure 1.15	A secondary level graph-set assignment. 51
Figure 3.1	An <i>ORTEP</i> diagram of 2,6-difluorophenylformamide 1a drawn with 50% probability displacement ellipsoids 88
Figure 3.2	Molecular structure of 1a 89
Figure 3.3	Histogram representing the C(7)=O(1) double bond (purple bars) and the N(1)-C(7) single bonds (yellow bars) in compounds 1 – 6 . 93
Figure 3.4	Packing in 2,6-difluorophenylformamide 96
Figure 3.5	Hydrogen bonding chain in 2,6-dichlorophenylformamide 2a 98

Figure 3.6	Hydrogen bonded chain (blue dashed lines) in 2,6-dimethylphenyl-formamide 3	101
Figure 3.7	Hydrogen bonded chains in the crystal of 2-chloro-6-methylphenyl-formamide 4a	103
Figure 3.8	N(1)-H(1)...O(1) hydrogen bonded chains (blue dashed lines) in 2,6-dibromophenylformamide 5	106
Figure 3.9	N-H...O hydrogen bonded chains in compound 6	107
Figure 3.10	Molecular structure of 2,4-dichlorophenylformamide 7	112
Figure 3.11	Packing diagram of compound 2,4-dichlorophenylformamide 7	117
Figure 3.12	An illustration of least squares planes through each of the two molecules in the asymmetric unit of the crystal structure of compound 8	118
Figure 3.13	Two layered N-H...O hydrogen bonded sheets of 2,4-dibromophenyl-formamide	119
Figure 3.14	View down the crystallographic <i>a</i> axis of a packing diagram for 2,4-dibromophenylformamide	120
Figure 3.15	<i>ORTEP</i> III diagram of 2,5-dichlorophenylformamide 9	121
Figure 3.16	Packing diagram for compound 9 as viewed down the crystallographic <i>a</i> axis.	123
Figure 3.17	Packing diagram of 2,5-dibromophenylformamide	125
Figure 3.18	Packing diagram of 5-chloro-2-methylphenylformamide showing intermolecular interactions between hydrogen-bonded chains	127
Figure 3.19	Packing diagrams of 3,4-dichlorophenylformamide	130
Figure 3.20	Packing diagram of 3,5-dichlorophenylformanilide as viewed down the crystallographic <i>a</i> axis. N-H...O hydrogen bonds in blue dashed lines	131
Figure 3.21	Packing diagram of 3,5-dichlorophenylformanilide. $\pi \dots \pi$ intermolecular interactions connecting adjacent N-H...O hydrogen bonded chains (in red dashed lines).	131
Figure 3.22	Histogram of C=S vs. C=N bond lengths for compounds 15 – 20 (compounds represented by numbers 1 – 6 respectively).	138
Figure 3.23	Molecular structures of (a) compound 15 and (b) compound 20 .	138
Figure 3.24	N-H...S hydrogen bonding chains of 2,6-difluorophenylthioamide as viewed down the crystallographic <i>a</i> axis.	140
Figure 3.25	Packing diagram of 2,6-difluorophenylthioamide	140

Figure 3.26	Packing diagram of 2,6-dichlorophenylthioamide as viewed down the <i>a</i> axis	142
Figure 3.27	Packing diagrams for 2,6-dimethylphenylthioamide.	145
Figure 3.28	Packing diagram of 2-chloro-6-methylphenylthioamide as viewed down the <i>a</i> axis.	147
Figure 3.29	Packing diagram of 2,6-dibromophenylthioamide showing ribbons formed by N-H...S (in blue) and C-H...S (in sky blue) hydrogen bonds.	148
Figure 3.30	Packing diagram for 2,6-diisopropylphenylthioamide.	150
Figure 3.31	The crystal structure of phenylformamide 21 showing the two molecules [(a) <i>cis</i> and (b) <i>trans</i>] in the asymmetric unit.	154
Figure 3.32	View along the crystallographic <i>c</i> axis showing one tetramer	158
Figure 3.33	View down the crystallographic <i>b</i> axis	158
Figure 3.34	Packing diagram of phenylformamide viewed down the <i>b</i> crystallographic axis, showing N-H...O hydrogen bonds, C-H... π and π ... π interactions	159
Figure 3.35	Packing diagram for cocrystal 22 showing hydrogen bond chains Cl...Cl interactions and π ... π interactions	164
Figure 3.36	Packing diagram for co-crystal 23 as viewed down the crystallographic <i>a</i> axis	165
Figure 3.37	Packing diagram for co-crystal 24 showing hydrogen bonding chains in blue and C-H... π interactions in orange dashed lines	167
Figure 4.1	DSC traces of compounds 2a (upper trace) and 4a (lower trace).	171
Figure 4.2	Experimental powder X-ray diffraction pattern showing the two phases of 2,6-dichlorophenylformamide.	172
Figure 4.3	Experimental powder X-ray diffraction pattern showing the two phases of 2-chloro-6-methylphenylformamide.	173
Figure 4.4	ORTEP diagrams for structures 2a and 4a	175
Figure 4.5	Hydrogen bonded chains in 2,6-dichlorophenylformamide 2a	179
Figure 4.6	Hydrogen bonded chains in 2-chloro-6-methylphenylformamide 4a	180
Figure 4.7	Crystal packing in the structure of 2a	181
Figure 4.8	View down (a) the <i>b</i> axis, and (b) down the <i>a</i> axis of a sheet of molecules from the structure of 2a	182
Figure 4.9	A sheet of molecules from the structure of 2b .	184
Figure 4.10	Crystal packing in 4b drawn as a projection down the <i>b</i> axis.	185

Figure 4.11	The arrangement of the three molecules contributing most to the stability of structure 2a .	188
Figure 4.12	Crystals of compound 15 (dark) and compound 1b (transparent and tiny)	192
Figure 4.13	ORTEP diagram for structure 1b .	193
Figure 4.14	Hydrogen bonded chains in 2,6-difluorophenylformamide 1a .	195
Figure 4.15	Crystal packing in the structure of 1a .	196
Figure 4.16	A view down the <i>a</i> crystallographic axis. Sheets of N-H...O hydrogen bonded molecules are linked by C-H...F (indicated in green dashed lines) and C-H...O interactions (in blue dashed lines).	197
Figure 4.17	Sheets of C-H...F (shown in purple dashed lines) and C-H...O (shown in red dashed lines) hydrogen bonded molecules of compound 1b .	198
Figure 4.18	The arrangement of the four molecules contributing most to the stability of structure 1a .	201
Figure 5.1	Crystal packing in compounds (a) 1a ; (b) 2a ; and (c) 4a as viewed down the crystallographic <i>a</i> axis	207
Figure 5.2	Bar graph comparing the closest non-bonding distances in compounds 1a , 2a and 4a	208
Figure 5.3	Powder patterns for 2,6-dichlorophenylformamide 2 , 2,6-dimethylphenylformamide 3 and the cocrystal 22	212
Figure 5.4	PXRD patterns for co-crystals of 2 and 3 with differing stoichiometries	213
Figure 5.5	Powder XRD patterns of 2,6-dimethylphenylthioamide 16 , 2-chloro-6-methylphenylthioamide 17 and cocrystal 23	217
Figure 5.6	Bar graph comparing of the closest non-bonding distances in compounds 6 , 20 and co-crystal 24	221
Figure 5.16	Powder patterns for 2,6-diisopropylphenylformamide 6 , 2,6-diisopropylphenylthioamide 20 and the cocrystal, 24	224
Figure 6.1	The four different categories generated by the N-H...O hydrogen bonds of compounds 1 – 14	235
Figure 6.2	The two different groups generated by the N-H...S hydrogen bonds of compounds 15 – 20	243
Figure 6.3	A scatter plot showing the correlation between the C-H...O angle and H...O distances for C-H...O hydrogen bonds in disubstituted phenyl formamides (1 – 14)	247

Figure 6.4	Hydrogen bonding motifs generated by C-H...O interactions in 2-chloro-6-methylphenylformamide.	249
Figure 6.5	Adjacent N-H...O hydrogen bond chains in N-Formyl-4-bromo-2,6-difluoroaniline linked up by C-H...O interactions	250
Figure 6.6	Hydrogen bonded ribbons of 2,6-dibromophenylthioamide.	252
Figure 6.7	Diagram showing X...X interactions in 2,5-dichlorophenyl formamide 9 , 2,5-dibromophenylformamide 10 and 5-chloro-2-methylphenylformamide 12	255
Figure 6.8	The two Cl...Cl interactions in 2,6-dichlorophenylthioamide	256
Figure 6.9	Hydrogen bond chains in category 1 and category 2 compounds and the support from C-H... π interactions.	258
Figure 6.10	Hydrogen bonded tetramers in phenylformamide supported by C-H... π interactions.	259
Figure 6.11	π ... π interactions in category 1 compounds and phenylthioamides linking up N-H...O and N-H...S hydrogen bond chains, and in category 3 and 4 compounds, linking up sheets of N-H...O hydrogen bond chains	261
Figure 6.12	The arrangement of the three molecules around a central molecule contributing most to the stability of structure 1a and 2a	268
Figure 6.13	The arrangement of the three molecules contributing most to the stability of 2,6-difluorophenylformamide 1a	270
Figure 6.14	The arrangement of the four molecules contributing most to the stability of 2,6-dibromophenylformamide 5	271
Figure 6.15	The arrangement of the three molecules contributing most to the stability of 2,6-dimethylphenylformamide 3	272
Figure 6.16	The arrangement of the three molecules contributing most to the stability of 2,5-dibromophenylformamide 8 and 14	276
Figure 6.17	The distance and general angle between adjacent and alternate molecules along hydrogen bonded chains in (I) 2,6-difluorophenylformamide and (II) 2,6-difluorophenylthioamide	280
Figure 7.1	The arrangement of aligned molecules between hydrogen bonded sheets in (a) 2,5-disubstituted phenylformamide and (b) 3,5-disubstituted phenylformamide.	287

List of tables	Page number
Table 1.1 Properties of strong, moderate and weak hydrogen bonds following the classification by Jeffrey [1997].	16
Table 1.2a R groups and the C=O...N angles of structures from literature: motifs (a) and (b).	41
Table 1.2b R groups and the C=O...N angles of structures from literature: motif (c).	44
Table 1.2c R groups and the C=O...N angles of structures from literature: motif (d).	46
Table 2.1 ¹ NMR data for arylformamides 1 – 14 and 21 (δ in ppm, ¹ H- ¹ H coupling constants in Hz)	74
Table 2.1 ¹ NMR data for arylformamides 15 – 20 (δ in ppm, ¹ H- ¹ H coupling constants in Hz)	77
Table 3.1 Some geometric parameters for compounds 1 to 6	88
Table 3.2 Crystal data for compounds 1a , 2a , 3 , 4a , 5 and 6	94
Table 3.3 Selected geometric parameters for compounds 7 to 14	113
Table 3.4 Crystal data for compounds 7 , 8 , 9 , 10 , 12 , 13 and 14	115
Table 3.5 Selected bond distances, bond and torsion angles for compounds 1-6	136
Table 3.6 Geometric parameters for compound 17 and 18 showing intermolecular distances and angles for π ... π and C-H... π interactions	146
Table 3.7 Geometric parameters for 2,6-diisopropylphenylthioamide	150
Table 3.8 NMR data for the phenylformamide powder and crystals	153
Table 3.9 Bond lengths and angles of both conformers of phenylformamide	156
Table 3.10 Showing the geometric parameters of compound 21	157
Table 3.11 Bond distances (Å) and angles (°) for compounds 22 , 23 and 24	161
Table 3.12 Unit cell parameters for co-crystals 22 , 23 and 24	162
Table 3.13 Geometric parameters for cocrystal 24	166
Table 4.1 Bond distances and angles for 2,6-dichlorophenylformamide 2 and 2-chloro-6-methylphenylformamide 4	176
Table 4.2 Hydrogen bonding distances and angles for 2,6-dichlorophenylformamide and 2-chloro-6-methylphenylformamide	176

Table 4.3	Bond distances and angles for compounds 1a and 1b	193
Table 4.4	Hydrogen bonding distances and angles for compounds 1a and 1b	194
Table 5.1	Bond distances (Å) and angles (°) for compounds 1a , 2a and 4a	206
Table 5.2	Unit cell parameters for compounds 1a , 2a and 4a	206
Table 5.3	Unit cell parameters of 2,6-dichlorophenylformamide 2a , 2,6-dimethylphenylformamide 3 , co-crystal 22 and 2-chloro-6-methylphenylformamide 4a	210
Table 5.4	Bond distances (Å) and angles (°) for compounds 1a , 2a and 4a	214
Table 5.5	Unit cell parameters for compounds 1a , 2a and 4a	214
Table 5.6	Unit cell parameters for 2,6-dimethylphenylthioamide 16 , 2-chloro-6-methylphenylthioamide 17 and cocystal 23	218
Table 5.7	Bond distances (Å) and angles (°) for compounds 6 and 20	220
Table 5.8	Unit cell parameters for compounds 6 and 20	220
Table 6.1	N-H...O=C geometry of <i>N</i> -disubstituted arylformamides 1-14	238
Table 6.2	N-H...S=C geometry of <i>N</i> -disubstituted arylthioamides 15-20	244
Table 6.3	C-H...O geometry of <i>N</i> -disubstituted arylformamides	248
Table 6.4	Geometric parameters for the C-H...S hydrogen bond for compounds 15-20	252
Table 6.5	Geometric parameters for halogen...halogen interactions in halogen substituted formamides and thioamides	256
Table 6.6	Geometric parameters for C-H... π , C-F... π and C-Cl... π interactions in compounds 1 – 21	257
Table 6.7	Geometric parameters for π ... π interactions in compounds 1 - 21	260
Table 6.8	Most stabilizing molecule-to-molecule interactions in compounds 1a , 2a , 4a and 6 [Category 1, (4) chains]	266
Table 6.9	Most stabilizing molecule-to-molecule interactions in compounds 1b , 2b , 4b , 3 , 5 and 12 . [Category 2 stacks]	269
Table 6.10	Most stabilizing molecule-to-molecule interactions in compounds 7 , 8 , 9 , 10 , 13 and 14 . [Category 3 sheets]	274
Table 6.11	Most stabilizing molecule-to-molecule interactions in compounds 15 and 20 . [Category 5]	277

List of Schemes

Scheme 1.1	Extended conjugation in aryl amides	5
Scheme 1.2	Useful formamides, thioamides and related amides from literature	7
Scheme 1.3	The two non-isomorphous derivatives of 2-benzyl-5-bromobenzylidene-cyclopentanone	59
Scheme 1.4	Resonance formulas for amides I – III	71
Scheme 3.1	Molecular representation of the 2,6-disubstituted arylformamides	87
Scheme 3.2	Resonance model in formamides	92
Scheme 3.3	Chemical structures of compounds 7 – 14 with their atom-numbering schemes	110
Scheme 3.4	Schematic diagrams for the 2,6-disubstituted arylthioamides 15 to 20	134
Scheme 3.5	Resonance structures around the thioamide moiety	136
Scheme 5.1	Non-isomorphous compounds 2a and 3 used in co-crystallization studies resulting in compound 22	210
Scheme 5.2	Non-isomorphous compounds 16 and 17 used in co-crystallization studies resulting in compound 23	217
Scheme 5.3	Isomorphous structures of 2,6-diisopropylphenylformamide 6 and 2,6-diisopropylphenylthioamide 20 used to grow an isomorphous co-crystal of both compounds (24)	223

List of Symbols

π - ρi - represents electrons clouds of a aryl ring

Å - Angstroms

$^{\circ}$ - Degree sign

δ - Delta – symbol for chemical shifts in NMR studies

θ - Theta – always used in reference to angles

d - the spacing of planes in the crystal

ρ - rho – symbol for density

α - alpha – angle between crystallographic b and c axes

β - beta – angle between crystallographic a and c axes

γ - gamma - angle between crystallographic a and b axes

λ - lambda – symbol for wavelength of X-rays

μ - mu -

Π - Symbol for unit cell similarity index

Σ - Summation.

Abbreviations

NADH – an enzyme - Neuron alcohol dehydrogenase.

NMR – Nuclear magnetic resonance

PXRD – Powder X-ray diffraction

DSC – Differential scanning calorimetry

DMSO – Dimethylsulphoxide

DMSO-d₆ – Deuterated Dimethylsulphoxide

CDCl₃ – Deuterated chloroform

DMF – Dimethylformamide

THF – Tetrahydrofuran

MHz – Mega Hertz

CCDC – Cambridge Crystallographic Data Center.

Me – Methyl

ⁱPr – Isopropyl

Br – Bromine

Cl – Chlorine

F – Fluorine

CSD – Cambridge structural database

Cg – Center of gravity (center of aryl ring)

B. O. – Bernard Omondi

1. Introduction and Literature background

1.1 Introduction

The search for simple theoretical and experimental models for important chemical and biological compounds continues to be important in science. In investigations like this one emphasis has always been on the importance of various functional groups, which contribute to the overall physical and chemical properties of the compounds. The understanding and control of the resulting physical and chemical properties has now developed into an important field in its own right. This has in turn been used in the discovery of several important new materials.

Solid-state studies of various compounds have been part of similar investigations and continue to be an important component of physical science as a discipline. Such investigations have therefore left chemists (involved in crystal engineering), physicists, material scientists and structural biologists with a principal goal of designing and preparing materials with desired properties.

For chemists such studies involve the systematic synthesis and in-depth investigation of properties of the synthesized compounds. This would for example involve changing one component or functional group in a molecule, which in turn changes the properties of this compound partially or completely. Some of the properties of current interest include

electrical conductivity, organic magnetic properties, photoconductivity and photovoltaicity, non-linear optical activity and second harmonic generation, chromogenic properties and thermal phase change properties. The study of changes of the above listed properties in materials has been supported with the use of a number of physical and analytical techniques used to detect and characterize the materials. These techniques include, hot-stage microscopy, thermal methods [which include DSC (differential scanning calorimetry), DTA (differential thermal analysis), TGA (thermo gravimetric analysis)], X-ray crystallography (single crystal and powder X-Ray diffraction), IR (infrared spectroscopy), RS (Raman spectroscopy), SSNMR (solid state nuclear magnetic resonance), SEM (Scanning electron microscopy), density measurements and theoretical analysis (computational calculations by means of scientific software) of compounds. Some of the properties and techniques that are relevant to this study will be discussed in more detail in later chapters.

In recent years studies involving the amide group and its relevance to biological and chemical systems have been carried out by several researchers. Amides and particularly formamides and thioamides have been known to be of fundamental chemical and biological interest as some of the features of these compounds can be manipulated to obtain certain distinct and useful physical and chemical properties [Zeller *et. al.*, 2005; Tam *et. al.*, 2006 and references therein]. Because of this a lot of effort has gone into the study (i.e. their synthesis and applications) of simple

***N*-aryl -formamides and -thioamides**

amides and thioamides. *N*-arylformamides and simple formamides can be singled out as ones that have been studied in detail. Most of these studies have only been theoretical, such as on conformational flexibility in arylformamides using *ab initio* calculations in comparison to results from microwave spectroscopy [Moreno *et. al.*; 2006], gas-phase molecular and supramolecular structures of formamide clusters containing water and ammonia [Federov and Cable, 2000; Dickinson *et. al.*, 1999] and gas phase conformations and relative stabilities of the *cis* and *trans* isomers [Manea *et. al.*, 1997]. Other studies have dealt with density functional studies of hydrogen-bonded formamide chains (simple formamides) [Moisan and Danneberg, 2003], the strength of N-H...O=C and C-H...O=C bonds in simple formamides [Vargas *et. al.*, 2001], study of the crystal and gas phase structures of formyl(2-pyridyl)amine [Bock *et. al.*, 1996], optical resolution studies of 1,2-bis(formylamino)benzene in crystals [Azumaya *et. al.*, 2003], restriction of rotation in *o*-formamides [Boeyens *et. al.*, 1988] and some on experimental NMR investigations [LaPlanche and Rogers, 1964; Bourn *et. al.*, 1964; Stewart and Siddall, 1970].

Despite the effort that has gone into the study of arylformamide, no crystal data of the compound has been reported, and not much has been done in terms of the structural studies of mono and disubstituted *N*-arylformamides and *N*-arylthioamides either. In fact until now (this work) only a few structures of arylformamides and arylthioamides have been reported and even then none has been investigated in any detail. Some

***N*-aryl -formamides and -thioamides**

single crystal structures of *N*-arylformamides that have been reported to date are: 2,6-dichlorophenylformamide [QIKNUT¹; Godwa *et. al.*, 2000], 4-bromo-2,6-difluorophenylformamide [SEDGAJ¹; Ferguson *et. al.*, 1998], *p*-chlorophenylformamide and 2-methylphenyl-formamide [Boeyens *et. al.*, 1988] (whose thio- analogue was also reported), *p*-nitroformamidobenzene and *p*-formamidoanisole [Zeller *et. al.*, 2005] and *p*-formamidobenzoic acid [de Armas *et. al.*, 2001]. The structures of some of these formamides and thioamides will be discussed in later Chapters of this thesis.

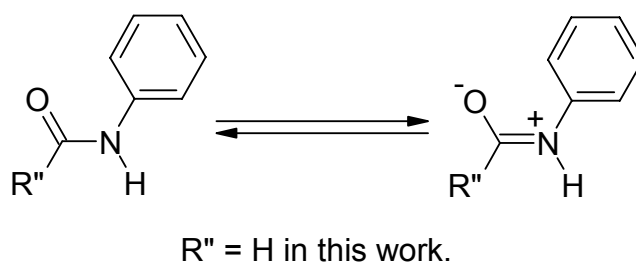
Formamides are amides containing the functional groups HCONH or HCONH₂. Thioamides therefore refer to a formamide in which the oxygen is replaced by a sulfur atom. Amides (formamides and thioamides) can be classified as primary, secondary or tertiary depending on the number of hydrogens attached to the nitrogen atom. For example the formamides and thioamides in this work are secondary since they only have one hydrogen atom attached to the nitrogen atom. Primary amides have two hydrogen atoms attached to the nitrogen and tertiary amides have no hydrogens attached to the nitrogen.

The arrangement of atoms or groups of atoms on the amide moiety in compounds can result in a *cis* or *trans* conformation. In this work the terms *cis* and *trans* are used in reference to the orientation of the hydrogen atom attached to the nitrogen in relation to the carbonyl oxygen

¹ CSD reference codes.

***N*-aryl -formamides and -thioamides**

in the formamides or the sulfur atom in the thioamides; when the hydrogen is on the same side as the oxygen or sulfur atom then *cis* is used and *vice versa*. Related to these two conformations (*cis* and *trans*) is conjugation around the amide moiety and the aryl ring. The delocalization of electrons in the aryl ring is believed to be extended to the amide moiety, especially when the two are co-planar, resulting in the two forms shown in scheme 1.1 [Pauling, 1960] which suggest a partial double bond character along the amide moiety (see scheme 1.1). This partial double bond character renders the amide moiety planar.



Scheme 1.1: Extended conjugation in aryl amides

Formamides and thioamides in general are versatile compounds that have found wide applications in the academic, industrial, biological and agricultural fields some of which are discussed briefly in the next section.

1.1.1 Relevance of formamides and thioamides

There are several areas in which the chemical and structural properties of compounds similar to formamides, acetamides and thioamides are relevant (see scheme 1.2). One such area is in pharmaceuticals, an example being that of paracetamol [$C_6H_5(OH-4)NHC(O)CH_3$ (see compound **I** in scheme 1.2)] where studies were focused on the behavior and prediction of its polymorphs [Haisa *et. al.*, 1976; Haisa *et. al.*, 1974; McGregor *et. al.*, 2002; Boldyreva *et. al.*, 2000; Nicholas and Frampton, 1998; Beyer *et. al.* 2001]. The compound has structural similarities to arylformamides. Another compound whose structure is related to that of the formamides that are discussed in this thesis is [6-Chloro-*N*-(2,6-dimethylphenyl)-3-pyridinecarboxamide (**II** in scheme 1.2)] an anticonvulsant agent with a high therapeutic ratio² and long half-life [Palmer *et al.*, 1993; Roberts, US patent]. *N*-alkylformamides such as *N*-methylformamide and *N*-ethylformamide (**IV** and **III** in scheme 1.2) have been found to possess hepatotoxic³ properties in that they have the ability to cause liver damage *in vivo* in mice [Shaw *et. al.* 1985].

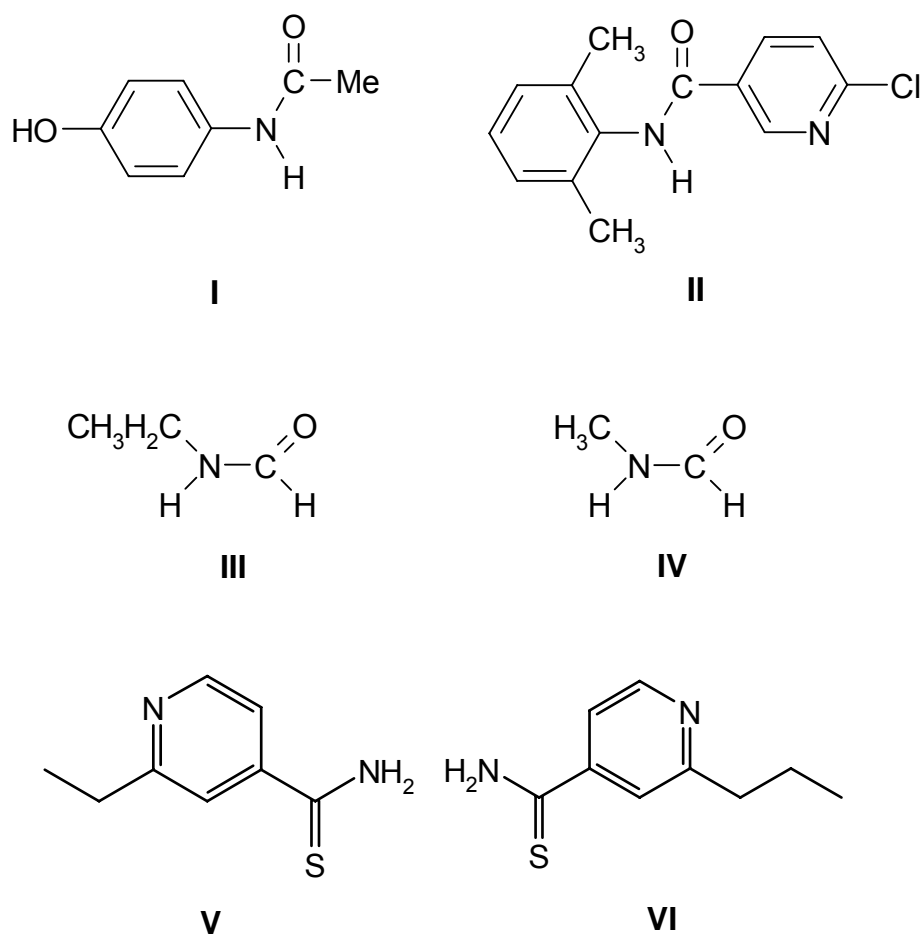
Biologically, due to their unreactive nature, formamides act as analogues of the aldehyde substrates of alcohol dehydrogenases, and are useful for structure-function studies, and for specific inhibition of alcohol metabolism. They bind preferentially to the enzyme-NADH complex thus

² A comparison of the amount of a therapeutic agent that causes the therapeutic effect to the amount that causes toxic effects (also = margin of safety).

³ Chemical-driven liver damage.

***N*-aryl -formamides and -thioamides**

inhibiting the binding of varied concentrations of alcohols. Such inhibitors could be especially useful for controlling alcohol metabolism since they are effective even at alcohol concentrations close to saturation [Venkataramaiah and Plapp, 2003].



Scheme 1.2: Useful formamides, thioamides and related amides from literature.

The amide group, well known as an important functional group in organic chemistry, forms the linkage in polypeptides, proteins and various

synthetic polymers [Jeffrey, 1997; Juranić, 2003] and plays a significant role in determining their special properties. Its planarity and hydrogen-bonding propensity is responsible for the formation of the secondary and tertiary structure of proteins, which lie at the heart of biological processes and also industrial processes such as the synthesis of polyamides.

With the increasing interest in biomacromolecules, it has become crucial to understand the structure, bonding and electronic properties of the amide group. Such properties are better studied by designing suitable molecules that mimic biomolecules. Such a study would either be theoretical (i.e. based on computer models) or studies on real molecules which possess similar features as those seen in biological systems. A model like this has to contain both C=O and N-H units which are able to form N-H...O hydrogen bonds. Proteins for example have only one amino hydrogen atom per formamide unit and the formation of multiple hydrogen bonds or bifurcated or trifurcated hydrogen bonds per amino group is therefore not easy due to the strain caused by R groups around amide bond. Thus when looking for structural model for the formation of hydrogen bonds in proteins secondary amides (as compared to primary or tertiary formamides) are a better choice [Juranić, 2003]. In this aspect the arylformamide as mentioned earlier has been regarded as a perfect model for the studies of stability and folding in peptides and protein [Barbooiu and Petrescu, 1973; Bourn et. al., 1964; Stewart and Siddall, 1970; Moreno et. al., 2006; Federov and Cable, 2000; Dickinson et. al., 1999;

***N*-aryl -formamides and -thioamides**

Manea et. al., 1997; Moisan and Danneberg, 2003; Vargas et. Al., 2001; Bock et. al., 1996; Azumaya et. al., 2003; Salzar et. al., 1993]

Thioamides are also relatively common in many biological systems such as amino acids (methionine, cystein and S-S bridged cystein, Vitamin B₁₂ – thiamine and penicillin). Thioamides in particular are versatile compounds that have found wide applications in the synthesis of pharmaceuticals as well as industrial and fine chemicals. In the pharmaceutical industry thioamides have been found to be bacteriostatic⁴ at therapeutic concentrations and important in treatment of tuberculosis. Ethionamide and prothionamide (**V** and **VI** respectively in scheme 1.2) have been used in treating drug resistant tuberculosis [Minton *et. al.*, 2004].

Thioamides have also attracted attention in peptide chemistry, in particular, α -substituted thioacetyl amides which are useful synthetic intermediates and provide an alternate route to phenylpropionic acids used in the synthesis of non-steroidal anti-inflammatory and analgesic drugs [Hoeg-Jensen and Holm, 1994]. In the industrial and fine chemicals field thioamides have been used as vulcanization accelerators, additives to lubricating oils, corrosion inhibitors, floatation agents, insecticides and fungicides, preservatives and intermediates for preparation of certain vitamins e.g. vitamin B₁) [Petrov and Andreev, 1969].

⁴ Antibiotics inhibit growth and reproduction of bacteria without killing them.

1.2 Aims of the project

The aim of this project was to prepare and comprehensively analyze the crystal structures of *N*-aryl -formamides and -thioamides with a view to understanding the influence of hydrogen bonds and other weak intermolecular interactions on the conformation and the overall crystal packing of these compounds. We chose aryl -formamides and -thioamides with steric constraints thereby introducing controlling features for intermolecular association. We also varied the nature of substituents (primarily alkyl and halide) and also their presence or absence the 2 or 6⁵ and other positions of the aryl ring.

The following summarizes our goals for the project.

- ❖ To synthesize formamides with different substituents at various positions of the ring and to structurally analyze these compounds.
- ❖ To synthesize the thio analogues of these formamides and analyze their structures.
- ❖ To investigate the possibility of the presence of different polymorphs of these compounds by comparing the various structures and growing crystals using various methods and examining their thermal behavior.

⁵ 2 and 6 refer to positions on the aryl rings only. Different in pyridines for example.

- ❖ To describe the relationships that may relate any existing polymorphs mathematically.
- ❖ To look at the influence the variation of substituents at the aryl ring will have with special focus on the chloro-methyl interchange.
- ❖ To compare any isomorphous compounds and to design and prepare suitable cocrystals of selected pairs of these compounds.

The presentation and analysis of the results obtained from the study is presented in 5 chapters. Apart from chapter 1 and 2 which deal with literature background and experimental procedures, respectively, chapter 3 describes the molecular and crystal structures of all 24 compounds, chapter 4 deals with polymorphism and phase transitions, chapter 5 assesses isomorphism and cocrystallization and chapter 6 gives an in-depth look at hydrogen bonding and weak intermolecular interactions in all 24 structures. The conclusions of all the findings are given in chapter 7. Because of the closeness of most chapters and use of the same structures in the different chapters, some sentences and figures appear in more than one chapter. This is done just for easy reading.

1.3 Literature background

Intermolecular interactions are major factors in governing crystal packing in solid state structures of many organic compounds. In designing a new and interesting crystalline material, which is the subject of crystal engineering, one of the main parameters that one might consider is the influence of hydrogen bonding. *N*-arylformamides and -thioamides are compounds that can be used to study the influence of such interactions in crystals. This class of compounds has proven to be a good tool for solid-state studies of small organic molecules, and more so for those compounds with the special C=O/C=S and the N-H bonds, that are responsible for the formation of interactions such as the N-H...O and N-H...S hydrogen bonds. A detailed knowledge of the amide group, for example, is required for making subtle changes in natural proteins (e.g. by just making point mutations as site directed metagenesis) and to design new materials mimicking biomolecules. Apart from these hydrogen bonds other weak and sometimes less directional forces such as C-H...O, Halogen...Halogen, Halogen...O, C-H... π and π ... π interactions are also important in generating the supramolecular architectures [Desiraju, 1991, 1995, 1996 and 2002; Desiraju and Steiner, 1999; Nishio *et. al.*, 1995; Nishio, 2004; Takahashi *et. al.*, 1999; Csöregi *et. al.*, 2001; Navon *et. al.*, 1997, Moulton and Zaworotko, 2001]. The ability of other groups of atoms such as chlorine to steer the local arrangement between two molecules in a structure has also been reported by several people [Addadi *et al.*, 1979;

Gnanaguru *et. al.*, 1985; Desiraju, 1991]. This steering ability can be important in crystal engineering [Price *et. al.*, 1994; Desiraju *et al.*, 1996; Bernstein, 1981] even though it's argued that it does not influence much crystal packing in organic molecules, and that even replacing it with a functional group of similar size does not result in significant changes in crystal packing [Kaitagorodsky *et al.*, 1973; Addadi *et al.*, 1979; van der Streek and Motherwell, 2005] with at least 25% effectiveness [van der Streek and Motherwell, 2005].

Analysis of crystal structures together with other studies such as thermal studies and computer based energy calculations [Price *et. al.*, 1994] can lead to the discovery of new polymorphs and the design of mixed crystals or cocrystals. Such processes could give access to a desirable packing arrangement and the improvement of physical (e.g. solubility, melting point and hygroscopicity) and chemical properties of useful compounds. The discovery of such polymorphs is important to a variety of disciplines such as for example the pharmaceutical and the dye and pigment industries.

1.3.1 *Hydrogen bonding and weak intermolecular interactions*

Hydrogen bonds and weak intermolecular interactions were discovered in the late 19th century and since then have received immense attention leading to a number of reviews with different definitions of the interaction [Steiner, 2003; Desiraju and Steiner, 1999; Aakeröy *et. al.*,

1999]. All these definitions are valid depending on ones point of interest. Generally hydrogen bonding as defined by Pauling [Pauling, 1939] is an interaction involving hydrogen atoms between a donor and an acceptor atom. This analogy is based on the Brönsted-Lewis acid, which is a proton donor, and a base, which is a proton acceptor. What it requires basically is that, if the letters A and D are used to represent acceptor and donor, where D bears the H atom in a covalent bond, then D needs to have a sufficiently high electronegativity to withdraw electrons to leave the proton partially unshielded. The acceptor atom A needs to have a lone-pair or polarizable π electrons [Atkins, 1990]. More recent definitions describe it as an interaction wherein a hydrogen atom is attracted to two atoms, D and A, rather than just one and so acts like a bridge between them [Desiraju, 2002]. This simple concept applies to a wider range of interactions (here referred to as weak intermolecular interactions) that are found in most organic and organometallic compounds. Depending on their properties hydrogen bonds can be categorized into different groups. Generally we have very strong hydrogen bonds, which resemble covalent bonds and weak hydrogen bonds, which resemble van der Waals forces. The rest of hydrogen bonds are distributed between the two extremes [Jeffrey, 1997].

Apart from the general chemical definitions, there exist many specialized definitions of hydrogen bonding most of which are in connection to the particular techniques used to study them. For example

infrared, Raman and microwave spectroscopists define hydrogen bonds with respect to their effect on the vibrational motions of the bonds directly bound. NMR spectroscopists observe the chemical shifts caused by the change in the electronic environment around the proton. Thermodynamicists measure hydrogen bond energies while theoreticians calculate them and determine the configurations associated with the energy minima. Diffractionists observe characteristics of bond lengths and bond angles associated with hydrogen bonding.

Other hydrogen bonding definitions include those by Pimentel and McClellan [1960]. According to them, a hydrogen bond is said to exist when (i) there is evidence of a bond, and (ii) there is evidence that this bond sterically involves a hydrogen atom already bonded to another atom. Another given by Steiner and Saenger [1998] says that, for a A-H...D system, a hydrogen bond is said to exist when there is a cohesive interaction where H (the hydrogen) carries a positive charge and A (the acceptor) a negative charge (partial or full) and the charge on the hydrogen is more positive than on D (the donor). All these definitions still fall within the wider scope of Pauling's definition.

1.3.2 The nature and properties of hydrogen bonds

The different definitions given in the previous section all provide a number of categories of hydrogen bonds. For practical reasons they are normally categorized as “strong”, “moderate” and “weak” hydrogen bonds

***N*-aryl -formamides and -thioamides**

(see Table 1) [Jeffrey, 1997] and for our purposes we shall use the same classification. Other definitions have classified them as “very strong”, “strong” and “weak” [Desiraju and Steiner, 1999]. However, there is normally not a clear demarcation between the boundaries of these three categories, hence the variance in names. These names, as in Pauling’s definition, are based on geometrical, energetic and thermodynamic features and have similar boundaries for the categories and therefore similar meanings.

Table 1.1: Properties of strong, moderate and weak hydrogen bonds following the classification by Jeffrey [1997]. The numerical data are only guiding values.

	<i>Strong</i>	<i>Moderate</i>	<i>Weak</i>
A-H...D interaction	Mostly covalent	Mostly electrostatic	Electrostatic
Interatomic distances	A-H \approx H...D	A-H < H...D	A-H \ll H...D
H...D (Å)	~1.2 – 1.5	~1.5 – 2.2	2.2 – 3.2
A...D (Å)	2.2 – 2.5	2.5 – 3.2	3.2 – 4.0
Bond angles (°)	170 - 180	130 - 180	90 - 150
Bond energy (kJ mol ⁻¹)	15 - 40	4 - 15	<4
Examples	O-H...O N-H...N	N-H...O N-H...S	C-H...O/N O/N... π C-H...F C-H...S

A “very strong” (strong according to Pauling’s nomenclature) hydrogen bond with a bond energy of between 15 and 40 kJ mol⁻¹ can be exemplified by an O-H...O bond. It has a donor to acceptor distance in the range of 2.2 to 2.5 Å, almost equal “O-H” and “H...O” distances and an <O-H...O angle close to 180°. Such hydrogen bonds (found only occasionally) demonstrate pronounced covalency, generate rigid or strong

***N*-aryl -formamides and -thioamides**

networks and are normally formed by groups in which there is a deficiency of electron density in the donor group or an excess of electron density in the acceptor group i.e. when the donor atom and the acceptor atoms are highly activated. An example is when the donor and acceptor atoms are related such as in a typical intermolecular arrangement of an 'acid and base conjugate'. Other examples with such strong hydrogen bonds can be found in situations where charge, resonance or cooperative assistance is involved [Steiner *et. al.*, 2001; Vishweshwar *et. al.*, 2001; Wilson, 2001; Pimentel and McClellan, 1960].

Moderate hydrogen bonds are mostly electrostatic and show bond distances shorter than the sum of the van der Waals radii. These bonds are formed generally by neutral donor and acceptor groups in which the donor atoms D are electronegative relative to hydrogen and the acceptor atoms A have a lone pair. They are the most frequent type found in natural and synthetic compounds.

In the case of the weak hydrogen bond, the bond energies are very low and their contribution to the overall packing of a crystal is normally viewed not individually but as a collective effect. In this type of interaction, one or both donor and acceptor atoms or group of atoms are only of moderate or low electronegativity. The hydrogen atom is bound to a slightly more electronegative atom. The described classifications are not strict when it comes to bond distances and angles and generally can only

serve as a guideline for differentiating the more common hydrogen bonds [Jeffrey, 1997].

1.3.3 Examples of hydrogen bonds and intermolecular interactions in molecular crystals of aryl -formamides and -thioamides

Molecular crystals can be viewed as supramolecular structures that are made up of millions of simple molecules in a regular periodic arrangement. These molecules are brought together through hydrogen bonds and intermolecular interactions to create the solid-state superstructures [Etter and Reutzel, 1991; Amabilino and Stoddart, 1994]. A proper understanding of molecular crystals is more comprehensive when one has a thorough knowledge of all the non-covalent intermolecular forces that can exist between the components of a supramolecular arrangement. The packing of molecules in the crystals is normally as a result of several different factors and the mere fact that an interaction exists in a crystal does not necessarily mean that the interaction is favourable [Desiraju and Steiner, 1999]. The existence of such an interaction, for example, could only be as a consequence of another more energetically favoured interaction. The above mentioned intermolecular forces can be favourable or unfavourable and together affect the overall arrangement or packing of molecules in a crystal. The forces are either maximised (for favourable interactions) or minimised (for unfavourable interactions) throughout the whole crystal and result in the different packing patterns observed. Thus to understand and control specific

interactions in crystals it is necessary to investigate families of compounds that have been chosen in such a way that effects of different factors on the resultant structural properties may be systematically analysed. A brief description and background of specific hydrogen bonds (strong and weak) that are relevant to this study is given below.

1.3.3.1 *N*-H...O=C hydrogen bonds

N-H...O=C linkages occur in several different classes of compounds, most commonly in biological systems in which they play a pivotal role in determining both their structure and activity [Jeffrey and Saenger, 1991] especially the structures such as that of peptide bonds in proteins. This type of hydrogen bond would be categorised as moderate and is present in all the arylformamides that are discussed in this thesis. Their energies are about 25 kJ/mol and have H...O bond distances in crystal structures, which range from 1.5 – 2.2 Å with N-H...O angles between 140 and 180°.

The C=O and the N-H groups (peptide groups) have their polar ends aligned [Juranić *et. al.* 2003 and references therein] resulting in hydrogen-bonded chains and networks. The geometry of the hydrogen-bonded networks in protein structures is mainly determined by the polarity of the peptide groups (see Figure 1.1 below). The partial double bond character in the C=O and N-H groups makes them polarizable through

***N*-aryl -formamides and -thioamides**

hydrogen bonding [Scheiner and Wang, 1993; Milner-White, 1997]. Hydrogen bonds in a peptide backbone can have a maximum bond energy (strength) of about 25 kJ mol^{-1} and in order to reach this value the C=O and N-H groups rotate in such a way that the O, H and N atoms of the amide groups lie along a straight line. There is a limit to the rotation since the formation of hydrogen bond induces π -character to the peptide C-N bond that increases its resistance to twisting from its planar conformation. The conformation formed is responsible for helical or sheet structures. The side groups on the peptide units contain a variety of hydrogen bond donor and acceptor groups, which form the hydrogen bonds between the polypeptide chains. There is conjugation between the peptide group and the side chains in proteins [Wiberg *et. al.*, 1997].

N-H...O=C hydrogen bonding plays a major factor in determining pairing in the structures of nucleic acids. [Watson and Crick, 1953; Saenger, 1984]. Examples of such pairings are between adenine and thymine, and guanine and cytosine which happen to be the only two that nature has selected for the purpose of genetic coding in DNA.

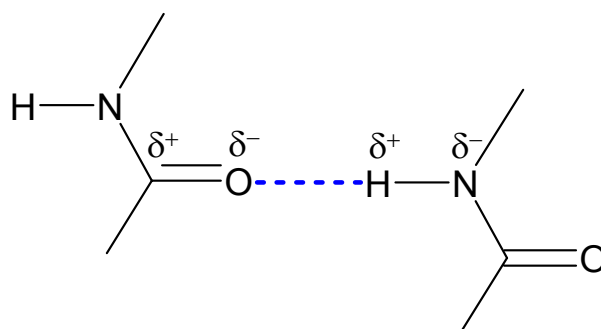


Figure 1.1: Hydrogen bonding (dashed line) between two peptide links. The backbone of the protein can form several of these bonds.

1.3.3.2 N-H...S=C hydrogen bond

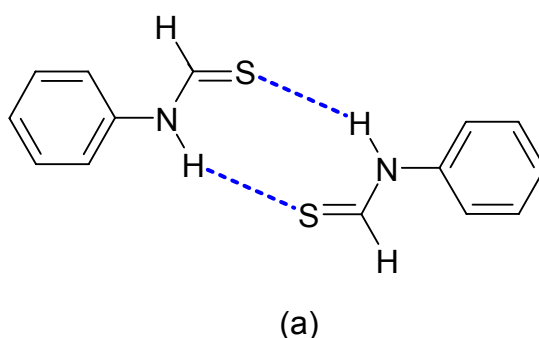
Just like the N-H...O=C hydrogen bond, N-H...S=C also is important in a number of chemical and biological processes as evident by the numerous investigations including X-ray [Rahman and van der Helm, 1980; Allen *et al.*, 1997a and b; Steiner, 1998] and neutron diffraction studies. Other studies on resonance-induced hydrogen bonding have been carried out using structures from the Cambridge Structural Database while others were on *ab initio* molecular orbital calculations done by Allen *et al.* [Allen *et al.*, 1997a and b].

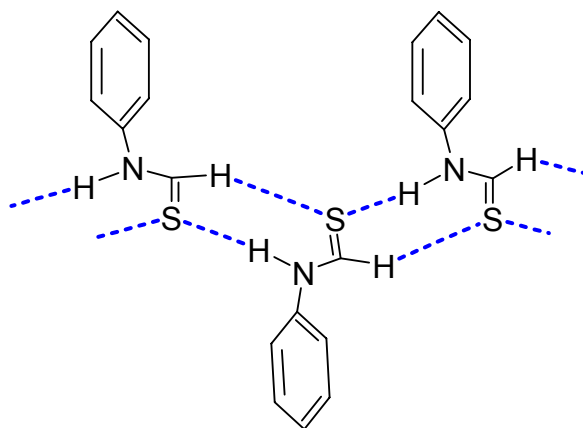
Very little work has been done with regards to the geometry of this weak hydrogen bond but there has been a study on conformational control of thioethers [Doerksen *et al.*, 2004 and references therein] in which the N-H...S hydrogen bond is discussed. In this study the distances for N...S and H...S are established to be 3.44(4) and 2.48(6) Å (neutron diffraction)

***N*-aryl -formamides and -thioamides**

and 3.58(3) and 2.74(2) Å (X-ray diffraction), respectively. From a study by Allen *et. al.* [1997a and b] it was concluded that a correlation existed between the length of the N-H bond and the H...S interatomic distance; the longest N-H bond (1.041 Å) was found for the shortest H...S distance (2.274 Å). According to their search, the H...S distance spans the range of 2.28-2.72 Å with the upper limit being 0.18 Å shorter than the sum of the van der Waals radii. The same kind of relation exists between N...S and H...S interatomic distances and these two distances point towards a strong tendency for linear N-H...S=C systems.

Because of the size of the sulphur atom, its involvement in the amide bond often results in a *cis* conformation (the hydrogen atom attached to nitrogen is *cis* to the sulphur atom). For this reason two common motifs are adopted by most arylthioamides. They either form isolated dimers with inversion-symmetry [as shown in Figure 1.2a] or they form extended zigzag chains, better known as ribbons (Figure 1.2b).





(b)

Figure 1.2: The main hydrogen bonding motifs in aryl thioamides. Hydrogen bonding chains are shown in dashed lines.

Motif (a) is formed mainly when the molecules are planar (i.e. the thioamide moiety is coplanar with the aryl ring). Molecules in this motif are often related by a centre of inversion. Motif (b) is formed when the two planes defined by N-H-C(X)=S and the aryl ring are not coplanar (like when there are substituents in the 2 and 6 position of the aryl ring). Molecules in this type of hydrogen bonding motif are normally related by a 2_1 -screw axis or by a glide plane.

1.3.3.3 *The C-H...O and C-H...S hydrogen bonds*

Initially the C-H...O hydrogen bond was not considered as an interaction with suggestions to the contrary by authors such as Sutor [1962 and 1963] back in the 60s receiving much scepticism. This hydrogen bond is now well established and has been studied in many

biological and chemical systems and in supramolecular design especially after the landmark study by Taylor and Kennard [1982], which provided unambiguous evidence for its existence. More accounts of its importance were given in the 90s by Desiraju [1991 and 1996] and Jeffrey [1997] and the mere fact that an oxygen atom is present in most organic or biological molecules just emphasises its importance.

These hydrogen bonds have been known to play a role in the stabilization and functioning of biological macromolecules for example in protein-protein interfaces [Jiang and Lai, 2002]. Their role in simple amine crystals structures was outlined by Czugler *et. al.* [2004] and Desiraju [1991 and 1996] showed its structural implications and importance in supramolecular design. As was mentioned earlier, it is becoming increasingly important to understand how molecules align themselves in crystals and the knowledge of such interactions is one way of doing this.

Early observations of the C-H...O hydrogen bond include Pauling's observation that the boiling point of acetyl chloride is substantially higher than that of trifluoroacetyl chloride [Pauling, 1960], Gladstone's suggestion of the existence of complexes of haloforms with ketones ($X_3C-H...O=C<$) [Gladstone, 1937] and Jeffrey's observation of the relatively high melting point of dimethyl oxalate due to methyl...carbonyl interactions in the solid state [Dougill and Jeffrey, 1953].

Taylor and Kennard [1982] showed that the C-H...O interactions were electrostatic in nature and that they occurred within wider distance and angle ranges than more directional and relatively stronger N-H...O, N-H...N and O-H...O interactions. In small molecules the significance of these C-H...O interactions increases with their number relative to the stronger N-H...O and O-H...O interactions and their energies (4-8 kJ/mol) is just in the range where it can compete with other conformational forces and forces responsible for tertiary structures of macromolecules.

In this thesis the criteria that are used for analysing stronger N-H...O, and O-H...O hydrogen bonds has been adopted. The description given below is a short summary of what is described by other authors such as Taylor and Kennard [1982] in their discussion of the C-H...O interaction. The discussion involved the study of the lengths and angles around the C-H...O interaction. The diagram below gives a description of the bond distances and angles of the C-H...O bond which are under scrutiny in this study.

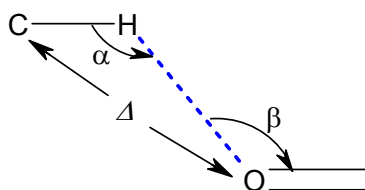


Figure 1.3: A general representation of the C-H...O hydrogen bond showing the relevant notation as used in this discussion.

The C-H...O interaction has a characteristic C...O distance (Δ). Unlike strong N...O and O...O distances which are normally significantly shorter than conventional van der Waals contacts [Desiraju, 1991] and whose value is more sensitive to the nature of the H atom than to the nature of the basic acceptor, the C-H...O bond, because of its weakness, can be distorted by other crystal forces and as a result the C...O distance varies over a large range (3.0 – 4.0 Å). The angles (α and β in Figure 1.3) of the C-H...O bond are in contrast relatively constant and tend towards linearity. The C...O repulsion, like N...O and O...O is not a major factor in determining bond linearity in these interactions and it has been suggested that perhaps the C...O distances are too long for any repulsions to exist. The directionality of these hydrogen bonds was illustrated by Gu and co-workers and they concluded that C-H...O bonds were sensitive to distortions from their equilibrium geometry in the same way as conventional hydrogen bonds [Gu *et. al.*, 1999].

It is important to note that the C-H...O interaction also exists in a variety of supramolecular motifs. Catemers, rings, dimers, chains are some of the very common motifs that have been observed in most organic compounds and are easily grouped using known graph set notations⁶. The formation of the motifs generated from C-H...O interactions is however usually dependent more on other stronger hydrogen bonds occurring in

⁶ Graph set notation is a mathematical way of describing patterns formed by hydrogen bonds. The full definition is given later in this chapter.

cooperation with it in the system of reference (in this study the N-H...O hydrogen bond).

Two major types of C-H...O hydrogen-bonds are recognized in our class of compounds (arylformamides and arylthioamides). These are the β -sheet type catemers that often occur in cooperation with the stronger N-H...O hydrogen bond, and the ring types, which often result in a motif with graph set $R_2^1(5)$ (Figure 1.4a) and, $R_2^1(5)$ and $R_2^2(4)$ [= $R_4^2(10)$] as illustrated in Figure 1.4b. The two types are closely related to the described specific categories of the N-H...O hydrogen bonds, with the β -sheet type structures found mainly amongst aromatic compounds with no substitutions on both the 2 and 6 positions of the aryl ring and the ring-type structures more commonly in category 2 compounds.

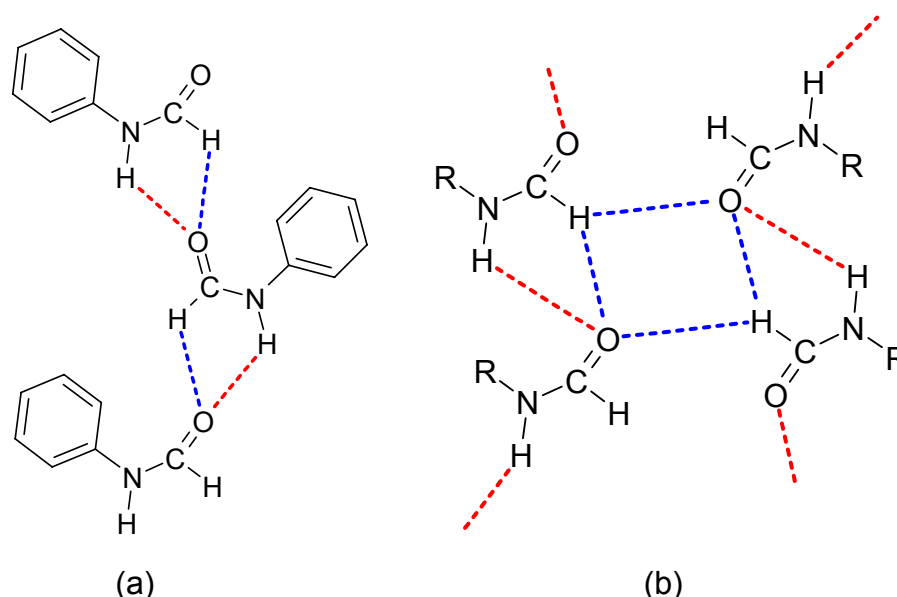
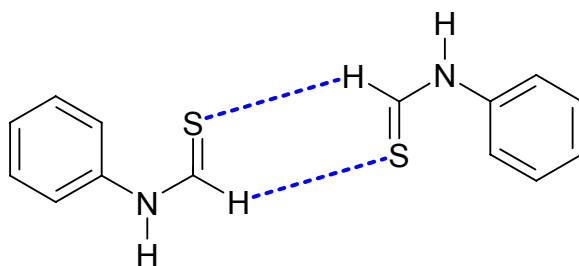


Figure 1.4: Two common motifs formed by the C-H...O hydrogen bond in aryl formamides and acetanilides from literature; (a) β -sheet type catemers

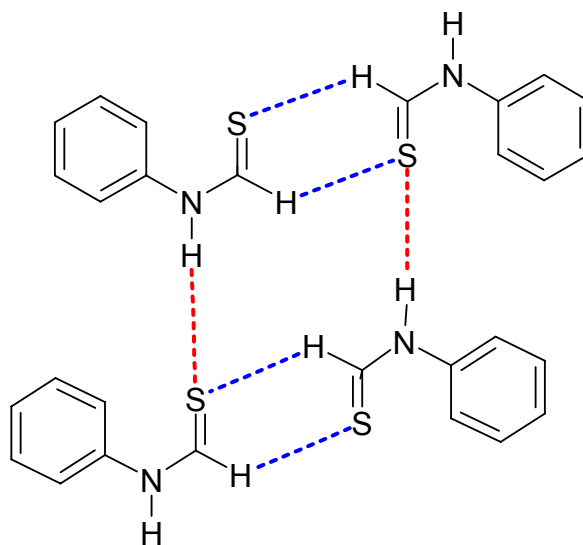
N-aryl -formamides and -thioamides

formed by C-H...O (in blue dashed lines) and N-H...O (in red dashed lines); (b) ring type motif.

The C-H...S hydrogen bonds behave in the same way as the C-H...O hydrogen bonds. Due to the larger size of the sulphur atom (in comparison to the oxygen atom) it can be involved in more than two interactions at a time. In most thioamides, in addition to the relatively strong N-H...S/O-H...S bond, the sulphur atom is involved in a second and sometimes even a third interaction. The result is the formation of dimers described by $R_2^2(6)$ graph set or ribbons composed $R_2^2(6)$ rings and $R_4^2(10)$ rings similar to the ones discussed in the formamides section. Since in most thioamides the conformation of the amide bonds is *cis*, this leaves the atom or the group of atoms attached to carbon (of the C-N single bond) available for interaction with the sulphur atom of the adjacent molecule along the hydrogen bond (see Figure 1.5).



(a)



(b)

Figure 1.5: Dimers of C-H...S hydrogen bonded formamides; (a) is adopted when N-H is not involved in a hydrogen bond and is described by $R_2^2(6)$ graph set, and (b) is adopted when the N-H is involved in a N-H...S hydrogen bond. The ring connecting the hydrogen bonded dimers is described by $R_4^2(10)$.

1.3.3.4 Halogen-H bonding and other related Halogen generated weak intermolecular interactions

Just like all electronegative atoms, the capability of halogens as hydrogen bond acceptors has in recent years attracted considerable attention. As ligands in coordination compounds and as halide ions, halogen atoms have been shown to be very good hydrogen bond acceptors [Aullón *et. al.*, 1998]. In organic compounds they have been described as weak hydrogen bond acceptors [Dunitz and Taylor, 1997]. Halogen substituted arylformamides and arylthioamides have also been

investigated in this context. Some applications of this important hydrogen bond were outlined by Brammer *et. al.* [2001] and their use in fields such as materials chemistry, biological and organometallic chemistry mentioned. Its influence in crystal engineering is of particular interest in this study. In previous studies molecular synthons formed by the halogen bonds were looked at with a view of manipulating structures in order to come up with new designs of the so-called “supramolecular assemblies or synthons” [Desiraju and Sharma, 1996].

The presence of halogens in organic compounds leads to a variety of intermolecular interactions; X...X, X...O, X...S, X...H, C-X... π (X = F, Cl, Br or I) etc. Whenever these interactions occur in the packing of molecules in crystals they are always considered to be just as important as hydrogen bonds. It is the X...X halogen bond that is mentioned a lot and has received quite some attention in recent studies. This halogen...halogen intermolecular interaction has a specific geometry. Two hypotheses have been put forward to account for it [observations were on the crystal structure of molecular chlorine Cl₂(s)] which can also accounts for the short X...X contacts in the crystal structures of other halogenated molecules [Bosch and Barnes, 2002; Price *et al.*, 1994; Murray *et al.*, 1994; Ramasubbu *et al.*, 1986].

One explanation [Bosch and Barnes, 2002] put forward is the existence of specific attractive forces, which result in short contacts in certain directions (responsible for short 4 Å axes). Another name for such

interaction is “donor-acceptor interaction” with one of the atoms acting as a donor and the other as an acceptor (or electrophile and nucleophile) in a weak form of covalent bonding⁷. Studies show that the majority of examples of X...X interactions that fall under this hypothesis are interactions between molecules that are related by a crystallographic center of symmetry.

The other explanation [Price et al., 1994; Murray et al., 1994; Ramasubbu et al., 1986] is based on the atomic charge density surrounding the halogen atoms. According to this explanation, the atomic charge density has a non-spherical shape and therefore produces a decreased repulsion and thus closer X...X contacts in certain directions. The reduced repulsion and an increase in the intermolecular attraction are not equivalent and influence the shape of the potential energy surface of the halogen (a smaller positive cap and larger negative tail is seen on the halogen atom as depicted in Figure 1.6a). These polarized nonspherical atomic moieties result in close packing of adjacent halogen atoms.

⁷ Covalent bond = A bond between closed shell species sharing electrons. In this instance, a single covalent bond is being referred to where the bond energies are relatively close.

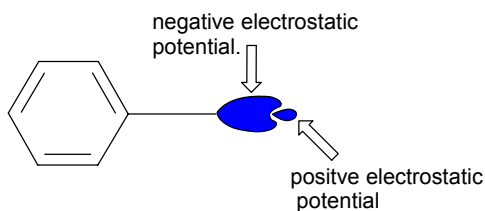


Figure 1.6a: A simplified representation of the electrostatic potential on a halo-benzene with negative and positive electrostatic potential indicated by arrows. The blue shaded part represents a halogen atom.

Other definitions [Desiraju and Parthasarathy, 1989; Pedireddi et al., 1994, Sakurai et al. 1963; Leser et al., 1978] have referred to the two hypotheses as **Type I** (same as the first hypothesis above) and **Type II** (same as the alternative hypothesis above). In these terms if we denote the larger of the two C-X...X angles as θ_1 and the smaller as θ_2 , then Type I interactions have $\theta_1 \approx \theta_2 \approx 180^\circ$ and Type II have $\theta_1 \approx 180^\circ$ and $\theta_2 \approx 90^\circ$ (see Figure 1.6b). Linear C-X...X-C systems with $\theta_1 \approx \theta_2 \approx 180^\circ$ are seldom observed. Intermolecular X...X distances in crystals are typically around 3.60 Å, slightly more than twice the van der Waals radius of 1.75 Å for Cl but normally range between 3.5 to as much as 3.8 Å. Most studies indicate that there are no orientations in which both angles are small as such geometries are unlikely to be sterically accessible. The two types of X...X interactions can also be referred to as close-packing (type 1) and L-type (type 2) [Saha et. al., 2006 and references therein]. A third type known as V-type is not common amongst the compounds discussed in this thesis.

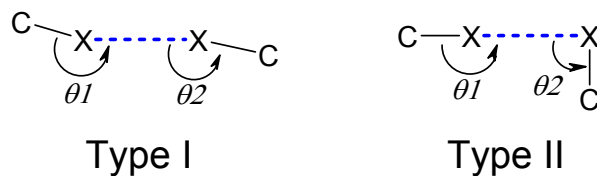


Figure 1.6b: An illustration of the two types of Cl...Cl interactions. For type I, $\theta_1 \approx \theta_2 \sim 180^\circ$ and for type II, $\theta_1 \approx 180$ and $\theta_2 \approx 90^\circ$

For fluorinated benzenes it has been shown that the formation of C-H...F and C-F... π interactions rather than F...F is favoured [Prasanna and Guru Row, 2000]. Oshrit *et. al.* [1997] and Lieberman *et. al.* [2000] showed the importance of the simultaneous occurrence of halogen-halogen and halogen-hydrogen interactions in crystal engineering. Lieberman and co-workers also showed that change in crystal density was reflected the change of molecular packing due to at least in part, the change in geometry of Br...Br and Br...H interactions. Another type of halogen bonds is discussed by Ouvrard *et. al.* [2003]. They look at the halogen bond geometry in about 141 structures between halogens and atoms such as oxygen, nitrogen, selenium, sulphur and phosphorus as Lewis bases while Kubicki [2004] looked at phase transitions of molecules that had Br...N and Br...Br interactions. These studies covered in one way or another all the other halogen bonds other than X...X.

1.3.3.5 C-H... π and π ... π interactions

The study of C-H... π and π ... π interactions has included investigations into molecular conformations, determining intermolecular interactions, π ... π stacked building blocks or supramolecular assembly for crystal engineering [Desiraju and Steiner, 1999; Amabilino and Stoddart, 1994 and references therein]. This attraction between C-H bonds and π systems first became evident in thermochemical observations and was later confirmed by IR and NMR spectroscopic and finally crystallographic studies [Nishio, 2004]. In most studies of this type of hydrogen bonds including theoretical calculations [Aoyama et al., 1979; Takagi et al., 1997; Sakaki et al., 1993; Jorgensen and Severence, 1990] it has been suggested that the interaction between CH bonds and π systems was 'attractive' - electrostatics plays a very small role and the stabilization is mainly a result of dispersion forces. In the case of π ... π hydrogen bonds, the interactions are not due to an attractive electrostatic force between two π systems but occur when the attractive interactions between π -electrons and the σ -framework outweigh unfavorable contributions such as π -electron repulsion [Hunter and Sanders, 1990].

The relevance of these intermolecular interactions is seen in many biological and chemical systems. They are known to control such diverse phenomena as the vertical base-base interactions which stabilize the double helical structure of DNA, the intercalation of drugs into DNA, the packing of aromatic molecules in crystals, the tertiary structures of

proteins, the conformational preferences and binding properties of polyaromatic macrocycles, complexation in many host-guest systems and porphyrin aggregations [Hunter and Sanders, 1990].

Figure 1.7 below shows the basic representations of the two interactions. In the face-to-face interaction the planes of the aromatic rings are parallel to each other while in the edge-to-face case the planes are perpendicular to each other. In the face-to-face arrangement there is some repulsion between the aromatic rings and therefore the rings are often slightly displaced relative to each other as indicated by the expression 'parallel-displaced $\pi \dots \pi$ interaction'. In the perpendicular arrangement one or two hydrogen atoms in one of the aromatic rings interact with the other ring resulting in a T-shaped interaction often referred to as a C-H... π interaction. The angle between the two aromatic rings in these two types of interactions range from 0° in an ideal 'face-to-face interaction' to 90° in an ideal 'edge-to-face interaction'. When the angle falls between 0° and 90° we have what is referred to as 'tilt angle $\pi \dots \pi$ interaction' which rarely occurs.

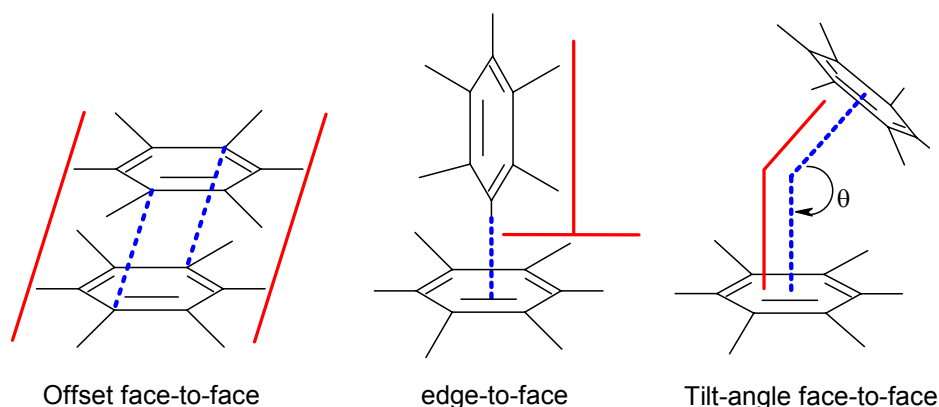


Figure 1.7: Representations of the two types of aromatic interactions with red lines showing the relative orientations of the interacting rings.

Another situation is found for acidic C-H groups (in instances where the C-H bond does not belong to an aromatic system) that can act as weak hydrogen bond donors. These sometimes interact with weaker (than O, N, Cl, Br) hydrogen bond acceptors such as π -bonded functional groups for instance $C\equiv C$, $C=C$, aryl rings, heteroarenes etc. These interactions also result in C-H... π interactions. In arylformamides and acetanilides such C-H... π interactions are formed preferentially between a hydrogen atom donated by the carbonyl carbon, or the hydrogen attached to the nitrogen atom, or one from a substituent on the aryl ring (for example a methyl group). Sometimes the weak donor involves heteroatoms as in X-H... π (X = N, O etc.) or C-X... π (X = halogen). A few of such examples are discussed later in this thesis.

The strength and directionality of these intermolecular interactions depends on a number of factors. It is found that the stronger the proton donating ability of the C-H bond, the stronger the stabilizing effect. As a consequence a *sp*-hybridized CH group will have a stronger interaction than an *sp*³-hybridized CH group. The C-H...acceptor distance also increases in the same order. The acceptor strength is influenced by the electron density of the π -donor and toluene is therefore a more effective C-H acceptor than benzene [Nishio, 2004]. With respect to the directionality of C-H... π interactions it is found that the more linear and shorter they are the stronger they are. The directionality also depends on the strength of the proton donor (*sp*-CH > *sp*³-CH; CHX₃ > CH₃X where X = any electron withdrawing group). The contribution of these individual interactions may be energetically small but collectively they add up to a significant component of the total stabilization energy of a crystal.

1.3.4 *N*-H...O=C hydrogen bonding motifs in aryl amides

A number of surveys based on data from the Cambridge Structural Database (CSD) have been carried out regarding the N-H...O hydrogen bond in amides [Taylor and Kennard, 1983; Taylor *et. al.*, 1983 and 1984; Leiserowitz and Tuval, 1978; Venkataramanan *et. al.*, 2004]. Presented here is a summary of the work reported by Taylor and co-workers [Taylor *et. al.*, 1983 and 1984] in which they examined the distributions of: (a) the hydrogen bond distances H...O and N...O; (b) the hydrogen bond angle

<N-H...O; (c) the donor bond length N-H, and (d) the acceptor bond length C=O. This method will later also be applied to the formamides presented in this thesis.

Previous investigations of secondary amides (of which our arylformamides are part of) have shown that the N-H...O=C system prefers three basic hydrogen bonding motifs [Haisa *et. al.*, 1980; Leiserowitz and Tuval, 1978]. These motifs are classified by the type of hydrogen-bonded chains whose component molecules are related in one of three ways: a 2_1 -screw axis, a glide plane or a unit cell translation. This is shown schematically in Figure 1.8. Geometries of N-H...O=C hydrogen bonds in the different motifs are normally fairly similar and the angular geometry of the motifs depends upon the tilt of the molecule relative to the glide plane or 2_1 -axis. This is significantly influenced by the electronic and steric effects of the R groups attached to the amide bond. As indicated in Figure 1.8, category⁸ 1, which includes (a), (b) and (c) have a C=O...N angle that varies from 130 – 155° for (a) and (b) and 155 – 180° for (c). Category 2 which refers to (d) in Figure 1.8 has molecules that are related by unit cell translation. In this category the N-H...O=C system tends to be collinear as well. Motifs (a) and (b) exemplify the two different patterns which category 1 compounds can adapt. This pattern type is largely dependent on the sizes of the R groups. When the R groups are large in volume then motif (a) is adopted (the R groups are further apart because

⁸ Category = our classification of the N-H...O hydrogen bonding patterns. Motifs (a), (b) and (c) belongs to category I while (d) belongs to category II.

N-aryl -formamides and -thioamides

of steric strain). When the R groups are not so large then they can easily fall on the same side of the hydrogen bonded chain since there is very little steric strain and adopt motif (b) (the positions of the R groups in the second motif induces steric and electronic effects which in turn affects the C=O...N angle).

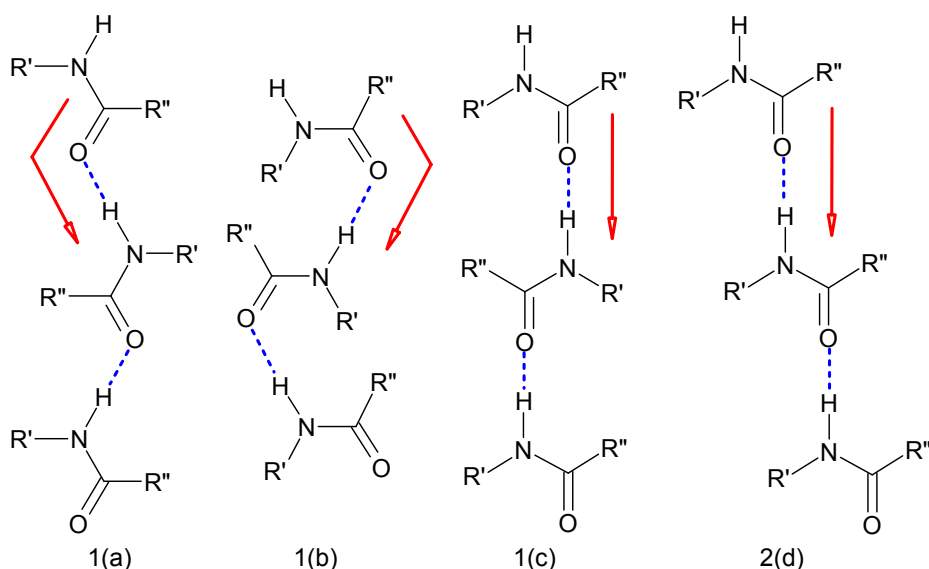


Figure 1.8: The three general motifs that are noticed in secondary and primary amides: glide plane (1(a), 1(b)), 2₁ axis (1(c)) and translation (2(d)). The arrows indicate the extent of linearity in the different motifs. Hydrogen bonds are shown in blue dashed lines and R' and R'' = alkyl or aryl.

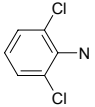
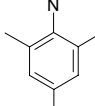
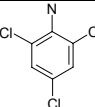
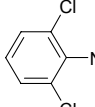
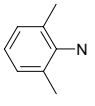
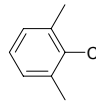
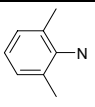
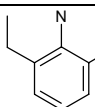
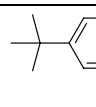
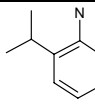
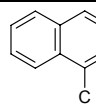
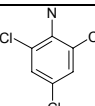
N-arylformamides, *N*-arylthioamides and acetanilides with bulky R groups all fall under the above presented motifs. Geometries of their N-H...O=C bonds vary depending on the absence or presence of substituents and also the position of these substituents on the aryl ring as

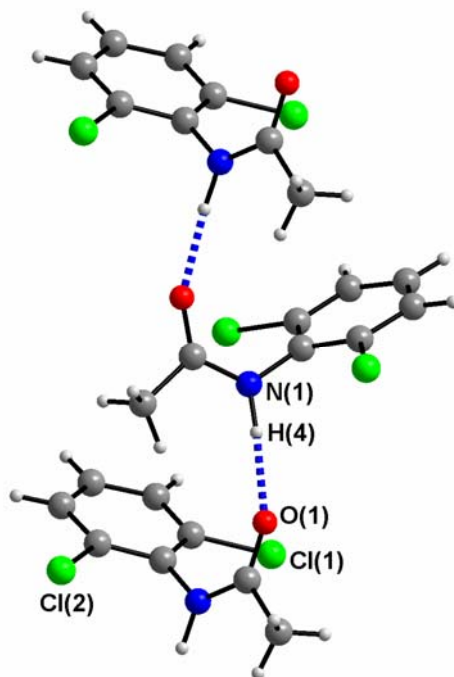
will be seen in later chapters. Alkyl formamides and acetanilides with single substituents adopt other motifs (Categories 3 and 4 in this thesis, discussed in later chapters). Tables 1.2 a - c give a summary of structures extracted from the CSD with substituents in the 2 and 6 and in the 2, 4 and 6 positions on the ring that are closely related to the structures discussed in this thesis. Each table gives a set of structures that adopt a similar motif. All the motifs fall under the ones discussed in Figure 1.8. Examples of the structures from the CSD of each motif are discussed below each of the tables. The tables show the influence of the nature of the two R groups on the C=O...N and the N-H...O angles.

There seems to be a small difference in the size of the C=O...N angle when the sizes of R' and R'' are changed slightly as in *N*-(2,6-dichloro phenyl)formamide down to *N*-(2,6-dichlorophenyl)neopentylamide in Table 1.2a. 2,6-dichloroacetanilide exemplifies compounds that adopt motif (b). It has Cl atoms as substituents in the 2 and 6 positions of the aryl ring and H atom as R''. There is very little steric interference between the two R groups and this results in a "V" shaped pattern when viewed down the axis of the hydrogen bonding chain (see Figure 1.9b).

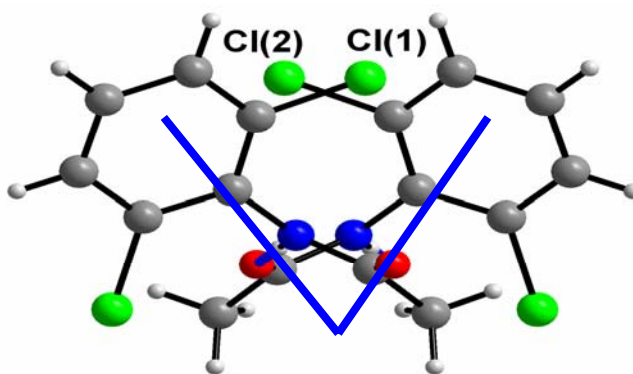
N-aryl -formamides and -thioamides

Table 1.2a: R groups and the C=O...N angles of structures from literature: motifs (a) and (b).

Name & ref code	Reference	R'	R''	Angle (°) C=O...N	Angle (°) N-H...O
N-(2,6-dichlorophenyl)formamide QIKNUT	Godwa et al., 2000		H	145	172
2,4,6-trimethylacetanilide UGUJIP	Upadhaya et al., 2002		CH ₃	153	162
2,4,6-trichloroacetanilide FUWPIW	Nyburg et al., 1987		CH ₃	153	159
N-(2,6-dichlorophenyl)isobutyramide QIKPEF	Godwa et al., 2000		CH(CH ₃) ₂	156	176
Trans-2,2',6,6'-tetramethylbenzanilide 2 mols. in Ass. Unt. YEGKAW	Azumaya et al., 1994			141 125	175 157
N-(2,6-dichlorophenyl)neopentylamide. 2 mols. in Ass. Unt. QIKPIJ	Godwa et al., 2000		C(CH ₃) ₃	147 151	159 171
N-2,6-diethylphenyl 4-t-butylbenzamide 3 mols. in Ass. Unt. ACAKUK	Adams et al., 2001			155 161 164	151 149 150
N-(2,6-Di-isopropylphenyl)anthracene-9-carboxamide 3 mols. in Ass. Unt. CABGES	Adams et al., 2001			134 152 151	170 170 151
N-(2,4,6-trichlorophenyl)-2,2,2-trichloroacetamide 2 mols. in ass. unit OBIBIK	Godwa et al. 2000		C-Cl ₃	151 141	159 133



(a)



(b)

Figure 1.9: (a) Hydrogen bonding pattern of 2,6-dichloroacetanilide [Nagarajan et. al., 1986]. R' = H and R'' = dichlorosubstituted aryl ring. Because the sizes of the two are immensely different the two R groups can favourably interact. (b) view down the *c* crystallographic axis showing

the alignment of the two R groups along the same sides of the N-H...O hydrogen bonded chains resulting in a “V” formation.

The introduction of larger R' and R'' groups as in *trans*-2,2',6,6'-tetramethylbenzalinide, *N*-(2,6-dichlorophenyl)neopentylamide, *N*-(2,6-diisopropylphenyl)anthracene-9-carboxamide and *N*-(2,6-diethylphenyl)-4-tertbutylbenzamide results in a variation of sizes of the C=O...N angle which range between 125 and 164°. All these compounds with larger R' and R'' groups have more than one molecule in the asymmetric unit and prefer motif (a) (see Figure 1.10). The R groups are slightly shifted away from each other and the “V” formation of the R groups when viewed down the hydrogen bonding chain is no longer seen.

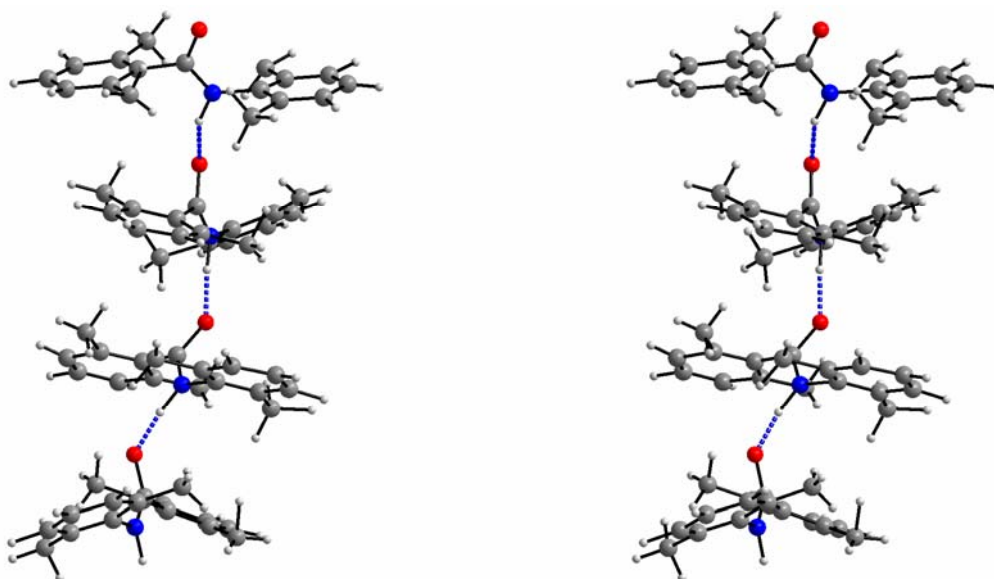
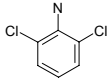
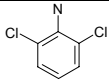
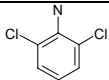
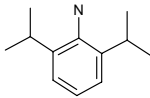
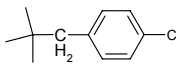


Figure 1.10: Stereo view of *trans*-2,2',6,6'-tetramethylbenzalinide showing N-H...O hydrogen bonded chains. There is little alignment of the two R groups along hydrogen bond chain.

N-aryl -formamides and -thioamides

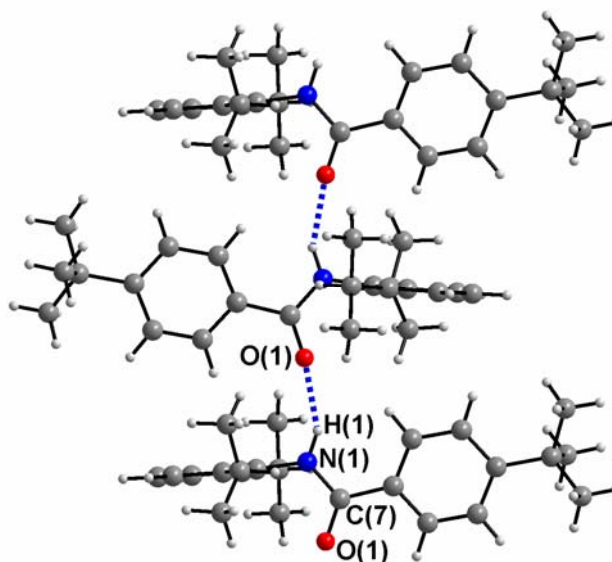
Table 1.2b: R groups and the C=O...N angles of structures from literature: motifs (c).

Name & ref code	Reference	R'	R''	Angle (°) C=O...N	Angle (°) N-H...O
2-Vinyl-N-(2,6-dimethylphenyl)benzamide JAWBIT	Vicente et. al., 2003			164	172
N-(2,6-Dichlorophenyl)-2,2,2-trichloroacetamide POBDEP	Groke et. al., 1994		C-Cl ₃	164	156
N-(2,6-Dichlorophenyl)-2,2,2-trichloroacetamide POBDEP01	Groke et. al., 1994		C-Cl ₃	164	155
N-(2,6-Dichlorophenyl)-2,2,2-trichloroacetamide POBDEP02	Groke et. al., 1994		C-Cl ₃	163	155
N-(2,6-Di-isopropylphenyl)p-t-butylbenzamide TODLIH	Adams et. al., 1996			163	150

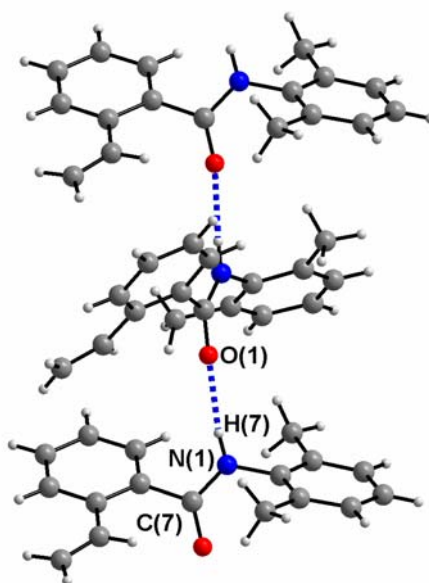
Compounds whose structures belong to motif (c) tend to have a co-linearity along C=O...N-H (see Table 1.2b). The C=O...N angle is more linear than the N-H...O angle and tends towards 180°. This class of compounds is best exemplified by 2-vinyl-N-(2,6-dimethylphenyl)benzamide and N-(2,6-diisopropylphenyl)p-tertbutylbenzamide (see Figure 1.11). The molecules along the hydrogen bonded chains are however related by 2₁-screw axes. The two R groups in

N-aryl -formamides and -thioamides

all except for *N*-(2,6-diisopropylphenyl)*p*-*t*-butylbenzamide form a narrower, compared to that in motif (b), “V” shape along the axis of the N-H...O hydrogen bond.



(a)

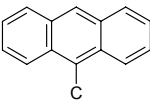


(b)

Figure 1.11: (a) N-H...O hydrogen bonded chains in *N*-(2,6-Diisopropylphenyl) *p*-*t*-butylbenzamide and (b) N-H...O hydrogen bonded chains in 2-Vinyl-*N*-(2,6-dimethylphenyl)benzamide.

N-aryl -formamides and -thioamides

Table 1.2c: R groups and the C=O...N angles of structures from literature: motifs (d).

REF Code	Reference	R'	R''	Angle (°) C=O...N	Angle (°) N-H...O
N-(2,6-Dimethylphenyl)anthracene-9-carboxamide CABGUI	Adams et. al., 2001			160	150
2,6-Dichloroacetanilide FEFSAK01	Nagarajan et. al., 1986		CH ₃	167	170
N-(2,4,6-Tri chlorophenyl)-2-chloroacetamide OBIBAC	Godwa et. al., 2000		CH ₂ Cl	160 162	165 163
N-(2,4,6-Tri chlorophenyl)-2,2-dichloroacetamide OBIBEG	Godwa et. al., 2000		CHCl ₂	157	156
N-(2,6-Dichlorophenyl)propionamide QIKPAB	Godwa et. al., 2000		CH ₂ CH ₃	164	169
N-Acetyl-4-bromo-2,6-dichloroaniline SEDFIQ	Ferguson et. al., 1998		CH ₃	163	159
N-Formyl-4-bromo-2,6-difluoroaniline SEDGAJ	Ferguson et. al., 1998		H	156	154

Structures from this motif have the C=O...N and the N-H...O angles fairly similar and generally more linear than the previous three motifs. The molecules along the N-H...O hydrogen bonded chains are all related by unit cell translation along an approximately 4 Å short axis. It can be seen that there is co-linearity along the N-H...O=C hydrogen bond with the

N-aryl -formamides and -thioamides

aryl rings parallel to each other along the short axis of the unit cell. The hydrogen bonded chains are shown in Figure 1.12 below.

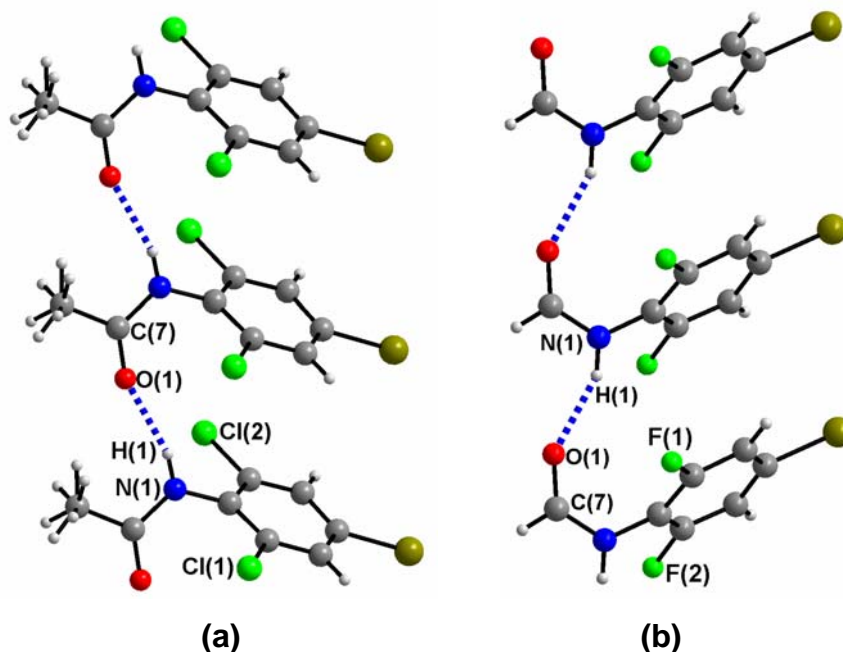
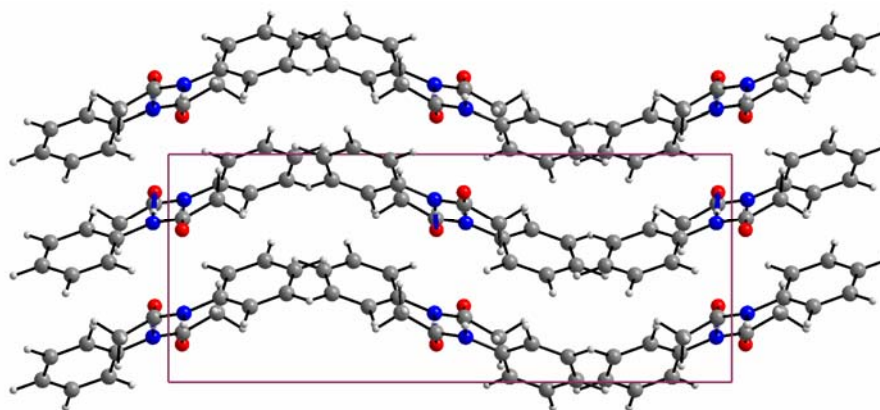


Figure 1.12: N-H...O hydrogen bonded chains of (a) N-Acetyl-4-bromo-2,6-dichloroaniline and (b) N-Formyl-4-bromo-2,6-difluoroaniline. This molecular stacking is observed in all the compounds that adopt motif (d).

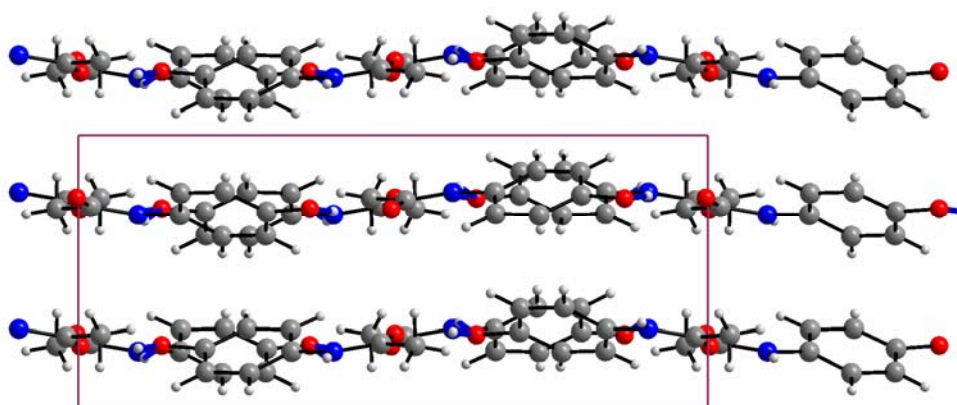
Motifs (a) – (d) are generally adopted by aryl amides that have substituents on the 2 and 6 positions of the R' group. A totally different motif is adopted when only one or none of the above positions is occupied. Examples of this kind of compound include *p*-chlorophenylformamide, acetanilide [Wasserman et. al., 1985; Johnson et. al., 1995], *p*-bromoacetanilide [Andreeti et. al., 1968], *p*-hydroxyacetanilide [Boldyreva et. al., 2000], *p*-acetotoluidine [Maeda et. al., 1976] etc. The amide moieties of these compounds are almost coplanar with their aryl rings. The molecules along a N-H...O hydrogen bonded chains are however still

N-aryl -formamides and -thioamides

related by either 2_1 -screw axis or a glide plane (same as in motifs (a) – (c) above). The arrangements shown in Figures 1.13 (a) and (b) are for acetanilide and *p*-hydroxyphenylformamide.



(a)



(b)

Figure 1.13: Sheets of hydrogen bonded chains in acetanilide (ACANIL) and *P*-hydroxyphenylformamide (HXACAN). The layered sheets can either be corrugated sheet type [as in (a)] or planar like in (b).

1.3.5 Use of graph-set notation and packing patterns to characterize hydrogen-bonding networks

It is important to have a general way of describing hydrogen-bonded networks. Graph sets have been commonly used for this purpose and they define in a simple way morphologies of hydrogen-bonded arrays. The 'graph set theory' was first suggested by Kuleshova and Zorkii [1980] and was then developed and used on organic crystal structures by Etter [Etter, 1990 and references therein], Bernstein and co-workers [Bernstein *et. al.*, 1995] and Grell and co-workers *et. al.* [Grell *et. al.*, 1999 and 2000] to account for schemes of hydrogen bonds.

The first step to the assignment of graph sets is to establish the number of different types of hydrogen bonds in a structure. The types of hydrogen bonds are defined by the nature of the donors and acceptors in the hydrogen bond. The motif, the set of molecules that are hydrogen bonded to one another by repetition of just one type of hydrogen bonds, is then established and is characterized by one of the four designators that indicate whether it is infinite or finite, cyclic or not. The designators for hydrogen bonded molecules are in the case of intermolecular interactions **C** (chain), **R** (ring) and **D** (dimer or other finite set) and in the case of intramolecular hydrogen bonds the designator **S**. The number of donors (**d**) and acceptors (**a**) used in each motif are assigned as subscripts and superscripts, respectively. The size or degree of the motif (corresponding to the number of atoms in the repeat unit) is indicated in parentheses (see

N-aryl -formamides and -thioamides

Figure 1.14). A general descriptor for a hydrogen bond pattern is given as $G_d^a(R)$ where G describes the type of hydrogen bond formed (**C**, **R**, **D** or **S**), a and d , number of acceptors and donors respectively and R in parentheses the size or the number of atoms in the repeat unit of the chain, ring or dimer [Etter, 1990].

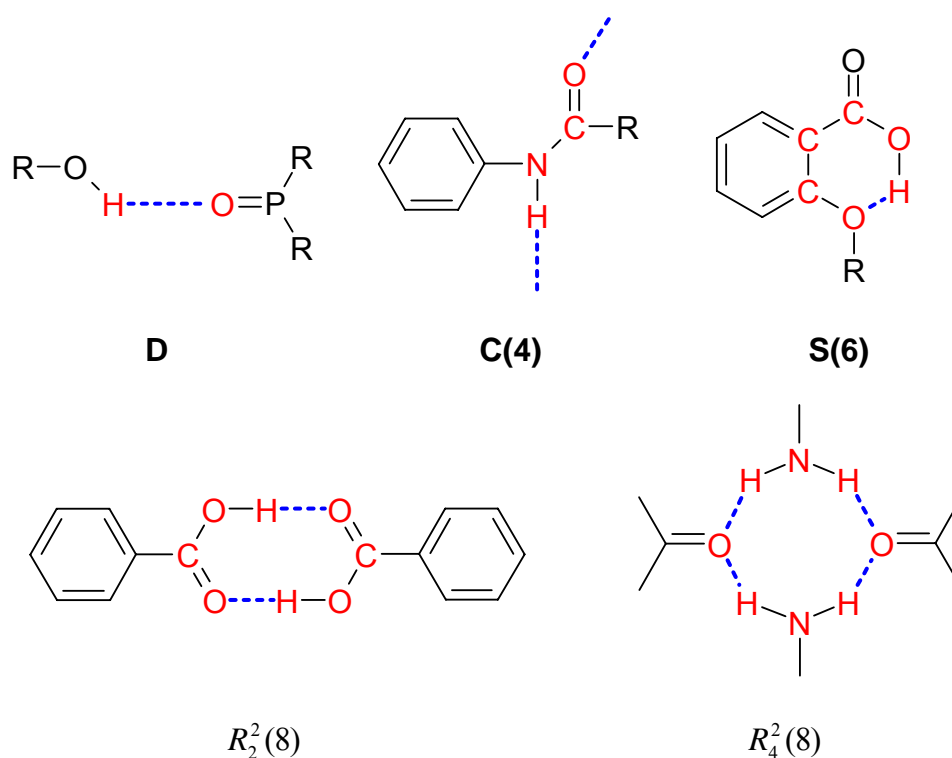


Figure 1.14: Examples of graph-set assignments for common hydrogen-bond motifs. Hydrogen bonds are shown in blue dashed lines [Etter, 1990].

One important aspect of this methodology involves differentiating between arrangements containing only one motif, and networks which contains several motifs. The first list of component patterns are referred to as 1st level graph sets (Figure 1.14). Networks are composed of more than one simple motif and can be described by 2nd level graph set and so on.

N-aryl -formamides and -thioamides

Unitary and secondary graph sets are normally denoted as N_1 and N_2 respectively. A good example is found in aryl amides that are similar to the aryl -formamides and -thioamides studied in this work. These can either form a cyclic dimer (*cis* amide) or a chain (*trans* amide) or can combine to form a network of both motifs. In cases where the two patterns co-exist, a new secondary level pattern is often generated (see Figure 1.15). By assigning the graph-sets to a series of crystal structures that contain one type of functional group, preferred patterns of hydrogen bonding may be identified.

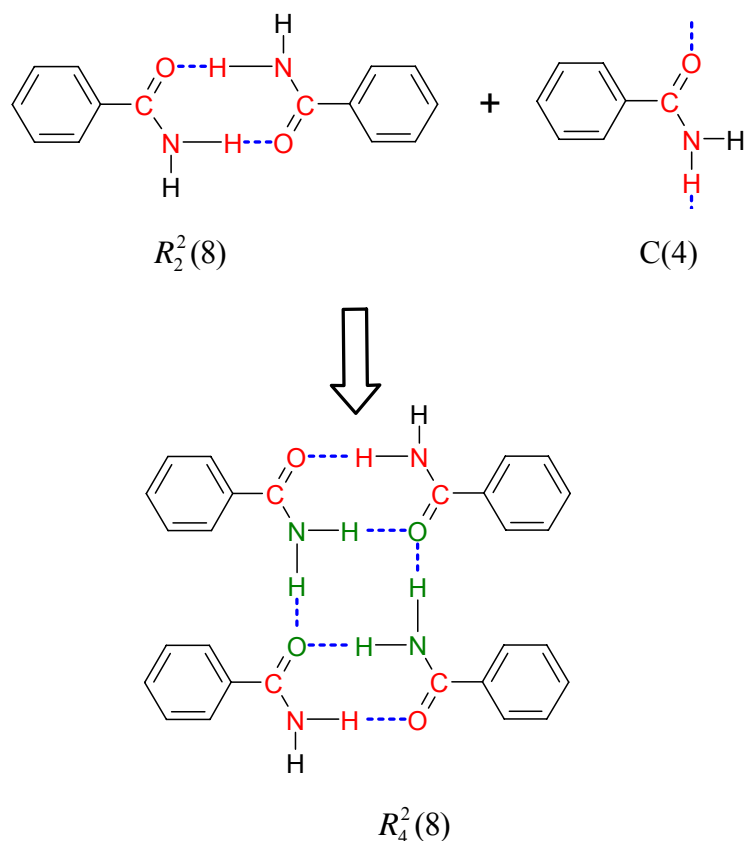


Figure 1.15: A secondary level graph-set assignment $R_4^2(8)$ resulting from the combination of two co-existing primary graph sets $R_2^2(8)$ rings and $C(4)$ chains.

1.3.6 *Isomorphism*

Isomorphism refers to the similarity of the spatial arrangement of the molecules of different compounds in their crystals [Fábián and Kálmán, 1999]. This phenomenon has been studied in some detail and the increased interest in the topic has helped in the understanding of significance of intermolecular interactions in crystals. Some early work in the field was carried out by Fábián et. al. [1993] on the similarities among related steroids.

It has been observed that solid-state structures of organic compounds can tolerate small changes in their molecular building blocks without visible effect on the original packing pattern. Possible changes include single atomic replacements and alterations in substituents (e.g. replacing a hydrogen atom with a methyl group). The most cooperative substituents according to the literature are halogen atoms. The similarity in van der Waals radii of groups of atoms or atoms (e.g. a methyl group and a chlorine atom) can lead to isomorphism. Besides the sizes of substituents, sizes of molecules can also lead to isomorphism. Large molecules often create voids large enough that atoms or groups of atoms that differ greatly in size (e.g. S and O atoms or methyl and ethyl groups) can replace each other without affecting the overall crystal structures of these compounds.

A number of methods have been used to determine the limits of Isomorphism. The degree of similarity between crystals cannot be based on packing patterns alone. Two compounds, whose molecules are similar may pack in similar ways but may not be isomorphous. The similarity in packing may be due to a similarity in space groups but their unit cell parameters and therefore their volume may be different. It has therefore been suggested that numerical descriptors be used to quantify the degree of similarity in organic crystals [Kálmán *et. al.* 1993].

Fábián *et al.* [1999] introduced new numerical descriptors based on the similarity of unit cells in the crystals. This unit-cell similarity index is given the symbol, Π . This measures the extent of similarity between the two unit cells in question. The comparison is based on the cell parameters, a , b , and c of both structures. One expression to describe the similarity of structures can therefore be given by:

$$\Pi = [(a + b + c)/(a' + b' + c')] - 1 \approx 0 \quad (i)$$

where a , b , c and a' , b' , c' are the orthogonalized unit cell parameters with the cell dimensions appropriately chosen such that $a + b + c$ is greater than $a' + b' + c'$. For this method the same orthogonalization scheme has to be employed for comparing corresponding unit cells.

A different and more useful descriptor (proposed by Rutherford [1997]) uses volume to measure the similarity in structures and works well

for all crystal systems. The symbol given to this descriptor is ϵ and it is termed '*mean elongation*'. The definition of ϵ is given by,

$$\epsilon = (V'/V)^{1/3} - 1 \approx 0 \quad (\text{ii})$$

where V and V' are the respective unit cell volumes and $V' > V$. This method has an advantage over Π in that one can avoid the use of orthogonalized unit cell parameters.

Another way of establishing Isomorphism is the comparison of the position of molecules in the unit cell [Kálmán *et. al.* 1993]. It is assumed that common atoms of the two structures in question have approximately the same coordinates. In this case the Isomorphism index is given by:

$$I_i(n) = \left[1 - \left(\sum \Delta R_i^2 / n \right)^{1/2} \right] \times 100\% \quad (\text{iii})$$

where ΔR_i values refers to the differences between the orthogonalized [Dunitz, 1979] coordinates [Fábián *et. al.* 1993] of n identical heavy atoms in related structures. Care has to be taken, that related structures have the same choice of asymmetric unit and origin. This method is quite similar to *root mean square deviation*, RMSD [Maierov and Crippen., 1994], a widely approved method for the analysis of protein structures.

Dzuibek and Katruziak [2004] have applied a graphical method and compared short intermolecular or interionic contacts for the analysis of isostructures and polymorphs. This was done by calculating the shortest

contacts of all atoms in both structures and then comparing them in a scatter plot or distance-distance plot. The plot has a diagonal line, which allows for measurements of direct differences between the distances. Each point in the plot is related to a pair of specific contacts. This is also similar to the use of computer programs such as NIPMAT which utilizes intermolecular contacts of the compounds in question through the creation of matrix diagrams [Rowland, 1995]. Other methods used bar graphs to compare the shortest intermolecular contacts of atoms or ions at different thermodynamic conditions [Boldyreva *et. al.*, 1997].

1.3.7 Cocrystallization

Cocrystallization continues to gain significance for its application to the design of new supramolecular structures with desired functional properties [Trask *et. al.*, 2004]. This has been an effective method, notably in the field of pharmaceuticals, to alter physical properties like solubility (or bioavailability), stability and melting point of the compounds [Remenar *et. al.*, 2003; Walsh *et. al.*, 2003, Oswald *et. al.*, 2002]; in materials with optoelectronic properties, to alter their conductivity, charge transfer and magnetism; in nonporous materials [Tan *et. al.*, 2006 and references therein] and also in the production of dyes and pigments.

The definition of a cocrystal is still in dispute at the moment [Desiraju, 2003; Dunitz, 2004; Aaker and Salmon, 2005]. In this work a cocrystal is defined as a structurally homogeneous crystalline material that

contains two or more neutral building blocks that are present in definite stoichiometric amounts [Aakeröy and Salmon, 2005]. Examples are cocrystals composed of two molecules of *cis*-Itraconazole⁹ and one molecule of a 1,4-dicarboxylic acid [Aoyama et al., 1997] to form a hydrogen bonded trimer, heteroatomic carboxylic acid and carboxylic acid to form hydrogen bonded dimers [Sarma and Desiraju, 1985] and pyridine and bis(hydroxymethyl)biphenyl to form hydrogen bonded trimers [Nassimbeni et al., 2004]. There are many reports on the synthesis of new materials using cocrystallization methods and in particular taking advantage of the hydrogen bonds in the starting materials to derive specific motifs and architectures [Aakeröy et al., 2005 and 2006]. Perhaps the most difficult task in cocrystallization is to control and reproduce the composition and polymorphism of the drugs or compounds in question.

A number of methods have been used for achieving mixed crystals or cocrystals most of which have been illustrated in publications. One of the methods that has become so effective in recent times has been solvent-drop grinding [Trask et al., 2004]. This technique involves grinding material for a given period of time under addition of organic solvents in a quantity just sufficient to moisten the crystalline powder. The grinding, which is done to reduce the particle size, may be carried out manually with a mortar and pestle or mechanically in a mill. In certain cases the

⁹ Itraconazole is an extremely water-insoluble antifungal drug, which is marketed, in the amorphous form to achieve the required bioavailability. Co-administration of this drug with acidic beverages is required to achieve maximum absorption.

energetic input in grinding is known to induce a variety of solid-state transformations. Examples are conversions from crystalline to amorphous [Crowley and Zografi, 2002], from amorphous to crystalline materials [Caira *et. al.*, 2003] as well as from one polymorph to another [Trask *et. al.*, 2004 and references therein].

Another method, which is more conventional, involves the dissolution of the material in large amounts of solvent and allowing for slow evaporation of the solvent. The solvent in use for this method should be one in which both materials that are being cocrystallized have the same solubility. Grinding of the samples may still be required in certain cases. Alternatively the solution can also be concentrated and then cooled down to allow the slow formation of crystals. Other crystallization methods include sublimation and crystallization from the melt.

A number of factors have an influence on the cocrystallization of compounds. One of the most important is intermolecular interactions in the solid state in general. It may also be possible to generate a solid solution by choosing atoms or groups of atoms that can easily be interchanged without significantly affecting the major interactions in the crystals. One such example is chloro-methyl interchange.

1.3.7.1 *Hydrogen bonding directed cocrystallization*

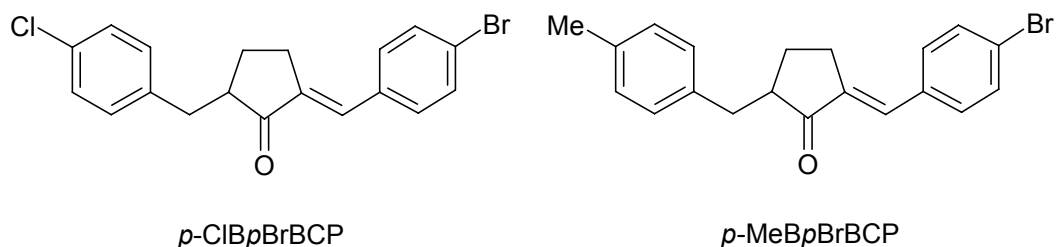
It has been shown before that hydrogen bonding in organic compounds can be used to influence the aggregation of different molecules in crystals, sometimes with predictable connectivity patterns [Etter, 1985; Etter *et. al.*, 1986; Panunto *et. al.*, 1987; Etter and Panunto, 1988; Etter and Baures, 1988]. For example Ducharme and Wuest [1988] demonstrated how dimeric hydrogen bond interactions of pyridones could be used to direct molecules with multiple pyridine sites into predictable aggregate structures. A similar idea could be used to cocrystallize different molecules. In this kind of cocrystallization the primary controlling feature that brings the different molecules together is intermolecular association through the hydrogen bonds. Other good examples have been given under the definition of cocrystals.

1.3.7.2 *Chloro-methyl exchange directed cocrystallization*

One of the strategies that has been useful in crystal engineering is the mutual exchange of groups that have equal or similar volumes. It has been demonstrated that the interchange of chlorine atoms and methyl groups (volumes 19.9 \AA^3 and 23.5 \AA^3 respectively) frequently resulted in isomorphous structures [Kitaigorodski, 1973]. Examples of the interchangeability of chlorine substituents with methyl groups where methyl derivative structures are isomorphous with those of correspondingly substituted chloro compounds have been presented in the

literature [Gnanaguru *et. al.*, 1985; Theocharis *et al.*, 1984; Edwards *et. al.*, 2001; Jones *et. al.*, 1981]. In a recent paper [Streek and Motherwell, 2005] it was found that of 1331 pairs of compounds in the November 2004 release of the CSD differing in the presence of either a methyl or chloro group (in essence a methyl group replacing a chloro group or vice versa) that approximately 25% of the structures were isomorphous. Chloro-methyl exchange as a concept has been used in cocrystallization of molecules with chlorine and methyl substituents since the two can, through positional disorder, occupy the same positions in the cocrystals.

Non-isomorphous molecules can also be used to grow cocrystals. In such systems one component of the cocrystals is forced to adopt a packing arrangement different from that which it adopts in the pure crystal. An example is that of the chlorinated and methylated derivatives of 2-benzyl-5-bromobenzylidene-cyclopentanone [Jones *et. al.*, 1983, Theocharis *et. al.*, 1984]. The two non-isomorphous derivatives presented as *p*-ClBpBrBCP and *p*-MeBpBrBCP are shown in the Scheme below.



Scheme 1.3: The two non-isomorphous derivatives of 2-benzyl-5-bromobenzylidene-cyclopentanone [Jones *et. al.*, 1983, Theocharis *et. al.*, 1984].

1.3.8 Polymorphism and phase transitions

Numerous methods are known for purifying substances from basic and commercial reactions. Of these methods crystallization is often the method of choice and is to a great extent employed in the pharmaceutical industry. One of the major problems that have arisen in the past and even more recently has been the ability of substances to crystallize in two or more forms, a phenomenon known as polymorphism. More specifically, the main problem has been the difficulty of controlling the formation of these new forms (polymorphs). However the accidental or intended discovery of a new polymorph is often regarded as an opportunity to better understand a material. In general a polymorph is a solid crystalline phase of a given compound resulting from the possibility of at least two arrangements of the molecules of that compound in the solid state [McCrone, 1965].

Polymorphism is a term that is used in chemistry or crystallography to refer to the structural diversity of a compound. This diversity may result from the variation of solvent, temperature, pressure, crystallization rate etc. Optimising these factors often is advantageous as novel polymorphs can be grown in a fairly controlled manner. Different terms are used in referring to different types of polymorphs. For example, conformational polymorphs are formed when a molecule can adopt different shapes due to internal degrees of freedom. Concomitant polymorphs are formed when a substance crystallizes with different amounts or types of solvent

molecules [Braga and Grepioni, 2000 and references therein; Bernstein, 2002].

Polymorphs often differ in chemical and physical properties such as solubility, dissolution rate, stability and mechanical properties. This is one of the reasons why there is so much interest in this subject in the pharmaceutical industry; to avoid dosage problems, processing and patent problems etc. Understanding the properties of polymorphs may lead to improving the stability of crystalline products without changing them [Beyer *et. al.* 2001]. Other known industrial processes where polymorphism plays an integral part are in the photographic industry and in the food industry especially in fat-based food products, for instance ice cream, chocolate and margarine.

The investigation of polymorphs requires a combination of structural and thermodynamic studies [Herbstein, 1996]. A good understanding of the two areas can lead to understanding the nature of polymorphism in organic and inorganic materials. Polymorphism in organic and organometallic materials involves the knowledge of a number of their physical and chemical properties. It is known that polymorphs often have different melting and boiling points and crystal densities and therefore thermal investigation methods can be used to study the transition from one polymorph to another. The different forms of a material can exist at a certain temperature range. For example a low-temperature form can only exist at a temperature below that of its transition to the high temperature

form. At the transition point the internal energies for the polymorphs are different. A small amount of energy, usually endothermic, is needed to change from one form to another. The high temperature form on the other hand could transform to the low temperature form as result of certain factors. Some of the factors that can cause this include mechanical shock, scratching or by heating the sample below the transition temperature. During transition from one form to another heat is either absorbed or released.

A number of analytical methods can be used to investigate and analyse polymorphs. Most analytical techniques can very easily be used to detect and characterize the differences and similarities between polymorphs. Because each of these techniques gives different information, it is often a good idea to employ these techniques together in order to meaningfully compare the different polymorphs of a given compound. Ordinarily one would use a technique that can detect the differences in crystal structures, as opposed to molecular structures, for a routine analysis.

These techniques include hot stage microscopy, a technique that involves the use of an optical microscope that is fixed with a polarizer and a hot stage to observe the physical behaviour of a crystalline material. Generally the use of this technique for the study of polymorphism is simply for observing the homogeneity and diversity of crystalline samples.

Variations in certain physical phenomena such as size, shape and colour may indicate the presence of different polymorphs.

Another important technique is differential scanning calorimetry (DSC). This technique is based on temperature differences between a substance and an inert reference material as the two specimens are subjected to identical temperature sources either heated or cooled at a controlled rate. As previously mentioned a change in the physical state of a material is accompanied by absorption or liberation of heat and this causes a detectable difference in temperature between the reference sample and the substance when a phase transition takes place. The main advantages of DSC are the requirement for only small samples (of the order of 10 mg) and that it can provide quantitative data with relative speed and ease.

X-ray crystallography is one of the most unambiguous ways of identifying and characterizing the differences between polymorphs. It can be divided in powder method and single crystal methods. Powder methods have been used for the qualitative identification of individual polymorphic phases or mixtures of phases whereas single crystal methods have been employed for the determination of detailed molecular and crystal structures. Both methods are often used in combination to derive more conclusive results. For example known crystal structure solutions are often used as an aid in *ab initio* calculation of structures from powder data. This has been used to solve larger and previously problematic structures

[Andreev *et. al.*, 1997; Shankland *et. al.*, 1997; David *et. al.*, 1998 and Tremayne *et. al.*, 1997] with subsequent refinement by Rietveld methods [Young, 1993].

1.3.8.1 *Thermodynamics of transformations in molecular structures*

The process by which molecular crystals are formed or grown can be considered to be thermodynamic (e.g. slow evaporation, slow cooling, slow sublimation etc.) or kinetic (e.g. high degree of supersaturation, rapid cooling of solution from melt, rapid evaporation of solvent etc.) [Bernstein, 2002]. The transformation of one polymorph to another can also be thermodynamic or kinetic and often depends on the amount of energy expended in deriving a specific form. However the transformation is classified as one of two types; first order changes and second order changes.

The main difference between the two types is that in the first-order phase transitions energy, volume and crystal structure change discontinuously while in changes of higher order, properties and crystal structure change continuously [Dunitz, 1995]. First order type transformations are normally accompanied by significant changes in the site symmetries of the structural units of the two phases. For systems that fall under this type of transformation there is often a small difference

between ΔH_{transf} and ΔH_{fus} ¹⁰ of the different polymorphs [Bernstein 2002; Kitaigorodski, 1971; Botoshansky *et. al.*, 1998]. The energies are normally endothermic and are accompanied by a change in volume (ΔV), which is positive. In most cases the crystal lattice is normally completely destroyed [Kaftory *et. al.*, 2001; Botoshansky *et. al.*, 1998]. For first order transformations therefore, except for the few single-crystal-to-single-crystal transformations, single crystal X-ray crystallography is not the method of choice for the study of the mechanism of transformation, but rather powder X-ray crystallography would be more informative.

In second-order phase transitions, the transformation from one form to the other is normally continuous and as such the crystal lattice remains intact even though the crystal habit might change. The changes in crystal parameters are easily monitored in this type of mechanism and this can easily be done using either single-crystal X-ray diffraction or powder X-ray diffraction methods.

1.3.9 Evaluation of intermolecular interactions via lattice energy calculations

The conformations and geometries of amide and thioamide molecules are to a considerable part determined by hydrogen bonding (e.g. N-H...O, N-H...S etc.) and other weak intermolecular interactions

¹⁰ ΔH_{transf} and ΔH_{fus} are the energies related with the enthalpy of transformation from one polymorph to another and with the melting of the second polymorph respectively.

(such as Cl...Cl, C-H... π etc.). Apart from the use of X-ray crystallographic data and NMR data advanced theoretical calculations have been used for in-depth analysis of molecular conformations and the nature of hydrogen bonds and other weak intermolecular interactions in organic and organometallic materials. Such analyses have given rise to methodologies that can be used to explore packing modes and intermolecular interactions in the crystals of compounds. This provides a picture of the types of intermolecular interactions present and also an approximate quantitative measure in terms of relative strengths of different interactions involved in holding together the molecules in a crystalline lattice.

A lot of effort has gone into theoretical studies of small (organic and organometallic) and big molecules (proteins) with emphasis on getting a better understanding of crystal structures for crystal engineering. Such efforts have been used successfully to estimate lattice energies of structures of molecular crystals and to predict and estimate the stability of new or probable polymorphs of the crystals [Gavezzotti *et. al.*, 1997; Beyer and Price, 2000; Beyer *et. al.*, 2001]. In these studies the approach involves the summing up of interactions of each atom in a molecule, at a convenient origin, with the atoms of surrounding molecules. Examples of programs that have been used in some of these studies are, *MPA* [Williams, 1996], *ZIP-PROMET* [Gavezzotti, 1991], *DMAREL* [Willock, 1995; Beyer *et. al.*, 2001], *Polymorph predictor* [Verwer and Leusen, 1998] *etc.*

Three blind tests [Lommerse *et. al.*, 2000; Motherwell *et. al.*, 2002; Day *et. al.*, 2005] have shown 3% success in predictions of crystal structures of simple organic molecules using lattice energy minimization techniques. One problem encountered during the first blind test was that for most molecules studied, more energetically feasible crystals were found than experimentally observed polymorphs. One successful study was carried out on paracetamol with the predicted polymorphs matching the experimentally observed polymorphs in the correct stability order [Beyer *et. al.*, 2001 and references therein]. The search for possible crystal structures was done using the systematic search programme MOLPAK [Holden *et. al.*, 1993] with lattice energy minimization calculations carried out using DMAREL [Willock *et. al.*, 1995; Beyer *et. al.*, 2001].

Moisan and Danneberg [2003] here looked at molecular orbital calculations of hydrogen bonding formamide chains, similar to those in proteins, using the DFT method in the Gaussian 98 suite of programs [Frisch *et. al.*, 1998]. In their work they studied the protonation of hydrogen bonding formamide chains that had up to 10 monomeric units and the effect of such protonations on the structures of the chains and the energies of individual hydrogen bonds in the chains.

Gavezzotti and Filippini [1994] in their work looked at the properties of intermolecular X-H...Y (X,Y = N,O) hydrogen bonds using crystal data from the CSD. The study entailed isolating the basic geometric and

energetic features of organic hydrogen bonds by looking at structures in which the donors and acceptors in the hydrogen bonds were N or O. Other works include calculations of packing energies [Gavezzotti, 1990] which addressed the effects of molecular size, shape and stoichiometry of hydrocarbons. Also related to this were the contributions other works of Gavezzotti, [1983, 1985, 1989] which have details and perspective on the methods applied for packing analysis. Others who have contributed ideas and techniques that contributed to the development of methods for calculation of packing energies include Kitaigorodski [1961], Williams and coworkers [see *e.g.* Williams & Houpt, 1986 and references therein; Leiserowitz & Schmidt, 1969; Leiserowitz & Hagler, 1983 and Sarma & Desiraju, 1986].

Despite all the effort that has gone into the above mentioned studies, the success rate of most of the programs used in structure prediction is low. As a consequence it has been suggested that other routine methods be used along with a knowledge of, for example, typical crystal density, crystal packing [Sarma and Desiraju, 2002], graph set analysis [Cross *et. al.*, 2003], evaluation of crystal morphology and mechanical properties [Beyer *et. al.*, 2001] and comparative CSD searches.

As part of a general study of the interactions of arylformamides and arylthioamides we have examined the influence of these interactions on their crystal structures by use of these lattice energy calculations. The

crystal structures of the compounds were studied using the ZipOpec module of the OPIX program suite¹¹ which allowed for calculations of lattice energies. In addition to lattice energies, ZipOpec calculates molecule-molecule interaction energies to identify which molecular arrangements contribute most to the overall lattice stabilization (see the description of OPIX in Chapter 2).

1.3.10 Nuclear Magnetic resonance studies of arylformamides, acetanilides and thioamides

Amides have been extensively studied by NMR. Most of these studies have dealt with rotational isomerization about the C-N bond, chemical shifts, *J* coupling constants and proton exchange and association. These studies have been carried out because of the relevance of amides to polypeptides and proteins. The general consensus is that the conformation of the amide group around the nitrogen atom is planar. This agreement is mainly based on NMR and crystallographic studies even though microwave studies suggest a slightly pyramidal conformation about the nitrogen atom.

It has been well established that the rate of rotation around the N-C(O) bond of formamides and amides is slow on the NMR time scale in solution at room temperature and as consequence *cis* (NH *cis* to CO) and

¹¹ OPIX, A computer program package for the calculation of intermolecular interactions and crystal energies [Gavezzotti, 2003].

trans (NH *trans* to CO) isomers can be observed in ¹H- and ¹³C-NMR spectra [Camilleri *et. al.*, 1988; Sidall *et. al.*, 1988; Quintanilla-Licea *et. al.*, 2002; Brown *et. al.*, 1968]. The barrier of rotation for the approximately planar amide group can be determined by variable temperature NMR spectroscopy and was found to be in the order of 75 – 105 kJ/mol [Kessler, 1970; Neumann, Jr. and Jones, 1968; Gasparro and Kolodny, 1977; Drakenberg and Forsén, 1970; Siddall, *et. al.*, 1970; Oberlander and Tebby, 2000; Bain *et. al.*, 1999; Stewart and Siddall, 1970.].

The hindered rotation has been attributed to a delocalization of electron density as represented by the resonance formulas **I** – **III** (in Scheme 1.4) and recently sparked a debate on the relative importance of **II** and **III**. In the classical resonance model as first proposed by Pauling [1960] the hindered rotation is explained by a partial double bond character of the C-N bond as represented by **II** [Quiñonero *et. al.*, 2001; Lauvergat and Hiberty, 1997; Bennet *et. al.*, 1990; Fogarasi and Szalay, 1997]. Others suggested that **II** is of minor importance compared to the ionic resonance structure **III** and attributed the hindered rotation to the alignment of the lone pair of electrons at N with the electron deficient *p* orbital at C and the preference for sp²-hybridisation at N [Wiberg and Laith, 1987; Wiberg and Breneman, 1992; Wiberg *et al.*, 1992; Wiberg and Rablen, 1995; Bader *et. al.*, 1990].

2 Experimental Methods

In this chapter the methods used to synthesize compounds 1 – 24 and to grow their crystals and also cocrystals of selected compounds are described. Methods of analysis are also described.

2.1 Synthesis of arylformamides (compounds 1 – 14)

Fourteen arylformamides (Table 2.1) were synthesized following a procedure by Ugi *et. al.* [1965]. The commercially available aniline, disubstituted and trisubstituted anilines (from Aldrich and Fluka with purity higher than 95%) were heated in a tenfold excess of formic acid for a period of 15 hrs at 90°. The excess of formic acid was then removed under vacuum to give a brown liquid (for arylformamide) or a white solid (off white and pale purple in the case of 2-methyl-5-chlorophenylformamide and 2,6-diisopropylphenylformamide, respectively) that was treated with dilute hydrochloric acid (0.1 M HCl) and ethyl acetate. The organic layer was separated from the aqueous layer, dried over magnesium sulphate and filtered. For arylformamide the brown liquid was distilled under vacuum to give an off-white solid which then yielded some suitable crystals. For the rest of the formamides crystals were grown directly from the filtrate. The crystals with different morphologies were obtained from different solvents (or mixture of solvents) in good yields. Some of the compounds were obtained as thin needle-shaped crystals while others

***N*-aryl -formamides and -thioamides**

were obtained as block shaped crystals. The solvents used were chloroform, ethyl acetate, acetonitrile, methanol, THF, DMF and DMSO. The purity of compounds was confirmed by NMR spectroscopy using a Bruker Avance 300 (^1H , 300.13 MHz) spectrometer and a Bruker Avance 400 (^1H , 400.12 MHz) spectrometer. Compounds were found to exist in solution [CDCl_3 , C_6D_6 or $(\text{CD}_3)_2\text{SO}$] as a mixture of isomers in a variety of ratios. For the 2,6-disubstitutedformamides (compounds **1a**, **2a**, **3**, **4a**, **5** and **6**), and the phenylformamide (**21**), compounds were found to exist in approximately equal ratios of *cis* and *trans* isomers. In the solid state the *trans* isomer was preferred. For compounds **7** to **14** the population of the *trans* isomer was higher in solution as compared to the *cis* isomer, however the *trans* conformation was preferred in the solid state, with exception of compound **13** which preferred the *cis* isomer.

N-aryl -formamides and -thioamides

Table 2.1: ¹NMR data for arylformamides **1 – 14** and **21** (δ in ppm, ¹H-¹H coupling constants in Hz)

Compound	Solvent	Conformer	Methyl H and Methine H	Ar H	CHO	NH
2,6-DiF (1a)	DMSO (not well resolved)	<i>cis and trans ~ 50%</i>	-	m, 7.66	s, broad, 9.68	12.65 11.89
2,6-DiCl (2a)	DMSO (not well resolved)	<i>cis and trans ~ 50%</i>	-	m, 7.35	d - broad 8.20	10.11
2,6-DiMe (3)	CDCl ₃	<i>trans and cis ~ 50%</i>	2.23 2.17	m, 7.05 m, 7.05	s, 7.15 d, 8.01 <i>J</i> = 11.9	s, 7.05 s, broad 8.29
2-Cl-6-Me (4a)	CDCl ₃	<i>trans and cis ~ 50%</i>	s, 2.36 s, 2.30	m, 7.22 -	s, 7.25 d, 8.21 <i>J</i> = 10.5	s, 8.40 s, 7.22
2,6-DiBr (5)	DMSO	<i>trans and cis ~ 50%</i>	- -	m, 7.27 -	d, 7.81 <i>J</i> = 8.04 d, 8.37 <i>J</i> = 3.24	s, broad 8.45 s, broad 10.10
2,6-Diiso (6)	CDCl ₃	<i>trans and cis ~ 50%</i>	s, 1.20 septet, 3.11 s, 1.23 septet, 3.21	m, 7.21 m, 7.32	d, 8.03 <i>J</i> = 11.93 s, 8.48	s, broad 7.01 s, broad 6.73
Phenyl-formamide (21)	DMSO	<i>trans and cis ~ 50%</i>	- -	m, 7.22 7.02 7.47	d, 8.37 <i>J</i> = 1.13 d, 8.70 <i>J</i> = 11.38	s, broad 8.46 -

N-aryl -formamides and -thioamides

2,4-DiCl (7)	DMSO	<i>trans</i>	-	d, 7.41 <i>J</i> = 8.84 d, 7.67 <i>J</i> = 2.31 d, 8.14 <i>J</i> = 8.84	s, 8.36	s, broad 9.97
2,4-DiBr (8)		<i>trans</i>	-	d, 7.65 <i>J</i> = 8.75 d, 7.97 <i>J</i> = 2.07 d, 8.06 <i>J</i> = 8.75	s, 8.42	s, broad 9.88
2,5-DiCl (9)	DMSO	<i>trans</i>	-	d, 7.24 <i>J</i> = 8.61 d, 7.55 <i>J</i> = 8.64 d, 8.28 <i>J</i> = 2.16	s, 8.39	s, broad 10.06
2,5-DiBr (10)	DMSO	<i>Trans and cis ~ 50%</i>		d, 6.65 <i>J</i> = 8.46 d, 7.01 <i>J</i> = 2.34 d, 7.32 <i>J</i> = 8.40 s, 5.65	s, 8.37 s, 8.43	d, 7.68 <i>J</i> = 8.52 s, broad 9.92
5-Cl-2-Me (12)	DMSO + CDCl ₃	<i>trans ~ 75%</i> <i>cis ~ 25%</i>	s, 2.19 s, 2.21	m, 7.03, s, 7.90 m, 7.03, s, 7.79	s, 8.28 d, 8.39 <i>J</i> = 10.76	s, 9.34 d, 9.62 <i>J</i> = 10.73
3,4-DiCl (13)	DMSO	<i>trans ~ 70%</i> <i>cis ~ 30%</i>	-	m, 7.24, m, 7.55 d, 8.02, <i>J</i> = 2.31	s, 8.37 d, 8.90 <i>J</i> = 10.76	s, 10.53 d, 10.34 <i>J</i> = 10.86
3,5-DiCl (14)	DMSO	<i>trans ~ 67%</i> <i>cis ~ 33%</i>	-	s, 7.30 s, 7.65 s, 7.30 s, 7.65	s, 8.34 d, 8.90 <i>J</i> = 10.65	s, 10.53 d, 10.34 <i>J</i> = 10.34

2.2 Synthesis of arylthioamides (compounds 15 – 20)

Compounds **15 – 20** (Table 2.2) were synthesized using a method described by Prof. Reid [Private communication]. The compounds were all refluxed in a mixture of THF and benzene for about 45 - 60 minutes (monitoring the progress of reaction using TLC plates). The solvent was then removed under vacuum and the product extracted from the remaining solid using benzene. The pale yellow solution was run through a column of silica gel in a 1:1 mixture of hexane and ethyl acetate as the carrier solvent. The products were grown straight from the carrier solutions. Pale yellow crystals of compounds **15 – 20** were obtained in good yields. As for the formamides, the purity of the arylthioamides was confirmed by NMR spectroscopy using a Bruker Avance 300 (1 H, 300.13 MHz) spectrometer. All compounds were found to exist in solution (CDCl₃ or d₆ -DMSO) as mixture of different ratios of *cis* and *trans* isomers.

N-aryl -formamides and -thioamides

Table 2.2: $^1\text{H-NMR}$ data for arylformamides **15** – **20** (δ in ppm, $^1\text{H-}^1\text{H}$ coupling constants in Hz)

Compound	Solvent	Conformer	Methyl H and Methine H	Ar H	CHS	NH
2,6-DiF-S (15)	DMSO	<i>trans</i> ~ 33%	-	m, 7.40	s, 9.71	s, 11.65
		<i>cis</i> ~ 66%	-	m, 7.53	s – broad, 9.98	d 11.91 $J = 13.86$
2,6-DiCl-S (16)	DMSO	<i>trans</i> ~ 33%	-	m, 7.40	d, 9.62 $J = 5.46$	s, broad 11.83
		<i>cis</i> ~ 66%	-	m, 7.59	d, broad, 9.38 $J = 13.68$	s, broad 11.85
2,6-DiMe-S (17)	C_6D_6	<i>trans</i> ~ 33%	s, 1.98	m, 6.66 6.80	d, 9.01 $J = 5.68$	s, broad 8.24
		<i>cis</i> ~ 66%	s, 1.78	6.92	d, broad, 8.82 $J = 14.75$	
2-Cl-6-Me-S (18)	DMSO	<i>Trans</i> ~ 33%	s, 2.33	m, 7.49	d, 9.63 $J = 3.18$	s, broad, 11.68
		<i>Cis</i> ~ 66%	s, 2.25	m, 7.38	d, 9.34 $J = 14.10$	s, broad, 11.68
2,6-DiBr-S (19)		<i>trans</i> ~ 33%	-	m, 7.02 7.29	s, 9.61	s, broad 8.68
		<i>cis</i> ~ 66%	-	7.57	d, 9.47 $J = 11.08$	
2,6-Diiso 6-S (20)	CDCl_3	<i>Trans</i> ~ 70%	s, 1.44 septet, 3.06	m, 7.15	d, 9.06 $J = 15.00$	d, 9.39
		<i>cis</i> - 30%	s, 1.17 septet, 2.96	m, 7.28	d, 8.90	s, 9.74

2.3 Crystal growth

Crystallization of all compounds was attempted from a choice of the following solvents: ethyl acetate, methanol, THF, DMSO, DMF, ethanol (all at 25 °C), and hexane (at 25, -20 and -60 °C). Powder X-ray diffraction patterns showed that a single polymorph was obtained for each compound grown from all solvents and temperatures indicating absence of possible concomitant polymorphs. Crystals suitable for single crystal X-ray analysis were selected from a solution of the formamides in their respective solvents. The high temperature phases of 2,6-dichlorophenyl formamide (**2b**) and 2-chloro-6-methylphenyl formamide (**4b**) were grown by sublimation of the powders at temperatures just below the melting points of the compounds, i.e. the powders were heated from room temperature to 160 °C (**2b**) or 125 °C (**4b**) over a period of 12 h to yield suitable single crystals. The second form of 2,6-difluorophenylformamide (**1b**) was by serendipity obtained during crystallization of a batch of crystals of 2,6-difluorophenylthioamide (**15**). We suspect that unreacted 2,6-difluorophenylformamide (**1a**) from the synthesis of 2,6-difluorophenylthioamide (**15**) must have grown as a different polymorph due to the influence of the thioamide (**15**).

2.4. Synthesis of cocrystals of compound 2 and 3, 16 and 17, and 6 and 20

Cocrystals **22**, **23** and **24** were prepared using similar methods. The starting materials (**2a** and **3** for **22**; **16** and **17** for **23**; **6** and **20** for **24**) were ground together using mortar and pestle for about three minutes. The resulting powder (pattern matched those of starting materials) was then dissolved in an appropriate solvent (a single solvent or a mixture that dissolved both ground compounds equally well) followed by crystallization via slow evaporation. For compound **22** a mixture of ethyl acetate and acetonitrile (in a ratio of 9:1) was used. For compound **23** a 1:1 mixture of methanol and chloroform was used while for compound **24**, ethyl acetate was used. Good quality colorless blocky crystals were obtained and analyzed using powder and single crystal X-Ray diffraction.

2.5 Single crystal X-ray diffraction

Intensity data were collected on a Bruker SMART 1 K CCD area detector diffractometer with graphite monochromated Mo K α radiation (50 kV, 30 mA). The collection method involved ω -scans of width 0.3°. Data reduction was carried out using the program SAINT+, version 6.02. [Bruker SAINT+, 1999]. Multi-scan absorption corrections were made using the program SADABS. [Sheldrick, 1996] The crystal structures were solved by direct methods using SHELXS-97 [Sheldrick, 1997]. Non-

hydrogen atoms were first refined isotropically followed by anisotropic refinement by full matrix least-squares calculation based on F^2 using SHELXL-97 [Sheldrick, 1997]. The 2-Cl atom and the 6-Me group are mutually disordered in both phases of 2-chloro-6-methylphenylformamide **2a** and **2b** with occupancies of 0.573(1):0.427(1) and 0.750(2):0.250(2) in **2a** and **2b**, respectively. The same applies for 2-chloro-6-methylphenylthioamide **18** with occupancies of 0.512(2):0.488(2) and cocrystal **22** 0.519(2):0.481(2) and **23** 0.868(2):0.132(2). The disorder was modeled by use of suitable restraints on C–Cl and C–CH₃ distances during refinement. For cocrystal **24** the oxygen and sulphur atoms are disordered over the same positions. The disorder was modeled by use of suitable restraints on C=O and C=S bond distances during refinement. With the exception of the hydrogen atoms involved in hydrogen-bonding [i.e. H(1)] all hydrogen atoms were positioned geometrically and allowed to ride on their respective parent atoms. H(1) was in all structures located in the difference map and refined freely. Further crystallographic data are summarized in Tables A1 to A5 in the appendix. Diagrams and publication material were generated using PLATON [Spek, 2003], ORTEP3 [Farrugia, 1997], DIAMOND3 [Brandenburg, 2006] and SCHAKAL-99 [Keller, 1999]. The general-purpose crystallographic tool PLATON was used for structure analysis.

2.6 Powder X-ray diffraction

Powder X-ray diffraction (PXRD) data were all recorded at room temperature using a Bruker AXS D8 equipped with a primary beam Göbel mirror, a radial Soller slit, a Vantec-1 detector and using Cu-K α radiation (40 kV, 40mA). Data were collected in the 2θ range 5 to 140° in 0.007° steps, using the scan speed resulting in an equivalent time of 110.4s per step. Powder patterns were recorded of finely ground powders of the solution-grown phases. In order to obtain data for the high temperature forms **2b** and **4b**, these same samples were heated to just below their respective melting points (but above their respective phase transition temperatures - see thermal analysis section below). These were then cooled and powder patterns of the high temperature forms (**1b** and **2b**) were recorded. The diffraction patterns were used as fingerprints to visually differentiate the low and high temperature polymorphs of each compound.

2.7 DSC measurements

Differential Scanning Calorimetry (DSC) was used to investigate the behavior of arylformamides and arylthioamides as a function of temperature. DSC measurements were carried out using a Mettler-Toledo Star DSC 822 instrument. Small amounts (5–10 mg) of sample were

weighed in aluminium pans and placed in the sample chamber of the calorimeter. The powders were then heated in the temperature range of 25 to 300 °C at a heating rate of 5 °C min under ambient atmosphere.

2.8 Lattice energy calculations

OPIX [Gavezzotti, 2003] is designed for molecular crystals and has a package for calculation of intermolecular properties and energies of crystals. The program contains a number of different modules namely Coor, ZipOpec, ZipPromet and Pixel each of which has set of functions that it can carry out.

Coor is the preliminary module and it provides interfacing between other modules and other program packages. This module reads files with extensions .oih or .oeh (which has coordinates of one reference molecular group, RMG) and uses them to prepare other file types. It calculates the explicit hydrogen atom positions (putting them in an output file with extension .oeh), prepares a file for input to ZipPromet (coo.pro), prepares a file for input to the lattice energy minimizer program (coo.pck) and a file for input to a graphics program [coo.dat, usually SCHAKAL-99 (Keller, 1999)].

ZipOpec is useful for calculating lattice energies by summing up interactions between atom pairs. This module reads an .oeh file. It

constructs a model based on the kind of RMG information in the .oeh file, e.g. if the RMG is for a crystal, then a crystal model will be constructed on the basis of the given symmetry operations of the space group and all the interatomic distances present calculated. However intramolecular interactions are not calculated. Some of the information that can be obtained from ZipOpec are, intermolecular bond distances and angles, the molecular volume [Gavezzotti, 1983], the molecular surface area [Gavezzotti, 1985] and the main moments of inertia.

The calculation of packing and potential energies (described by the UNI force field [Filippini and Gavezzotti, 1993/4 / unpublished results]) for one fragment in the RMG is done using the equations below;

$$E_{(\text{pot,tot})} = \sum_i \sum_j E(i,j); E(i,j) = A \exp(-BR_{ij}) - CR_{ij}^{(-6)} + q_i q_j / R_{ij} \quad (\text{i})$$

$$E_{(\text{latt})} = -\Delta H_{(\text{subl})} = \frac{1}{2} E \quad (\text{ii})$$

where *i* labels any atom in the RMG and *j* labels any atom in any SMG. *E* is the potential energy of one mole of molecules in the crystal, while 1/2*E* is the gain in energy when one mole of molecules at infinity are brought into contact in the crystal (the computational equivalent of the sublimation energy). There is no cutoff and sums are extended over a large number of neutral units so that convergence of the sums in (1) is good even without forced convergence procedures. The coulombic part of the sums does not

***N*-aryl -formamides and -thioamides**

converge properly only for structures with a large cell dipole in polar space groups.

3. Structural analyses of disubstituted arylformamides and arylthioamides

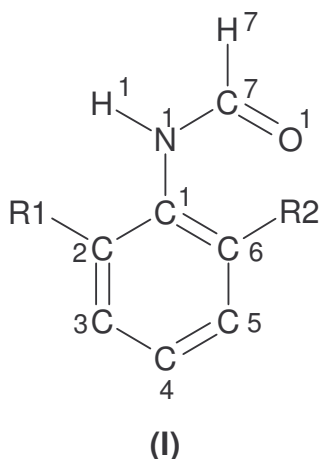
In this chapter the crystallographic structures of each of the 21 *N*-aryl -formamides and -thioamides and their cocrystals are discussed. The discussion of the crystallographic data is divided into five sections. First the 2,6-disubstituted arylformamides (section 3.1), then the formamides with substitutions in other positions (section 3.2), then the 2,6-disubstituted arylthioamides (section 3.3), then the arylformamide (section 3.4) and finally their cocrystals (section 3.5). The arylformamide is discussed on its own because it has no substituents on the aryl ring like the others. Only the room temperature polymorphs of 2,6-difluorophenylformamide (**1a**), 2,6-dichlorophenylformamide (**2a**) and 2-chloro-6-methylphenylformamide (**4a**) are discussed in this chapter. The other polymorphs of these compounds (**1b**, **2b** and **4b**) are discussed in chapter 4 which deals with polymorphism and phase transitions of 2,6-difluorophenylformamide, 2,6-dichlorophenylformamide and 2-chloro-6-methylphenylformamide. The different categories under which all the structures of this work fall in are discussed in chapter 6.

3.1 *2,6-disubstituted arylformamides*

3.1.1 *Introduction*

A series of 2,6 disubstituted arylformamides were synthesized and crystallized from a variety of solvents. The formamides were varied in the type of substituents on the 2 and 6 positions of the aryl rings. The range of synthesized formamides included substitution by fluorine atom, chlorine atom, methyl group, bromine atom and isopropyl group and a combination of chlorine atom and methyl group in the 2 and 6 positions of the aryl ring. This was done with a view to investigate the influence of factors such as steric bulk and electronic properties on the hydrogen bonding patterns and crystal packing and also the role of these substituents in the formation of possible polymorphs. It was hoped that these studies would further our understanding of solid-state properties of disubstituted arylformamides and thioamides, and help us understand the factors that govern polymorphism in simple organic compounds. Initial research work indicated that some of the synthesized formamides existed in more than one phase and that the change from one phase to the other was temperature dependent.

3.1.2 Molecular structures of 2,6 disubstituted arylformamides



Scheme 3.1: Molecular representation of the 2,6-disubstituted arylformamides. R1 = R2 = F (**1a**); Cl (**2a**); Me (**3**); Br (**5**); iPr (**6**); R1 = Cl and R2 = Me (**4**).

The structural diagram and general atom-numbering scheme for the 2,6-*N*-disubstituted arylformamides (compounds **1a** – **6**) is given in Scheme 3.1 above. The six compounds discussed are 2,6-difluorophenylformamide **1a**, 2,6-dichlorophenylformamide **2a**, 2,6-dimethylphenylformamide **3**, 2-chloro-6-methylphenylformamide **4a**, 2,6-dibromophenylformamide **5** and 2,6-diisopropylphenylformamide **6**. Each of the six compounds is distinctly different with respect to the nature and size of the substituents in the *ortho*-position of the aryl rings. All compounds were crystallized from a variety of solvents in accordance with their solubilities and their purity was confirmed by NMR spectroscopy. The *ORTEP* diagrams representing the molecular structures of compounds **1** – **6** are given in Appendix 2. A representative *ORTEP* drawing for compounds **1** – **6** is shown in Figure 3.1. Important bond distances and

angles as well as intermolecular hydrogen bonds are presented in Table 3.1. The crystal structure of compound **2** has been reported [Godwa *et. al.*, 2000] previously but was repeated for reasons of comparison.

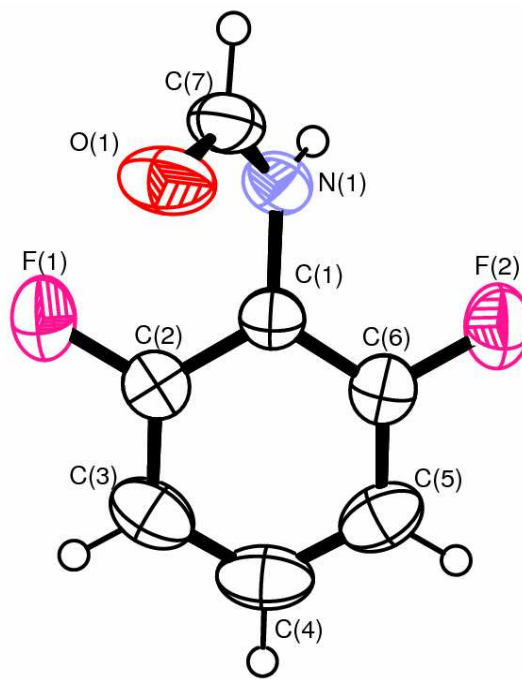


Figure 3.1: An *ORTEP* diagram of 2,6-difluorophenylformamide **1a** drawn with 50% probability displacement ellipsoids. The will serve as representation of the 2,6-disubstituted arylformamides.

Table 3.1 Some geometric parameters for compounds **1** to **6**. Bond distances in (Å), bond angles and torsion angles in (°)

Parameter	1	2	3	4	5	6
N(1)-C(7)	1.330(3)	1.337(3)	1.333(2)	1.337(2)	1.313(7)	1.331(2)
N(1)-C(1)	1.414(2)	1.418(2)	1.431(2)	1.424(2)	1.437(7)	1.442(2)
O(1)-C(7)	1.216(3)	1.221(3)	1.220(3)	1.221(2)	1.234(7)	1.220(2)
C(2)-X(1)	1.352(2)	1.738(2)	1.505(2)	1.738(2)	1.886(6)	1.515(2)
C(6)-X(2)	1.352(2)	1.736(2)	1.506(3)	1.489(4)	1.899(6)	1.521(2)
C(1)-N(1)-C(7)	122.6(2)	123.4(2)	124.2(1)	124.1(1)	122.5(5)	123.4(2)
N(1)-C(7)-O(1)	125.6(2)	126.0(2)	125.8(2)	126.3(1)	124.9(6)	125.8(2)
C(7)-N(1)-C(1)-C(2)	60.3(3)	67.3(3)	69.4(2)	67.2(2)	82.7(8)	78.9(2)
Volume of substituent In Å ³	~15	~20	~23	~20 & 23	~26	>26

X1 and X2 = F **1**, Cl **2**, Me **3**, Br **5** and ⁱPr **6**, X1 = Cl and X2 = Me **4**

The molecular geometry of compounds **1** - **6** is similar in that all show a *trans* conformation with the plane formed by the formamide moiety [defined by C(1)-N(1)-C(7)-O(1)] being out of the plane of the aromatic ring [defined by C(1) to C(6)] and the substituents on the 2 and 6 positions (Figure 3.2) by an angle of between 60 and 83°. Among the 2,6 disubstituted arylformamides synthesized in this thesis, none adopts a *cis* conformation in the solid state.

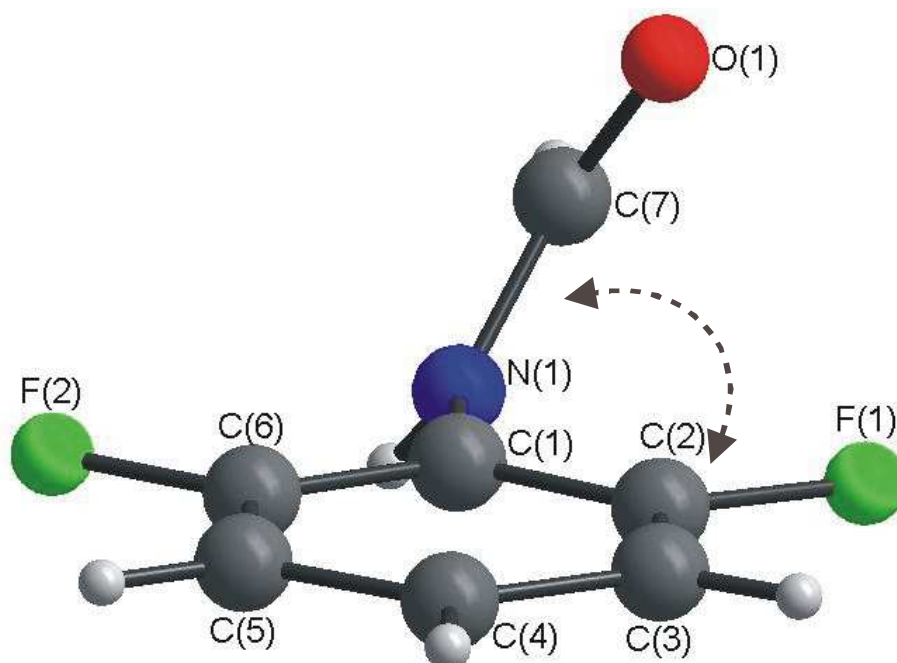


Figure 3.2: Molecular structure of **1a**. The angle referred to in the text above is defined as the angle between the planes formed by the aryl ring [C(1)–C(6)] and the formamide moiety [C(1)–N(1)–C(7)–O(1)].

The angles between the two planes defined above are different for all compounds and seem to be subtly dependent on the size of the substituents in the ortho positions of the aryl ring (see Table 3.1). This

torsion angle increases with an increase in geometric volume of the substituent e.g. from fluorine (60.2°) to isopropyl group (78.9°) (Table 3.1). The angle is slightly larger in 2,6-dibromophenylformamide **5** as compared to 2,6-diisopropylphenylformamide **6**, even though the volume that the isopropyl groups occupy in compound **6** is greater than the one occupied by the bromine groups in compound **5**. The orientation of the two methyl groups in the isopropyl group is such that they do not interfere much sterically with the formamide group when compared to the bromine groups in 2,6-dibromophenylformamide. The two methyl groups in each isopropyl group face away from the formamide group hence the smaller torsion angle in 2,6-diisopropylphenylformamide as compared to 2,6-dibromophenylformamide.

Electronic factors do not seem to significantly affect the general geometric parameters of the six compounds. The replacement of an electron-withdrawing group (as in 2,6-dichlorophenylformamide **2**) with an electron rich group (as in 2,6-dimethylphenylformamide **3**) leaves the geometry between the two planes virtually unchanged. The similarity of these torsion angles in compounds **2** and **3** is therefore likely to be a result of the similar size or volume of the Cl atom and the methyl group (19 Å³ for Cl atom and 23 Å³ for the CH₃ group) in compounds **2** and **3**, respectively. This phenomenon has been explored extensively in the literature [Gnanaguru et al., 1985; Jones et al., 1981; Edwards et al., 2001; Streek and Motherwell, 2005].

Other factors that may contribute to the similarity in torsion angle could be the presence of additional intramolecular interactions (such as C-H...O) in compound **3**, as will be shown later in this chapter, as well as the type of N-H...O hydrogen bond chain category referred in chapter 1. The relevant angle is different in each of the polymorphic compounds 2,6-difluorophenylformamide **1a** and **1b**, 2,6-dichlorophenylformamide **2a** and **2b** and 2-chloro-6-methylphenylformamide **4a** and **4b**. This torsion angle compares well to other related formamides and acetamides that have been studied previously and fits the above-discussed trend; the angle increases with the increase in the size of R' and R" (see Tables 2.2a - c) and is found to be greater in compounds that belong to category 1 as compared to those in category 2.

The bond distances and angles of all six compounds are similar and also compare well to previously reported structures of formamides and acetamides. The N(1)-C(7) bond distances are in the region of 1.33 Å (Table 3.1) and show considerable double bond character if compared to typical N-C single or double bonds (1.45 or 1.26 – 1.28 Å respectively) [Pauling, 1960]. The expected lengthening of the C=O bond distances is, however, not observed and they are at approximately 1.22 Å, only slightly longer than those in a typical C=O double bond (1.198 Å) [Abrahams *et al.*, 1956; Allen *et al.*, 1997]. This observation was brought forward as counter argument to the resonance model description (see Scheme 3.2) for the rotation barrier in formamides [Quintanilla-Licea *et al.*, 2002 and

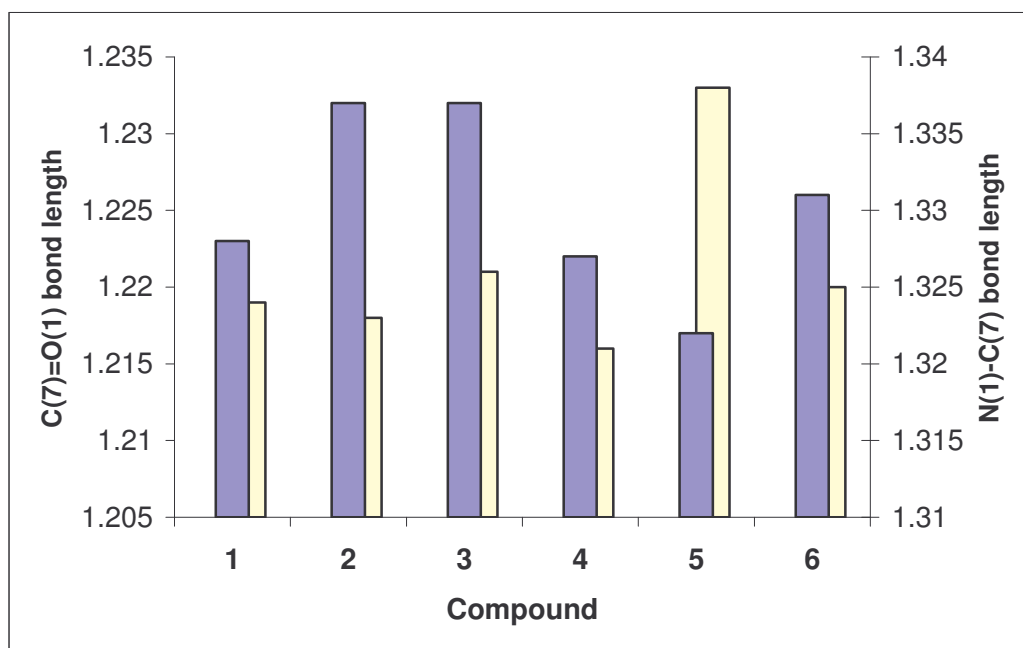


Figure 3.3: Histogram comparing the C(7)=O(1) double bond (purple bars) and the N(1)-C(7) single bonds (yellow bars) in 2,6-disubstituted arylformamides (represented by the numbers **1** – **6** on the histogram). The bond lengths are given in Angstroms.

There are only a few known formamides with substituents in the 2 and 6 positions of the aryl ring that have been characterized by X-ray diffraction (see discussion in Chapter 1), leaving acetanilides as the only other closely related compounds from the Cambridge Structural Database (CSD) that can be compared to compounds **1** – **6**. Most of these acetamides have similar general geometries to the formamides discussed in this thesis.

3.1.3 Crystal packing and intermolecular interactions in 2,6 disubstituted arylformamides

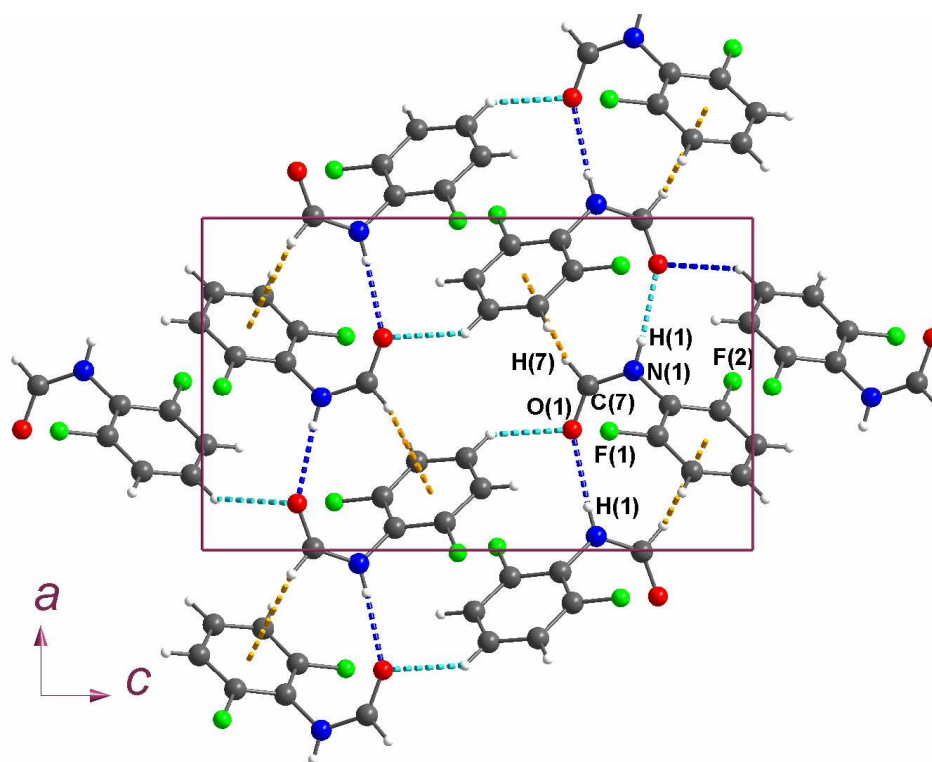
Table 3.2 summarizes crystal data for compounds **1a**, **2a**, **3**, **4a**, **5** and **6**.

Table 3.2: Crystal data for compounds **1a**, **2a**, **3**, **4a**, **5** and **6**.

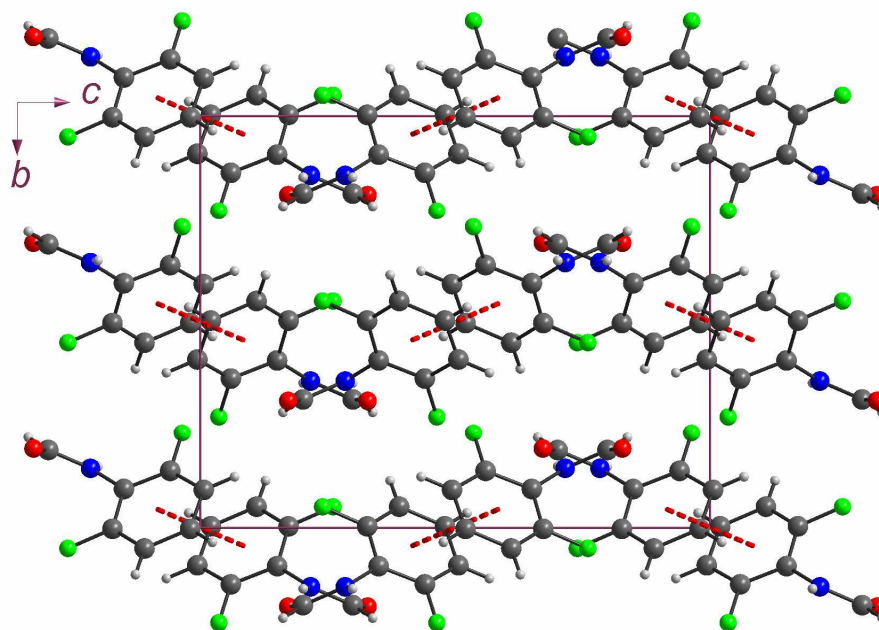
Parameter	1a	2a	3	4a	5	6
Formula	C ₇ H ₅ F ₂ NO	C ₇ H ₅ Cl ₂ NO	C ₉ H ₁₁ NO	C ₈ H ₈ ClNO	C ₇ H ₅ Br ₂ NO	C ₁₃ H ₁₉ NO
<i>W</i>	157.1	190.0	149.2	169.6	278.9	205.3
<i>T</i> (K)	293(2)	293(2)	293(2)	173(2)	293(2)	293(2)
λ , Å	0.7107	0.7107	0.7107	0.7107	0.7107	0.7107
Space group	<i>Pbca</i>	<i>Pbca</i>	<i>P2₁2₁2₁</i>	<i>Pbca</i>	<i>P2₁2₁2₁</i>	<i>P2₁/c</i>
<i>a</i> , Å	8.503(2)	8.604(1)	4.502(4)	8.445(2)	4.315(1)	9.034(1)
<i>b</i> , Å	11.387(2)	12.743(2)	8.589(8)	12.903(3)	13.976(3)	8.858(1)
<i>c</i> , Å	14.075(3)	14.402(2)	21.297(2)	14.419(3)	14.325(3)	16.001(2)
α, β, γ (°)	90, 90, 90	90, 90, 90	90, 90, 90	90, 90, 90	90, 90, 90	90, 104.90(3), 90
<i>V</i> Å ³	1362.8(4)	1578.9(3)	823.5(1)	1571.0(6)	864.0(3)	12.375(3)
$\rho_{(calc)}$ Mg/m ³	1.532	1.599	1.203	1.434	2.145	1.102
<i>Z</i>	8	8	4	8	4	4

Compound **1a** crystallizes in the orthorhombic space group *Pbca*, *Z* = 8 with one molecule in the asymmetric unit. The molecules are linked together by N-H...O [N(1)...O(1) = 2.843 Å] hydrogen bonds. These hydrogen bonds form infinite chains of molecules related by a glide plane in the crystallographic *a* direction. This results in the formamide molecules pointing in alternate directions (Figure 3.4). Adjacent chains are held together through weak C-H...O interactions [O(1)...H(4) = 2.750 Å] between molecules forming corrugated sheets that run in the crystallographic *c* direction. Besides the N-H...O hydrogen bond, each of

these corrugated sheets are linked together through C-F... π [C(6)... π = 3.815, F(2)... π = 3.613 Å and C(6)-F(2)... π = 71°] and π ... π intermolecular interactions. The C-H... π interactions are between adjacent molecules along the N-H...O hydrogen bonded chains that are related by a glide plane. The face-to-face π ... π interactions are between molecules from adjacent N-H...O hydrogen bonded chains; the molecules are related by a center of inversion. The distances between the centers of gravity (*Cg*...*Cg*) for these interactions are 3.903 Å with the closest distances of approach for the two interactions being 3.485 Å [symmetry operators = -*x*, 1 - *y*, 1 - *z*] (Figure 3.4b). Other intermolecular interactions contributing to the overall packing of the molecules in the crystal include C-H...F [H(3)...F(2) = 2.680] intermolecular interactions.



(a)



(b)

Figure 3.4: Packing in 2,6-difluorophenylformamide. (a) View down the *b* axis showing N-H...O hydrogen bond chains (in dashed blue lines) and C-H...O interactions (in light blue dashed lines) linking the hydrogen bonded chains. C-H... π interactions are shown in gold. (b) View down the crystallographic *a* axis. The dashed red lines represent π ... π intermolecular interactions.

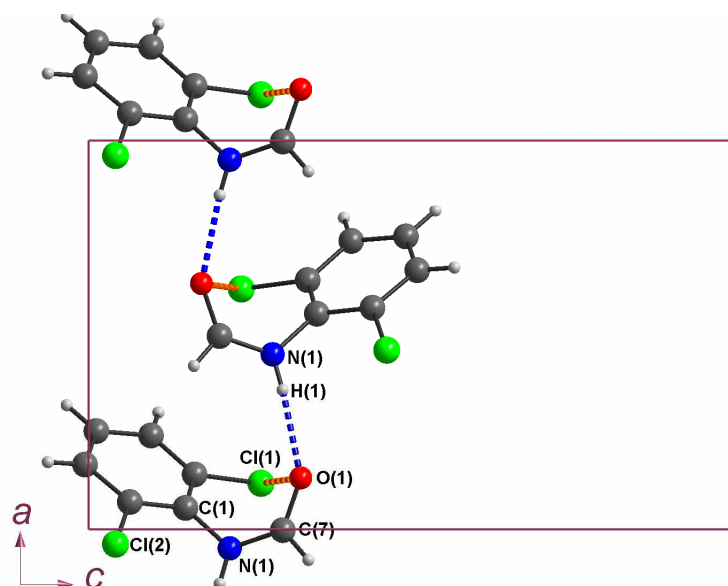
Ferguson *et. al.* [1998] analyzed a closely related compound with fluorine as the substituents in the 2 and 6 positions of the aryl ring and bromine in the 4 position. *N*-formyl-4-bromo-2,6-difluoroaniline crystallizes in the orthorhombic space group $P2_12_12_1$ and is structurally very different to compound **1a**. Both compounds have a different arrangement of molecules along the N-H...O hydrogen bonded chains. In the solid-state

***N*-aryl -formamides and -thioamides**

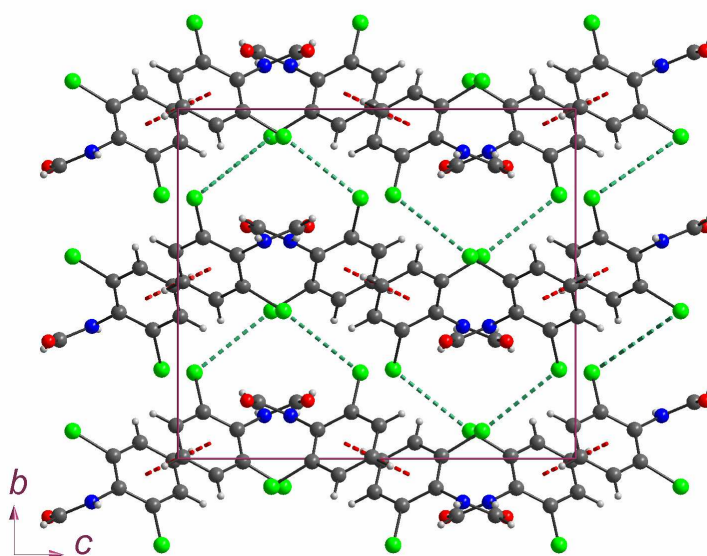
molecules of *N*-formyl-4-bromo-2,6-difluoroaniline are related by translation forming infinite chains along the crystallographic *a* direction. As in compound **1a** the hydrogen-bonded chains are linked to one another by weak C-H...O interactions, which run in the crystallographic *c* direction (see Figure 3.4 above). This intermolecular distance in compound **1a** is similar to the one in *N*-formyl-4-bromo-2,6-difluoroaniline (N...O distance in **1a** is 2.841 and in *N*-formyl-4-bromo-2,6-difluoroaniline it is 2.801 Å) and is found between molecules from adjacent hydrogen bonded chains related by a 2-fold screw axis. The two C-H...O interactions together with the N-H...O hydrogen bond complete a trimeric pattern that link adjacent hydrogen bonded chains in *N*-formyl-4-bromo-2,6-difluoroaniline. There are also a C-H... π interaction and π ... π interactions between molecules related by translation along the hydrogen-bonded chains. *N*-formyl-4-bromo-2,6-difluoroaniline unlike 2,6-difluorophenylformamide has F...F interactions. This is in addition to F...Br and F...O interactions.

2,6-dichlorophenylformamide (**2a**) crystallizes in the orthorhombic space group *Pbca*, *Z* = 8 with one molecule in the asymmetric unit similar to compound **1a**. Compound **2a** has its molecules linked together by N-H...O [N(1)...O(1) = 2.872 Å] hydrogen bonds forming chains of molecules related by glide planes in the crystallographic *a* direction. This results in the formamide molecules pointing in alternating directions (Figure 3.5a). Adjacent chains are held together through π ... π interactions [*Cg*...*Cg* 3.678 Å] between aryl rings from neighboring chains forming sheets of

molecules parallel to (010) (Figure 3.5b). Neighboring sheets interact with each other through Cl...Cl [Cl(1)...Cl(2) = 3.640 Å] interactions (Figure 3.5b).



(a)



(b)

Figure 3.5: (a) Hydrogen bonding chain in compound **2a** showing spirals in which each molecule is related to the next one by a glide plane and

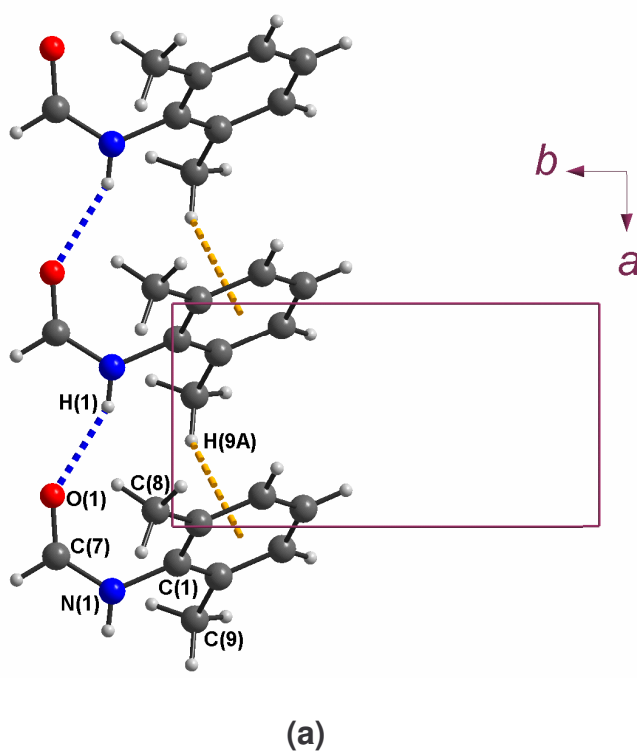
intramolecular Cl(1)...O(1) interactions (orange dashed lines); (b) Crystal packing in **2a** showing chains of N-H...O hydrogen bonded molecules running down the *a* axis and linked to each other through $\pi\cdots\pi$ (red dashed lines). Between each sheet of molecules are Cl(1)...Cl(2) interactions (green dashed lines).

Compounds **1a** and **2a** are isomorphous with minor packing differences. The unit cell parameters are similar with the *b* parameter shorter by 1.4 Å in compound **1a**. The other difference is in the torsion angle between the plane of the aryl ring and that of amide moiety. This angle is smaller by about 6° in **1a**. 2,6-difluoroacetanilide [Hanson *et. al.*, 2004] and 2,6-dichloroacetanilide [Nagarajan *et. al.*, 1986] have torsion angles of about 54 and 70° between the plane of the aryl ring and that of amide moiety but these two crystallize in the monoclinic space group $P2_1/n$.

2,6-dimethylphenylformamide (**3**) exhibits a different hydrogen bonding pattern when compared to compounds **1a** and **2a**. Compound **3** crystallizes in the orthorhombic chiral space group $P2_12_12_1$, $Z = 4$, with just one molecule in the asymmetric unit. The absolute structure could not be determined from the X-ray diffraction experiment due to a lack of atoms capable of anomalous scattering in Mo $K\alpha$ radiation. In the solid state, molecules of the compound are joined by N-H...O [N(1)...O(1) = 2.854 Å] hydrogen-bonded chains which run along the crystallographic *a* direction. The molecules are related by unit cell translation along the N-H...O

N-aryl -formamides and -thioamides

hydrogen bonded chains and are linearly stacked with aryl groups parallel to each other (Figure 3.6). Neighboring N-H...O hydrogen-bonded chains are connected to one another along the *b* axis through intermolecular C-H...O interactions [O(1)...H(7) = 2.900 Å] between molecules (also related by unit cell translation) forming sheets parallel to the (001) plane. A second intramolecular C-H...O interaction [C(8)...O(1) = 3.227, 0.01 Å shorter than the sum of van der Waals radii of carbon and hydrogen) we believe influences the conformation of the formamide moiety relative to the aryl ring.



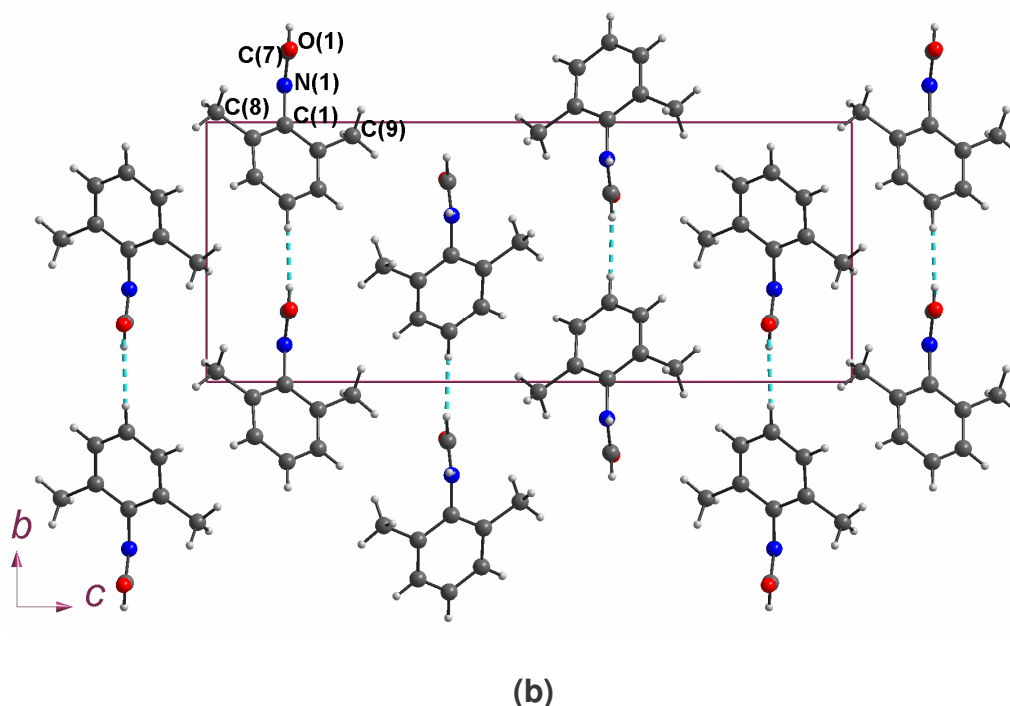


Figure 3.6: (a) Hydrogen bonded chain (blue dashed lines) in 2,6-dimethylphenylformamide (**3**) showing the stacking relationship in each chain with molecules related to another by unit cell translation. Also shown is C-H... π interactions (in gold); (b) Crystal packing in **3** as a projection down the crystallographic *a* axis. C(4)-H(4)...O(1) interactions (indicated with the blue dashed lines) linking N-H...O hydrogen bonded chains.

Hydrogen bonding and crystal packing in 2,6-dimethylphenylformamide **3** can easily be compared to similar dimethyl substituted acetamides and benzamides. The replacement of H(7) of compound **3** by a methyl group (as in 2,4,6-trimethylacetanilide [Upadhaya *et. al.*, 2002]) or a aryl group (as in *trans*-2,2'6,6'-tetramethylbenzanilide, [Azumaya *et. al.*, 1994] changes the packing in the crystal completely. In these compounds hydrogen-bonded chains (as in compounds **1** and **2**) in which molecules are pointing in alternate directions are formed. However

the stacking chains are also formed in *N*-(2,6-dimethylphenyl)anthracene-9-carboxiamide [Adams *et. al.*, 2001] in which the vertical separation between molecules along a hydrogen-bonded chain is 4.5 Å and has a C-H... π interaction between the molecules along the N-H...O hydrogen bond as in compound **3**.

2-chloro-6-methylphenylformamide (**4a**) crystallizes in the space group *Pbca*, $Z = 8$ with one molecule in the asymmetric unit. In the crystal of compound **4a**, molecules are linked together by N-H...O hydrogen bonds forming chains that run in the crystallographic *a* direction. A glide plane relates the molecules along the N-H...O hydrogen-bonded chain resulting in an arrangement with formamide molecules pointing in alternating directions. In addition to this there are intramolecular Cl...O interactions [Lommerse *et. al.*, 1996]. Adjacent chains are held together through π ... π interactions (*Cg*...*Cg* 3.675 Å) between aryl groups of neighboring N-H...O hydrogen-bonded chains hereby forming sheets of molecules parallel to (010). Neighboring sheets interact with each other through Cl...Cl [Cl(1)...Cl(2): 3.64 Å] and C-H...Cl interactions (see Figure 3.7). This compound is isomorphous with 2,6-dichlorophenylthioamide (see discussion in Chapter 5 of this thesis).

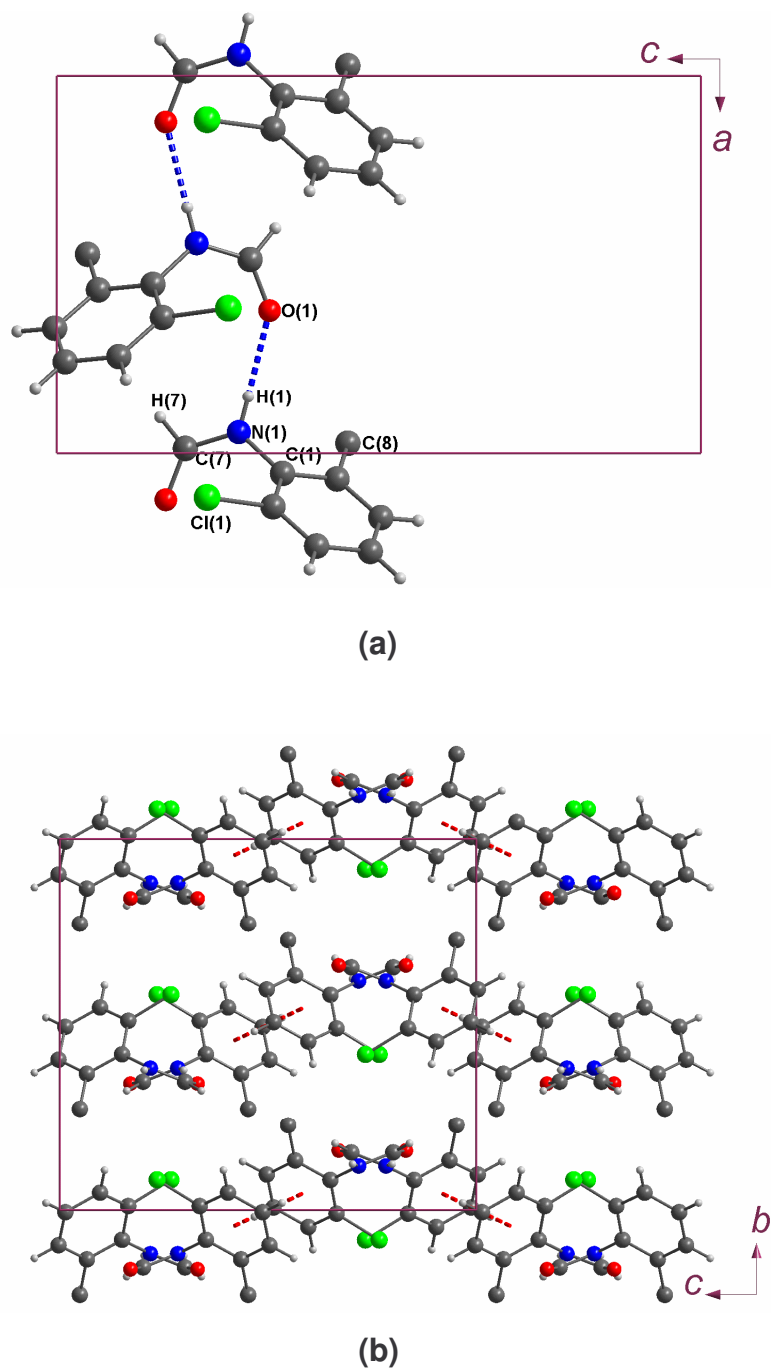
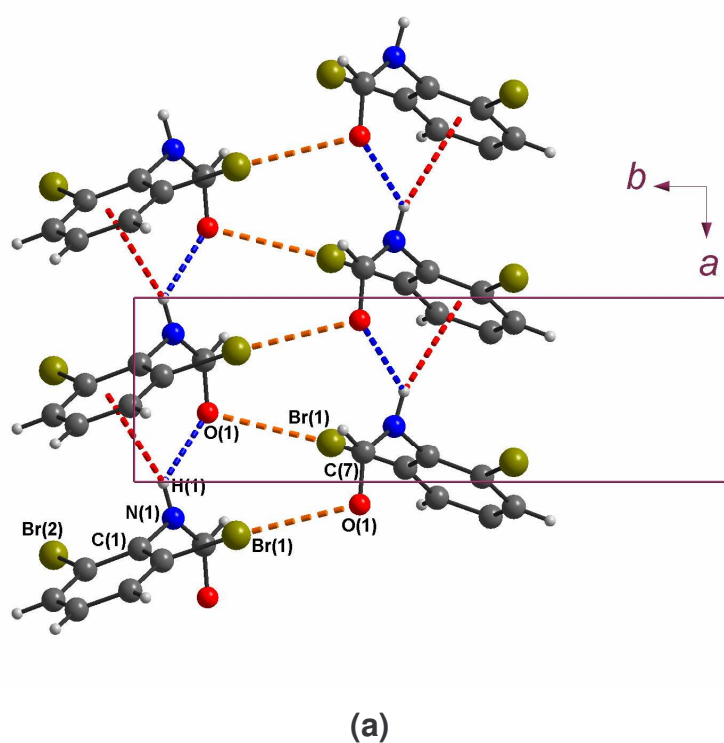


Figure 3.7: (a) Hydrogen bonded chains in the crystal of 2-chloro-6-methylphenylformamide **4a** showing molecules that are related to each other by a glide plane; (b) Crystal packing in **4a** drawn as a projection down the crystallographic *a* axis. $\pi \dots \pi$ interactions linking pairs of N–H...O chains are indicated with dashed lines.

2,6-dibromophenylformamide (**5**) crystallizes in the chiral orthorhombic space group $P2_12_12_1$ (same as compound **3**), $Z = 4$ with one molecule in the asymmetric unit. The colorless crystals (very thin needles) were grown by evaporation of the solvents from a 1:1 mixture of ethyl acetate and chloroform. Molecules of compound **5** are linked through N-H...O hydrogen bonds [$N(1)\dots O(1) = 2.806 \text{ \AA}$] forming chains running along the crystallographic a direction. The molecules in the chains are related by translation with the aryl rings stacked parallel to each other along the N-H...O hydrogen-bonded chains. In addition to the N-H...O hydrogen bonds, there are intermolecular N-H... π interactions [Desiraju and Steiner, 1999; $H(1)\dots\pi = 3.230$ and $N(1)\dots\pi = 3.800 \text{ \AA}$] between adjacent molecules along the same N-H...O hydrogen-bonded chains.

Connecting each of these chains, in the crystallographic b direction are Br...O interactions [Kubicki, 2004 and references therein; $Br(2)\dots O(1) = 3.178 \text{ \AA}$] between molecules related by a 2_1 screw axis, and in the crystallographic c direction C-H...O [$O(1)\dots H(4) = 2.650 \text{ \AA}$] and Br...Br intermolecular interactions [$Br(1)\dots Br(2) = 3.570 \text{ \AA}$] between molecules related by a 2_1 screw axis (Figure 3.8). The Br...Br interactions result in sheets of molecules, which form layers parallel to the bc (011) plane. The Br...Br distance is 0.13 \AA shorter than the sum of the van der Waals radii of the bromine atoms and is within the expected range of Br...Br intermolecular distance.

Bromine atoms in this compound are involved in two intermolecular interactions as indicated in Figure 3.8b. It has been reported that the Br atom is frequently involved in such contacts as a result of its non-spherical shape [Liebermann et al., 2000; Lommerse et al., 1996; Beyer et al., 2001]. The Br atoms in this crystal interact with O(1) head-on and with Br(2) side-on (oxygen being a nucleophile and bromine the electrophile). This leads to a two dimensional network similar to that in 2,3,6,7-tetrabromonaphthalene (space group $P2_1/c$) or the cocrystal of 2,3,6,7-tetrabromonaphthalene and bromobenzene [Navon et al., 1997].



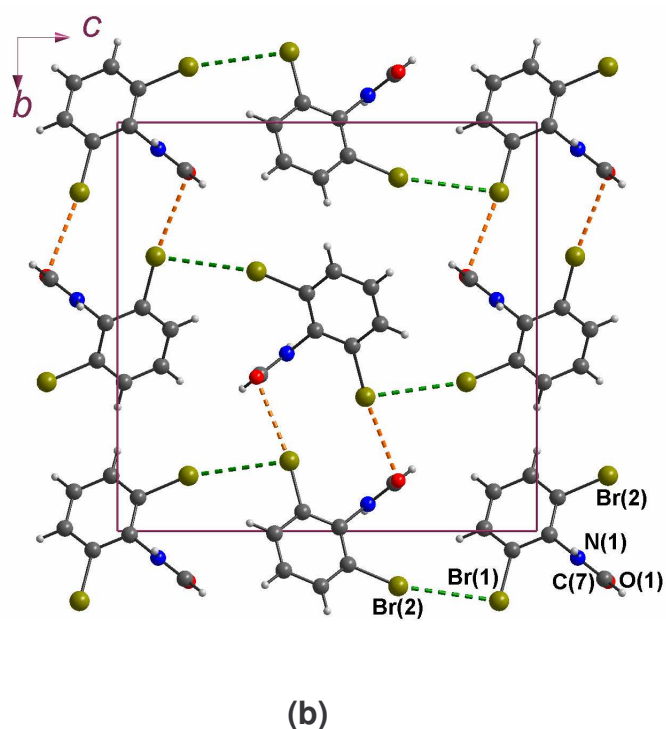


Figure 3.8: (a) N(1)-H(1)...O(1) hydrogen bonded chains (blue dashed lines) in 2,6-dibromophenylformamide (**5**) showing the stacking relationship in each chain. The molecules along the chain are related by unit cell translation. In addition to the N(1)-H(1)...O(1) hydrogen bonds, there are N(1)-H(1)... π interactions (red dashed lines). The gold dashed lines show Br(2)...O(1) interactions (shown in gold) that link up the hydrogen bonded chains; (b) Crystal packing in compound **5** as a projection down the crystallographic *a* axis. Also shown are Br(1)...O(1) and Br(1)...Br(2) interactions linking hydrogen-bonded chains (shown in gold).

2,6-diisopropylphenylformamide (**6**) crystallizes in the monoclinic space group $P2_1/c$, $Z = 4$ with one molecule in the asymmetric unit. The plate-like, colorless crystals were grown from ethyl acetate by slow evaporation of the solvent. The packing is dominated by the formation of N-H...O hydrogen bonds giving rise to the formation of chains that run

along the crystallographic *b* direction resulting in the formamide molecules pointing in alternate directions (see Figure 3.9).

Adjacent chains are held together through two interactions made by the aryl rings resulting in centrosymmetric dimers on the *ab* and *ac* faces of the unit cell. Each ring is involved in two C-H... π interactions; through C(10) [C(10)... π = 3.569 Å], between the dimers on the *ab* and *ac* faces, and through C(7) [C(7)... π = 3.768 Å], along the N-H...O hydrogen bonded chains, between adjoining molecules that are related by a glide plane (Figure 3.9). The C(7)-H(7)... π angle is closer to 180° than the C(10)-H(10)... π angle [157° and 143° respectively]. These C-H... π interactions together with the N-H...O hydrogen bond chains complete packing in the solid-state structure of compound **6**.

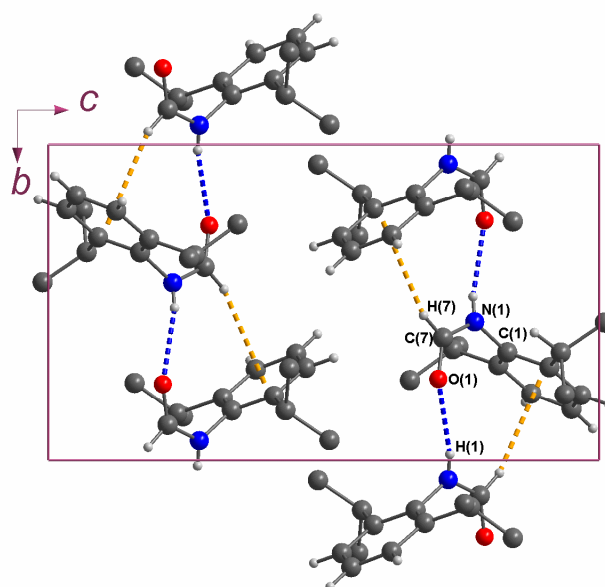


Figure 3.9: N-H...O hydrogen bonded chains in compound **6** (blue dashed lines). The N-H...O hydrogen bonded chains are linked by C-H... π interactions (gold dashed lines) between molecules that are related by a

center of inversion. Methyl and methine hydrogens have been omitted for the sake of clarity.

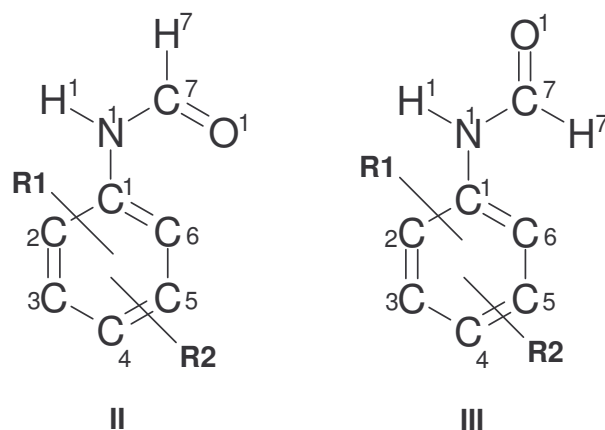
3.1.4 Discussion of crystal packing and intermolecular interactions in 2,6 disubstituted arylformamides

Two categories of packing patterns based on the kind of N-H...O hydrogen bond chains formed are generated from the six compounds discussed above. The first set (Category 1) has its molecules related by glide planes or 2_1 -screw axes (compounds **1a**, **2a**, **4a** and **6**) and the second set (category 2) has its molecules related by translation (compounds **3** and **5**) along the N-H...O hydrogen bonded chains. The π ... π interactions seem to be important in category 1 compounds as they are present in all of them. C-H...Cl interactions play a part of bringing Cl atoms closer in 2-chloro-6-methylphenylformamide resulting in Cl...Cl interactions. Similar interactions (C-H...F) occur in 2,6-difluorophenylformamide but in this case fluorine atom (being highly electronegative) does not allow for F...F interactions. Other halogen interactions are found in 2,6-dichlorophenylformamide (Cl...Cl and Cl...O) and 2,6-dibromophenylformamide (Br...O and Br...Br). Generally N-H...O hydrogen bond seems to be the most important interaction in category 1 and 2 compounds, followed by π ... π interactions (in category 1 compounds) or the others mentioned above (C-H... π , C-H...O, Br...O and Br...O) in category 2 compounds.

3.2 Disubstituted arylformamides with substituents in positions other than 2,6

3.2.1 Introduction

Substituents in the 2,6 positions to some extent restricted the free rotation of the formamide moiety. We therefore altered our compounds by varying the positions of the substituents on the aryl ring. In this category of formamides, substituents were put in positions 2 and/or 3, 4 and 5 as shown in Scheme 3.3 below. The variation of the substituents and their position on the aryl ring was however limited to chlorine, bromine and methyl due to a lack of commercially available starting materials and also (basing our argument on experience of studying the 2,6-disubstituted formamides) due to the fact that they behaved more or less similarly in solid state. It was hoped that this kind of variation would further our understanding of the effect of not having a substituent in position 6 and thereby not limiting the rotation of the formamide moiety [defined by the torsion angle C(1)-N(1)-C(7)=O(1)].



Scheme 3.3: Chemical structures of compounds **7** – **14** with their atom-numbering schemes. R1 = R2 = Cl, position 2,4 (**7**) - II; R1 = R2 = Br, position 2,4 (**8**) - II; R1 = R2 = Cl, position 2,5 (**9**) - II; R1 = R2 = Br, position 2,5 (**10**) - II; R1 = R2 = Me, position 2,5 (**11**) - unknown; R1 = Me, R2 = Cl, position 2,5 respectively (**12**) - II; R1 = R2 = Cl, position 3,4 (**13**) – III; R1 = R2 = Cl, position 3,5 (**14**) – II.

Eight compounds of this nature were synthesized. Their synthesis was done by refluxing their respective anilines in formic acid followed by a work up similar to the one used for the 2,6-disubstituted formamides. The compounds synthesized were: 2,4-dichlorophenylformamide **7**, 2,4-dibromophenylformamide **8**, 2,5-dichlorophenylformamide **9**, 2,5-dibromophenylformamide **10**, 2,5-dimethylphenylformamide **11**, 5-chloro-2-methylphenylformamide **12**, 3,4-dichlorophenylformamide **13** and 3,5-dichlorophenylformamide **14**. The structures of all but compound **11** were solved by single crystal X-ray diffraction. Crystals of compound **11** were not suitable for single crystal X-ray studies thus the only evidence of the composition of the compound is NMR spectroscopic data.

3.2.2 Molecular structures of compounds 7 – 14

Scheme 3.3 above gives the molecular representations of the compounds with the general atom-labeling scheme as used throughout the discussion. Important bond distances and bond angles (including important torsion angles) are presented in Table 3.3. The molecular geometries of compounds **7 - 14** are similar in that all (with exception of compound **13**, which shows a *cis* conformation) show a *trans* conformation as the 2,6-disubstituted phenylformamides. All of them with the exception of compound **12** have the formamide moiety coplanar with the plane of the aryl ring (Figure 3.10). One reason for this planarity may be the absence of a substituent in position 6 of the aryl ring (**6 – 12**) or in positions 2 and 6 (**13** and **14**) hence very little steric interference with the rotation of the formamide moiety. Electronic factors may also be responsible for the planarity [Boeyens et. al., 1988]. The respective dihedral angles between the two planes are close to 0° in all the planar compounds (see Table 3.3 and Figure 3.10). Compound **12** has a conformation similar to that of the 2,6-disubstituted arylformamides. One of the possible contributors to non-planarity of this arylformamide is the presence of the methyl group in position 2 of the aryl ring. There is steric interference between the methyl group and H(6) on the aryl ring twisting the formamide moiety to an angle of 51.7° - much smaller when compared to category 2 compounds of the 2,6-disubstituted formamides. This in turn orientates the methyl group in a manner that results in the methyl group interacting with the aryl ring in a C-

H... π interaction [H(8C)... π = 2.777 Å and C(8)-H(8C)... π = 145.4°] with adjacent molecules along the N-H...O hydrogen bond chain.

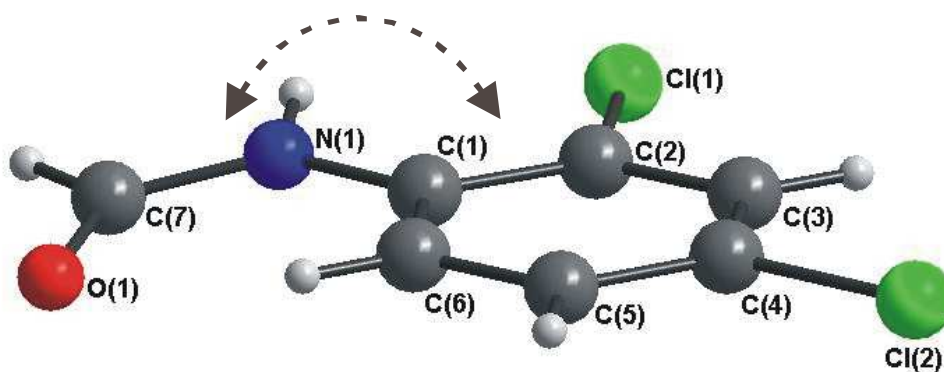


Figure 3.10: Molecular structure of 2,4-dichlorophenylformamide **7**. The arrow shows the angle between planes defined by the aryl ring (C(1)–C(6)) and C(1)–N(1)–C(7)–O(1) which is close to 0°.

N-aryl -formamides and -thioamides

Table 3.3: Selected geometric parameters for compounds **7** to **14**. Bond distances are given in (Å), bond angles and torsion angles are given in (°)

Parameter	7	8/(8A)	9	10	12	13	14
N(1)-C(7)	1.348(5)	1.358(6) 1.331(6)	1.355(4)	1.336(4)	1.364(1)	1.341(8)	1.335(3)
N(1)-C(1)	1.394(5)	1.405(5) 1.399(5)	1.403(3)	1.397(4)	1.396(1)	1.410(8)	1.403(3)
O(1)-C(7)	1.216(5)	1.206(6) 1.218(6)	1.212(4)	1.227(4)	1.201(1)	1.223(9)	1.212(3)
C(Y)-X(1)	1.745(4)	1.898(4) 1.902(4)	1.729(3)	1.501(4)	1.903(7)	1.728(6)	1.740(2)
C(Z)-X(2)	1.741(4)	1.888(5) 1.901(4)	1.732(3)	1.743(3)	1.911(8)	1.738(6)	1.742(2)
C(1)-N(1)-C(7)	128.3(4)	128.0(4) 128.5(4)	127.3(3)	124.6(3)	128.6(7)	127.2(5)	129.0(2)
N(1)-C(7)-O(1)	126.2(4)	127.2(5) 126.7(5)	125.8(3)	126.0(3)	126.0(8)	124.3(6)	126.7(2)
C(7)-N(1)-C(1)-C(6)	11.2(7)	3.4(8) 15.4(8)	11.9(5)	50.9(4)	6.9(1)	6.7(1)	8.7(4)

R1 = R2 = Cl, position 2,4 (**7**); R1 = R2 = Br, position 2,4 (**8**); R1 = R2 = Cl, position 2,5 (**9**); R1 = R2 = Br, position 2,5 (**10**); R1 = R2 = Me, position 2,5 (**11**) - unknown; R1 = Me, R2 = Cl, position 2,5 respectively (**12**); R1 = R2 = Cl, position 3,4 (**13**); R1 = R2 = Cl, position 3,5 (**14**).

Bond distances and angles of compounds **7** to **14** are similar to those of compounds **1** to **6** and compare well to previously reported values of structurally characterized formamides and related acetanilides. The N(1)-C(7) bond distances are in the region of 1.33 – 1.36 Å (Table 3.2) and show considerable double bond character. Again, the expected lengthening of the C=O bond distances is not observed and range between 1.21 – 1.23 Å. The N(1)-C(1) bond distances represent single bonds and the C–C bond distances and angles within the aryl ring are not significantly different from those of known aryl aromatic systems.

3.2.3 Crystal packing and intermolecular interactions

Compounds in this section will be discussed in groups of similar positional substitutions, e.g. the 2,4-disubstituted formamides are discussed together, the 2,5- together etc. The crystal data for the 7 compounds are given in Table 3.4.

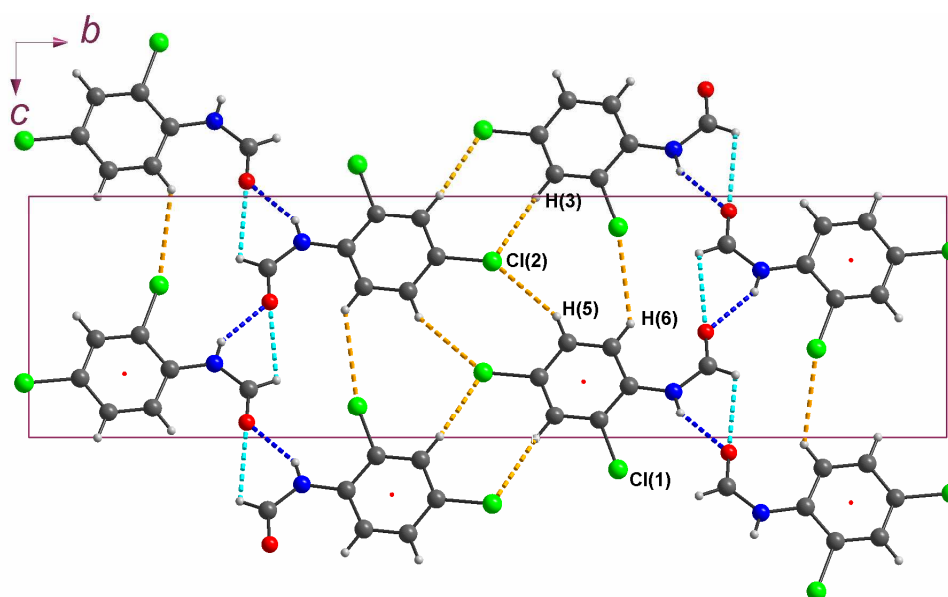
N-aryl -formamides and -thioamides

Table 3.4: Crystal data for compounds **7**, **8**, **9**, **10**, **12**, **13** and **14**.

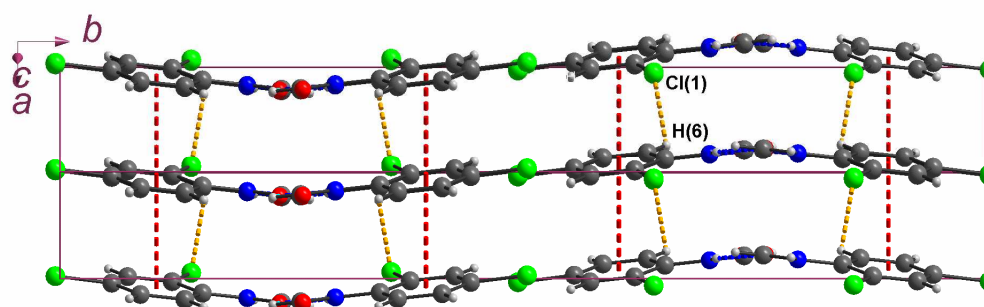
Parameter	7	8	9	10	12	13	14
Formula	C ₇ H ₅ Cl ₂ NO	C ₇ H ₅ Br ₂ NO	C ₇ H ₅ Cl ₂ NO	C ₇ H ₅ Br ₂ NO	C ₈ H ₈ CINO	C ₇ H ₅ Cl ₂ NO	C ₇ H ₅ Cl ₂ NO
<i>W</i>	190.0	278.9	190.0	278.9	169.6	190.0	190.0
<i>T</i> (K)	293(2)	293(2)	293(2)	173(2)	293(2)	293(2)	293(2)
<i>λ</i> , Å	0.7107	0.7107	0.7107	0.7107	0.7107	0.7107	0.7107
Space group	<i>P</i> 2 ₁ / <i>n</i>	<i>P</i> 2 ₁ / <i>c</i>	<i>P</i> 2 ₁	<i>P</i> 2 ₁ 2 ₁ 2 ₁	<i>P</i> 2 ₁ / <i>c</i>	<i>P</i> 2 ₁ / <i>c</i>	<i>P</i> 2 ₁ / <i>n</i>
<i>a</i> , Å	3.839(3)	27.774(2)	3.970(3)	4.011(3)	6.073(1)	9.489(3)	7.371(2)
<i>b</i> , Å	27.900(2)	4.021(4)	8.661(6)	7.043(3)	4.644(1)	12.393(4)	14.787(5)
<i>c</i> , Å	7.424(6)	15.067(1)	11.328(9)	28.895(2)	28.439(7)	6.705(2)	8.016(3)
<i>α, β, γ</i> (°)	90, 97.7(1), 90	90, 98.3(5), 90	90, 91.2(6), 90	90, 90, 90	90, 93.9(4), 90	90, 100.7(7), 90	90, 110.1(6), 90
<i>V</i> Å ³	788.3(1)	1664.8(3)	389.3(2)	816.7(1)	800.3(3)	774.7(5)	820.3(5)
<i>ρ</i> _(calc) Mg/m ³	1.601	2.226	1.621	2.269	1.408	1.629	1.539
<i>Z</i>	4	8	2	4	4	4	4

3.2.3.1 2,4-dichlorophenyl- and 2,4-dibromophenyl- formamides

ORTEP diagrams for structures of 2,4-dichlorophenylformamide and 2,4-dibromophenylformamide are given in the appendix. 2,4-dichlorophenylformamide (**7**) crystallizes in the monoclinic space group $P2_1/n$, $Z = 4$ with one molecule in the asymmetric unit. In the crystal two of the four molecules in the unit cell are linked together via N-H...O hydrogen bonds [$N(1)...O(1) = 2.885 \text{ \AA}$] forming chains of molecules that run diagonally across the crystallographic *ac* plane. Adjacent chains are connected via C-H...Cl intermolecular interactions [$H(5)...Cl(2) = 3.086 \text{ \AA}$, shown in golden dashed lines in Figure 3.11] between molecules related by a center of inversion resulting in a $R_2^2(8)$ graph set. The chains form parallel sheets of molecules that are linked by another C-H...Cl intermolecular interactions [$H(6)...Cl(1) = 3.024 \text{ \AA}$, between molecules related by translation) and weak $\pi... \pi$ intermolecular interactions [$Cg...Cg = 3.839 \text{ \AA}$]. These sheets are layered in the crystallographic *a* direction.



(a)



(b)

Figure 3.11: Packing diagram of compound 2,4-dichlorophenylformamide. (a) Sheets of N-H...O hydrogen bonded chains (blue dashed lines), C-H...O interactions (in pale blue color) and Cl...H interactions linking the hydrogen bonded chains (in gold). The Cl...H intermolecular interactions result in $R_2^2(8)$ graph set formations; and (b) Sheets of the N-H...O hydrogen bonded chains connected by Cl...H interactions (in gold).

2,4-dibromophenylformamide on the other hand crystallizes in the monoclinic space group $P2_1/c$, $Z = 8$ with two molecules in the asymmetric unit. The two molecules have a dihedral angle equal to $14.63(3)^\circ$ - the angle between least squares plane defined by the 11 non-hydrogen atoms of each molecule (see Figure 3.12 for illustration).

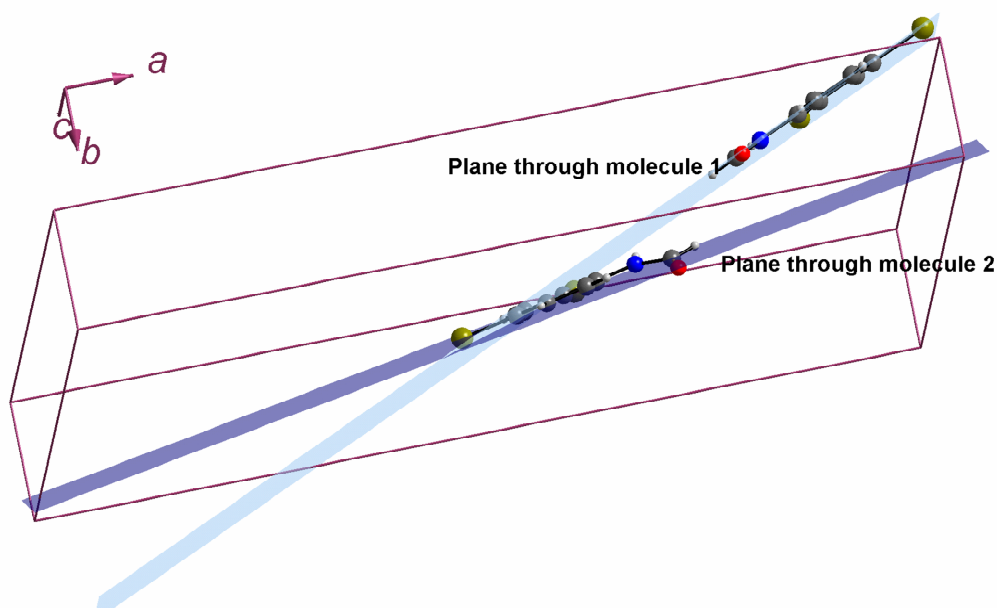


Figure 3.12: An illustration of least squares planes through each of the two molecules in the asymmetric unit of the crystal structure of compound **8**.

In the solid-state structure the pair of molecules in the asymmetric unit are involved in separate N-H...O hydrogen bonding [$N(1A)\dots O(1) = 2.908 \text{ \AA}$ and $N(1)\dots O(1A) = 2.730 \text{ \AA}$] to form sheets that runs in the crystallographic b direction. The molecules along each hydrogen bond alternate between molecule 1 and 2 (see Figure 3.13). These molecules along the hydrogen bonded chains are related by a 2-fold screw axes and

N-aryl -formamides and -thioamides

face alternate directions. Adjacent chains are also linked through Br...H interactions [Br(1A)...H(7) = 2.964 Å] between molecules that are related by a center of inversion. The separate hydrogen bonded chains are layered directly on top of each other forming sheets parallel to the (1 0 1) plane. These sheets are linked by C...O contacts [C(7A)...O(1) = 3.203 Å] (see Figure 3.14).

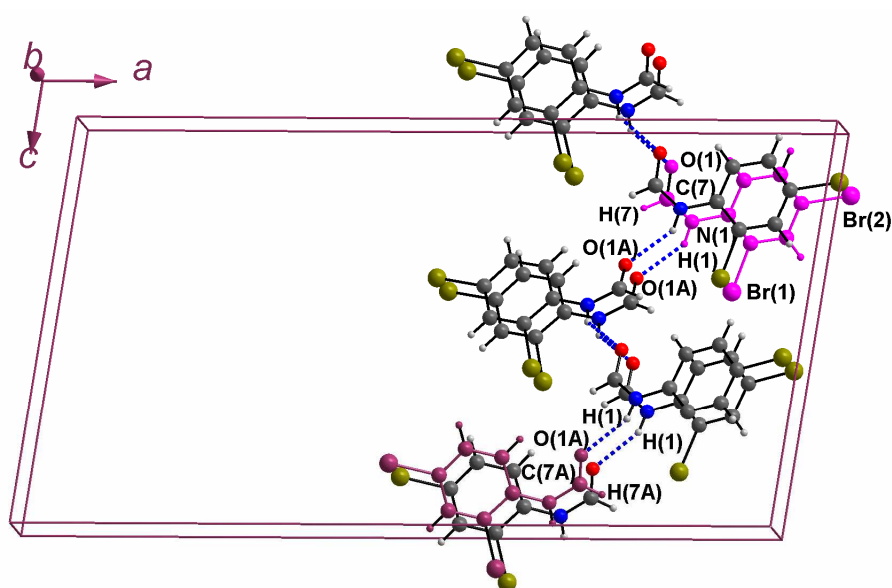


Figure 3.13: Two layered N-H...O hydrogen bonded sheets (in blue dashed lines) running down the crystallographic *c* direction in the solid state structure of 2,4-dibromophenylformamide. The two layers show the separate sheets which the two molecules in the asymmetric unit (colored purple and maroon) belong to.

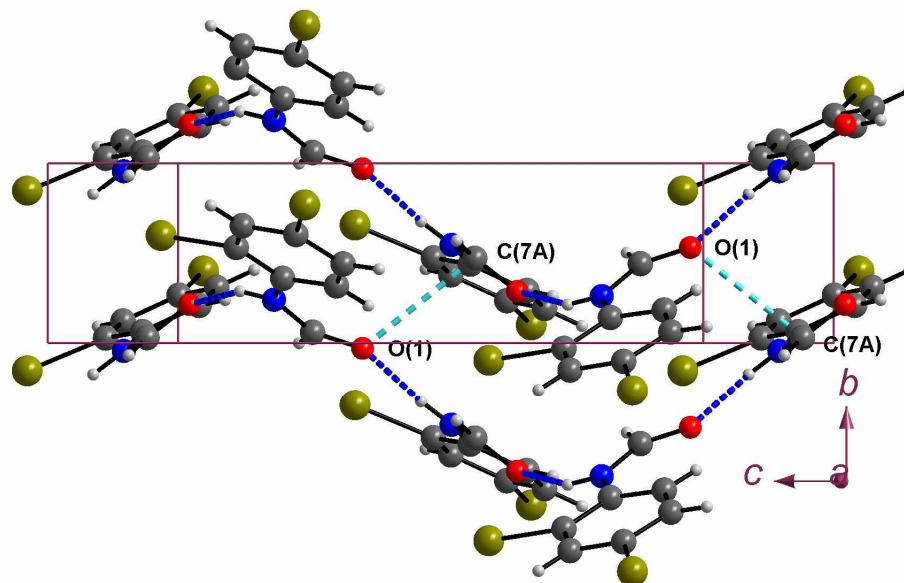


Figure 3.14: View down the crystallographic *a* axis of a packing diagram for 2,4-dibromophenylformamide showing close C...O contacts (in sky blue dashed lines) that connect the N-H...O hydrogen bonded sheets.

3.2.3.2 2,5-dichlorophenylformamide, 2,5-dibromophenylformamide and 5-chloro-2-methylphenylformamide

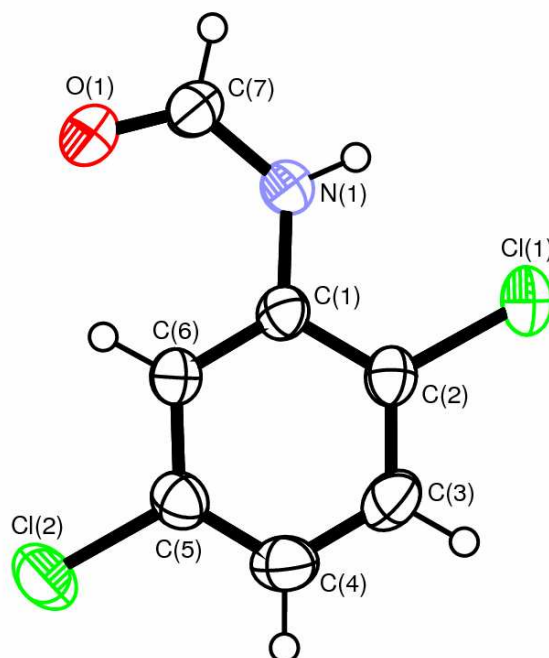
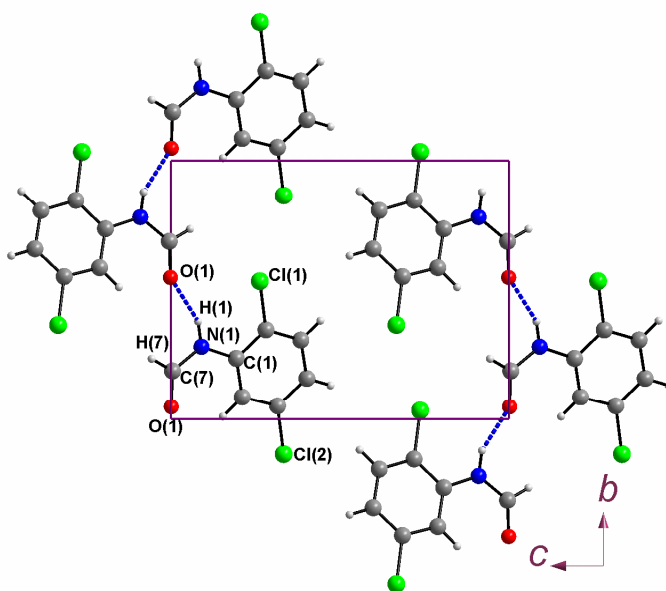


Figure 3.15: *ORTEP* diagram of 2,5-dichlorophenylformamide **9**. Ellipsoids are given at 50% probability level. The diagrams for 2,5-dibromophenylformamide **10** and 5-chloro-2-methylphenylformamide **12** can be found in the appendix.

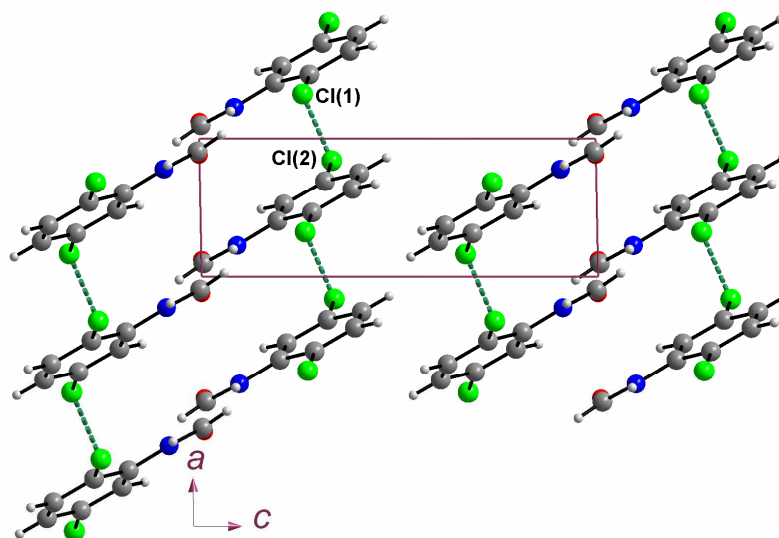
The molecular structure of 2,5-dichlorophenylformamide (**9**) accompanied with the atom numbering scheme as used in this discussion is given in Figure 3.15. The same numbering scheme is used in 2,5-dibromophenylformamide (**10**) and 5-chloro-2-methylphenylformamide (**12**). 2,5-dichlorophenylformamide crystallizes in the monoclinic space group $P2_1$, $Z = 2$ with one molecule in the asymmetric unit. The two

N-aryl -formamides and -thioamides

molecules in the unit cell are involved in N-H...O hydrogen bonding [N(1)...O(1) = 2.877(5) Å] resulting in chains that run down the crystallographic *b* axis. The molecules along the chains are related by a 2_1 -screw axis. Adjacent hydrogen bonded chains are linked together by two Cl...Cl interactions [Cl(1)...Cl(2) = 3.548(1) Å symmetry code -1+x,1+y,z, Cl(1)...Cl(2) = 3.603(1) Å, symmetry code x,1+y,z] that run diagonally across the crystallographic *ac* plane (see Figure 3.16b).



(a)

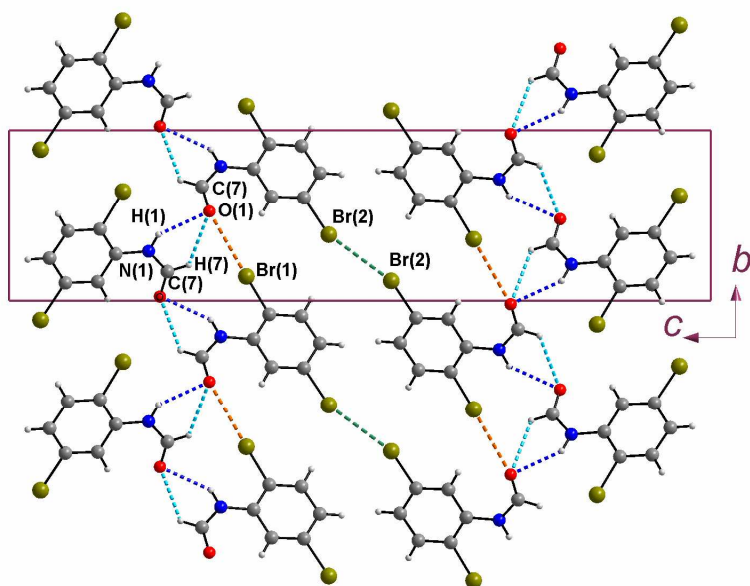


(b)

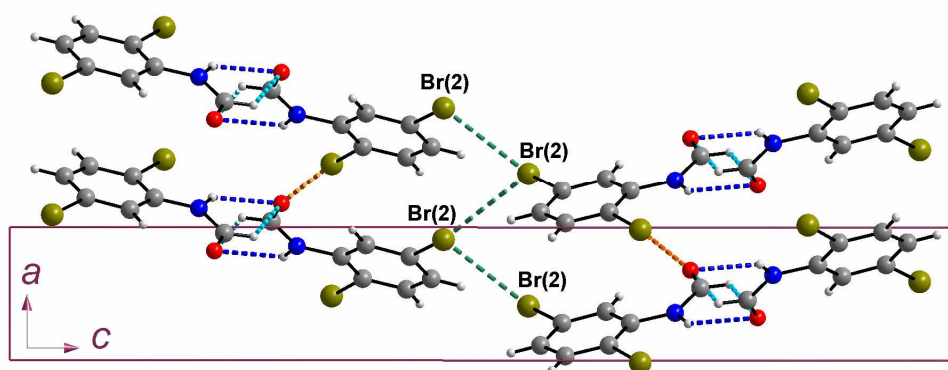
Figure 3.16: Packing diagram for 2,5-dichlorophenylformamide **9** as viewed down the crystallographic *a* axis. (a) N-H...O hydrogen bonds (b) view down the *b* axis showing Cl...Cl interactions (in green dashed lines) between N-H...O hydrogen bonded chains.

2, 5-dibromophenylformamide crystallizes with one molecule in the asymmetric unit in the chiral orthorhombic space group $P2_12_12_1$, $Z = 4$. The most significant intermolecular interaction is the N-H...O hydrogen bond [$N(1)...O(1) = 3.002 \text{ \AA}$] generating chains that run along the crystallographic *b* axis (see Figure 3.17a). The molecules along the chain are arranged in alternate directions. These chains are arranged in sheets parallel to the crystallographic *bc* plane. These sheets are connected *via* intermolecular Br...O interactions [$Br(1)...O(1) = 3.325 \text{ \AA}$], which result in a mesh-like network of symmetrically arranged formamide molecules (see

Figure 3.17b). Along the hydrogen bonded chain adjacent molecules are twisted out of the plane of one another by about 58.19° and are related by a 2_1 -screw axis (Figure 3.17c).



(a)



(b)

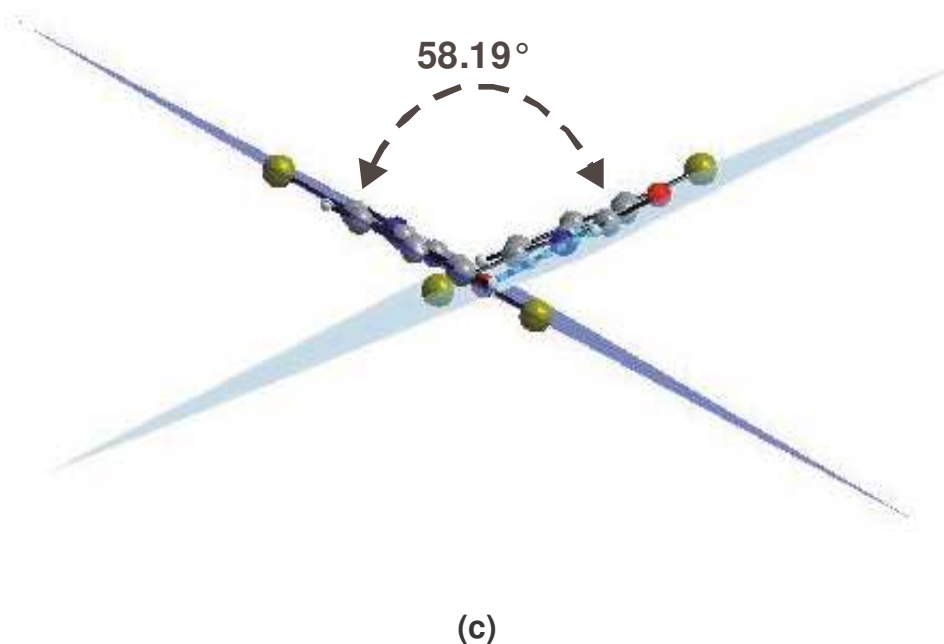
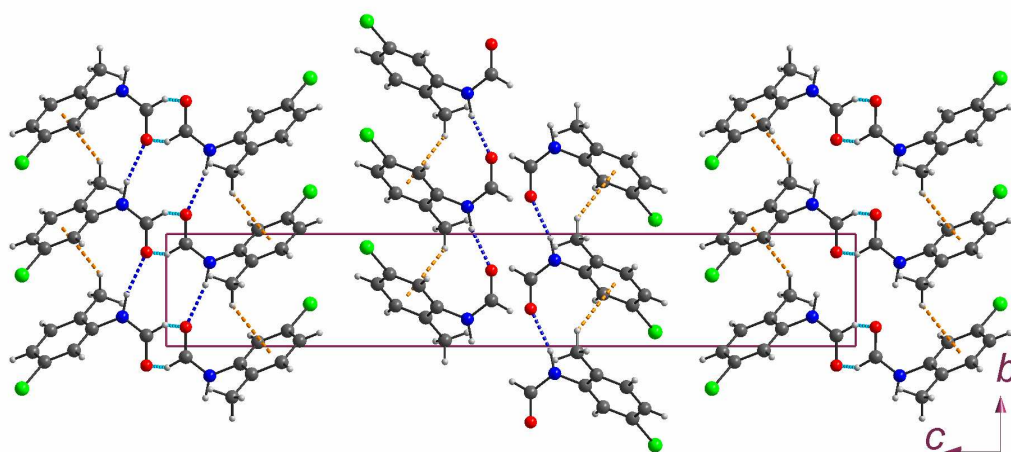


Figure 3.17: Packing diagram of 2,5-dibromophenylformamide; (a) View down the crystallographic *a* axis showing N-H...O hydrogen bonds (in blue dashed lines), C-H...O hydrogen bonds (in light blue) and Br...O interactions (in orange) between sheets of hydrogen bonded chains; (b) View down the crystallographic *b* axis. The Br...Br interactions shown in green are slightly longer than the sum of van der Waals radii of the two bromine atoms; and (c) the angle between adjacent molecules in a N-H...O hydrogen bonded chain.

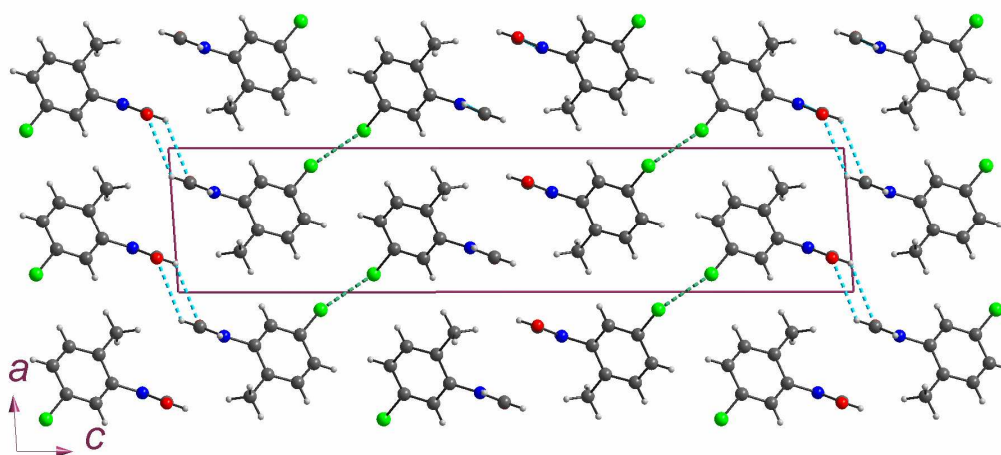
5-chloro-2-methylphenylformanilide crystallizes in the monoclinic space group $P2_1/c$ with one molecule in asymmetric unit, $Z = 4$. Each of the four molecules in the unit cell is involved in separate N-H...O hydrogen-bonded chains [$N(1)...O(1) = 2.874 \text{ \AA}$] which run in the crystallographic *b* direction (see Figure 3.18a). The molecules along the

N-aryl -formamides and -thioamides

chains are arranged in such a way that the aryl rings are stacked directly on top of each other (in a similar fashion as some of the 2,6 disubstituted arylformamides) resulting in C-H... π interactions [C(8)...Cg = 3.609 Å, C(8)-H(8)...Cg = 145.4°]. The molecules along these N-H...O hydrogen bonded chains are related by translation along *b*. Adjacent chains are linked together by C-H...O interactions between molecules related by a center of inversion on one side and by bifurcated Cl...Cl interactions [Cl(1)...Cl(1) = 3.551 Å, between molecules related by a 2₁ screw axis] on another side extending along the crystallographic *c* direction (see Figure 3.18b).



(a)



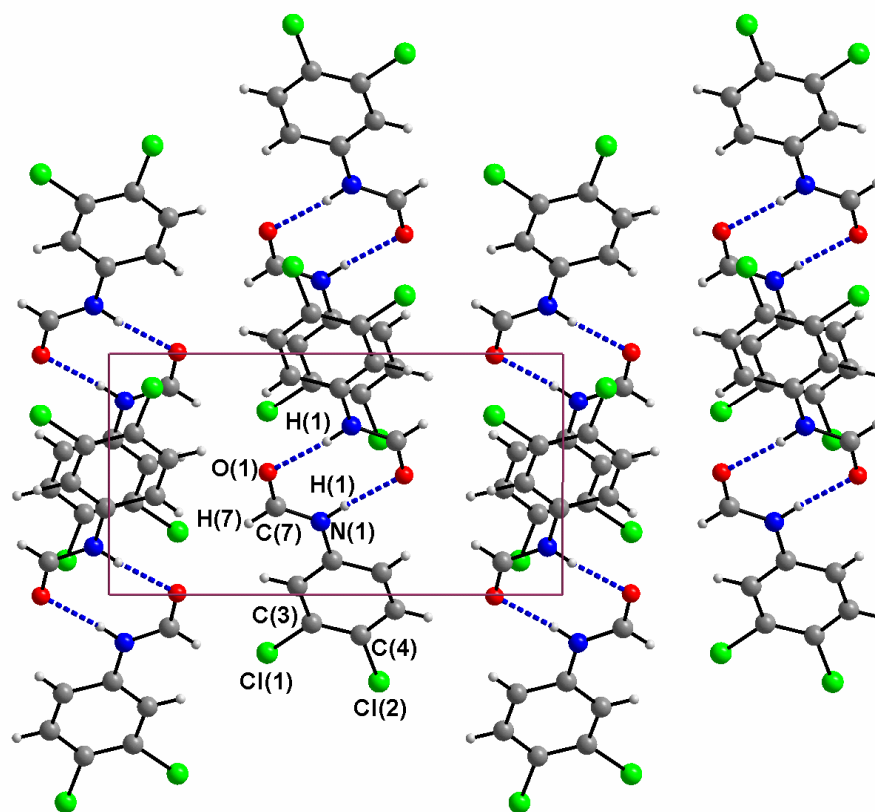
(b)

Figure 3.18: (a) Packing diagram of 5-chloro-2-methylphenylformamide showing intermolecular interactions between hydrogen-bonded chains, N-H...O hydrogen bonds (in blue dashed lines), C-H...O hydrogen bonds connecting adjacent N-H...O hydrogen bonded chains (in sky blue) and C-H... π intermolecular interactions (in gold). The C-H...O interactions result in a $R_2^2(6)$ graph set; and (b) Cl...Cl interactions in green dashed lines.

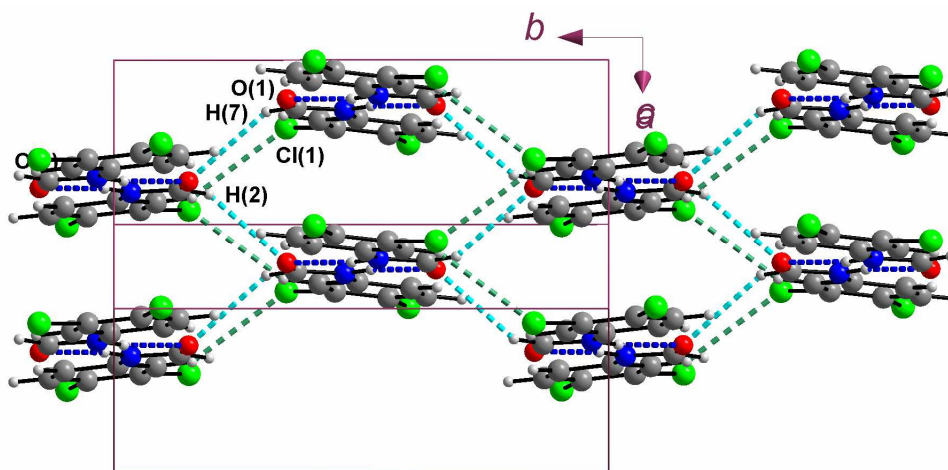
3.2.3.3 3,4-dichlorophenylformamide and 3,5-dichlorophenylformamide

3,4-dichlorophenylformamide forms crystals in the monoclinic space group $P2_1/c$ with one molecule in the asymmetric unit, $Z = 4$. The formamide moiety adapts a *cis* conformation as opposed to the *trans*-amide conformation that is common in the other formamides and most acetanilides from the literature. Unlike the other formamides discussed

here, this molecule forms N-H...O hydrogen bonded dimers [N(1)...O(1) = 2.907 Å] between molecules that are related by a center of inversion. The four molecules in the unit cell also form inversion-symmetry related pairs all involved in separate N-H...O hydrogen bonds. The hydrogen-bonded dimers are almost co-planar and result in sheets that run diagonally across the crystallographic *ac* plane when viewed down the crystallographic *b* axis (see Figure 3.19a). This inversion symmetry however is only approximately satisfied thus the molecules within each pair are not exactly parallel - Interplanar angles: molecule 1/molecule 2 = 0.60(3)°, 1/3 = 6.50(7)°, 1/4 = 0.50(3)°, 2/3 = 6.70(7)°, 2/4 = 0.60(1)° and 3/4 = 7.00(7)° with planes calculated through all non hydrogen atoms. The hydrogen bonded dimers are related to one another by a 2₁ screw axis. The sheets of dimers are connected to adjacent ones through C-H...O interactions [H(7)...O(1) = 2.771, <C(7)-H(7)...O(1) = 146.0°] and C-H...Cl interactions [H(2)...Cl(1) = 2.771 Å] between molecules that are related by a 2₁-screw axis (see Figure 3.19a and b). The formation of a N-H...O hydrogen bonded dimer and the existence of the compound in a *cis*-amide conformation occur at the same time (its hard to say which one leads to the other). We note that, apart from 2-methylphenylformamide [Boeyens et. al., 1988], this is the only other formamide that crystallizes in the *cis* conformation.



(a)



(b)

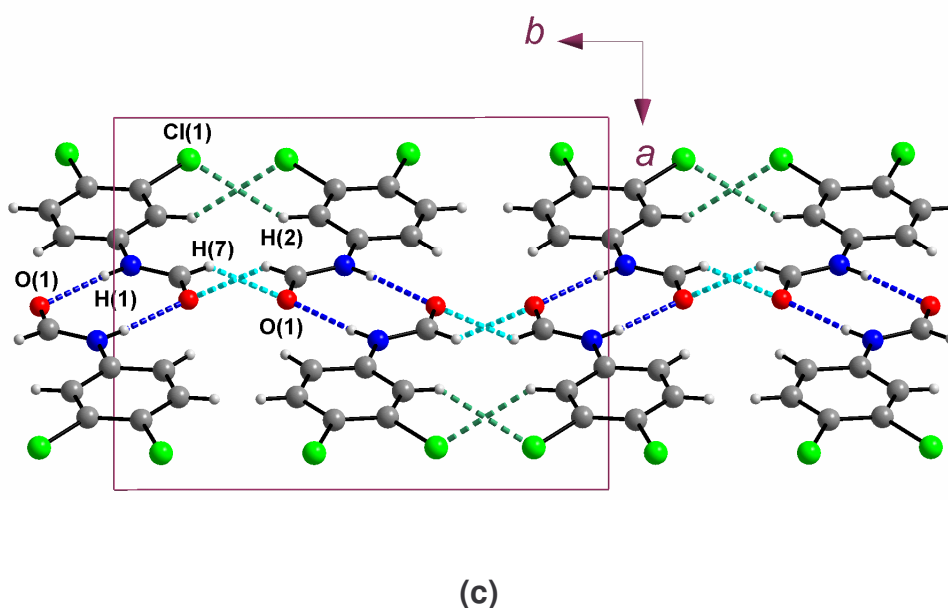


Figure 3.19: Packing diagrams of *cis*-3,4-dichlorophenylformamide; (a) N-H...O hydrogen bonded dimers (hydrogen bonds are shown in dashed blue lines) as viewed along the crystallographic *a* axis; (b) C-H...O interactions (in light blue) and C-H...Cl in green dashed lines) connecting the hydrogen bonded dimers; and (c) a viewed down the crystallographic *c* direction showing the N-H...O, C-H...O and the C-H...Cl interactions.

3,5-dichlorophenylformamide crystallizes in the monoclinic space group $P2_1/n$ $Z = 4$, with one molecule in the asymmetric unit. In the crystal the molecules are joined via N-H...O hydrogen bonds forming sheets (see Figure 3.20) of molecules related by a 2_1 -screw axis that run diagonally across the crystallographic *ac* plane. Adjacent hydrogen bonded chains are connected through π ... π interactions [$Cg...Cg = 3.694 \text{ \AA}$] (Figure 3.21) between molecules that are related by a center of inversion.

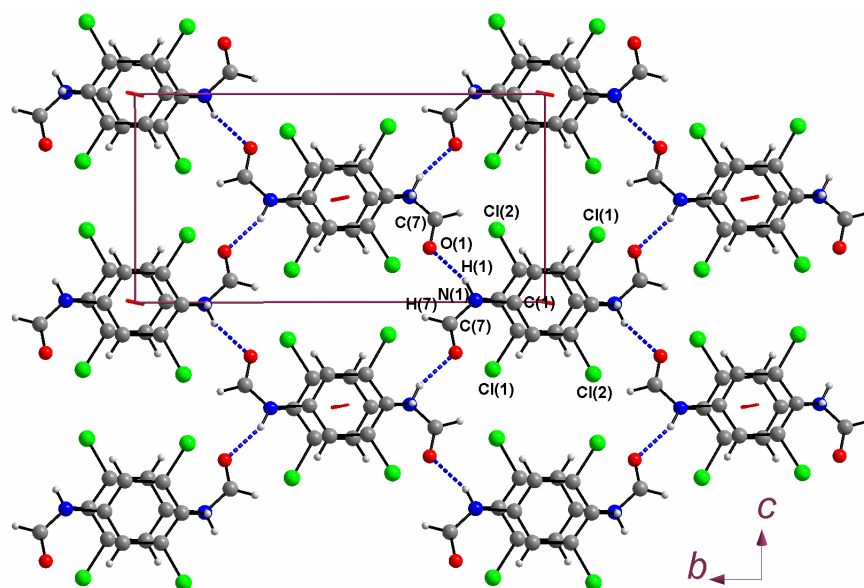


Figure 3.20: Packing diagram of 3,5-dichlorophenylformanilide as viewed down the crystallographic *a* axis. N-H...O hydrogen bonds in blue dashed lines.

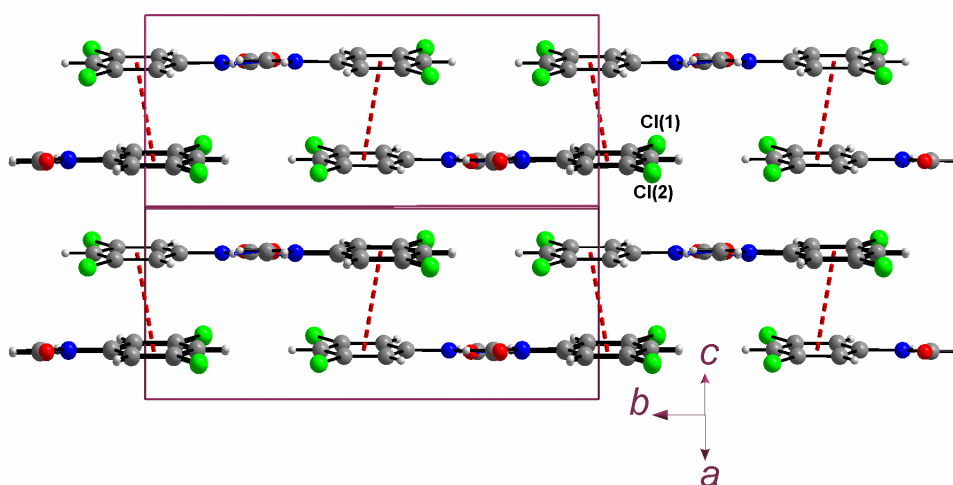


Figure 3.21: Packing diagram of 3,5-dichlorophenylformanilide. π ... π Intermolecular interactions connecting adjacent N-H...O hydrogen bonded chains (in red dashed lines).

3.2.4 Discussion of crystal packing and intermolecular interactions in compounds 7 - 14

Although compounds **7 - 14** are all planar [except for 5-chloro-2-methylphenylformamide (**12**)] and in *trans*-conformation [except for compound (**13**)] there are significant differences in their packing. The N-H...O hydrogen bond is important in each of the structures (as it is in all of them). The 2,4-disubstituted formamides **7** and **8** form sheets of N-H...O hydrogen bonded chains which are either planar (**7**) or corrugated (**8**). The sheets are connected C-H...Cl interactions and are almost planar in **7** and by C-H...O interactions and corrugated in **8**.

The 2,5-disubstituted arylformamides **9**, **10** and **12** have halogen contacts Cl...Cl for **9**, Br...Br and Br...O for **10** and Cl...Cl for **12**. The methyl group in compounds **12** besides making the aryl ring electron rich acts as a proton donor in a C-H... π interaction which stabilizes the N-H...O hydrogen bond. Whereas **9** makes hydrogen bonded sheets diagonally across the *ac* face, **10** forms corrugated sheets extending in the *c* direction and **12** stacks similar to the ones formed by Category 2 compounds.

3,4-dichlorophenylformamide (**13**) has no π ... π interactions with closest distance between two overlaying aryl rings being 4.687 Å. C-H...O and C-H...Cl interactions are important in this compound. 3,5-dichlorophenylformamides (**14**) on the other hand has π ... π interactions

which are important in the solid state structure. Amongst the compounds discussed in this section (**7** to **14**), **14** has the strongest $\pi\cdots\pi$ interactions and the longest Cl...Cl contacts (3.665 Å). The rest of the compounds have fairly long *Cg*...*Cg* distances (between 3.8 and 4.1 Å) between the centers of overlaying aryl rings and as such the $\pi\cdots\pi$ interactions are not as important as the other interactions (C-H...Cl, C-H...O, Cl...Cl, Br...Br) in their structures.

All compounds form chains described by C(4) graph set notation except for 3,4-dichlorophenylformamide (**13**) which forms hydrogen bonded dimers. This compound adopts a *cis* conformation and forms hydrogen bonded dimers described by a $R_2^2(8)$. Adjacent C(4) chains in 5-chloro-2-methylphenylformamide are joined together by C-H...O interactions resulting in rings described by $R_2^2(6)$ graph set notation, or together with N-H...O interactions, rings described by $R_4^2(10)$.

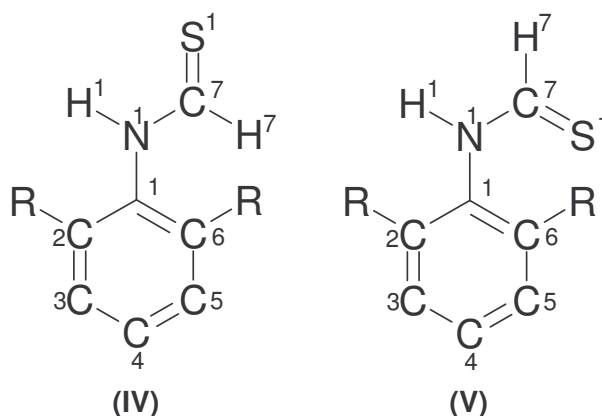
3.3 2,6-disubstituted arylthioamides

3.3.1 Introduction

Another variation to the 2,6 disubstituted amides was to change the C=O group to a C=S group. Six arylthioamides of this nature were synthesized from their formamide analogues. It was hoped that electronic influences as well as the difference in size of the oxygen atom and sulphur

atom would give a totally different kind of hydrogen bonding pattern. Further these compounds could have a different amide conformation to the common *trans* conformation that arylformamides adopt. It would also be of interest if a change from the formamide to thioamide would result in a variety of interesting structural polymorphs. Our comparison of the two systems will expand on the investigation carried out by Allen *et al.* [1997] since we also include lattice energy calculations as well as energies relating molecule-to-molecule interactions. The compounds synthesized in this category were: 2,6-difluoro- **15**, 2,6-dichloro- **16**, 2,6-dimethyl- **17**, 2-chloro-6-methyl- **18**, 2,6-dibromo- **19** and 2,6-diisopropyl- **20**, arylthioamides. Interestingly all but compound **20** had a *cis*-amide conformation.

3.3.2 Molecular structures of 2,6-disubstituted arylthioamides



Scheme 3.4: Schematic diagrams for the 2,6-disubstituted arylthioamides **15** to **20** together with the atom numbering scheme. R = F (**15**), Cl (**16**), Me (**17**), Cl and Me (**18**) and Br (**19**), [IV] and iPr (**20**), [V].

Scheme 3.4 [(IV) and (V)] is a schematic representation of the thioamides discussed in this section. Important bond distances and angles are given in Table 3.5. Compounds **15** to **19** adopt a *cis* conformation (IV in Scheme 3.4) in which the sulfur atom is on the same side as the hydrogen atom attached to the nitrogen atom. 2,6-diisopropylphenylthioamide **20** is the only exception. It adopts a *trans* conformation (V), same as its formamide analogue. All six molecules have two planes defined by the aryl ring [C(1) – C(6)] and the thioamide moiety [C(1)-N(1)-C(7)=S(1)]. The angle between these two planes ranges between 53 and 77° for the six compounds (see Table 3.5). Substitution at the 2 and 6 positions of the aryl ring and hydrogen bonding are some reasons for the non-planarity. Another reason could be a reduced overall effective conjugation of the π -orbitals of the aromatic ring and the thioamide moieties [Pauling, 1960]. The π components of the C=S bond are relatively weak due to the poor overlap between $2p$ and $3p$ orbitals (weaker also in relation to their formamide analogues) and the electronegativity of S is also low and closer to that of C [Pauling, 1960]. These factors are known reasons for the elongation of C=S bond distance and the planarity of the thioamide moiety [Allen et al., 1987]. The ionic resonance structure $\text{RN}^+(\text{H})=\text{C}(\text{H})-\text{S}^-$, (III) in Scheme 3.4 [Allen et al., 1997] is preferred hence a high rotation barrier for the thioamides moiety. This has been also established by NMR studies in which there is always one major conformer. This *cis* conformer exists as the major conformer in

are shorter than that of a typical C=N double bond of 1.334 Å by as much as 0.042 Å for 2,6-diisopropylphenylthioamide and as little as 0.019 Å for 2,6-dichlorophenylthioamide. Because of this shortening of the N=C double bond, the C=S double bond is as expected considerably elongated and is longer than that of a typical C=S double bond (1.61 Å) [Steiner et al., 1998; Allen et. al.,1997]. These C=S bond lengths normally span a wide range, from 1.58 Å in pure thiones to 1.75 Å in thioureido species. This is according to a CSD search [Allen et. al., 1997] in which it was found that for thioamides the distance was slightly longer than for a standard C=S double bond. In compounds **15** to **20** the difference between the C=S bond and that of a typical C=S bond ranges between 0.029 Å and 0.037 Å. It is also notable that there is no general relationship between the formally double C=S and single N-C bond distances [C(7)=S(1) and N(1)-C(7)] for compounds **15** to **20**, similar to the one known for RN₃C=O systems [Blessing, 1993] (see Figure 3.22).

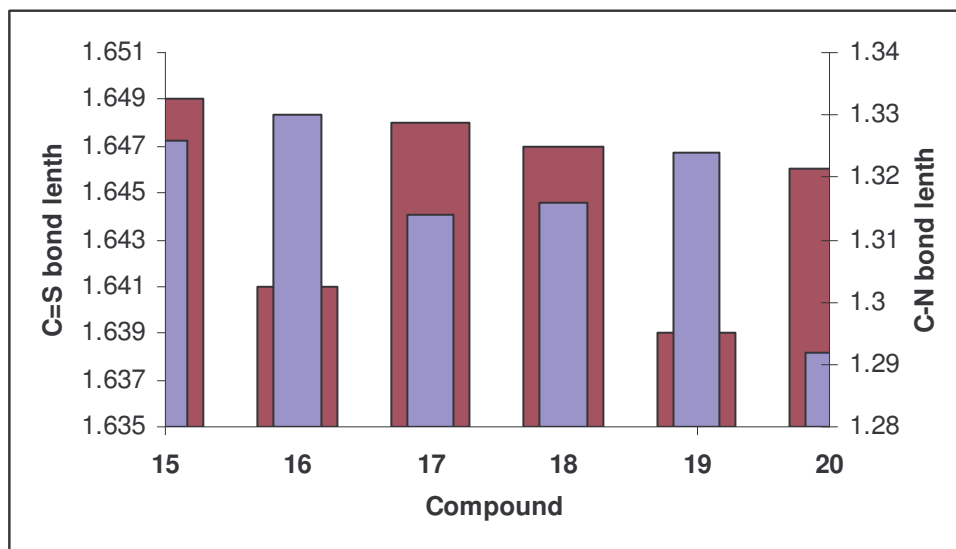


Figure 3.22: Histogram of C=S (shown in maroon) vs. C=N (shown in purple) bond lengths for compounds **15** – **20**.

3.3.3 Crystal packing and intermolecular interactions

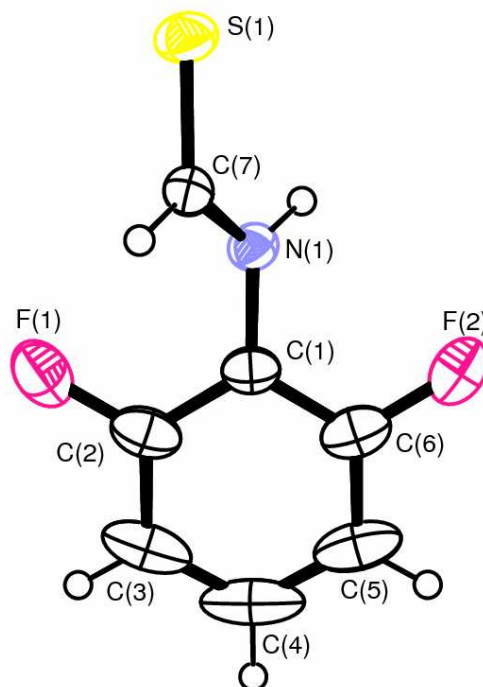


Figure 3.23: ORTEP diagram of 2,6-difluorophenylthioamide **15**. Thermal ellipsoids of non-H atoms are given at 50% probability level and only non-hydrogen atoms are labeled (H atoms are shown at an arbitrary radius).

Figure 3.23 shows the molecular structures of 2,6-difluorophenylthioamide with the atom-labeling scheme as used throughout this section. The structures of compounds **16**, **17**, **18** and **19** resemble that of compound **15** and are therefore given in the appendix.

2,6-difluorophenylthioamide **15** crystallizes in the orthorhombic space group *Pbca*, $Z = 8$ with one molecule in the asymmetric unit. Each of the eight molecules are involved in separate N-H...S hydrogen-bonded chains [N(1)...S(1) = 3.307 Å]. The hydrogen bonds form infinite chains of molecules related to each other by a glide plane in the crystallographic *b* direction resulting in the arylthioamide molecules pointing in alternating directions (see Figure 3.24). Adjacent chains are held together through weak C-H...S interactions [H(4)...S(1) = 2.860 Å] between molecules forming sheets that run along the crystallographic *a* axis and almost perpendicular to the N-H...S hydrogen-bonded chains. Besides the C-H...S interaction π ... π intermolecular interactions [*Cg*...*Cg* = 4.262 Å symmetry operators = $1/2-x, -1/2+y, z$ and $1/2-x, 1/2+y, z$ respectively] between molecules related by inversion symmetry connect the N-H...S hydrogen bonded chains completing a supramolecular assembly of molecules in the crystal. Other weak interactions contributing to the overall packing pattern in the crystal include intramolecular H...F interactions [H(7)...F(2) = 2.680 Å].

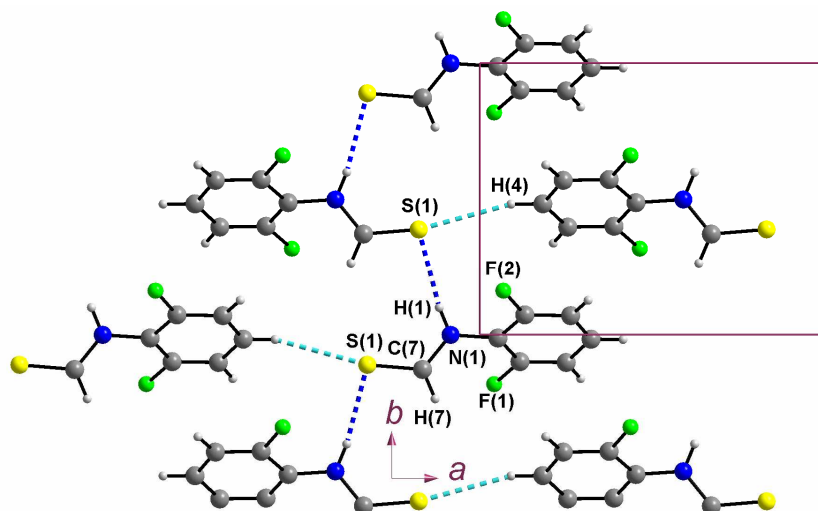


Figure 3.24: N-H...S hydrogen bonding chains of 2,6-difluorophenylthioamide as viewed down the crystallographic *c* axis (shown in blue dashed lines). Neighboring hydrogen bond chains are connected via C-H...S hydrogen bonds (light blue dashed lines).

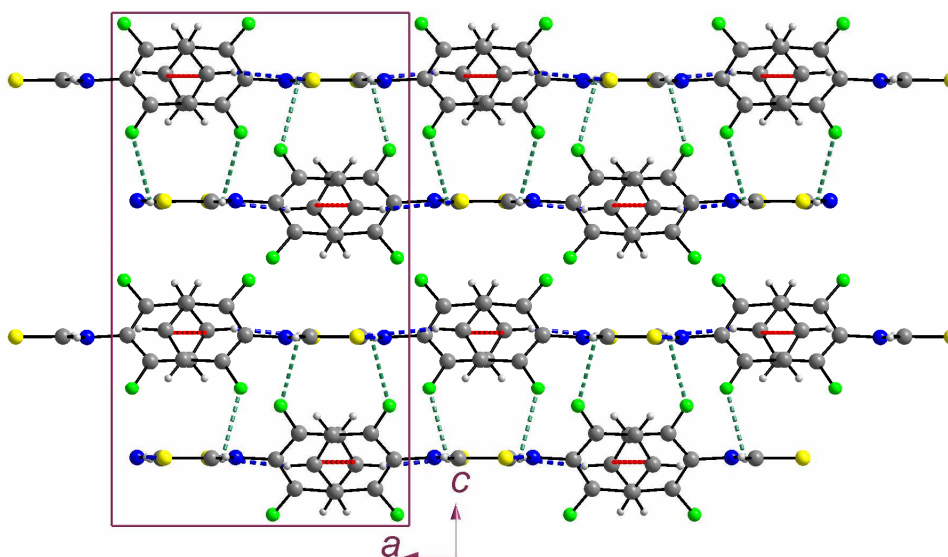
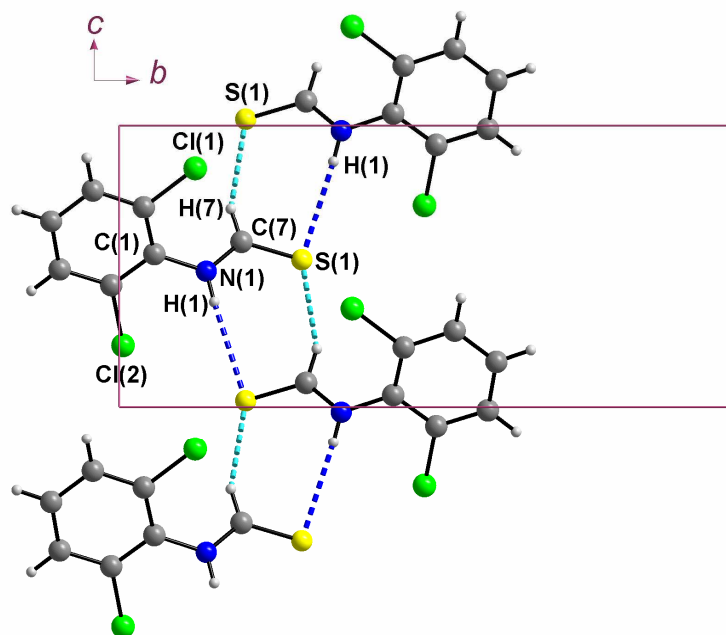
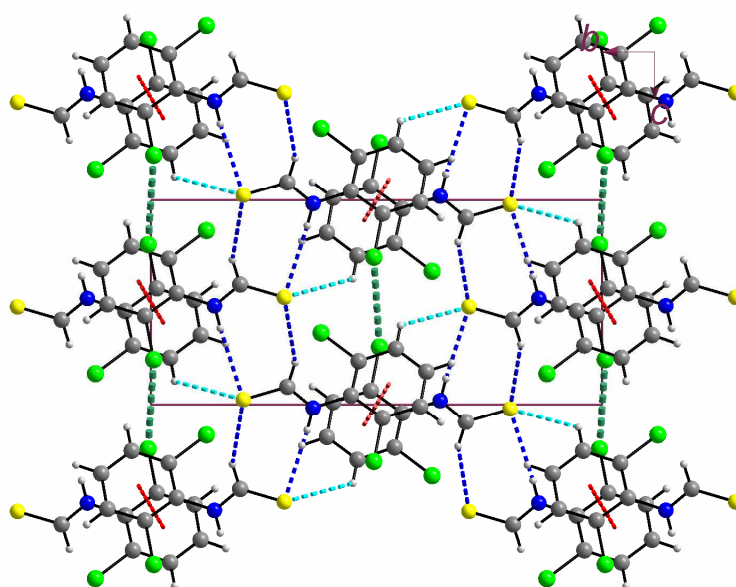


Figure 3.25: Packing diagram for 2,6-difluorophenylthioamide as viewed down the crystallographic *b* axis showing F...H (in green dashed lines) and π ... π (in red dashed lines) interactions that also link the hydrogen bonded chains.

2,6-dichlorophenylthioamide, compound **16** crystallizes in the monoclinic space group $P2_1/c$, $Z = 4$ with one molecule in the asymmetric unit. The crystal packing of this compound is governed mainly by a set of weak intermolecular interactions: planar ribbons of the arylthioamide molecules are obtained through the formation of N-H...S and a C-H...S intermolecular hydrogen bonds hereby forming a ring described by a $R_2^2(7)$ graph set (see Figure 3.26). The ribbons are between molecules that are related by a glide plane and run parallel to the crystallographic c direction with the thioamide molecules along the ribbons pointing in alternate directions. These ribbons are connected by a second C-H...S interaction [$H(3)...S(1) = 3.100 \text{ \AA}$] and a $\pi... \pi$ interaction [$Cg...Cg = 4.9887 \text{ \AA}$] between molecules that are related by inversion symmetry. In addition to the $\pi... \pi$ interactions, there are Cl...Cl interactions [$Cl(2)...Cl(2) = 3.591 \text{ \AA}$, see Figure 3.26] between molecules that are related by a center of inversion. This Cl...Cl contact is slightly longer than the sum of van der Waals radii of the Cl atoms.



(a)



(b)

Figure 3.26: (a) Diagram of 2,6-dichlorophenylthioamide as viewed down the *a* axis. N-H...S hydrogen bonds and C-H...S interactions which form ribbons running along the crystallographic *c* axis are indicated by blue and

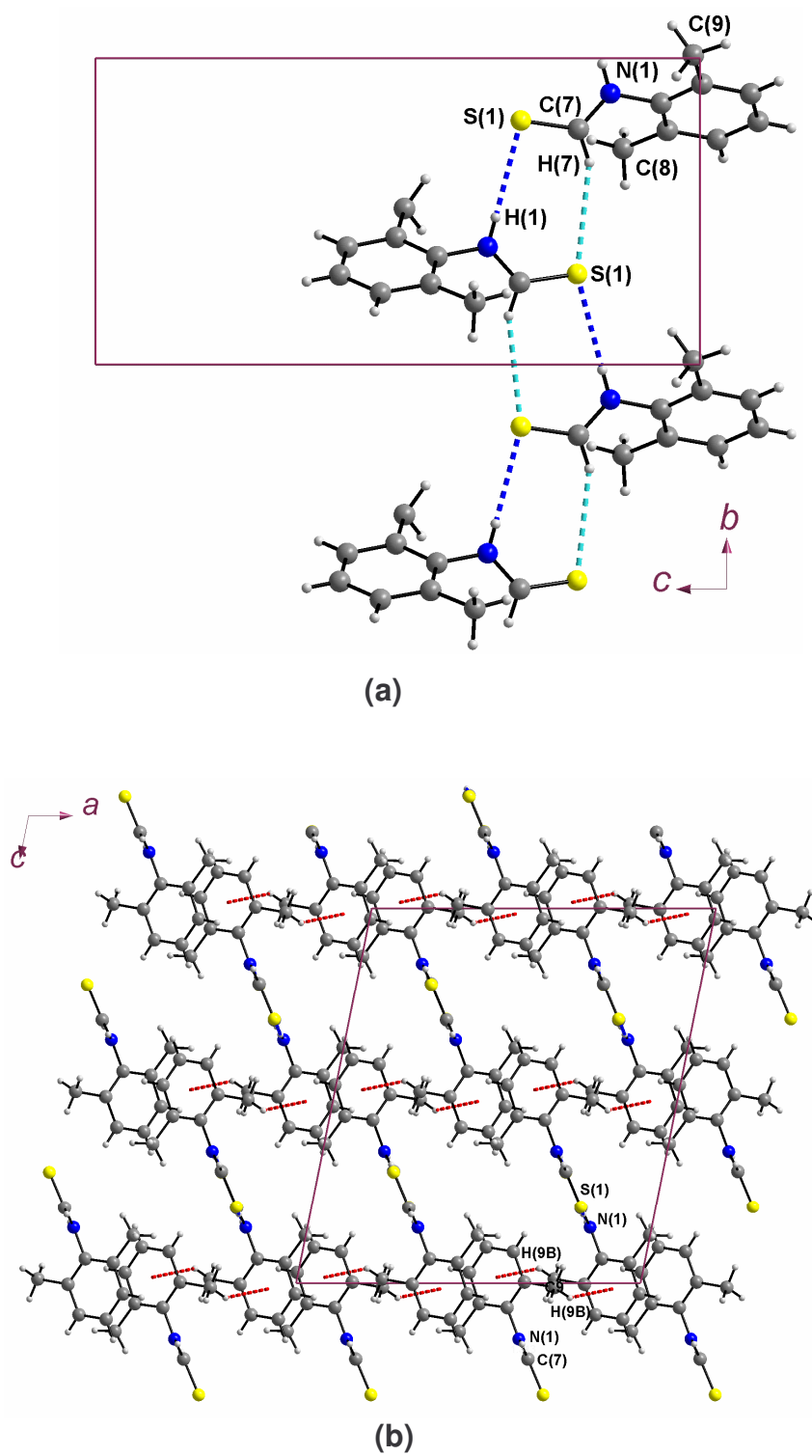
***N*-aryl -formamides and -thioamides**

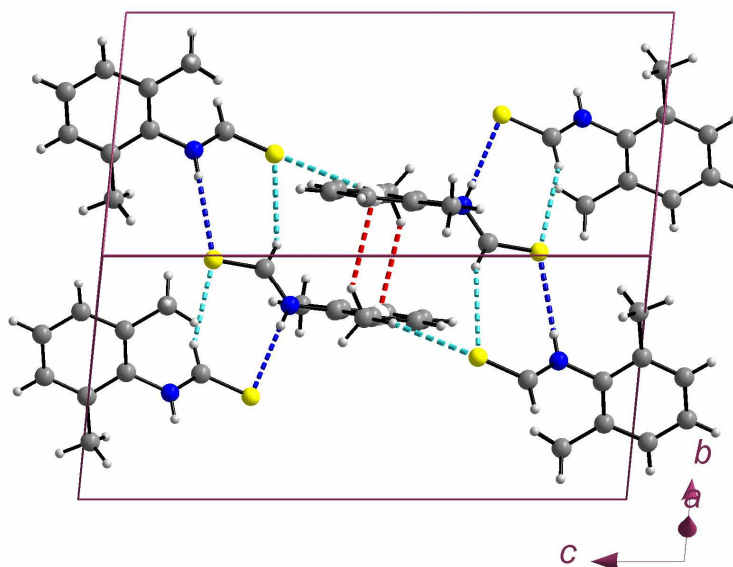
sky blue dashed lines respectively. (b) Packing diagram of 2,6-dichlorophenylformamide showing the ribbons connected via $\pi\cdots\pi$ interactions (indicated by red dashed lines) and Cl...Cl interactions (green dashed lines).

2,6-dimethylphenylthioamide, compound **17** crystallizes in the monoclinic space group $C2/c$, $Z = 8$. In the crystal the sulfur atom S(1) is involved in three intermolecular interactions (see Figure 3.27a). Symmetry related molecules of $C_6H_3(CH_3)_2N(H)C(H)S$ associate to form centrosymmetric thioamide dimers. These dimers are composed of molecules that are related by a glide plane and are connected by the main N-H...S hydrogen bond [N(1)...S(1) = 3.453 Å] together with a C-H...S hydrogen bond [H(1)...S(1) = 2.640 Å, see geometric parameters in Table 3.4]. This results in infinite ribbons that run along the crystallographic b direction. The second molecule of the dimers is generated by the symmetry operator $3/2-x, 1/2+y, 3/2-z$. The thioamide S(1) is involved in a third interaction. This interaction connects neighboring ribbons and is between molecules that are related by symmetry operators $[x, 1-y, 1/2+z]$ and $[3/2-x, 1/2-y, 1-z]$ resulting in tetrameric units composed of four arylthioamide molecules, two from each ribbon (Figure 3.27c). Each hexameric unit is formed via C-H...S [H(9A)...S(1) = 2.940 Å] and N-H...S interactions, which also form chains running parallel to the crystallographic b axis. The hexameric units are in addition held together by C-H... π

N-aryl -formamides and -thioamides

[H(9b)...Cg = 2.828 Å, C(9)-H(9b)...Cg = 144°] between molecules from neighboring ladders (Figure 3.27b and Table 3.4).





(c)

Figure 3.27: Packing diagrams for 2,6-dimethylphenylthioamide. (a) View down the *a* axis showing N-H...S and C-H...S hydrogen bonds which form ribbons that run down the crystallographic *b* axis, indicated by blue and light blue dashed lines respectively; (b) View down the crystallographic *b* axis showing C-H... π interactions that linked up the ribbons (indicated by red dashed lines); and (c) C-H...S and C-H... π interactions forming units of molecules each between adjacent ribbons (light blue dashed lines).

2-chloro-6-methylphenylthioamide **18**, also crystallizes in the monoclinic space group $C2/c$, $Z = 8$. This compound is isomorphous to compound **17**. The hydrogen bonding patterns are similar. The respective hydrogen bonding distances and angles are in Table 3.6. Further comparison of the two compounds is done in chapter 5. Figure 3.28 shows C-Cl... π interactions [$\text{Cl}(1a)\dots\text{Cg} = 3.582$] indicated by red dashed lines

N-aryl -formamides and -thioamides

and Cl...Cl interactions [Cl(1a)...Cl(1a) = 3.682] indicated by the green dashed line that link up the ribbons in compound **18**.

Table 3.6: Geometric parameters for compound **17** and **18** showing intermolecular distances and angles for π ... π and C-H... π interactions

Donor-H...Acceptor	D-H (Å) 17 / 18	H...A (Å) 17 / 18	D...A (Å) 17 / 18	<D-H...A (°) 17 / 18
N(1)-H(1)...S(1) ¹	0.84 / 0.84	2.650 / 2.610	3.455 / 3.434	177.0 / 176.9
C(X)-H(X)...S(1) ¹	0.98 / 0.98	2.430 / 2.940	2.922(2) / 2.936	111.0 / 106.0
π ... π	<i>Cg</i> ... <i>Cg</i> (°)	Closest distance of approach (Å)	Interplanar angle (°)	
<i>Cg</i> (1)... <i>Cg</i> (2) ²	3.723(2) / 3.676(3)	3.664/3.618	0.02/0.00	
X(I)-H(I)... π (J)	H(I)... π (J) (Å)	X(I)... π (Å)	<X(I)-H(I)... π (°)	
C(8)-H(8c) ... <i>Cg</i> (1) ⁵	2.893 / 3.008	3.768/ 3.679	157.30 /	

Symmetry operators (1) 1/2-x,-1/2+y,1/2-z; (2) -x, 1 - y, -z; (3) -x, 2 - y, -z; (4) 1/2 - x, 3/2 - y, -z.; (5) 1/2 - x, 3/2 - y, - z. / Symmetry operators (1) -x+3/2, y+1/2, -z+1/2; (2) 2-x, -y, 1-z; (3) 2-x, 1-y, 1-z; (4) 3/2-x, 1/2-y, 1-z; (5) 3/2-x,1/2-y,1-z.

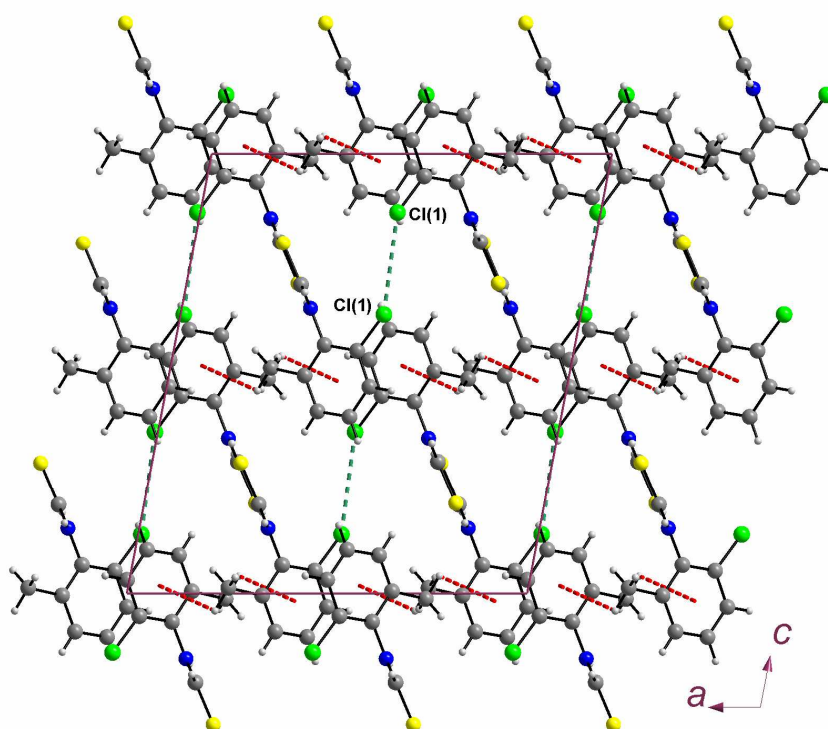


Figure 3.28: Packing diagram of 2-chloro-6-methylphenylthioamide as viewed down the *a* axis. Cl...Cl and C-H... π interactions which link up the ribbons are indicated by green and red dashed lines respectively.

Compound **19**, 2,6-dibromophenylthioamide crystallizes in the monoclinic space group, $P2_1/c$, $Z = 4$ with one molecule in the asymmetric unit. The molecules form hydrogen bonded chains in the solid state. A ribbon-like arrangement similar to that found in compounds **17** and **18** is formed through hydrogen-bonded chains of molecules that are involved in N-H...S hydrogen bonds [$N(1)...S(1) = 3.465 \text{ \AA}$] and C-H...S intermolecular interactions [$H(7)...S(1) = 3.160 \text{ \AA}$]. The sulphur atom of the thioamide is involved in a bifurcated C-H...S interaction and a N-H...S hydrogen bond. The second C-H...S interaction [$H4...S1 = 2.903 \text{ \AA}$] links

N-aryl -formamides and -thioamides

adjacent ribbons forming sheets that run diagonally along the crystallographic *bc* plane (see Figure 3.29). A glide plane relates the molecules along these ribbons, which run down the crystallographic *b* axis. Adjacent ribbons are further stabilized by π ... π interactions [Cg ... Cg = 3.537 Å] between molecules that are related by an inversion center. There are no Br...Br interactions in the solid state structure of this compound but C-Br... π interactions [$Br(2)$... Cg = 3.492 Å, $C(6)$ - $Br(2)$... Cg = 176°].

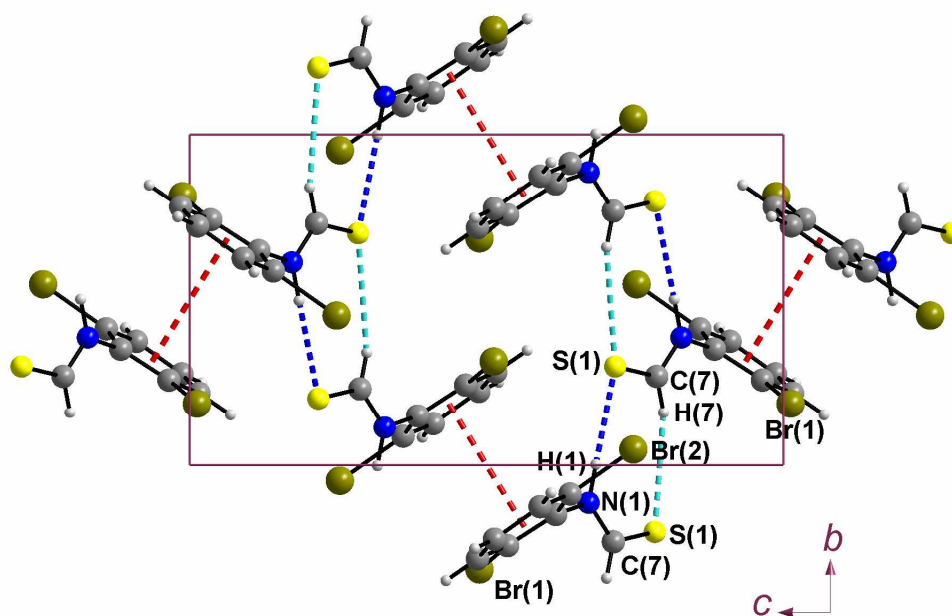


Figure 3.29: Packing diagram of 2,6-dibromophenylthioamide showing ribbons formed by N-H...S (in blue) and C-H...S (in light blue) hydrogen bonds and π ... π interactions (in red dashed lines) that link up adjacent hydrogen bonded ribbons.

The crystal morphology of 2,6-diisopropylphenylthioamide **20** may be described as pale yellow blocks. Like 2,6-diisopropylphenylformamide, this compound crystallizes in the centrosymmetric monoclinic space group $P2_1/c$, $Z = 4$. Unlike compounds **15** to **19** and also most of other aryl thioamides reported in the literature this compound prefers the *cis* conformation in the solid state similar to the one preferred by their formamide analogues. In the solid state molecules are connected via N-H...S hydrogen bonds [N(1)...S(1) = 3.318 Å] resulting in chains that run in the crystallographic *b* direction. Unlike in the formamide analogue, in which each of the molecules in the unit cell is part of a separate N-H...O hydrogen bond, in this crystal two of the four molecules in the unit cell belong to the same N-H...S hydrogen bond. There are also two intramolecular hydrogen bonds between the methine hydrogens of C(8) and C(9) [H(8) and H(9) respectively] and N(1) with distances of about 2.904 for C(8)...N(1) and 2.861 Å for C(9)...N(1). These two C-H...N interactions and steric bulk of the isopropyl groups together could be the cause of the large angle between the plane of the aryl ring and that of the thioamide moiety (77.57°). There are also two C-H... π and two π ... π intermolecular interactions (distances are in Table 3.7) in the solid state structure of compound **20**. One of the C-H... π interactions is to be found along the N-H...S hydrogen bond and is between adjacent molecules that are related by a glide plane. The other C-H... π interaction is between molecules from adjacent N-H...S hydrogen bonded chains. These molecules are related by an inversion center in the centers of *ac* and *bc*

faces of the unit cell. The $\pi\cdots\pi$ interactions which link the N-H...O hydrogen bonded chains are between molecules that are related by an inversion center.

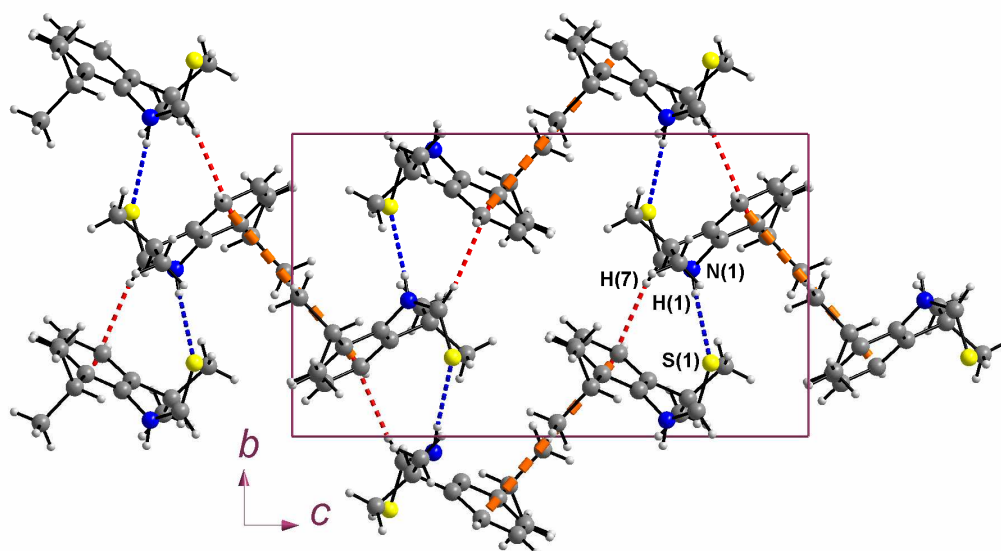


Figure 3.30: Packing diagram for 2,6-diisopropylphenylthioamide. N-H...S hydrogen bonded chains shown in blue dashed lines while C-H... π and $\pi\cdots\pi$ interactions are shown in red and orange dashed lines.

Table 3.7: Geometric parameters for 2,6-diisopropylphenylthioamide.

Donor-H...Acceptor	D-H (Å)	H...A (Å)	D...A (Å)	<D-H...A (°)
N(1)-H(1)...S(1) ¹	0.83(3)	2.50(3)	3.318(3)	167(3)
C(8)-H(8)...N(1) ¹	0.98	2.54	2.902(4)	108
C(9)-H(9)...N(1) ¹	0.98	2.34	2.861(5)	109
$\pi\cdots\pi$	Cg...Cg (Å)	Closest distance of approach (Å)	Interplanar angle (°)	
Cg(1)...Cg(2) ²	5.936(4)	5.221	0.00	
X(l)-H(l)... π (j)	H(l)... π (j) (Å)	X(l)... π (Å)	<X(l)-H(l)... π (°)	
C(7)-H(7) ...Cg(1) ³	2.7478	3.637(4)	160.36	
C(10)-H(10) ...Cg(1) ⁴	3.2556	3.740(4)	113.25	

Symmetry operators (1) 1-x, 1/2+y, 1/2-z; (2) 1-x, 2-y, 1-z; (3) 1-x, 1/2+y, 1-z; (4) 1-x, 2-y, 1-z.

3.3.4 Discussion of crystal packing and intermolecular interactions in compounds 15 - 20

In this class of compounds N-H...S hydrogen bonds and $\pi\cdots\pi$ intermolecular interactions are the most important interactions. The $\pi\cdots\pi$ interactions are present in the structures of every compound except for 2,6-dimethylphenylthioamide **17**. This compound has however a C-H... π interaction that links adjacent ribbons the same way as $\pi\cdots\pi$ does in the other structures. A look at the torsion angles between the plane of the aryl ring and the thioamide moiety shows that this angle is slightly larger in 2,6-dimethylphenylthioamide **17** (63.9°), 2,6-bromophenylthioamide **18** (62.6°) and 2,6-diisopropylphenylthioamide **20** (80.7° *trans* conformation) as compared to the other compounds (\approx 53, 54 and 60°). The size of this angle together with the presence of methyl groups in compounds **17** and **20** could be the reason for the absence of significant $\pi\cdots\pi$ interaction in their structures. The methyl groups lead to the formation of C-H... π .

Compounds **15** and **20** form C(4) chains, **16** – **19** ribbons via C-H...S and N-H...S interactions described by the $R_2^2(7)$ graph set. The ribbons are connected by $\pi\cdots\pi$ or C-H... π intermolecular interactions between molecules related by inversion centers.

3.4 Phenylformamide

3.4.1 Introduction

The structure of phenylformamide has been discussed separately in this thesis because it has no substituents on the aryl ring and also because of the interest it has attracted in a number of previous studies. Until this work crystallographic data on phenylformamide has not been reported. Studies of the compound have been largely theoretical [see Chapter 1, Moisan and Danneberg, 2003; Kobko and Danneberg, 2003; Vargas *et. al.*, 2001; Bock *et. al.*, 1995; Manea *et. al.*, 1997; Pliego and Riveros, 2002]; the investigations include, resonant two-photon ionization spectroscopy [Federov and Cable, 2000], laser-induced fluorescence excitation [Dickinson *et. al.*, 1999], Density functional theory studies (DFT) [Doerksen *et. al.*, 2004], molecular orbital calculations and infrared ultra-violet double resonance spectroscopy. The study of this compound has been immensely valuable in the theoretical investigation of the structure of proteins, mainly protein folding and stability. This is because experimental measurements have almost always been indirect and typically have been based upon a theoretical interpretation of the infrared resonance, Raman or NMR spectra of model systems such as formamide (the simplest example), or *N*-alkyl or *N*-aryl amide-water clusters, either isolated in a matrix or dispersed in an aqueous solution [Dickinson *et. al.*, 1999].

Phenylformamide was synthesized using the same method as the previously discussed formamides but gives a brown liquid which is distilled

under vacuum to give a cream powder. The solution NMR spectrum for this powder in CDCl_3 showed equal concentrations of both *cis* and *trans*-isomers. Crystals of the compound were grown from chloroform, ethanol, dichloromethane and THF all of which gave crystals of the same conformational form as was evident from powder XRD experiments. Another portion was grown from DMF. The powder XRD pattern differed from crystals obtained from other solutions, implying that it is a different polymorph or solvate.

3.4.2 NMR spectroscopic studies of compound 21

Proton magnetic resonance spectra of an equilibrium mixture of the *cis* and *trans* isomers in CDCl_3 were recorded at room temperature for the powder sample and the crystalline sample. Table 3.8 lists the chemical shift values for both samples.

Table 3.8: NMR data for the phenylformamide. The NMR spectrum is given in Appendix C5.

Isomer	NH	CHO	Aromatic Protons
<i>cis</i> δ (ppm)	broad s, 8.46	d, 8.70, J_3 H-H = 11.38	m, <i>o</i> -H 7.22 m, <i>m</i> -H 7.05
<i>Trans</i> δ (ppm)	-	d, 8.37, J_3 H-H = 1.13	m, <i>p</i> -H 7.47

S = singlet, d = doublet and m = multiplet

At this temperature the *meta* and *ortho* aromatic protons appear as a multiplet. The *para* aromatic protons appear as two almost overlapping singlets. However the *cis* and *trans* are not separately identifiable. For the

cis and the *trans* isomers, the formyl protons appear as doublets with coupling constants for the *cis* isomer being larger (see Table 3.8). For mono and some disubstituted phenylformamides the *cis* isomer always has the larger coupling constant [Bourn *et. al.*, 1964]. The protons attached to N appear as somewhat broad singlets. The formyl proton and the proton attached to the N atom form what is referred to as an AB pattern similar to what was observed for the monosubstituted 2-methylphenylformamide [Siddall *et. al.*, 1968]. This is possibly the *trans* isomer as it is expected to be smaller in intensity when compared to the *cis* isomer. The signal from this proton is also known to be dynamic in solution and can move more upfield at higher temperatures.

3.4.3 Molecular structure of phenylformamide

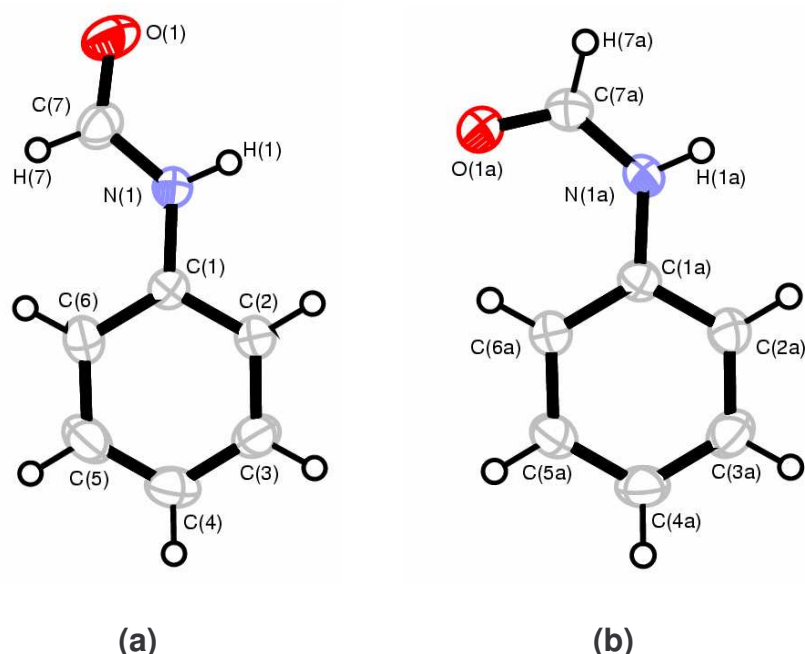


Figure 3.31: The crystal structure of phenylformamide **21** showing the two molecules [(a) *cis* and (b) *trans*] in the asymmetric unit. Ellipsoids are drawn at 50% probability level.

Figure 3.31 shows the *trans*- and *cis*- conformers of the molecular structure of phenylformamide as it exists in the crystal. Despite the existence of the two conformers, most of the bond lengths and angles have typical values and these parameters are quite similar in both molecules (see Table 3.9). The notable differences are in the angles between the planes defined by the aryl ring [C(1) – C(6)] or [C(1A) – C(6A)] and that defined by the formamide moiety [C(1)-N(1)-C(7)-O(1)] or [C(1A)-N(1A)-C(7A)-O(1A)]. In the *cis* isomer the two planes are completely coplanar whereas in the *trans* isomer the formamide moiety is slightly out of the plane of the aryl ring by about 9.1° [between 17 and 21° for acetanilide, Wasserman *et. al.*, 1985]. This is contrary to theoretical studies done by Moreno and Coworkers [Moreno *et. al.*, 2006] and Manea and Coworkers [Manea *et. al.*, 1997] in which the *cis* conformer was found to be non-planar and the *trans* conformers planar. The size of the angle between the above mentioned planes in *trans* isomer has been shown to be for a number of reasons. In most cases hydrogen bonding, aryl ring to amide conjugation and intramolecular interactions between the carbonyl oxygen and the *ortho*-aryl substituents (hydrogen atom in this case). This should be the preferred geometry in order to extend π conjugation from the ring system to the formamide moiety. The conjugation does not however shorten the N(1)-C(1) significantly. For formamides the N(1)-C(7) bond length is as expected to be in the 1.33 Å region with the O(1)-C(7) expected to be about 1.22 Å.

Table 3.9: Bond lengths (Å) and angles (°) of both conformers of phenylformamide

Parameter	cis	trans	Parameter	cis	trans
N(1)-C(7)	1.324(2)	1.336(2)	C(3)-C(4)	1.371(2)	1.383(2)
N(1)-C(1)	1.411(2)	1.410(2)	C(4)-C(5)	1.373(2)	1.376(2)
O(1)-C(7)	1.226(2)	1.223(2)	C(5)-C(6)	1.385(2)	1.379(2)
C(1)-C(2)	1.385(2)	1.388(2)	C(6)-C(1)	1.386(2)	1.387(2)
C(2)-C(3)	1.378(2)	1.378(2)			
C(1)-N(1)-C(7)	128.2(1)	128.3(1)			
N(1)-C(7)-O(1)	123.2(2)	123.1(1)			
C(7)-N(1)-C(1)-C(2)	179.4(1)	170.3(2)			

3.4.4 *Crystal packing and intermolecular interactions in phenylformamide*

This compound crystallizes with two molecules in the asymmetric unit in the monoclinic space group $C2c$, with $Z = 16$. One of the molecules has a *cis*- conformation while the other shows a *trans*- conformation. N-H...O hydrogen bonding plays a significant role in the packing of molecules in the crystal. Due to molecular planarity the hydrogen bonds are, nearly linear with N-H...O angles being 178 and 176° for the *cis* and the *trans* conformers, respectively (see Table 3.10). The N...O distances are slightly shorter [2.844 and 2.821 Å respectively] when compared to that of acetanilide [Wasserman et al., 1985; Johnson et al., 1995] which also adopts a *trans* conformation.

The two molecules in the unit cell are almost coplanar and have a dihedral angle of about 19.07° between their mean planes. Each molecule of a particular conformation (*cis* or *trans*) is related to its nearest neighbor

N-aryl -formamides and -thioamides

of the same conformation through a two-fold screw axis along the crystallographic *c* axis (see highlighted molecules in Figure 3.33). Looking down the crystallographic *a* and *b* axes the molecules are translated by half the distance of the cell dimension. Each molecule is connected to another one of different conformation through N-H...O hydrogen bonding resulting in characteristic tetrameric arrangement (Figure 3.32) with each of the hydrogen bonded tetramers having two molecules of each conformer. These tetramers are then linked to one another through a series of several edge-to-face C-H... π and face-to-face π ... π interactions (See Table 10 and Figure 3.33 and 3.34). The geometric parameters of the interactions suggest that all of them have close-to ideal T-shaped (for C-H... π , thinner red dashed lines) and parallel-displaced (thicker red dashed lines in Figure 3.32b for π ... π) geometry (Figure 3.34).

Table 3.10 Showing the geometric parameters of compound **21**.

Donor-H...Acceptor	Dist. D-H (Å)	Dist. H...A (Å)	Dist. D...A (Å)	Angle D-H...A (°)
N(1)-H(1)...O(1A) ¹	0.88	1.97	2.844(2)	176
N(1A)-H(1A)...O(1) ¹	0.88	1.94	2.821(2)	178
C(6 ^a)-H(6A)...O(1A) ²	0.95	2.30	2.895(2)	120
π ... π	Cg...Cg (Å)	Closest distance of approach (Å)	Interplanar angle (°)	
Cg(1)...Cg(1) ³	4.946(1)	2.025	44.89	
Cg(1)...Cg(1) ⁴	4.278(1)	3.586	0.03	
X(I)-H(I)... π (J)	H(I)... π (J) (Å)	X(I)... π (Å)	<X(I)-H(I)... π (°)	
C(3)-H(3)...Cg(1) ⁸	3.106	3.798(2)	131.09	
C(6)-H(6)...Cg(1) ⁹	3.330	4.111(2)	141.01	
C(7)-H(7)...Cg(1) ¹⁰	3.085	3.873(2)	141.50	

Symmetry operators (1) $x, 1 + y, z$; (2) $-x, -y, 1 - z$; (3) $1/2 - x, -1/2 + y, 3/2 - z$; (4) $1/2 - x, 1/2 - y, 2 - z$; (5) x, y, z ; (6) $x, 1 - y, 1/2 + z$; (7) $x, -y, -1/2 + z$; (8) $1/2 - x, 1/2 + y$; (9) $3/2 - z, x, -y, 1/2 + z$.

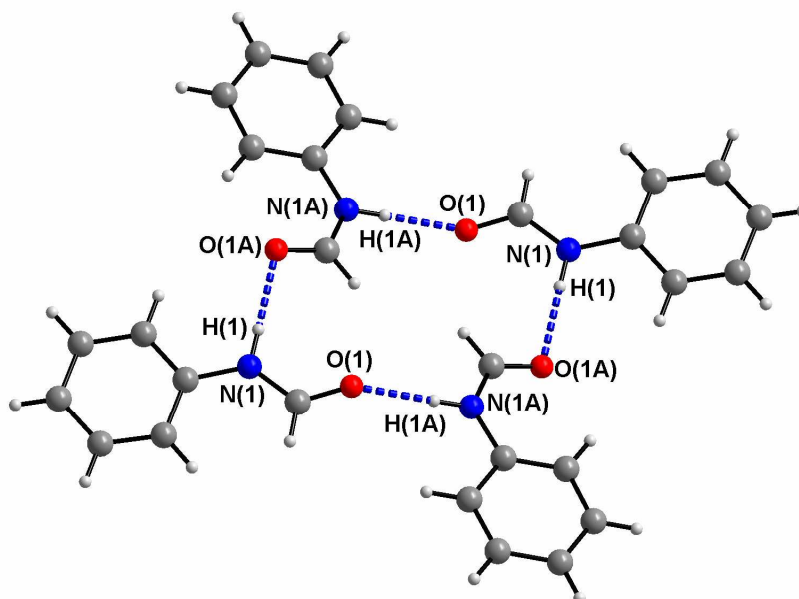


Figure 3.32: View along the crystallographic *c* axis showing one tetramer unit of phenylformamide. The ring formed by the four molecules can be described by a $R_4^4(14)$ graph set.

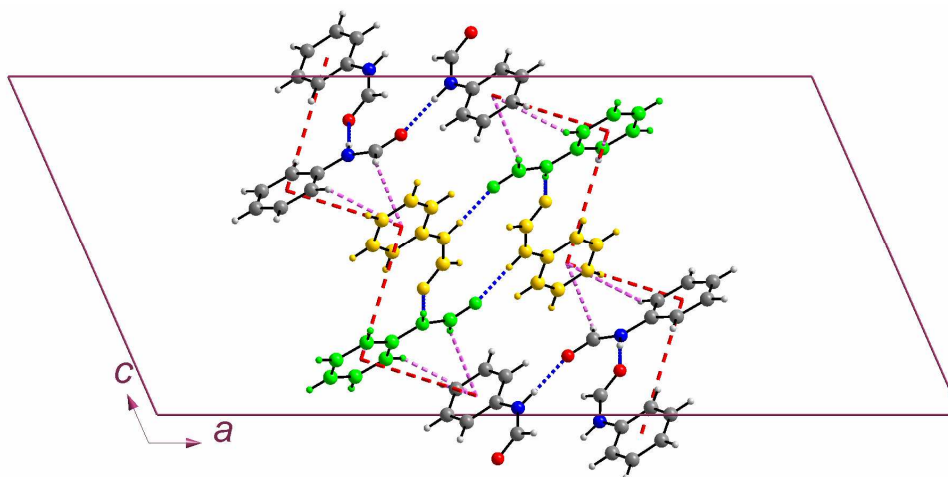


Figure 3.33: View down the crystallographic *b* axis. In one tetramer the *cis* and *trans* isomers are highlighted in green and yellow colors respectively. Adjacent tetramers are connected to this one via a series of C-H... π and π ... π intermolecular interactions.

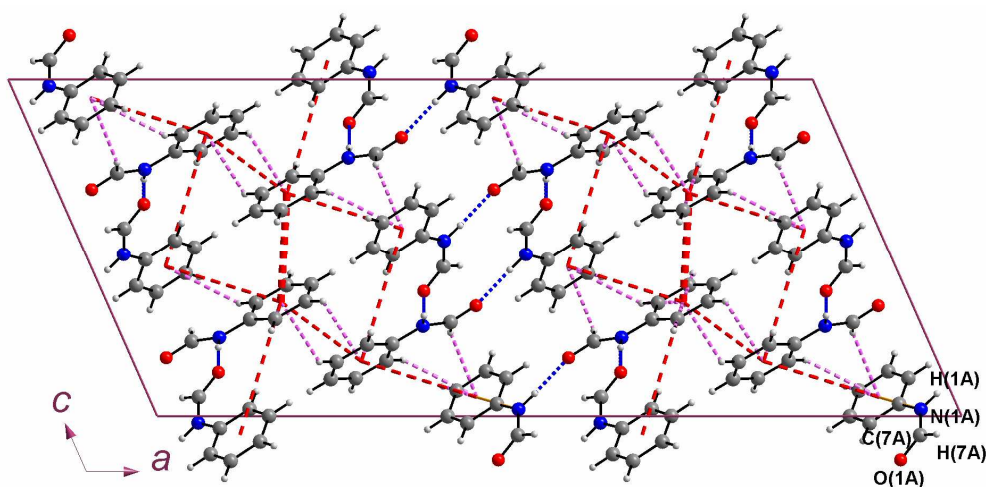


Figure 3.34: Packing diagram of phenylformamide viewed down the *b* crystallographic axis, showing N-H...O hydrogen bonds (in blue), C-H... π (in purple) and π ... π interactions (in red dashed lines). The C-H... π and π ... π interactions link up the N-H...O hydrogen bonded tetramers.

3.4.5 DISCUSSION

As mentioned earlier the study of phenylformamide has been done by a number of people. From previous studies of phenylformamide and acetanilide a number of conclusions were drawn based on the data from NMR spectroscopy and on that presented in Tables 3.11. The NMR studies (in this and also from literature) resulted in a general conclusion that both the *trans* and *cis* isomers of phenylformamide existed in equal abundances in solution. For acetanilide it was found that it existed almost

exclusively as the *trans* isomer [Bourn et. al., 1966] where it was also found to be planar [Cater, 1967].

Studies of phenylformamide in gas phase and through Hartree-Fock calculations (with either 3-21G or 6-31G* basis sets) show and predict the *trans* isomer to be more stable and planar as opposed to the *cis* isomer which has the amide moiety out of plane of the aryl ring. The ratios of the two isomers *cis:trans* was found to be 6.5:93.5 [Manea et. al., 1997].

Geometrically parameters around the formyl group and the *ortho* aryl hydrogens seem to play a role in determining which of the *cis* and *trans* isomers of phenylformamide, formamide or *N*-methylformamide is energetically favored. The key factors with regards to stability of the two isomers are the bond angles about the carbonyl carbon (see Table 3.11). There seems to be a relationship between the angles N-C-O and N-C-H, and the distance between either the carbonyl oxygen or the carbonyl hydrogen atom and the *ortho*-aryl hydrogen [Manea et. al., 1997 and references therein]. Contrary to what is reported for the gas phase calculations of phenylformamide, the *trans* conformer is not planar. Further the two conformers seem not to be thermodynamically stable on their own in solid state as it has been shown in this work.

3.5 Cocystals of aryl -formamides and -thioamides

3.5.1 Introduction

As a part of a series of structural investigations on molecular recognition of arylformamides and arylthioamides cocrystallization of selected formamides and/or thioamides has been done in this work. Three pairs of compounds were cocrystallized; 2,6-dichlorophenylformamide **2** and 2,6-dimethylphenylformamide **3**, and 2,6-dichlorophenylthioamide **16** and 2,6-dimethylphenylthioamide **17** and 2,6-diisopropylphenylformamide **6** and 2,6-diisopropylphenylthioamide **20** which lead to new structures, cocrystals **22**, **23** and **24**, respectively.

3.5.2 Molecular structures of cocrystal 22, 23 and 24

ORTEP diagrams for these three structures can be found in the Appendix.

Table 3.11: Bond distances (Å) and angles (°) for compounds **22**, **23** and **24**

Parameter	22	23	24
C(1)-N(1)	1.418(3)	1.433(2)	1.437(3)
N(1)-C(7)	1.326(3)	1.315(2)	1.269(3)
C(7)-O(1)/S(1)	1.218(3)	1.648(2)	1.211(8)/1.620(8)
C(1)-N(1)-C(7)	124.6(2)	125.1(1)	127.4(2)
N(1)-C(7)-O(1)	125.8(3)	127.3(1)	128.3(2)/127.6(2)
C(2)-C(1)-N(1)-C(7)	62.5(2)	81.7(2)	77.5(3)

Table 3.12: Unit cell parameters for cocrystals **22**, **23** and **24**.

Compounds	Space group	Unit cell parameters	
22	<i>Pbca</i>	$a = 8.507(1)$ $b = 13.093(2)$ $c = 14.448(2)$	$\alpha = \beta = \gamma = 90^\circ$ $1609.3(4) \text{ \AA}^3$ 1.400 Mg/m^3
23	<i>Pbca</i>	$a = 9.208(5)$ $b = 13.142(5)$ $c = 14.617(5)$	$\alpha = \beta = \gamma = 90^\circ$ $1768.8(1) \text{ \AA}^3$ 2.120 Mg/m^3
24	<i>P2₁/c</i>	$a = 9.022(5)$ $b = 9.003(5)$ $c = 16.005(5)$	$\beta = 103.170(5)^\circ$ $1265.8(1) \text{ \AA}^3$ 1.443 Mg/m^3

Cocrystals **22** and **23** crystallizes in the same space group *Pbca* while **24** crystallizes in the space group *P2₁/c*. **22** and **23** are isomorphous with **1a**, **2a** and **4a**. The three cocrystals adopt a *trans* conformation in which the formamide moiety (defined by [C(1)-N(1)-C(7)-O(1)]) is out of the plane of the aryl ring (defined by [C(1)-C(6)]). The angles between the planes defined by the aryl rings and the formamide groups for the three structures are 62.5(2), 81.7(2) and 77.5(3)° for **22**, **23** and **24** respectively which fall in the ranges for the aryl -formamides and -thioamides discussed in this work.

The molecules of the three compounds are disordered over two positions and as such not much can be deduced from the three structures in terms of bond distances and angles. This is especially so for C(2)/C(6)-Cl(1)/Cl(2) for **22** and **23**, and C(7)-O(1)/S(1) for **24**. The rest of the molecule in the three structures is not much disordered and this affects

only slightly the bond distances and angles which are comparatively close to those of the pure compounds (see Table 3.11).

3.5.3 Crystal structure of cocrystal 22

Common features are observed in the hydrogen-bonded networks of compounds **22** and some 2,6-disubstituted arylformamides (Category 1). The cocrystal crystallizes with one molecule in the asymmetric unit. In the crystal, molecules are linked together by N-H...O hydrogen bonds [N(1)...O(1) = 2.868 Å] forming chains that run in the crystallographic *a* direction. A glide plane relates the molecules along the N-H...O hydrogen bonded chain. This results in the formamide molecules pointing in alternate directions. In addition to this the structure has intramolecular Cl(1)...O(1) interactions [3.254 Å] supporting the N-H...O hydrogen bonds. Adjacent chains are held together through π ... π interactions [*Cg*...*Cg* = 3.6915 Å] between aryl groups on neighbouring chains forming sheets of molecules parallel to (010). Neighbouring sheets interact with each other through Cl...Cl [Cl(1)...Cl(2) = 3.717 Å] and C-H...Cl interactions [Cl(2)...H(5) = 2.920 Å] (see Figure 3.35).

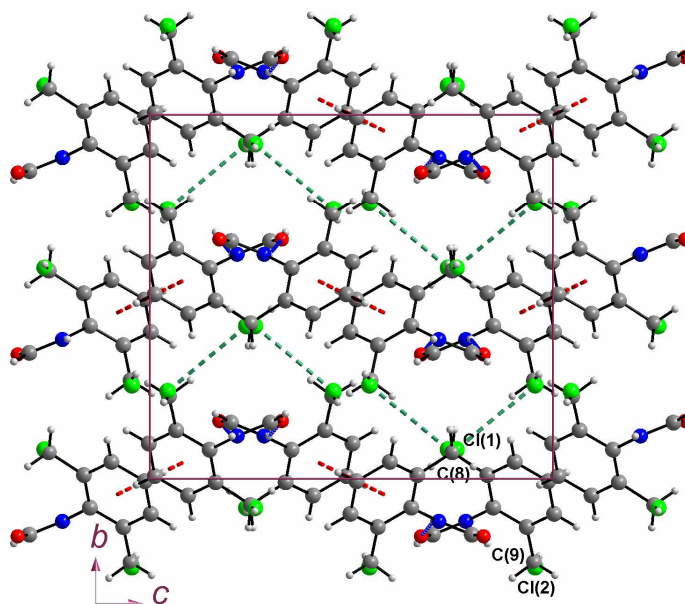


Figure 3.35: Packing diagram for cocrystal **22** showing hydrogen bond chains (running into the page), Cl...Cl interactions (in green) and π ... π interactions (in red dashed lines)

3.5.4 Crystal structure of cocrystal **23**

Cocrystal **23** crystallizes in the space group *Pbca* with $Z = 8$ and one molecule in the asymmetric unit. The molecular geometry of compound **23** is different from that of compounds **16** - **19** showing a *trans*-thioamide conformation with the thioamide moiety being orientated out of the plane of the aromatic ring. The reason for the *trans* conformation adopted by this cocrystal is not yet fully understood.

In the crystal, molecules are linked together by N-H...S hydrogen bonds [$N(1)\dots S(1) = 3.2730 \text{ \AA}$] forming chains that run in the crystallographic *a* direction. A glide plane as in compound **22** relates the

N-aryl -formamides and -thioamides

molecules along the N-H...S hydrogen bonded chain, which results in the formamide molecules pointing in alternate directions. In addition to this there are intramolecular Cl...S interactions. Adjacent chains are held together though π ... π interactions [$Cg...Cg = 3.998 \text{ \AA}$] between aryl groups on neighbouring chains forming sheets of molecules parallel to (010). Neighbouring sheets interact with each other through Cl...Cl and C-H...Cl interactions (see Figure 3.36). Compounds **22** and **23** are isomorphous.

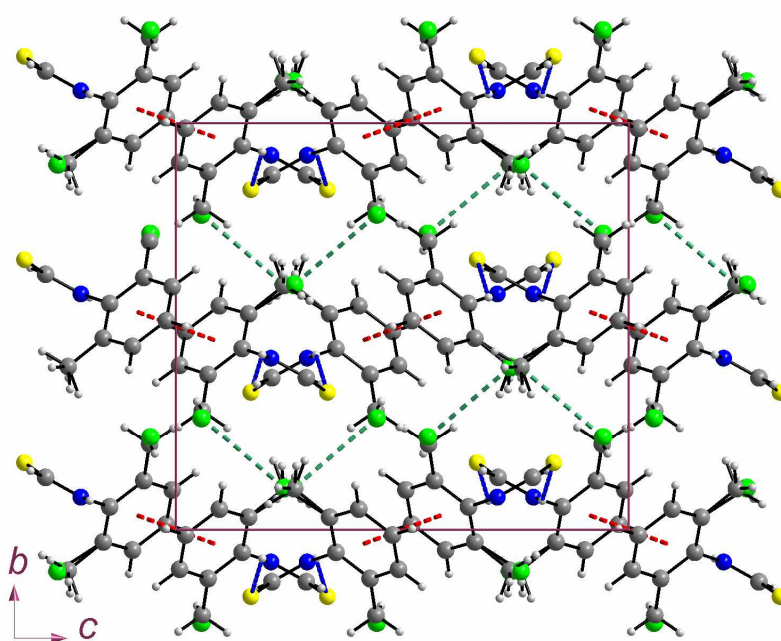


Figure 3.36: Packing diagram for cocrystal **23** as viewed down the crystallographic *a* axis. N-H...O hydrogen bonds are shown in blue while Cl...Cl and π ... π interactions are shown in green and red dashed lines, respectively.

3.5.5 Crystal structure of cocrystal 24

The ORTEP diagram for cocrystal **24** can be found in the appendix. Cocrystal **24** crystallizes in the same space group ($P2_1/c$) as compounds **6** and **20** with one molecule in the asymmetric unit. Some hydrogen bonding parameters for the compound are given in Table 3.13.

The packing is dominated by the formation of N-H...O/S hydrogen bonds [$N(1)...S(1) = 3.028 \text{ \AA}$] which form chains that run in the crystallographic b direction resulting in the formamide molecules pointing in alternate directions (see Figure 3.37). In addition to the N-H...O hydrogen bonds are C-H... π interactions [$H(7)... \pi = 2.740 \text{ \AA}$, $C(7)-H(7)... \pi = 163^\circ$]. The C-H... π interactions are along the N-H...O hydrogen bonded chain and occur between adjacent molecules that are related by a glide plane along the hydrogen bond chains. Adjacent chains are held together through C-H... π interactions [$H(11a)... \pi = 2.740 \text{ \AA}$, $C(11a)-H(11a)... \pi = 127^\circ$].

Table 3.13: Geometric parameters for cocrystal **24**.

Donor-H...Acceptor	D-H (Å)	H...A (Å)	D...A (Å)	<D-H...A (°)
N(1)...O(1) ¹	0.83	2.226	3.034	163
N(1)...S(1) ¹	0.84	2.426	3.246	167
C(8)-H(8)...N(1) ¹	0.98	2.440	2.933	110 (intra)
C(9)-H(9)...N(1) ¹	0.98	2.490	2.879	116 (intra)
X(I)-H(I)... π (J)	H(I)... π (J) (Å)	X(I)... π (Å)	<X(I)-H(I)... π (°)	
C(7)-H(7) ...Cg(2) ³	2.76	3.673	161	
C(11)-H(11) ...Cg(2) ²	2.94	3.612	127	

Symmetry operators (1) $-x, 1/2+y, 1/2-z$; (2) $1-x, 1-y, -z$; (3) $1-x, 1/2+y, 1/2-z$.

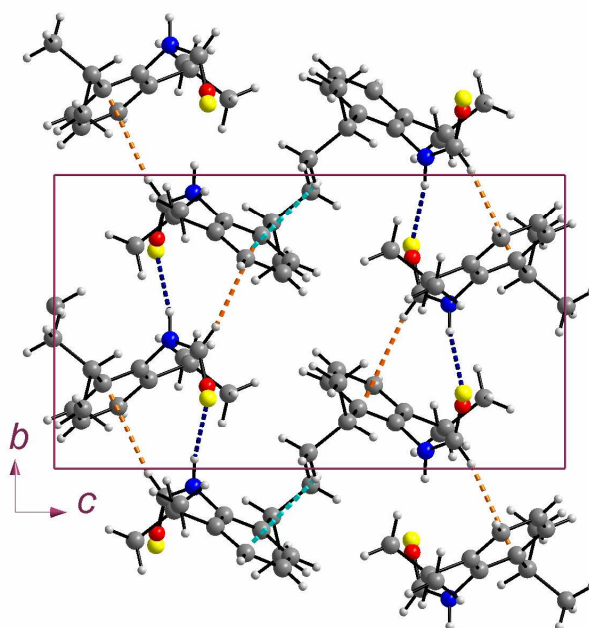


Figure 3.37: Packing diagram for cocrystal **24** showing hydrogen bonding chains in blue and C-H... π interactions in orange dashed lines.

Cocrystals **22** and **23** are isomorphous with 2,6-difluorophenylformamide **1a**, 2,6-dichlorophenylformamide **2a** and 2-chloro-6-methylphenylformamide **4a**. Cocrystal **24** is isomorphous with 2,6-diisopropylphenylformamide **6** and 2,6-diisopropylphenylthioamide **20**. Further comparison of these structures is done in chapter 5.

4. Polymorphism and phase changes in compounds 2,6-difluoro-, 2,6-dichloro- and 2-chloro-6-methylphenylformamides

4.1 Introduction

In this work we decided to investigate in a systematic manner polymorphism in all disubstituted arylformamides and thioamides that were synthesized. One method to establish the presence of new phases of compounds is the use of DSC. From the series of arylformamides and arylthioamides that were investigated, only three existed in more than one phase. Only two of the three new phases (2,6-dichlorophenylformamide **2b** and 2-chloro-6-methylphenylformamide **4b**) were discovered using DSC while the third, the new phase of 2,6-difluorophenylformamide **1a**, was fortuitously isolated from a batch of 2,6-difluorophenylthioamide crystals. The DSC traces of 3,4-dichlorophenylformamide and 2,4-dibromophenylformamide also showed endothermic peaks before reaching their melting points, corresponding to possible new phases of the compounds. However, attempts to try and show the existence of any new phases for the two compounds were not successful. The DSC traces for the remaining compounds did not show any phase transitions before reaching the melting points. Melting points of these compounds were also confirmed by optical hot stage microscopy, which showed a smooth change from solid state to liquid state for all compounds. Attempts were made using variable temperature powder XRD to follow the phase change by which the low temperature forms of 2,6-

dichlorophenylformamide **2a** and 2-chloro-6-methylphenylformamide **4a** transformed into their high temperature forms (**2b** and **4b** respectively). Such experiments could not be carried out for the phases of 2,6-difluorophenylformamide **1a** since only a few crystals of **1b** were available. The stable room-temperature forms of these three compounds will be referred to as forms 'a' while the unstable high-temperature phases will be referred to as forms 'b'. The chloro and methyl groups in the structures of **4a** and **4b** are disordered over two positions. The ratios of the disordered components are given later in this chapter.

4.2 Polymorphism in 2,6-dichloro- and 2-chloro-6-methylphenylformamides

The two forms of 2,6-dichlorophenylformamide and 2-chloro-6-methylphenylformamide were obtained using different methods. The low temperature forms were grown from solutions in ethyl acetate at room temperature and the high temperature forms were derived via sublimation of the room temperature form materials. The four compounds were analysed using a number of methods, which included DSC, powder XRD, single crystal XRD and lattice energy calculations. The results of each of these methods are outlined below.

4.2.1 Thermal Analysis

The thermal behaviour of the two 2,6 substituted *N*-arylformamides was analysed using differential scanning calorimetry. 2,6-dichloro- and 2-chloro-6-methyl-phenylformamides displayed small endothermic peaks at 155.34 °C (3.26 kJ/mol) and 106.10 °C (1.36 kJ/mol), respectively, before reaching their melting points of 179.55 °C and 165.30 °C (Figure 4.1). No peak was observed during the cooling cycle implying that both phase transitions were irreversible during the time frame of the DSC measurements. Subsequent powder diffraction studies showed, however, that the high-temperature form of 2,6-dichlorophenylformamide reverted to the room-temperature form over a period of several days, a behaviour consistent with similar observations described by Weiss *et. al.*, [1986] for *N*-2,6-dichlorophenylacetamide. The high-temperature form of 2-chloro-6-methylphenylformamide appeared, in contrast, to be stable at room temperature (no transformations were observed over a period of 48 hours or even after several weeks, see Powder X-ray diffraction discussion below). Monitoring the phase change in single crystals of **2a** and **4a**, through optical hot stage microscopy, indicated that the phase transition occurred in both compounds with significant disruption to the crystal habit. In addition, it was not possible to follow changes in unit cell parameters through the phase transitions in **2a** and **4a**, using single crystal diffraction, due to the significant

N-aryl -formamides and -thioamides

structural changes involved. Consequently both phase changes can be regarded as being first order.

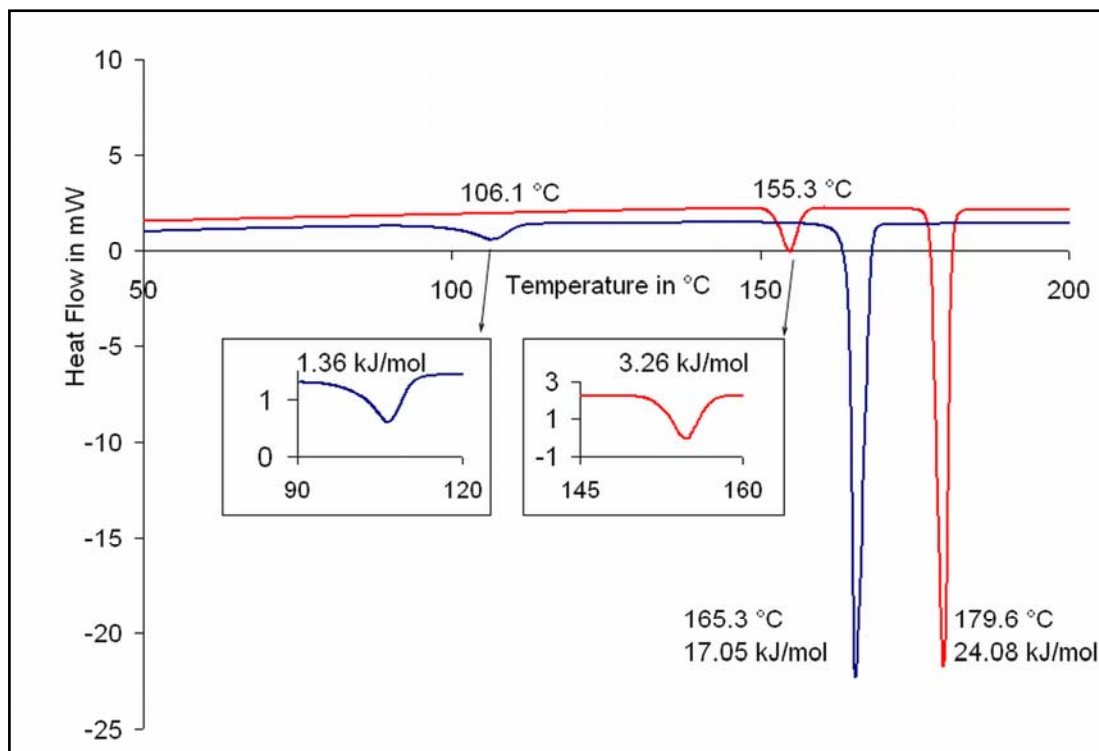


Figure 4.1: DSC traces of compounds **2a** (upper trace) and **4a** (lower trace).

4.2.2 Powder X-ray diffraction

PXRD patterns of the low and high-temperature forms of 2,6-dichlorophenylformamide **2a** and **b** and 2-chloro-6-methylphenylformamide **4a** and **b** are shown in Figures 4.2 and 4.3. As the powder patterns indicate the two phases of each compound differ significantly. Crystals of the high

***N*-aryl -formamides and -thioamides**

temperature forms **2b** and **4b**, grown by sublimation have calculated PXRD patterns matching that of the corresponding powders heated beyond their respective phase transition temperatures, demonstrating that the structures of the sublimed crystals and heated bulk powder are identical.

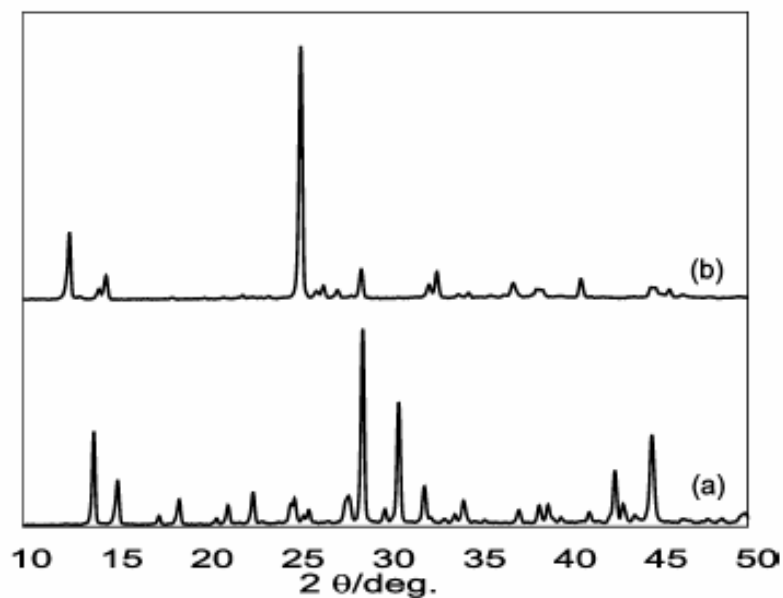


Figure 4.2: Experimental powder X-ray diffraction pattern showing the two phases of 2,6-dichlorophenylformamide.

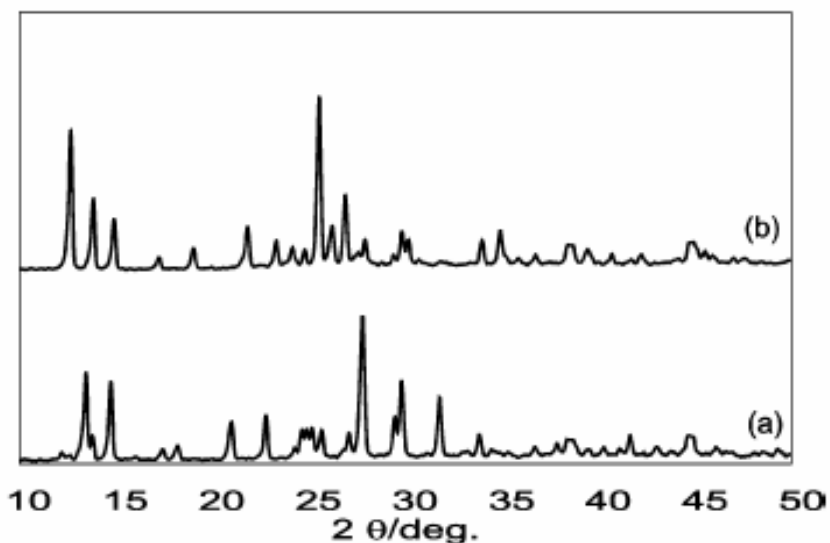


Figure 4.3: Experimental powder X-ray diffraction pattern showing the two phases of 2-chloro-6-methylphenylformamide.

The phase change behaviour of the high temperature forms of the two compounds (**2b** and **4b**) differ. Both single crystal and powder samples of the high temperature form of 2,6-dichlorophenylformamide (**2b**) revert back to the low temperature phase (**2a**) after several days at room temperature. Below T_c the conversion to the thermodynamically more stable **2a** begins and can be accelerated by heating at a temperature just below T_c . Keeping the high-temperature form (**2b**) at about 140 °C in an oven, i.e. just below the phase transition temperature, accelerates its re-conversion to the low-temperature form (**2a**). After 2 days, less than 5% of the high temperature phase (**2b**) remains and after 4 days the sample has completely reverted back to the low

temperature phase (**2a**). Between the phase transformation temperature ($T_c = 156\text{ }^\circ\text{C}$) and the melting point ($180\text{ }^\circ\text{C}$) compound **2b** is thermodynamically more stable than **2a**.

Unlike compound **2b**, **4b** does not revert back to the low temperature form even after several weeks at room temperature. Attempts to initiate the process by heating it (keeping the sample in the oven at $80\text{ }^\circ\text{C}$ for 12 hours then at $96\text{ }^\circ\text{C}$ for another 12 hours) caused no change back to form **4a** as monitored by PXRD.

4.2.3 Molecular structure of compounds 2a, 2b, 4a and 4b

The molecular structures of **2a** and **4a** (only low temperature forms shown) with the atom-labelling scheme are shown in Figure 4.4. Important bond distances and angles as well as intermolecular hydrogen bond parameters are given in Tables 4.1 and 4.2. The crystal structure of **2a** has been described previously [Godwa *et. al.*, 2000] but was repeated for reasons of comparison.

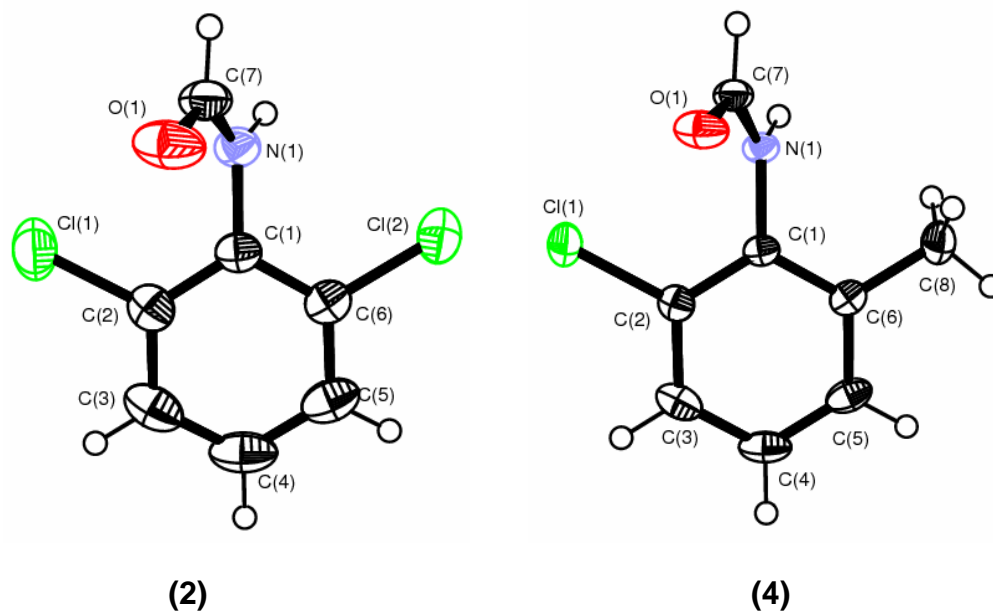


Figure 4.4: ORTEP diagrams for structures **2a** and **4a** (only one of the disordered arrangements shown). Thermal ellipsoids are given at 50% probability.

N-aryl -formamides and -thioamides

Table 4.1: Bond distances and angles for 2,6-dichlorophenylformamide **2** and 2-chloro-6-methylphenylformamide **4** (units in Å and °, respectively).

Parameter	2a	2b	4a	4b
N(1)–C(7)	1.337(2)	1.327(3)	1.337(2)	1.335(2)
N(1)–C(1)	1.416(2)	1.413(3)	1.425(2)	1.425(2)
O(1)–C(7)	1.218(2)	1.216(3)	1.221(2)	1.224(2)
C(2)–X(1)	1.738(2)	1.730(2)	1.704(3)	1.750(5)
C(6)–X(2)	1.736(2)	1.729(3)	1.569(7)	1.515(5)
C(1)–N(1)–C(7)	123.4(1)	123.3(2)	124.1(1)	122.2(1)
N(1)–C(7)–O(1)	126.0(2)	125.1(2)	126.4(1)	124.5(1)
C(1)–C(2)–X(1)	119.9(1)	119.5(2)	119.8(3)	117.9(1)
C(1)–C(6)–X(2)	119.1(1)	118.8(2)	120.7(4)	121.2(6)
C(7)–N(1)–C(1)–C(2)	67.4(2)	76.8(3)	67.2(2)	79.3(2)
Density _(calc) (mg/m ³)	1.599	1.538	1.434	1.389

X(1) = Cl(1) for **2a**, **2b**, **4a** and **4b**, X2 = Cl(2) for **2a**, **2b** and C(8) for **4a** and **4b**.

Table 4.2: Hydrogen bonding distances and angles for 2,6-dichlorophenylformamide and 2-chloro-6-methylphenylformamide (units in Å and °, respectively).

Compound	N–H (Å)	H ... O (Å)	N ... O (Å)	N–H ... O (°)
1a	0.79(2)	2.09(2)	2.872(2)	173(2)
2a	0.83(2)	2.04(2)	2.859(2)	171(2)
1b	0.81(3)	2.10(3)	2.782(2)	142(3)
2b	0.83(2)	2.07(2)	2.789(2)	146(2)

Symmetry operators; **1a** = $x + \frac{1}{2}, y, -z + \frac{1}{2}$; **2a** = $x - \frac{1}{2}, y, -z + \frac{1}{2}$; **1b** = $x - 1, y, z$;
2b = $x, y + 1, z$.

***N*-aryl -formamides and -thioamides**

The molecular geometry of 2,6-dichlorophenylformamide and 2-chloro-6-methylphenylformamide is similar in that both show a *trans* conformation with the formamide moiety out of the plane of the aromatic ring (Figure 3.1 in Chapter 3). However, the angles between the planes defined by the aryl ring [C(1)-C(6)] and the formamide group [C(1)-N(1)-C(7)-O(1)] are smaller for the low temperature forms (**2a** = 67.3°, **4a** = 67.2°) than for the high temperature forms (**2b** = 76.8°, **4b** = 79.3°).

The geometry of the different polymorphs were also modelled theoretically with *ab initio* calculations being carried out using second order Møller-Plesset (MP2) correlation energies and the 6-31G** basis set as implemented in Gaussian98 [Gaussian 98, Revision A.7, 1998]. Geometry optimization starting from structures **2a** and **2b** converged to the same stationary point, with an angle of 62.6° between the phenyl and formamide planes. The small value of this angle in the low temperature forms and calculated structures may indicate a stabilizing interaction between the oxygen atom of the formamide group and the substituent in 2 position (Cl for **2a** and **2b** and Cl or Me for **4a** and **4b**). In the high temperature forms the larger angle precludes such interaction in the observed crystal structure (intramolecular Cl...O interactions are only observed in the high temperature forms).

***N*-aryl -formamides and -thioamides**

In 2-chloro-6-methylphenylformamide the formamide group can bend towards either the chlorine or methyl ligand, so both C-H...O and Cl...O interactions are possible. The substituents in the 2 and 6 positions are disordered, consistent with the chloro-methyl interchange effect and resulting in increased entropy. Each disordered component was optimized¹ for both the low and high temperature forms and all four starting geometries converged to equivalent structures with a C-H...O interaction and an angle between the aryl and formamide plane of 57.2°. In the structure of the observed low temperature form, **4a**, the ratio of Cl...O to C-H...O interactions (which varies according to the site of occupancy) is 0.573(1):0.427(1) (see Chapter 2 for refinement details). This ratio changes to 0.750(2):0.250(2) in the high temperature crystals **4b** (after sublimation). This increased differentiation in the location of the methyl and chloro groups is likely to be a property of this crystal form being grown *via* sublimation, and may have no relationship to the structure created by the phase transition itself.

¹ The methyl and chlorine groups are disordered such that one of two interactions (C-H...O or Cl...O) are possible depending on whether the chloro group or methyl group is in position 2 on the aryl ring. During the calculations the two possible models of each polymorph are worked on separately (optimizing a specific interaction).

4.2.4 Crystal packing, hydrogen bonding and intermolecular interactions

Hydrogen bonding patterns of the crystal structures are shown in Figures 4.5 and 4.6. The hydrogen bonding distances and angles are given in Table 4.2.

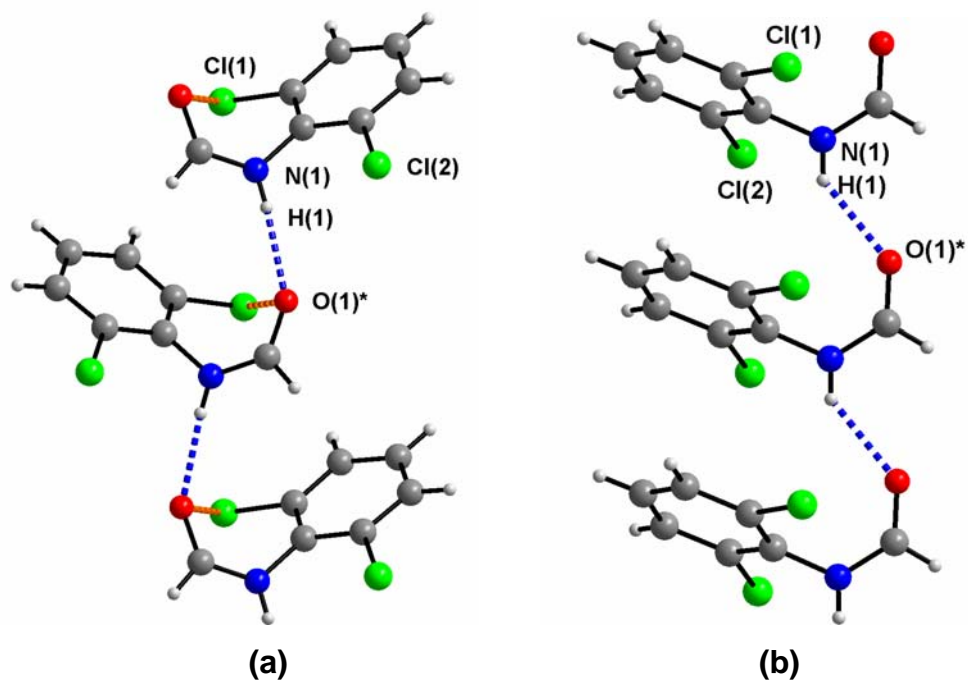


Figure 4.5: Hydrogen bonded chains in 2,6-dichlorophenylformamide showing (a) the alternating arrangement due to a glide plane in **2a** (Symmetry operator $* = \frac{1}{2} + x, y, \frac{1}{2} - z$) and (b) the stacked relationship of molecules related by unit cell translation in **2b** (Symmetry operator $* = -1 + x, y, z$).

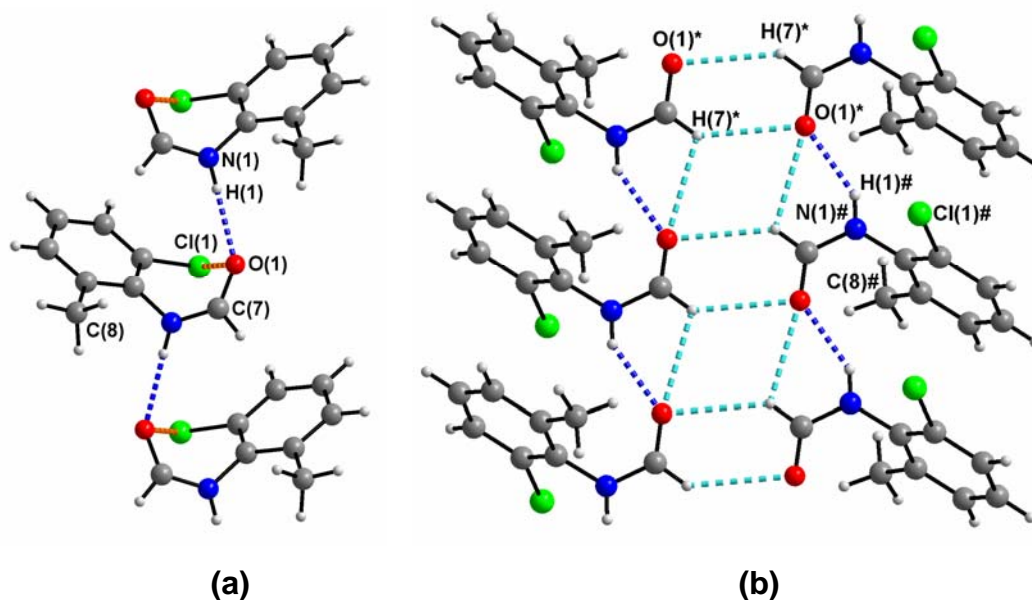


Figure 4.6: Hydrogen bonded chains in (a) **4a** (Symmetry operator * = $\frac{1}{2} + x$, y , $\frac{1}{2} - z$) and (b) **4b** (Symmetry operator * = $1 - x$, $1 - y$, $1 - z$, # = $1 - x$, $2 - y$, $1 - z$). While chains of molecules are kept together by N–H...O hydrogen bonding in **4a** with molecules alternating within the chain in a manner identical to **2a**, the molecules in **4b** are aligned in a stacking arrangement similar to **2b**. However, in **4b** these chains are further stabilized by C–H ... O interactions.

Both room-temperature forms, compounds **2a** and **4a**, are isomorphous and crystallize in the orthorhombic space group *Pbca*, with $Z = 8$. The high-temperature forms, **2b** and **4b** are both monoclinic but not isomorphous (**1b**: $P2_1/n$, $Z = 4$; **2b**: $P2_1/c$, $Z = 4$). As mentioned in Chapters 1 and 3 the N–H...O hydrogen bond plays a significant role in amides and is present in the structures presented here. The isomorphous structures of **2a**

and **4a** have molecules linked together by N-H...O hydrogen bonds (Table 4.1) forming chains of molecules related by a glide plane in the crystallographic *a* direction. This results in the formamide molecules pointing in alternating directions [Figures 4.5a and 4.6a]. Adjacent chains are held together through π ... π interactions [*Cg*...*Cg* = 3.678 and 3.675 Å for **2a** and **4a**, respectively] between aryl groups on neighbouring chains forming sheets of molecules parallel to (010) [Figures 4.7 and 4.8]. Neighbouring sheets interact with each other through Cl...Cl [Cl(1)...Cl(2): 3.640 Å; Figure 4.7] and C-H...Cl interactions.

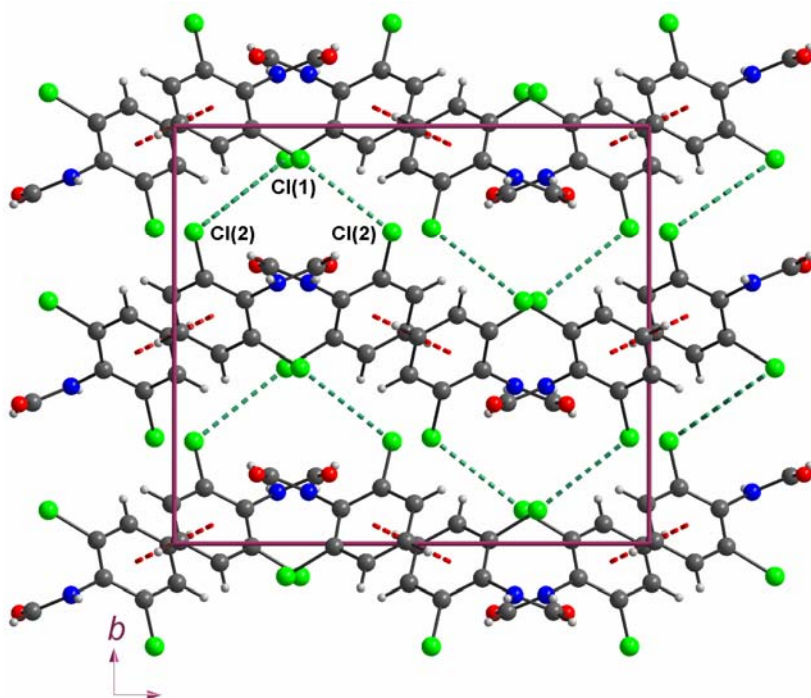
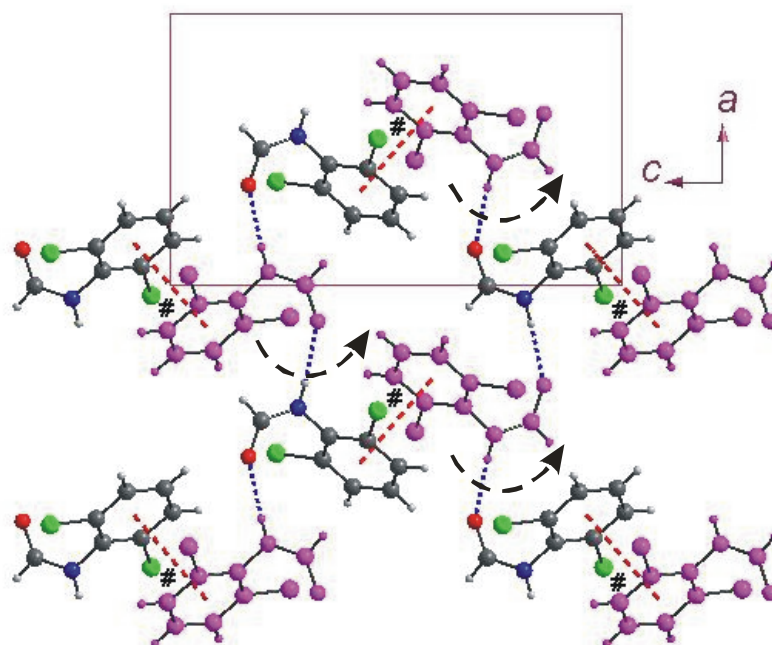


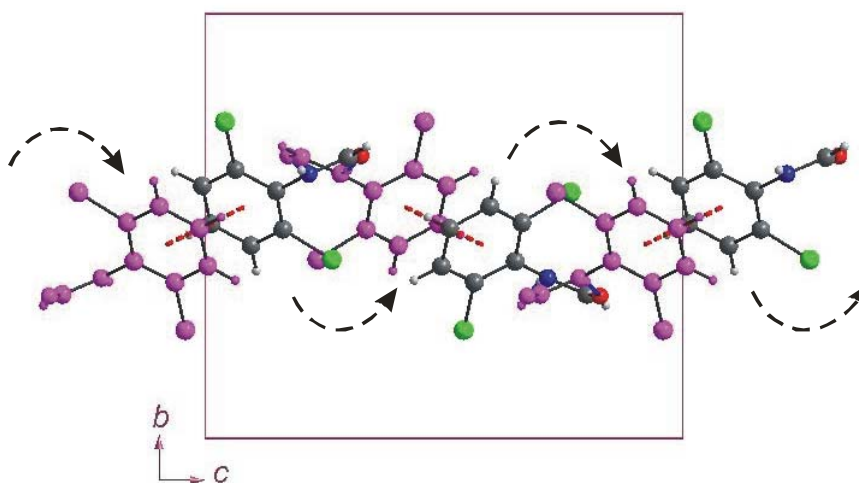
Figure 4.7: Crystal packing in the structure of **2a** showing chains of N-H...O hydrogen bonded molecules running down the *a* axis (perpendicular to the plane of the page) and linked to each other through π ... π interactions (red

N-aryl -formamides and -thioamides

dashed lines). Between each sheet of molecules are Cl...Cl interactions shown with green dashed lines.



(a)



(b)

Figures 4.8: View down (a) the *b* axis, and (b) down the *a* axis of a sheet of molecules from the structure of **2a**. N–H...O hydrogen bonding within molecular chains are shown as well as the π ... π interactions (indicated with #)

between adjacent chains. Molecules surrounding the # contribute significantly to the stability of the structure of **2a** (see energy calculations in text). Arrows indicate the rotation direction needed to form the N–H...O chains found in **2b**.

Although the structures of the two high-temperature forms in this study, **2b** and **4b**, are not isomorphous the hydrogen bonded chains in the two forms are very similar. In both structures the molecules stack linearly through translation along a crystallographic axis (the *a* axis for **2b** and the *b* axis for **4b**). This results in the molecules being parallel to each other forming chains through N-H...O hydrogen bonding along the crystallographic *a* direction for **2b** and crystallographic *b* direction for **4b** [Table 4.1 & Figs. 4.5b and 4.6b]. Neighbouring chains in **2b** are further connected through Cl...Cl interactions [Cl(1)...Cl(2) = 3.491 Å] along the *b* axis to form sheets of molecules parallel to the (001) plane (Figure 4.9). Adjacent sheets are held together by other van der Waals interactions such as Cl...H interactions. In **4b** hydrogen bonded chains are further connected through bifurcated C-H...O hydrogen bonds acting between formamide groups related by centres of symmetry in the structure and formamide groups related by unit cell translation along the *b* axis (Figure 4.6b). These reinforce the N-H...O hydrogen bonded chain. As a consequence of these weak interactions the arrangement of N-H...O chains and hence the crystal packing in the structures of **2b** and **4b** are very different (compare Figures 4.9 and 4.10). The stability of the C-H...O interactions and the fact that the crystal packing in the structure of **4b** differs substantially from

4a may explain why this compound is unable to undergo the phase transition back to the low temperature form.

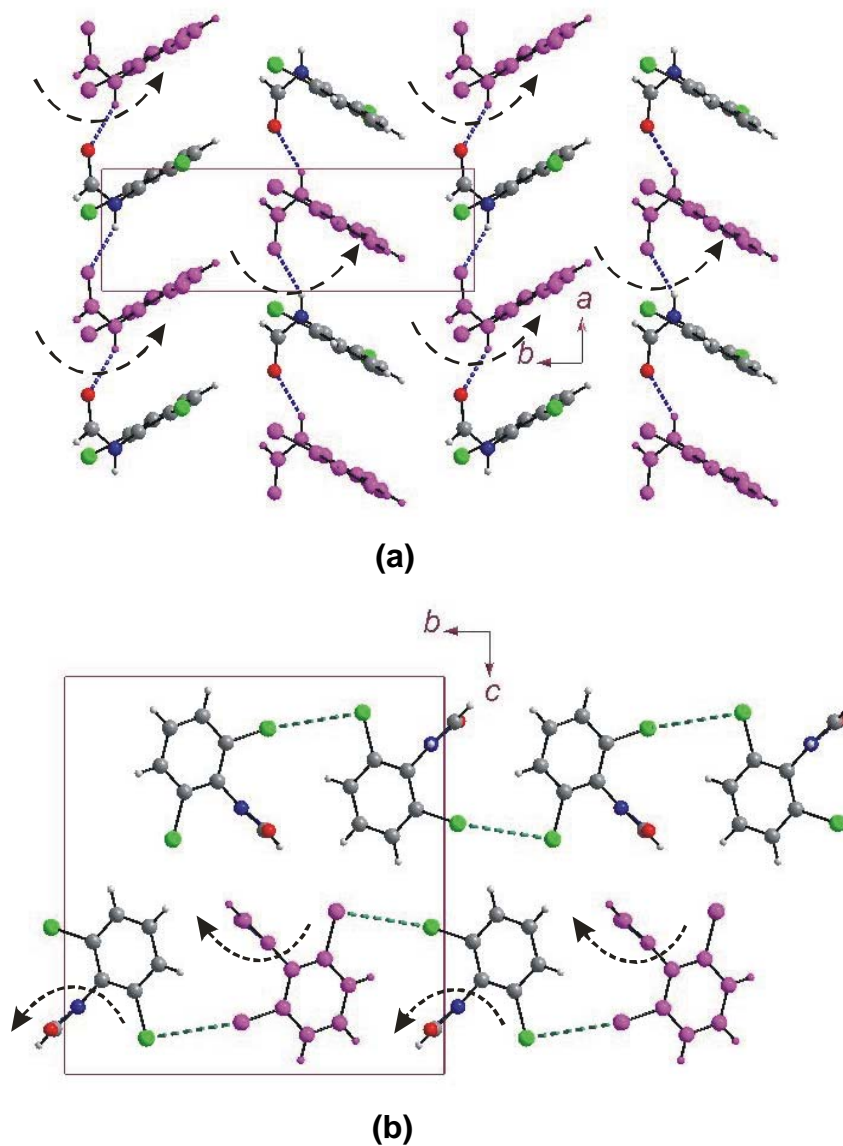


Figure 4.9: A sheet of molecules from the structure of **2b**: (a) N–H...O interactions within molecular chains; (b) Cl...Cl interactions between adjacent chains. Arrows indicate the rotation direction needed to form the N–H...O chains found in **2a**.

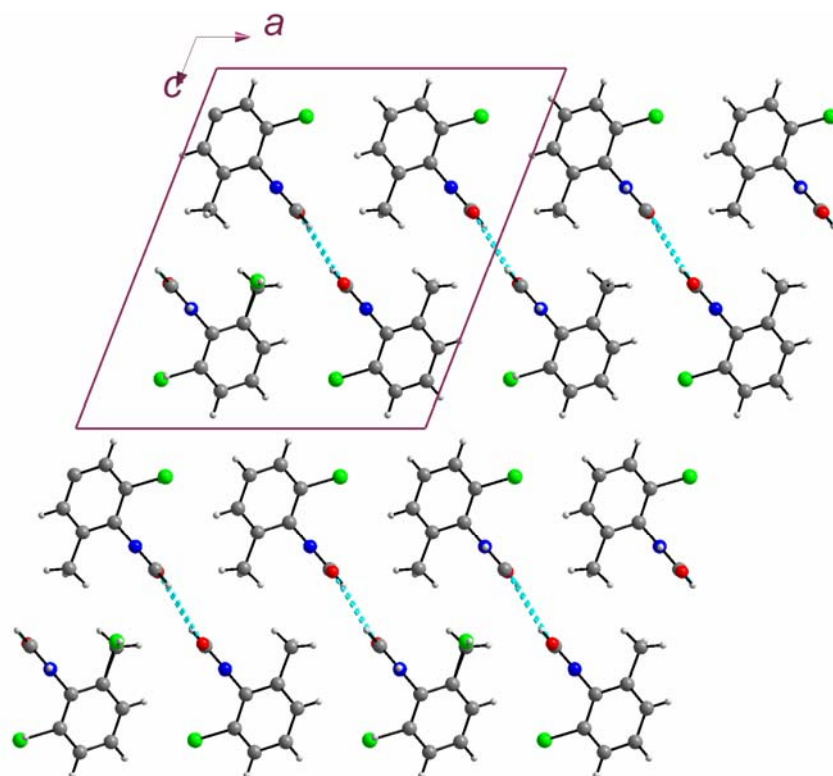


Figure 4.10: Crystal packing in **4b** drawn as a projection down the *b* axis. C–H...O interactions linking pairs of N–H...O chains are indicated with dashed lines. The C–H...O interactions probably play a significant role in inhibiting the reverse phase change to the low temperature form (**4a**).

4.2.5 Proposed mechanism for the phase change of 2a to 2b

A possible mechanism describing part of the phase change between the low and high temperature forms of 2,6-dichlorophenylformamide is shown in Figures 4.8 and 4.9. The mechanism depends on the similarity between the two forms and involves the rotation of every alternate formamide aryl ring in a N–H...O chain into a neighbouring chain. The reverse happens on going from

the high temperature form to the low temperature form. Since the movements required achieving the phase change are quite substantial it is probable that the phase change depends on space available at either the crystal surface or at crystal defects. However, lattice energy calculations indicate that the geometry relating the molecules through the $\pi\dots\pi$ interaction in **2a** (Figure 4.9b) is energetically very favourable and provides a strong driving force for the reverse phase change from **2b** to **2a**. The activation energy required to undergo the reverse phase transition is however reasonably high. This explains the slow rate of phase change at room temperature and the significant rate acceleration at higher temperatures. It has been reported that phase changes in some compounds can be inhibited in the presence of impurities (dopants) [Nagarajan *et. al.*, 1986, Fernandes *et. al.*, 2004] or if weak interactions are present between two groups that would normally be able to move – see Lieberman *et. al.* [2000] where C-H...Br and Br...Br interactions between two crystal twins are believed to inhibit a phase change in 1,2,4,5-tetrabromobenzene. In a similar manner it is likely that the C-H...O interactions between the N-H...O chains in **4b** prevent the reverse phase change to **4a**.

Crystal densities are sometimes used as indicators to assess the stability of polymorphs – the higher the crystal density the higher the stability. In this study **2a** and **4a** are the thermodynamically more stable forms at low temperatures - otherwise structure **2b** would not spontaneously revert to **2a** -

***N*-aryl -formamides and -thioamides**

and their crystal densities are correspondingly higher (by 0.061 and 0.045 g cm⁻³, respectively – see Table 4.2) than those of the high temperature forms.

The $\langle U_{\text{iso}} \rangle$ values [average of U_{iso} values for the atoms common to all the structures, i.e. C(1)-C(7), N(1) and O(1)] are 0.044 and 0.058 for **2a** and **2b**, respectively at 293 K, and 0.027 and 0.041 at 173K for **4a** and **4b**, respectively. Therefore, not only do the low temperature forms of 2,6-dichlorophenylformamide and 2-chloro-6-methylphenylformamide have higher crystal densities, they also have lower thermal displacement parameters compared to their respective high temperature forms. The phase transition from the low to high temperature forms of the two compounds may be necessary to accommodate extra thermal vibrations at temperatures near their respective melting points.

The ZipOpec module of the OPIX program suite [Gavezzotti, 2003] was used to estimate lattice energies by summation of atom-atom pair wise potential energies or atom-atom interaction energies (described by the UNI force field [Filippini and Gavezzotti, 1993/4/unpublished results]). Values of -103.5 and -96.0 kJ/mol were obtained for **2a** and **2b**, respectively. The difference between these energy values gives an indication of the magnitude of the entropy contribution to the stability of **2b** at high temperatures. The difference in intramolecular energies is significantly smaller than the lattice energy difference (**2a** is more stable by 1.4 kJ/mol and **4a** is more stable by

N-aryl -formamides and -thioamides

1.8 kJ/mol when Cl...O interactions are important or 3.7 kJ/mol when C-H...O interactions are important).²

In addition to lattice energies, ZipOpec calculates molecule-molecule interaction energies to identify which molecular arrangements contribute most to the overall lattice stabilization. To identify each molecule pair (or geometry) we have specified one interaction that links up the pair (see Figure 4.11a and b); however, all interactions (attractive and repulsive) between the molecules contribute to listed energies.

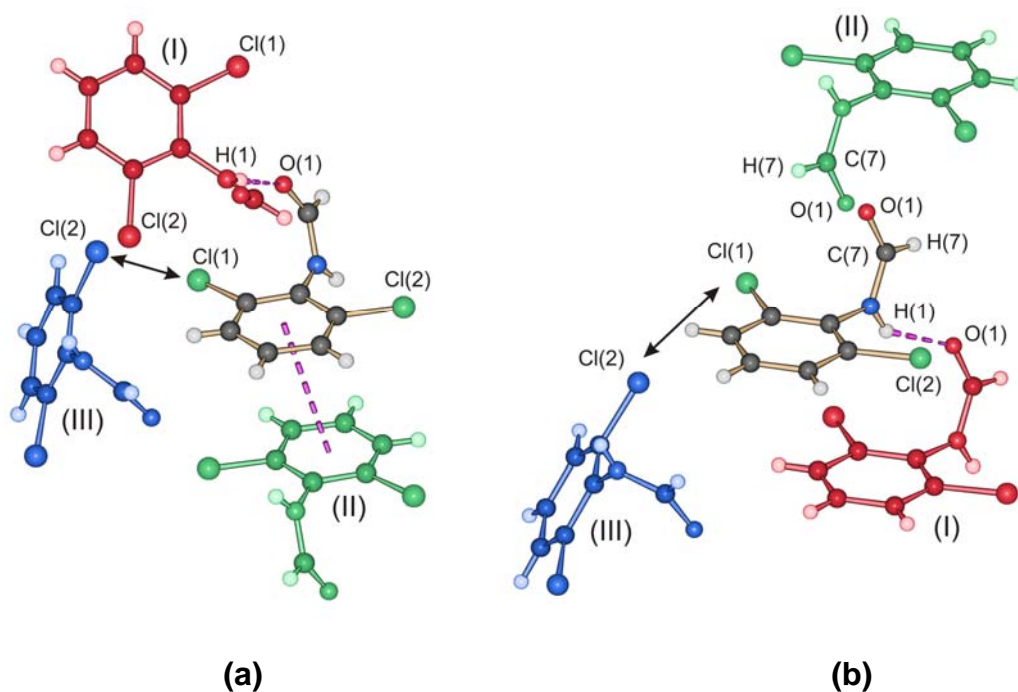


Figure 4.11: (a) The arrangement of the three molecules contributing most to the stability of structure **2a**; (I) molecules involved in hydrogen bonding

² Calculated with Gaussian98 for the geometries of **2a** and **2b** in the crystals (without optimization). These values have not been (and cannot be) corrected for zero point vibrational energy because the necessary frequency calculations are only valid at stationary point geometries.

***N*-aryl -formamides and -thioamides**

(-0.5+x, y, 0.5-z; -39.8 kJ/mol); (II) molecules involved in the $\pi\dots\pi$ interaction (-x, 1-y, -z; -29.8 kJ/mol); (III) molecules involved in the Cl...Cl interaction (-x, 0.5+y, 0.5-z; -8.9 kJ/mol), (b) The arrangement of the three molecules contributing most to the stability of structure **2b**; (I) molecules involved in hydrogen bonding (-1+x, y, z; -42.1 kJ/mol); (II) molecules related by a centre of inversion (2-x, 2-y, 2-z; -11.7 kJ/mol); (III) molecules involved in the Cl...Cl interaction (1.5-x, -0.5+y, 1.5-z; -11.0 kJ/mol).

For **2a**, the most stabilizing interaction is between molecules involved in the N-H...O chain (-39.8 kJ/mol), followed by molecules arranged in a $\pi\dots\pi$ interaction configuration (-29.8 kJ/mol). The third most stabilizing interaction (-8.9 kJ/mol) brings neighboring Cl and H atoms into close proximity and enables Cl...Cl and Cl...H interactions. In **2b**, the most stabilizing interaction is again between those involved in the N-H...O chain (-41.1 kJ/mol). The next most stabilizing geometries contribute -11.7 and -11.0 kJ/mol, respectively towards the lattice stability. The former involves a pair of molecules related by an inversion centre, leading to significant dipole-dipole interactions, while the latter brings two molecules into close enough contact to allow the Cl...Cl interaction associated with **2b** (Figure 4.9b). It is clear that the $\pi\dots\pi$ interaction configuration in **2a** (which is not present in **2b**) contributes to the thermodynamic preference for **2a** (at room temperature) and provides a driving force for the conversion of **2b** into **2a**. Both disordered components of structure **4a** also show a significantly stabilizing $\pi\dots\pi$ interaction

configuration, which is absent from structure **4b** (more of energies relating these interactions is outlined in Chapter 6).

2,6-dichloroacetanilide was reported to undergo a similar phase change from monoclinic to orthorhombic and has similar hydrogen bonding patterns and packing motifs to both phases of 2,6-dichlorophenylformamide and 2-chloro-6-methylphenylformamide [Nagarajan *et. al.*, 1986]. The corresponding phases also have similarities in the sequence of interaction energies. The three most important energies in the structure are arranged in some order depending on their magnitudes. The interactions have either big or small values of energy. Thus the low temperature structures have -big...big...small³ (e.g. structure **2a** has -39.8, -29.8 and -8.9 kJ/mol) while the high temperature forms have big...small...small (e.g. structure **2b** has -42.1, -11.7 and -8.9 kJ/mol) as the order of the most important interactions.

In summary the phase transformation of **2a** and **4a** involves rotation of the aryl group, leaving the N–H...O hydrogen bonding chain intact. This transformation is entropically driven, and reverts back to the low temperature form (for **2a**) in large part because of the stabilizing π ... π interactions. For 2-chloro-6-methylphenylformamide, no reverse phase change is observed and is probably inhibited by intermolecular C–H...O interactions present in the high

³ Refers to the similarities in the sequence of interaction energies for the low temperature structures (big...big...small) versus those of the high temperature forms (big...small...small).

temperature polymorph of this compound but not present in the high temperature polymorph of 2,6-dichlorophenylformamide.

4.3 Polymorphism in 2,6-difluorophenylformamide

Crystals of form II of 2,6-difluorophenylformamide (**1b**) were found by accident in a batch of crystals of 2,6-difluorophenylthioamide (**15**). Since 2,6-difluorophenylformamide (**1a**) is a starting material in the synthesis of 2,6-difluorophenylthioamide it was assumed that unconverted 2,6-difluorophenylformamide from the reaction crystallized out under the influence of 2,6-difluorophenylthioamide thereby obtaining compound **1b**. Attempts to grow crystals of **1b** under controlled conditions were not successful as only the starting crystals (**1a** and **15**) were obtained in their original forms. Figure 4.12 shows crystals of **1b** in a batch of crystals of compound **15**.

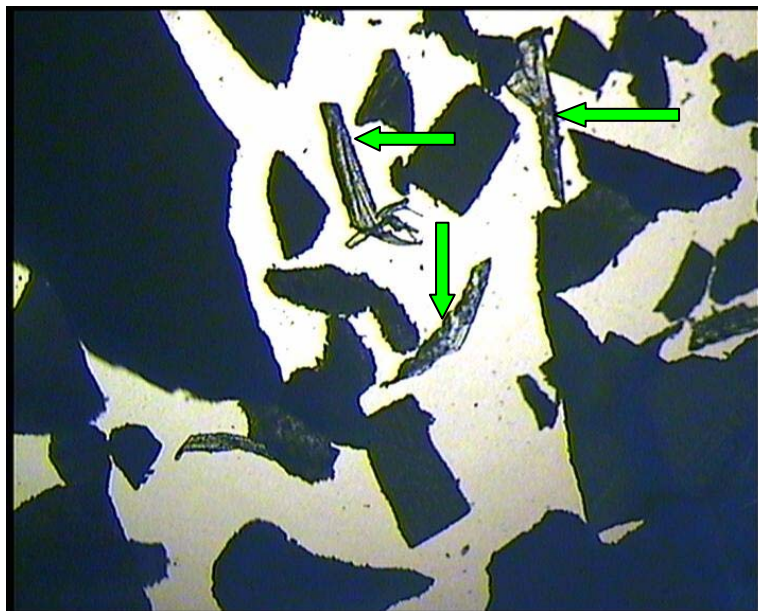


Figure 4.12: Crystals of compound **15** (dark) and compound **1b** (transparent and tiny; indicated by green arrows).

4.3.1 Molecular structure of 2,6-difluorophenylformamide (1a and 1b)

The molecular structures of **1a** and **1b** are similar. **1b** is shown with the atom-labelling scheme in Figure 4.13. Important bond distances and angles as well as intermolecular hydrogen bond parameters were presented in Chapter 3 but are repeated here in Tables 4.3 and 4.4 for comparison.

N-aryl -formamides and -thioamides

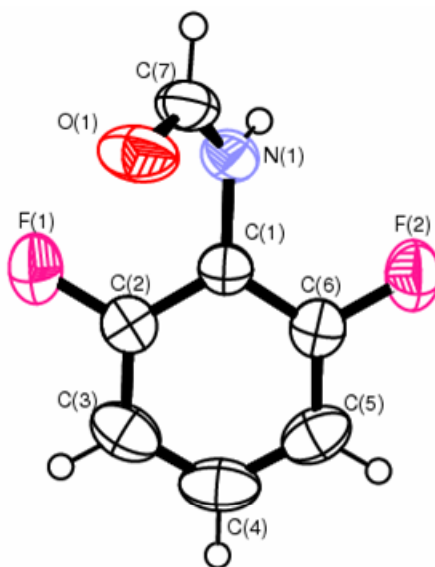


Figure 4.13: ORTEP diagram for structure **1b**. Thermal ellipsoids are given at 50% probability.

Table 4.3: Bond distances and angles for compounds **1a** and **1b** (units in Å and °, respectively). The densities of the two compounds are also included in this table.

Parameter	1a	1b
N(1)–C(7)	1.328(2)	1.334(3)
N(1)–C(1)	1.416(2)	1.416(3)
O(1)–C(7)	1.219(2)	1.224(3)
C(2)–F(1)	1.352(2)	1.354(3)
C(6)–F(2)	1.353(2)	1.351(3)
C(1)–N(1)–C(7)	122.4(1)	123.2(2)
N(1)–C(7)–O(1)	125.8(2)	125.9(2)
C(1)–C(2)–F(1)	118.0(1)	117.9(2)
C(1)–C(6)–F(2)	117.0(2)	116.9(2)
C(7)–N(1)–C(1)–C(2)	60.2(2)	56.6(3)
Densities (mg/m³)	1.532	1.577

***N*-aryl -formamides and -thioamides**

Table 4.4: Hydrogen bonding distances and angles for compounds **1a** and **1b** (units in Å and °, respectively).

Compound	N–H	H ... O	N ... O	N–H ... O	Symmetry operator
1a	0.79(2)	2.06(2)	2.843(2)	170(2)	$-\frac{1}{2} -x, y, \frac{1}{2} -z$
1b	0.86(3)	2.00(3)	2.807(4)	157(3)	$-1+x, y, z$

The molecular geometry of compounds **1a** and **1b** is similar in that all show a *trans* conformation with the formamide moiety being out of the plane of the aromatic ring (Figure 3.1 in Chapter 3). The angle between the planes defined by the aryl ring [C(1)-C(6)] and the formamide group [C(1)-N(1)-C(7)-O(1)] is smaller for **1b** (56.6°) than for **1a** (60.2°). This is different from what is observed in the two forms of 2,6-dichlorophenylformamide and 2-chloro-6-methylphenylformamide as well as from the previously reported 2,6-dichloroacetanilide [Nagarajan *et. al.*, 1986], where the low temperature forms have a lower value of this torsion angle as compared to the high temperature forms.

4.3.2 Crystal packing, Hydrogen bonding and intermolecular interactions

Hydrogen bonding patterns of the crystal structures are shown in Figures 4.14 and 4.15. The hydrogen bond distances and angles are given in Table 4.3.

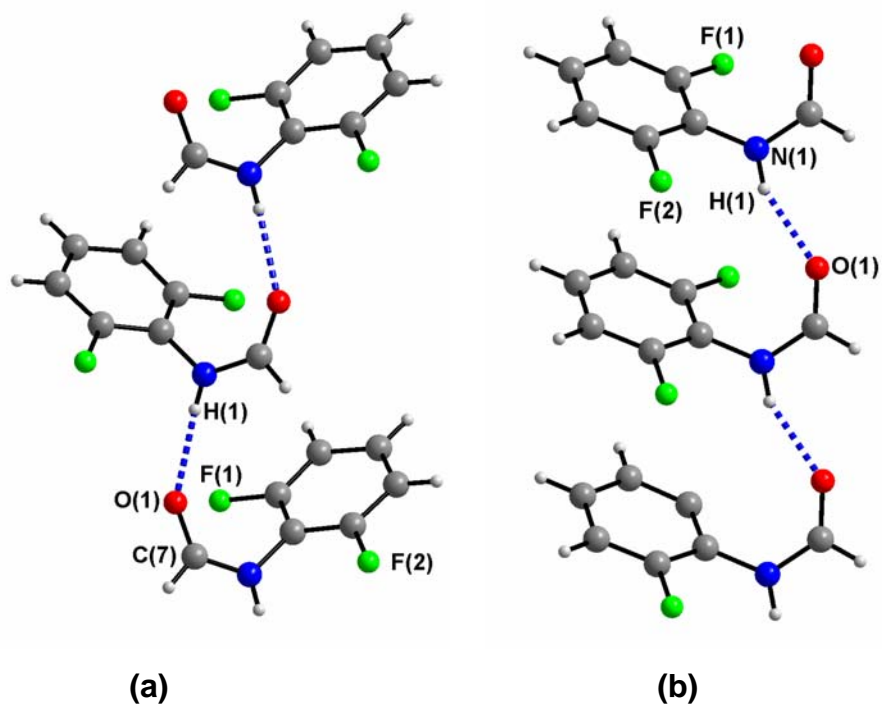


Figure 4.14: Hydrogen bonded chains in 2,6-difluorophenylformamide showing (a) the alternating arrangement due to a glide plane in **1a** (Symmetry operator = $-\frac{1}{2} + x, y, \frac{1}{2} - z$) and (b) the stacked relationship of molecules related by unit cell translation in **1b** (Symmetry operator = $-1 + x, y, z$).

N-H...O hydrogen bond is present in **1a** and **1b**. Form I (**1a**) has molecules linked together by the N-H...O hydrogen bonds (Table 4.3) forming

N-aryl -formamides and -thioamides

chains of molecules related by a glide plane in the crystallographic *a* direction. This results in the formamide molecules pointing in alternating directions (Figure 4.14a). Adjacent chains are held together through $\pi\cdots\pi$ interactions [$Cg\cdots Cg = 3.903 \text{ \AA}$] between aryl groups on neighbouring chains forming sheets of molecules parallel to (101) [Figure 4.15]. Neighbouring sheets interact with each other through C-H \cdots F interactions (see Figures 4.16) and bifurcated C-H \cdots O interactions.

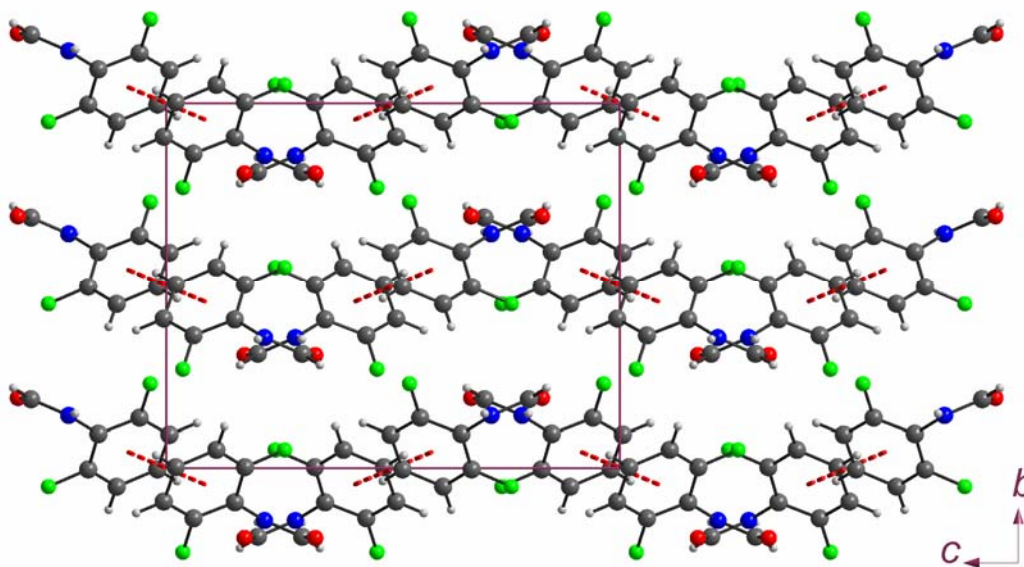


Figure 4.15: Crystal packing in the structure of **1a** showing chains of N-H \cdots O hydrogen bonded molecules running down the *a* axis (perpendicular to the plane of the page) and linked to each other through $\pi\cdots\pi$ interactions.

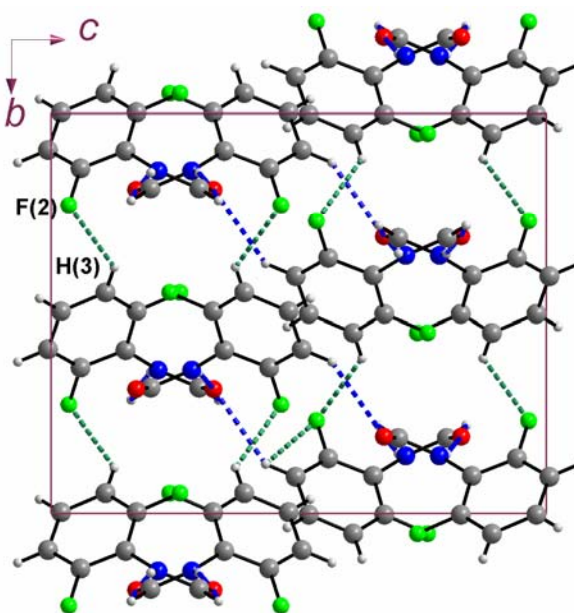


Figure 4.16: A view down the *a* crystallographic axis of **1a**. Sheets of N-H...O hydrogen bonded molecules are linked by C-H...F (indicated in green dashed lines) and C-H...O interactions (in blue dashed lines).

The hydrogen bonded chains in **1b** are very similar to that of the high temperature forms of 2,6-dichlorophenylformamide and 2-chloro-6-methylphenylformamide **2b** and **4b**. In these structures the molecules are stacked with the aryl rings linearly arranged on top of one another and related by translation along a crystallographic axis (the *a* axis for **1b** and **2b** and the *b* axis for **4b**). This results in the molecules being parallel to each other forming chains though N-H...O hydrogen bonding [$N(1)\dots O(1) = 2.807$ Å] along the crystallographic *a* direction (Table 4.4 and Figure 4.14). These stacks are further strengthened by two C-F... π intermolecular interactions

N-aryl -formamides and -thioamides

between molecules related by a 2_1 -screw axis [$F(1)\dots Cg = 3.824 \text{ \AA}$] and by translation [$F(2)\dots Cg = 3.433 \text{ \AA}$]. Neighbouring chains in **1b** are further connected through C-H...F [$F(2)\dots H(5) = 2.650 \text{ \AA}$, $F(1)\dots H(3) = 2.450 \text{ \AA}$] and C-H...O interactions [$H(4)\dots O(1) = 2.600$] along the *b* axis to form sheets of molecules parallel to the (001) plane (Figure 4.17). Adjacent sheets are held together by van der Waals interactions such as F...H interactions.

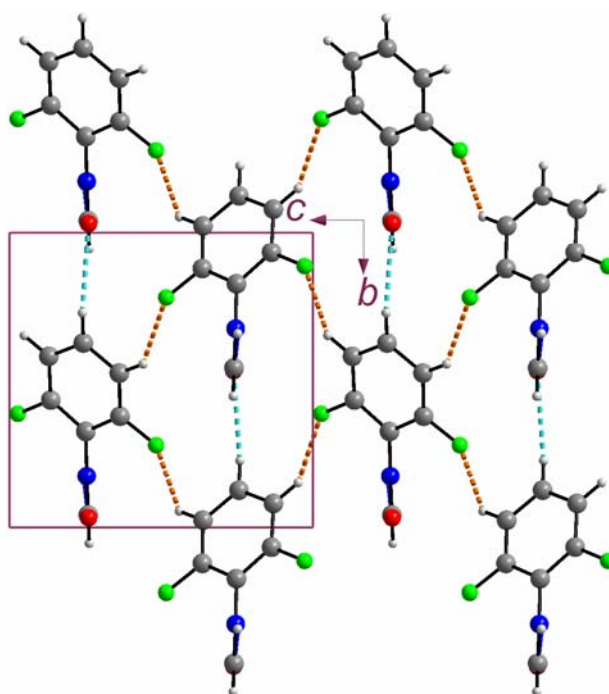


Figure 4.17: Sheets of C-H...F (shown in purple dashed lines) and C-H...O (shown in red dashed lines) hydrogen bonded molecules of compound **1b**.

4.3.3 Results from lattice energy calculations

Estimation and description of lattice energies by summation of potential energies between interacting atoms (or atom-atom interaction energies) was carried out using the ZipOpec module of the OPIX program suite [Gavezzotti, 2003] described by the UNI force field [Filippini and Gavezzotti, 1993/4 / unpublished results] in similar manner as was done for 2,6-dichlorophenylformamide and 2-chloro-6-methylphenylformamide. Values of -91.3 and -89.9 kJ/mol were obtained for the lattice energies of **1a** and **1b**, respectively. The difference between these energy values could be an indication of the relative stability of the two polymorphs. However the two polymorphs remain stable at room temperature. Sublimation of **1a** did not result in **1b**. The difference in N-H...O hydrogen bond energies is the same as the lattice energy difference (**1a** is more stable by 1.4 kJ/mol).⁴ The energy contribution of C-H...F interaction in **1b** is bigger than in **1a**. This compensates for the lack of π ... π interactions in **1b** which contribute more than twice the amount of energy C-H...F interactions contributes in **1a**.

A look at molecule-molecule interaction energies as calculated by ZipOpec helped identify the molecular arrangements that contribute most to the overall lattice stabilization (see Chapter 6 also). This was done in the

⁴ Calculated with Gaussian98 for the geometries of **1a** and **1b** in the crystals (without optimization). These values have not been (and cannot be) corrected for zero point vibrational energy because the necessary frequency calculations are only valid at stationary point geometries.

***N*-aryl -formamides and -thioamides**

same way as for 2,6-dichlorophenylformamide and 2-chloro-6-methylphenylformamide.

For **1a** (Figure 4.18), the most stabilizing interaction is between molecules involved in the N-H...O chain (-35.2 kJ/mol), followed by molecules arranged in a π ... π interaction configuration (-21.9 kJ/mol). The third most stabilizing interaction (-9.1 kJ/mol) brings neighboring F and H atoms into close proximity to form C-H...F interactions. In **1b**, the most stabilizing interaction is again between those involved in the N-H...O chain (-36.9 kJ/mol). The next most stabilizing geometries contribute -12.6 and -12.4 kJ/mol and these involve molecules interacting via C-H...F and C-F... π interactions, respectively towards the lattice stability. As we mentioned earlier it seems like the π ... π interaction configuration in **1a** (which is not present in **1b**) contributes to the thermodynamic preference for **1a** at room temperature.

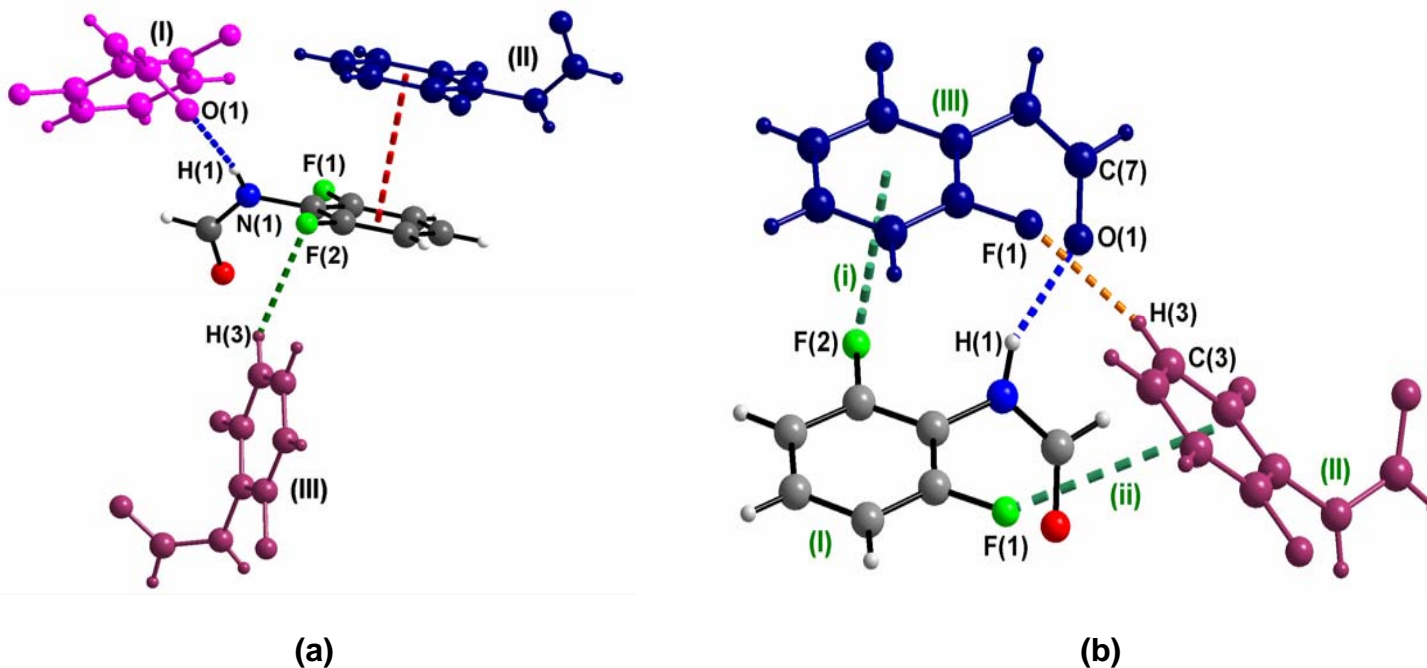


Figure 4.18: (a) The arrangement of the four molecules contributing most to the stability of structure **1a**; (I) molecules involved in hydrogen bonding ($-0.5+x, y, 1.5-z$; -35.2 kJ/mol); (II) molecules involved in the $\pi\dots\pi$ interaction ($2-x, 1-y, 1-z$; -21.9 kJ/mol); (III) molecules involved in the F...H interaction ($1.5-x, -0.5+y, z$; -9.1 kJ/mol), (b) The arrangement of the three molecules contributing most to the stability of structure **1b**; (III) molecules involved in hydrogen bonding ($-1+x, y, z$; -36.9 kJ/mol); (II and I) molecules related by F... π interaction ($1-x, -0.5+y, 1-z$; -12.4 kJ/mol); (III and II) molecules involved in the F...H interaction ($1-x, -0.5+y, 2-z, 0.5-z$; -12.6 kJ/mol).

***N*-aryl -formamides and -thioamides**

In summary we have outlined the three interactions for each polymorph that contribute the most to stabilization of the crystals. The two sets of energies follow the same order in terms of magnitudes [-35, -21 and -9.1 kJ/mol (big...big...small) and -36.9, -12.6 and -12.4 (big...small...small) for **1a** and **1b** respectively] as in the polymorphs of 2,6-dichlorophenylformamide and 2-chloro-6-methylphenylformamide. The $\pi\cdots\pi$ interactions in **1a** might be the cause of higher lattice energy when compared to **1b** which does not have the interactions. **1b** does not seem to revert to **1a** an indication of its stability after formation. **1a** is more stable than **1b** by only 1.4 kJ/mol. The packing patterns for the two polymorphs of 2,6-difluorophenylformamide (**1a** and **1b**) are similar to those of 2,6-dichlorophenylformamides (**2a** and **2b**) and 2-chloro-6-methylphenylformamide (**4a** and **4b**). It is possible that the same mechanism proposed for the transformation of **2a**, **4a** to **2b**, **4b**, takes **1a** to **1b**.

5. Isomorphism and Cocrystallization of some aryl -formamides and -thioamides

5.1 Introduction

The formation of identical packing motifs can be expected if the related molecules exhibit only small differences on their surfaces. The differences may often be in atomic replacements and minor alterations in substitutions and or epimerization (when the chiral centre is changed).

A number of factors are known to be the driving forces to isomorphism in organic structures. Studies have shown that, under appropriate circumstances, interchanging parts (with similar volumes) of a molecule such as chlorine atom for a methyl group [also known as chloro-methyl interchange; Edwards *et. al.*, 2001] might not change much the crystal packing [Kitaigorodskii, 1973]. Apart from chloro-methyl interchange, other interchanges such as chloro-bromo, bromo-methyl *etc.* have been reported [Bar and Bernstein, 1987 and references therein].

Other studies have shown that isomorphism can also be as result of overall volume of a molecule. It is argued that when a molecule is sufficiently big, it is possible to replace one atom in a molecule with another atom (even if the two are greatly different in size) and still keep the structural features of the former. This is only possible as long as the void left by the atom that is being replaced can accommodate the

replacing atom comfortably. Small molecules such as urea (CH₄N₂O) and thiourea (CH₄N₂S) cannot develop isomorphous lattices since the difference in volume of S and O is significant with respect to the small molecules themselves [Kitaigorodskii, 1961].

The degree of isomorphism can be defined in a number of ways (see discussion in Chapter 1) and in this work the *unit-cells similarity index* [Kalman *et. al.*, 1991; Rutherford, 1997] as well as the graphical method for comparing short intermolecular distances similar to the ones described by Dziubek and Katrusiak [2004] are used.

Related to isomorphism in the aryl -formamides and -thioamides discussed in this work is structural mimicry, where non-isomorphous molecules can cocrystallize to give mixed crystals in which one component is forced to adopt a packing arrangement different from which it adopts in the pure crystal [Edwards *et. al.*, 2001]. An example from literature is that of the cocrystallization of the non-isomorphous chlorinated and methylated derivatives of 2-benzyl-5-bromobenzylidene-cyclopentanone [Jones *et. al.*, 1983].

We now report isomorphism and cocrystallization of selected aryl -formamides and -thioamides synthesized in this work. The isomorphous structures were 2,6-difluorophenylformamide (**1a**), 2,6-dichlorophenylformamide (**2a**) and 2-chloro-6-methyl-phenylformamide

(**4a**); 2,6-dimethylphenylthioamide (**17**) and 2-chloro-6-methylphenylthioamide (**18**); and 2,6-diisopropylphenyl -formamide (**6**) and -thioamide (**20**). From these sets of structures, three cocrystals were generated; the cocrystal of - 2,6-difluorophenylformamide (**1a**) and 2,6-dimethylphenylformamide (**3**); 2,6-dichlorophenylthiomamide (**16**) and 2,6-dimethylphenylthiomamide (**17**); and 2,6-diisopropylphenylformamide (**6**) and 2,6-diisopropylphenylthiomamide (**20**).

5.2 Isomorphism and cocrystallization in 2,6 disubstituted aryllformamides

5.2.1 Isomorphism

The *ORTEP* diagrams for the isomorphous crystal structures of 2,6-difluorophenylformamide (**1a**), 2,6-dichlorophenylformamide (**2a**) and 2-chloro-6-methyl-phenylformamide (**4a**) are in the appendix. Isomorphism between the structures of **1a**, **2a** and **4a** is shown by the use of important bond distances and angles (Tables 5.1), crystal data (Table 5.2), calculation of *unit cell similarity indices* and comparison of the closest non-bonding distances of the three structures (Figure 5.2).

N-aryl -formamides and -thioamides

Table 5.1 Bond distances (Å) and angles (°) for compounds **1a**, **2a** and **4a**

Parameter	1a	2a	4a
C(1)-N(1)	1.414(2)	1.418(2)	1.424(2)
N(1)-C(7)	1.330(3)	1.337(2)	1.337(2)
C(7)-O(1)	1.216(3)	1.221(2)	1.221(2)
C(1)-N(1)-C(7)	122.6(2)	123.4(2)	124.1(2)
N(1)-C(7)-O(1)	125.6(2)	125.9(2)	125.9(2)
C(2)-C(1)-N(1)-C(7)	60.3(2)	67.3(3)	67.2(2)

Table 5.2: Unit cell parameters for compounds **1a**, **2a** and **4a**

Compound	Space group	Cell Parameters
1a	<i>Pbca</i>	8.503(2), 11.387(2), 14.075(3) [Å] 90, 90, 90 [°] 1362.8(4) Å ³
2a	<i>Pbca</i>	8.604(1), 12.743(2), 14.402(2) [Å] 90, 90, 90 [°] 1578.9(3) Å ³
4a	<i>Pbca</i>	8.445(2), 12.903(3), 14.419(3) [Å] 90, 90, 90 [°] 1571.0(6) Å ³

The bond distances and angles of the three structures show great similarities with the exception of the torsion angle [C(2)-C(1)-N(1)-C(7)] of 2,6-difluorophenylformamide (**1a**) which is smaller by about 7° (see Table 5.1). The unit cell parameters for the three structures are also similar. This is evident from the *unit cell similarity indices* between **1a** and **2a**, **2a** and **4a** and between **1a** and **4a** which are very close to zero (0.053, 0.005 and 0.053 respectively).

The packing of molecules in the crystals of the three compounds are similar (see Figure 5.1). N-H...O and C-H...O hydrogen bonds, and C-H... π and π ... π interactions are important in the solid state structures of **1a**, **2a** and **4a** (see Chapter 3). All compounds form N-H...O hydrogen bonded chains which are linked by C-H...O and π ... π interactions. The substituents on the phenyl ring of compound **4a** are disordered over two positions (in a ratio = 0.57:0.43). This disorder in the structure of **4a** allows for similar regions of halogen interactions and hydrocarbon interactions.

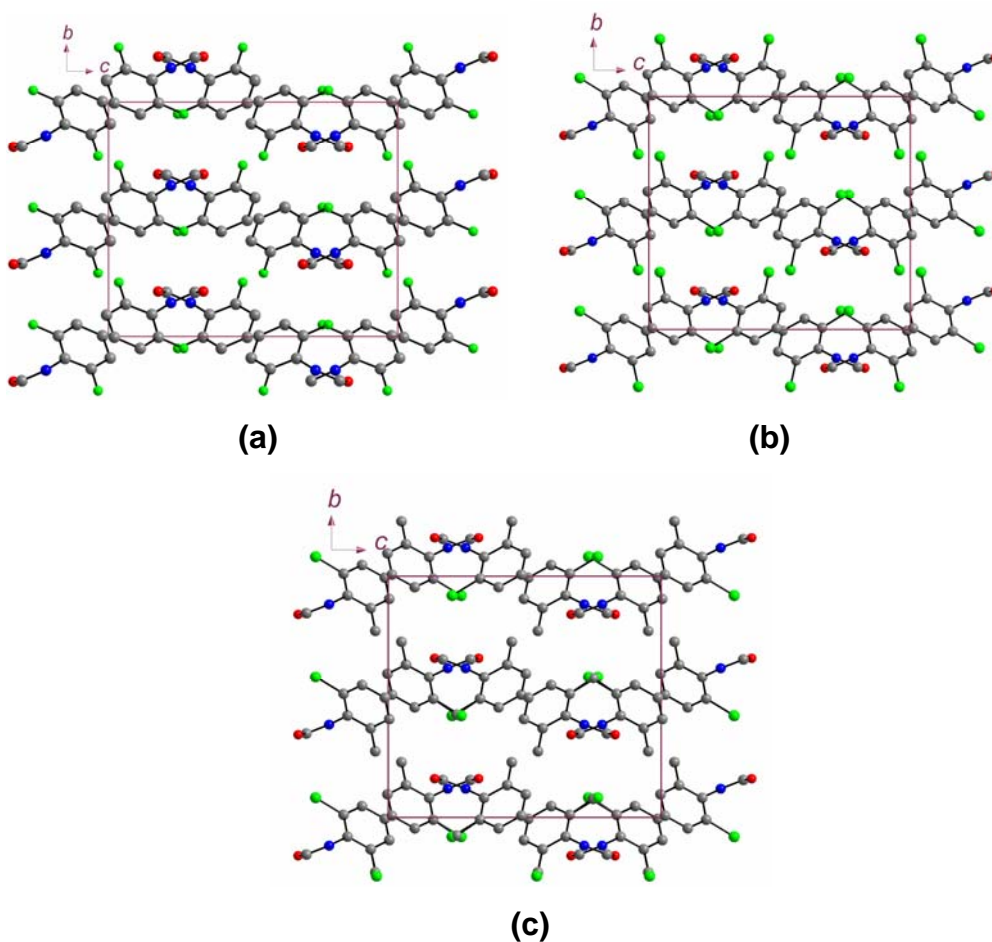


Figure 5.1: Crystal packing in compounds (a) **1a**; (b) **2a**; and (c) **4a** as viewed down the crystallographic *a* axis. Hydrogen atoms have been omitted for clarity.

N-aryl -formamides and -thioamides

The shortest intermolecular contacts for all atoms were calculated using *PLATON* and compared using a bar graph (Figures 5.2). Each of the distances on the plot is related to three of specific contacts in the structures of **1a**, **2a** and **4a**. Six non-hydrogen distances were compared for each of the three isomorphous compounds and this showed that the compared contacts are similar.

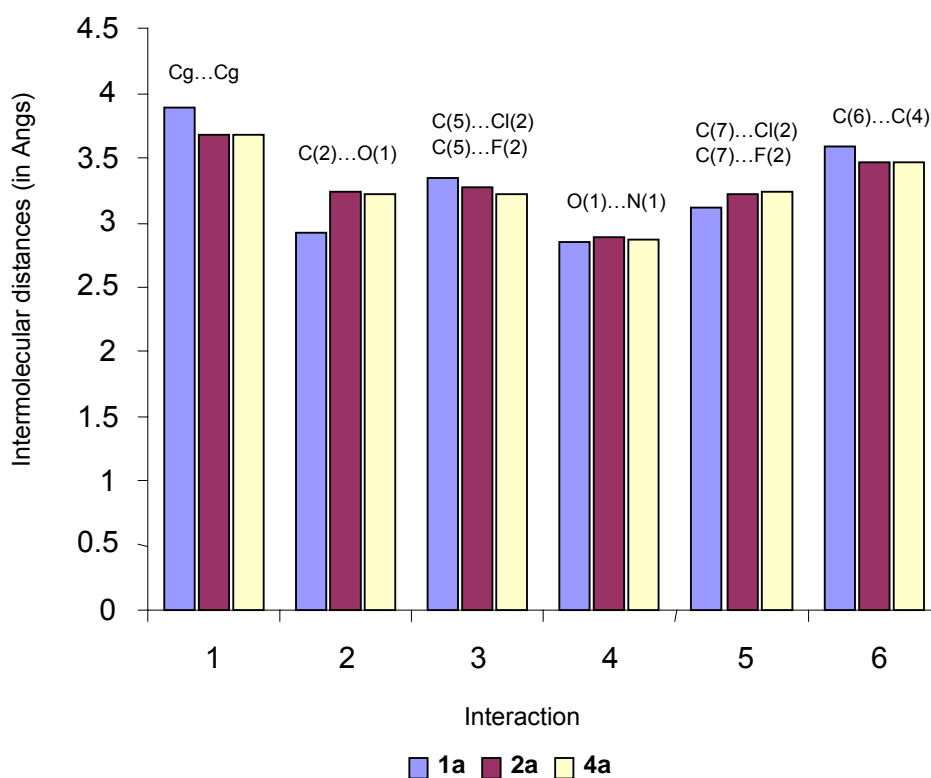
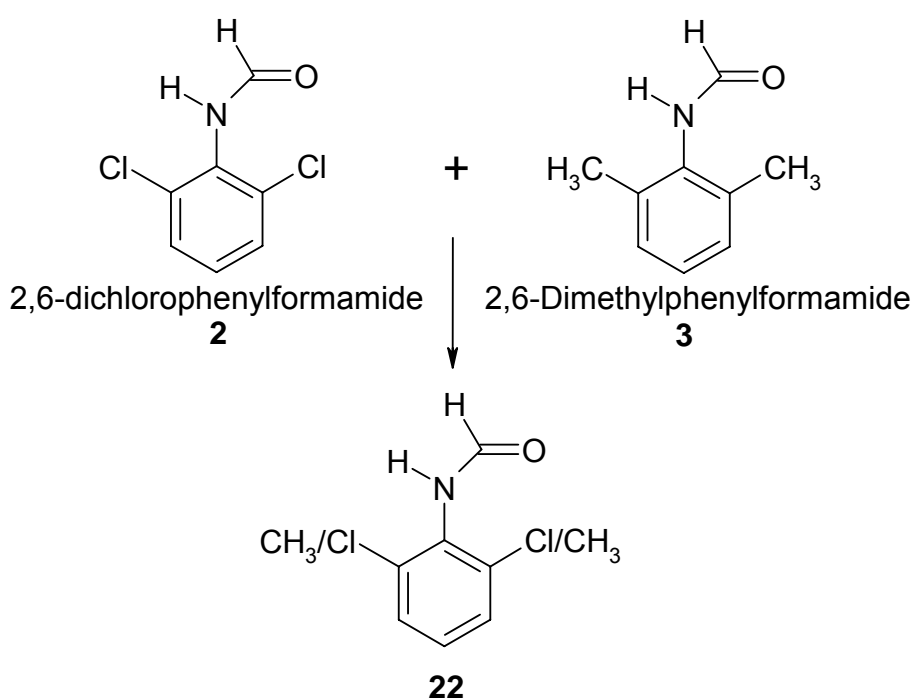


Figure 5.2: Bar graph comparing isomorphous compounds; a comparison of the closest non-bonding distances in compounds **1a**, **2a** and **4a**.

5.2.2 Cocrystallization of 2,6-dichlorophenylformamide (2a) and 2,6-dimethylphenylformamide (3)

The cocrystallization of 2,6-dichlorophenylformamide and 2,6-dimethylphenylformamide resulted in the 1:1 cocrystal **22** (see Scheme 5.1) which was confirmed by X-ray powder and single crystal diffraction studies. DSC was also used for further analysis of the cocrystals.



Scheme 5.1: Non-isomorphous compounds **2a** and **3** used in cocrystallization studies resulting in compound **22**

2,6-dichlorophenylformamide **2a** and 2,6-dimethylphenylformamide **3** are non-isomorphous and crystallize in the space groups *Pbca* and *P2₁2₁2₁* respectively. The two are however conformationally similar in so far as both adopt a *cis* conformation (see Chapter 3). Two polymorphic

***N*-aryl -formamides and -thioamides**

forms of 2,6-dichlorophenylformamide have been reported [Omondi *et. al.*, 2005] and are also discussed in this thesis: the room temperature polymorph (**2a**) grown from solution and the higher temperature polymorph (**2b**) obtained by sublimation of the room temperature polymorph. One structure is known for 2,6-dimethylphenylformamide. Mixed crystals of 2,6-dichlorophenylformamide and 2,6-dimethylphenylformamide were examined from the viewpoint of structural mimicry. The crystals were obtained by grinding the two starting compounds together followed by crystallization by slow evaporation from a 9:1 solution of ethyl acetate and acetonitrile. A comparison of the unit cell parameters for the starting materials and the cocrystal are given in Table 5.3.

Table 5.3: Unit cell parameters of 2,6-dichlorophenylformamide **2a**, 2,6-dimethylphenylformamide **3**, cocrystal **22** and 2-chloro-6-methylphenylformamide **4a**.

Compounds	Space group	Unit cell parameters
2a	<i>Pbca</i>	$a = 8.604(1)$ $b = 12.743(2)$ $c = 14.402(2)$ $\alpha = \beta = \gamma = 90^\circ$
3	<i>P2₁2₁2₁</i>	$a = 4.502(4)$ $b = 8.589(8)$ $c = 21.297(2)$ $\alpha = \beta = \gamma = 90^\circ$
22	<i>Pbca</i>	$a = 8.507(1)$ $b = 13.093(2)$ $c = 14.448(2)$ $\alpha = \beta = \gamma = 90^\circ$

The cocrystal **22**, 2,6-dichlorophenylformamide **2** and 2-chloro-6-methylphenylformamide **4a** were found to be isomorphous hence the similar powder patterns. Comparison of the calculated powder patterns against the experimental powder patterns indicated the isomorphism of the three structures. The calculated PXRD patterns (calculated using *PLATON* and atom coordinates from the single crystal analyses) matched the experimental powder patterns of the bulk material of 2,6-dichlorophenylformamide **2a** and 2,6-dimethylphenylformamide **3** and the cocrystal **22**, demonstrating that the powder and the single crystals were the same.

5.2.2.1 Powder X-ray diffraction analysis

PXRD patterns of 2,6-dichlorophenylformamide, 2,6-dimethylphenylformamide and the cocrystal **22** are shown in Figure 5.3. As the powder patterns indicate, the indices of the peaks of the three compounds are significantly different. Most of the peaks for the pattern of structure **22** have 2θ values that correspond to those of 2,6-dichlorophenylformamide (but are slightly shifted) an indication that it (cocrystal **22**) adopts the packing pattern of 2,6-dichlorophenylformamide.

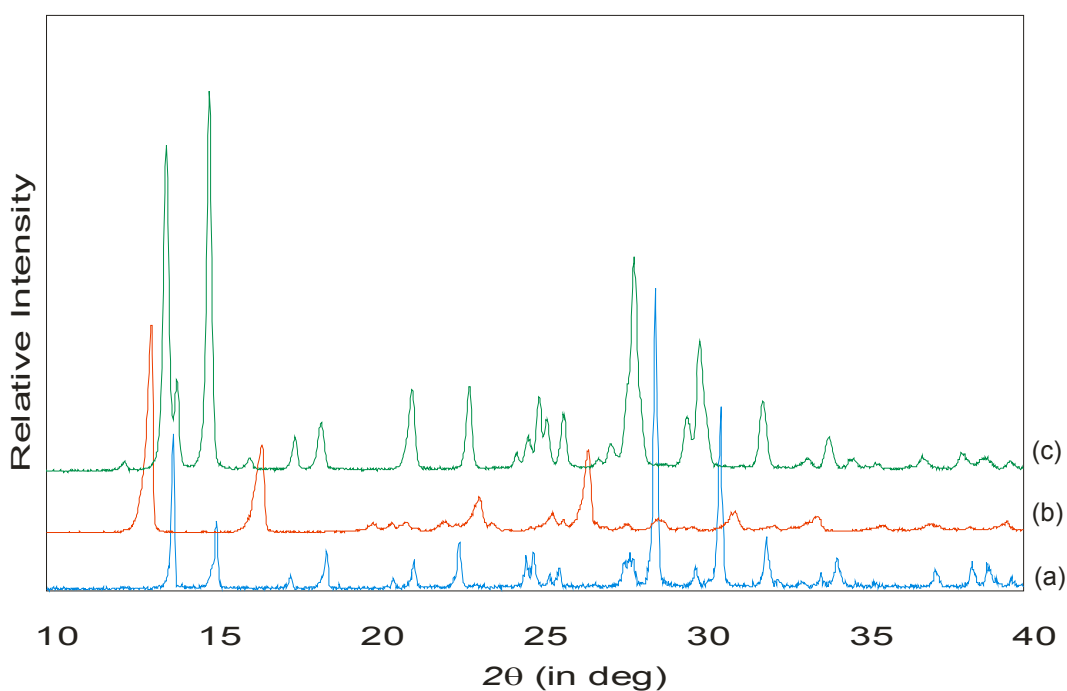


Figure 5.3: Experimental powder patterns for (a) 2,6-dichlorophenylformamide **2** (in blue), (b) 2,6-dimethylphenylformamide **3** (in red) and (c) the cocrystal **22** in (green lines).

Cocrystallization was also done using various compositions of 2,6-dichlorophenylformamide (in blue) and 2,6-dimethylphenylformamide and the powder patterns were recorded at room temperature (Figure 5.4). This was done to examine the extent to which changing the ratios of the two compounds can still result in cocrystals. Single crystals were obtained for a 1:1 mixture. This corresponded to a 1:1 mixture of the two compounds.

The results given in Figure 5.4 are consistent with the formation of cocrystals at varying stoichiometries. This seems particularly obvious for intermediate adduct ratios (i.e. 3:7 and 7:3, (c) and (e) in Figure 5.4). The extreme compositions (1:9 and 9:1, (b) and (f) in Figure 5.4) did not result

in the formation of cocrystals but rather in the separate pure crystals of both starting materials (with peaks of the sample with the higher percentage being prominent). There is evidently a systematic shift of the peaks, which could be a possible indication that the overall structure adopted amongst the different compositions was that of compound **2** (*c.f.* cell parameters in Table 5.2).

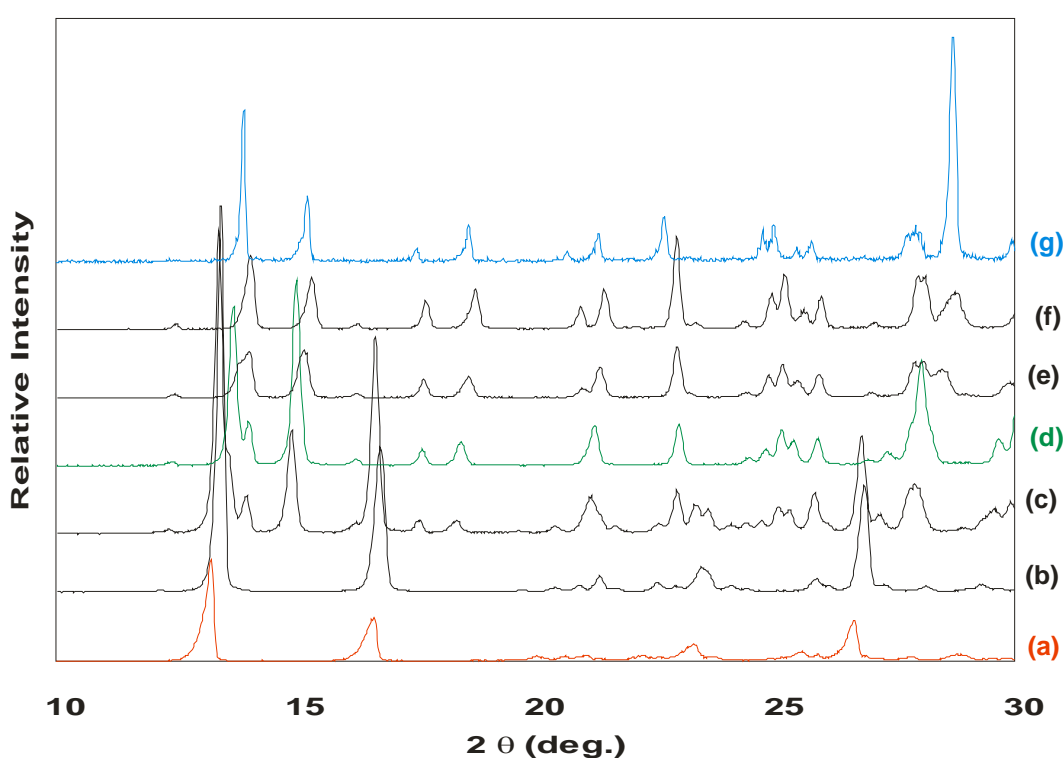


Figure 5.4: Experimental powder patterns for cocrystals of **2** and **3** with differing stoichiometry. The ratios are as follows; 2,6-dichlorophenylformamide : 2,6-dimethylphenylformamide (a) 10:0, (b) 9:1, (c) 7:3, (d)1:1, (e) 3:7, (f) 1:9 and (g) 0:10.

5.3 Isomorphism and cocrystallization in 2,6 disubstituted arylthioamides**5.3.1 Isomorphism**

The *ORTEP* diagrams for the isomorphous crystal structures of 2,6-dimethylphenylthioamide (**17**) and 2-chloro-6-methyl-phenylthiomamide (**18**) are in the appendix. Isomorphism in the structures of **17** and **18** was shown using similar methods as mentioned in section 5.2.1. Table 5.4 shows important bond distances and angles and Table 5.5 the crystal data of the two structures.

Table 5.4 Bond distances (Å) and angles (°) for compounds **1a**, **2a** and **4a**

Parameter	17	18
C(1)-N(1)	1.436(3)	1.427(2)
N(1)-C(7)	1.315(3)	1.316(3)
C(7)-S(1)	1.646(2)	1.647(2)
C(1)-N(1)-C(7)	124.3(2)	124.0(2)
N(1)-C(7)-S(1)	126.9(2)	125.9(2)
C(2)-C(1)-N(1)-C(7)	64.0(2)	60.3(2)

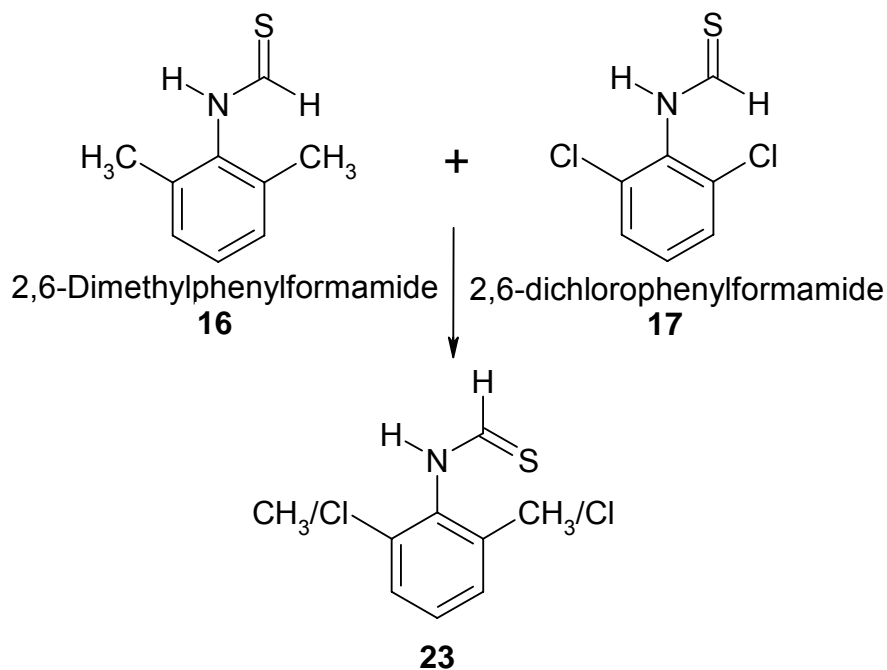
Table 5.5: Unit cell parameters for compounds **1a**, **2a** and **4a**

Compound	Space group	Cell Parameters
17	<i>C2/c</i>	14.555(3), 8.060(2), 16.133(3) [Å] 90, 101.422(10), 90 [°] 1855.1(6) Å ³
18	<i>C2/c</i>	14.367(5), 8.022(5), 16.068(5) [Å] 90, 100.920(5), 90 [°] 1578.9(3) Å ³

The bond distances and angles of the two structures show great similarities with the *unit cell similarity indices* between them being close to zero (-0.709). The packing of molecules in the crystals of the two compounds is similar and are determined mainly by N-H...S, C-H...S, C-H... π and π ... π (see Chapter 3). The substituents on the aryl ring of compound **18** are disordered over two positions (in a ratio = 0.57:0.43). This disorder in the structure of **18** allows for similar regions of halogen interactions. A comparison of the packing patterns of the two isomorphous structures and a bar graph comparing corresponding non-hydrogen intermolecular distances can be found in Appendix D1.

5.3.2 Cocrystallization of 2,6-dimethylphenylthioamide 16 and 2-chloro-6-methylphenylthioamide 17

The cocrystallization of 2,6-dimethylphenylthioamide **16** and 2-chloro-6-methylphenylthioamide **17** gave cocrystals as was confirmed by X-ray powder diffraction and single crystal studies (see Scheme 5.2).



Scheme 5.2: Non-isomorphous compounds **16** and **17** used in cocrystallization studies resulting in compound **23**

2,6-dimethylphenylthioamide and 2-chloro-6-methylphenylthioamide are non-isomorphous and crystallize in the space groups $P2_1/c$ and $C2/c$. The two are however conformationally similar and have a *trans* conformation (see Chapter 3). Grinding the two compounds together, then crystallizing from a solution of methanol and chloroform gave crystals of the cocrystal which did not adopt neither the structures nor the conformation of the starting materials. It is noted here that attempts to grow the cocrystal straight from solution without grinding did not result in the desired product but rather a mixture of the pure starting materials.

5.3.2.1 Powder X-ray diffraction analysis

PXRD patterns of 2,6-dimethylphenylthioamide and 2-chloro-6-methylphenylthioamide and cocrystal **23** are shown in Figure 5.5. As the powder patterns in Figure 5.5 indicate, the indices of the peaks of the three compounds are significantly different.

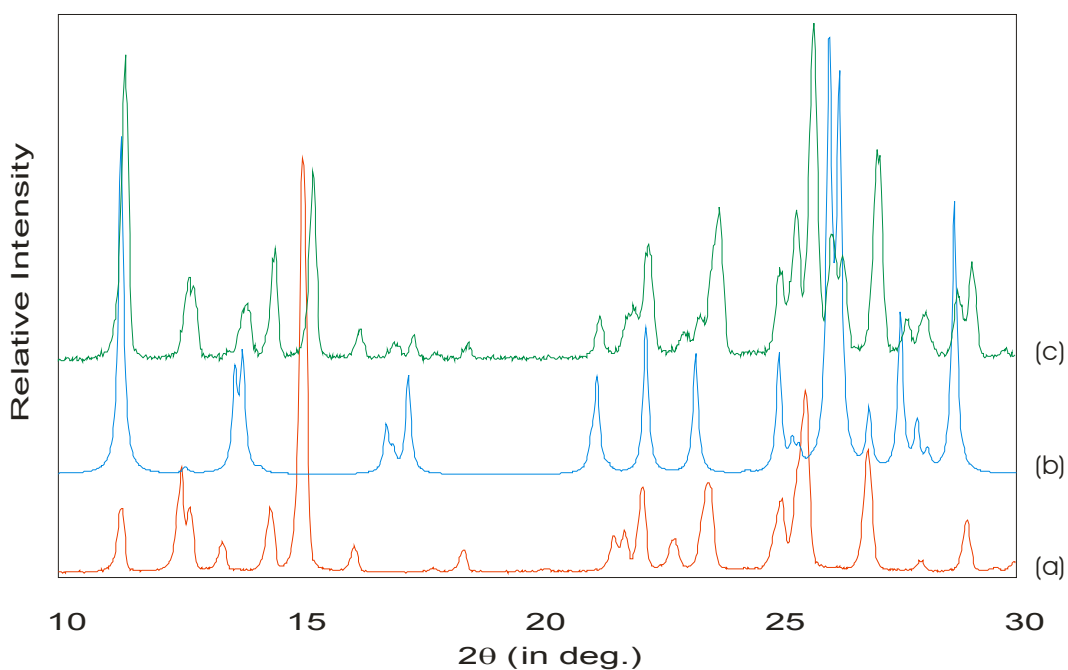


Figure 5.5: Experimental powder patterns of (a) 2,6-dimethylphenylthioamide **16** (in red), (b) 2-chloro-6-methylphenylthioamide **17** (in blue) and (c) cocrystal **23** (in green lines)

Table 5.6: Unit cell parameters for 2,6-dimethylphenylthioamide **16**, 2-chloro-6-methylphenylthioamide **17** and cocrystal **23**

Compounds	Space group	Unit cell parameters
16	<i>P2₁/c</i>	$a = 7.873(2)$ $b = 15.643(4)$ $\beta = 117.336(5)^\circ$. $c = 7.991(2)$
17	<i>C2/c</i>	$a = 14.555(3)$ Å $b = 8.0597(16)$ $\beta = 101.422(4)$ $c = 16.133(3)$
23	<i>Pbca</i>	$a = 9.208(5)$ $b = 13.142(5)$ $c = 14.617(5)$ $\alpha = \beta = \gamma = 90^\circ$

Table 5.6 lists the unit cell parameters for 2,6-dimethylphenylthioamide **16**, 2-chloro-6-methylphenylthioamide **17** and cocrystal **23**. The cocrystal crystallizes in the space group *Pbca* with $Z = 8$ and one molecule in the asymmetric unit. The molecular geometry of compound **23** is different from that of compounds **16** and **17** showing a *trans*-thioamide conformation (the N-H hydrogen being *trans* to the C=S group) with the thioamide moiety being orientated out of the plane of the aromatic ring. The reason for the formation of the *trans* conformation is not yet fully understood. The angle between the planes defined by the aryl ring [C(1)-C(6)] and the formamides group [C(1)-N(1)-C(7)-O(1)] is 81.67° . This is slightly larger than that of the other isomorphous structures **1a**, **2a**, **4a** and cocrystal **22**.

There are no common features observed in the hydrogen-bonding network of compounds **16**, **17** and **23**. The crystal structures of compounds **16**, **17** and **23** are discussed in Chapters 3. In the crystal structure of **23**, molecules are linked together by N-H...S hydrogen bonds forming chains that run in the crystallographic *a* direction similar to the ones of the isomorphous structures **1a**, **2a**, **4a** and cocrystal **22**.

5.4 Isomorphism and cocrystallization of 2,6-diisopropylphenyl-formamide and 2,6-diisopropylphenylthioamide

5.4.1 Isomorphism

The crystal structures together with the atom-numbering scheme of 2,6-diisopropylphenyl -formamide and -thioamide can be found in the appendix. A comparison of the geometric parameters of the two compounds is shown in Table 5.7 and the unit cell parameters are given in Table 5.8. The two tables also include data for the structure of cocrystal (**24**) since the three are isomorphous. Comparison of the two isomorphous structures was done using the *unit cell similarity index* [Fábián and Kálmán, 1999] and by the use of a bar graph comparing non-hydrogen intermolecular interactions.

Table 5.7 Bond distances (Å) and angles (°) for compounds **6** and **20**

Parameter	6	20	24
C(1)-N(1)	1.442(2)	1.438(3)	1.438(3)
N(1)-C(7)	1.330(2)	1.292(4)	1.292(4)
C(7)-O(1)/S(1)	1.220(2)	1.646(3)	1.220(2)/1.646(3)
C(1)-N(1)-C(7)	123.3(2)	127.2(2)	127.2(2)
N(1)-C(7)-O(1)/S(1)	126.1(2)	128.9(2)	125.8(2)/128.9(2)
C(2)-C(1)-N(1)-C(7)	78.9(2)	80.7(3)	77.5(3)

Table 5.8: Unit cell parameters for compounds **6** and **20**

Compound	Space group	Cell Parameters
6	<i>P2₁/c</i>	9.034(1), 8.858(1), 16.001(2) [Å] 90, 104.896(3), 90 [°] 1237.5(3) Å ³
20	<i>P2₁/c</i>	9.023(5), 9.367(5), 16.269(5) [Å] 90, 101.453(5), 90 [°] 1347.7(1) Å ³
24	<i>P2₁/c</i>	9.022(5), 9.003(5), 16.605(5) 90, 103.17(5), 90 [°] 1265.8(1) Å ³

A number of similarities can be drawn from the solid state structures of 2,6-diisopropylphenylformamide (**6**) and 2,6-diisopropylphenylthioamide (**20**). The unit cell parameters for the two compounds are very similar resulting in a *unit cell similarity index* close to zero (0.022). The hydrogen bonding patterns are also similar where N-H...O or N-H...S hydrogen bonds form chains that run down the crystallographic *b* axis (see Chapter 3). This is so despite the fact that the amide bond distances and angles for the formamide and the thioamide are different. The difference in N(1)...O(1) and N(1)...S(1) hydrogen bond distances in the two

compounds is compensated for in the difference in the angles around their amide moieties. Corresponding intermolecular distances also have no marked differences (see Figure 5.6). The comparison of non-hydrogen intermolecular distances in Figure 5.6 also includes that of the cocrystal of compounds **6** and **20**.

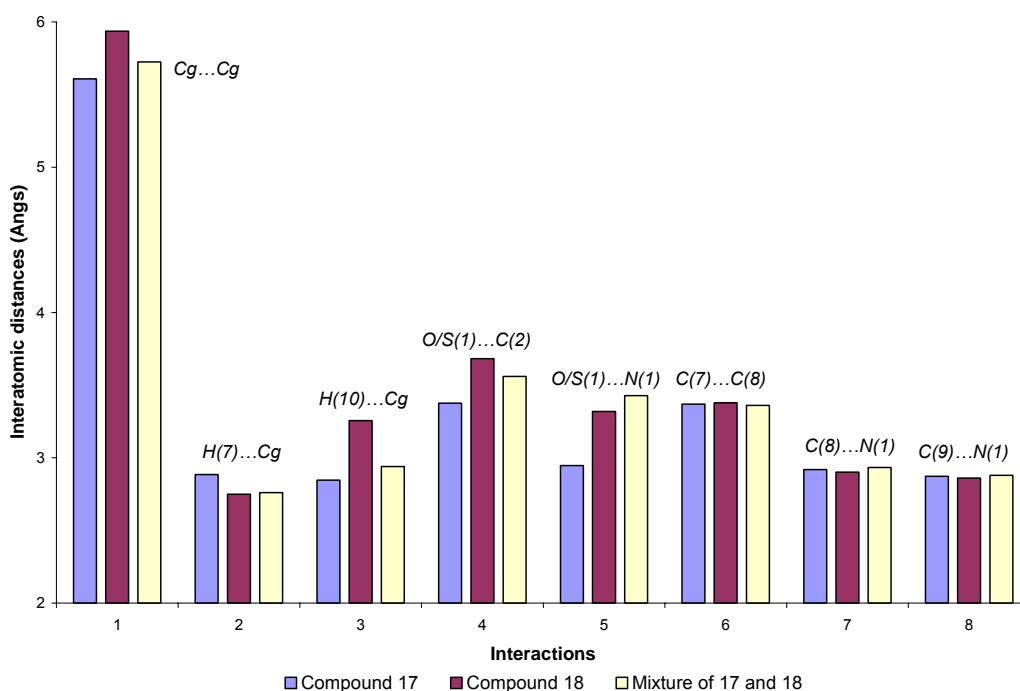


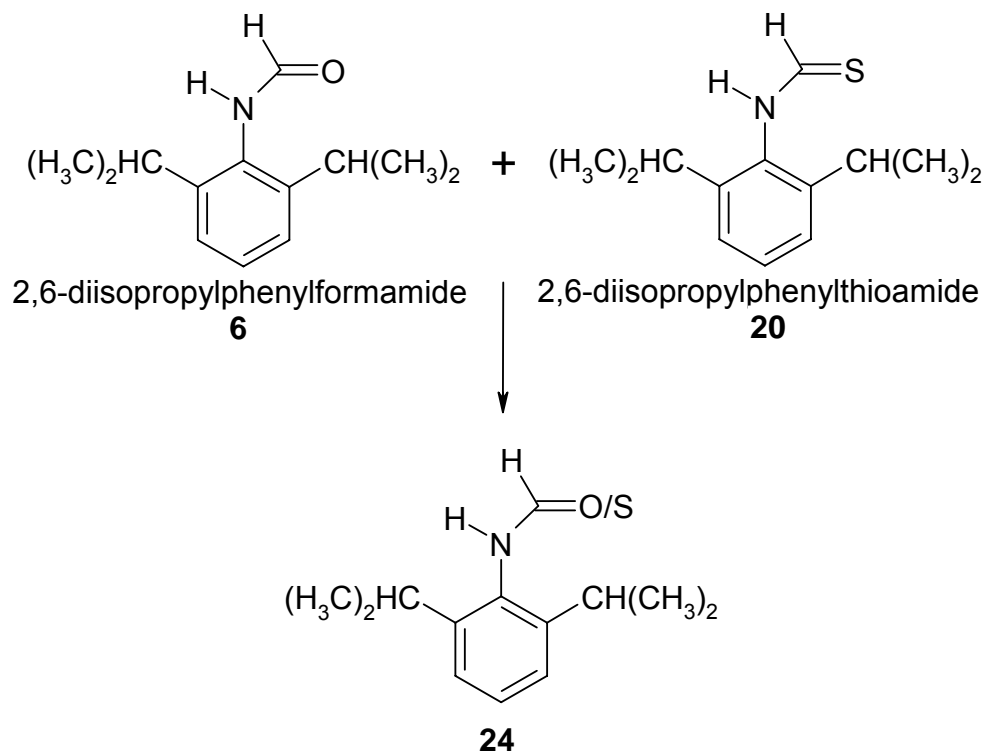
Figure 5.6: Bar graph comparing of the closest non-bonding distances in isomorphous compounds **6** and **20** and of a cocrystal of **6** and **20**.

5.4.2 Cocrystallization of 2,6-diisopropylphenylformamide and 2,6-diisopropylphenylthioamide

The cocrystallization of 2,6-diisopropylphenylformamide **6** and 2,6-diisopropylphenylthioamide **20** gave a cocrystal as was confirmed by X-ray

N-aryl -formamides and -thioamides

powder and single crystal diffraction studies. The synthesis was carried out using the room temperature forms of compounds **6** and **20** (see Scheme 5.3).



Scheme 5.3: Isomorphous structures of 2,6-diisopropylphenylformamide **6** and 2,6-diisopropylphenylthioamide **20** used to grow an isomorphous cocrystal of both compounds (**24**).

2,6-diisopropylphenyl -formamide (**6**) and -thioamide (**20**) are isomorphous and crystallize in the space group $P2_1/c$. The two compounds are conformationally similar and adopt a *trans* conformation (see Chapter 3). One structure is known for each of the two compounds (**6**) and (**20**). Mixed crystals of compound **6** and **20** were obtained by grinding the two starting materials followed by crystallization from a 1:1 solution of ethyl

acetate and acetonitrile by slow evaporation of the solvent. Attempts to grow the cocrystals straight from solution without first grinding the two starting materials did not yield the desired cocrystals.

5.4.2.1 Powder X-ray diffraction analysis

PXRD patterns of compound 2,6-diisopropylphenylformamide **6** and 2,6-diisopropylphenylthioamide **20** and cocrystal **24** are shown in Figure 5.16 indicating significant differences in the three structures. The cocrystallization took place in a 1:1 ratio and cell parameters as well as the powder pattern indicate that the structure of cocrystal **24** adopts an average structure of compounds **6** and **20** - most of the peaks of structure **24** have 2θ positions that fall in between the corresponding peaks of **6** and **20**.

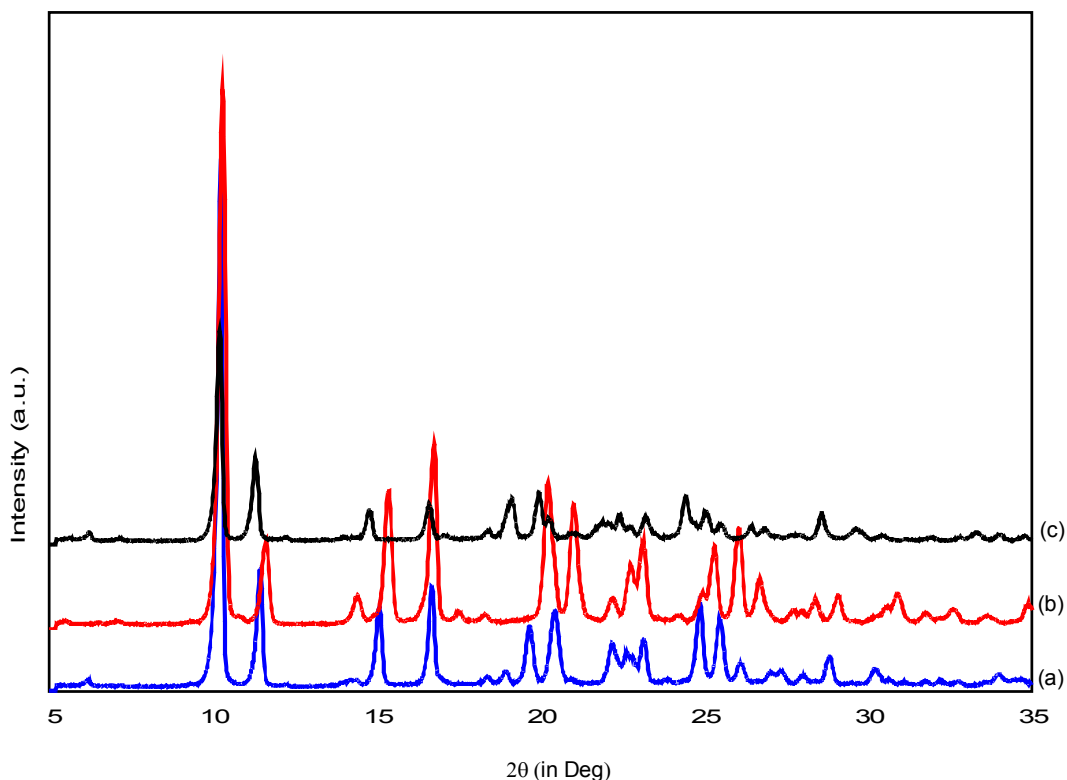


Figure 5.7 Experimental powder patterns for (a) 2,6-diisopropylphenylformamide and **6**, (b) 2,6-diisopropylphenylthioamide **20** and (c) the cocrystal, **24**.

The cocrystal crystallizes in the same space group ($P2_1/c$) as compounds **6** and **20** (see Table 5.8). The molecular geometry is similar to that of the two starting compounds showing a *trans* conformation (the N-H hydrogen being *cis* to the carbonyl group) with the formamide moiety being out of the plane of the aromatic ring. The angle between the planes defined by the aryl ring [C(1)-C(6)] and the formamide group [C(1)-N(1)-C(7)-O(1)] is 77.5° and is slightly smaller when compared to that of 2,6-diisopropylphenylformamide [78.9°] and 2,6-diisopropylphenylthioamide [80.7°].

5.5 Discussion of isomorphism and cocrystallization in aryl -formamides and -thioamides

5.5.1 Isomorphism

From our results it has been shown that a number of chemically distinct aryl -formamides and -thioamides exhibit isomorphous crystal structures depending on different conditions. Three sets of compounds showed isomorphic structures; the first and second sets of compounds contained fluorine, chlorine and methyl groups as substituents on the aryl ring, while the third set of compounds differed in one core atom of the molecule i.e. oxygen vs. sulfur atom.

Two compounds of the first and second sets of compounds (**4a** and **18**) are disordered – the disorder being in the positions occupied by the chloro and methyl groups. The known reason for disorder between these two groups' atoms is related to their sizes. It has been shown that because of the similarity in sizes of Cl and Me groups they can be easily interchanged in molecules without changing the crystal structures of compounds [Kitaigorodskii, 1973]. This is one reason why the structures of 2,6-dichlorophenylformamide (**2a**) and 2-chloro-6-methylphenylformamide (**4a**) are very similar.

Isomorphism in 2,6-difluorophenylformamide (**1a**), 2,6-dichlorophenylformamide (**2a**) and 2-chloro-6-methylphenylformamide (**4a**) can also be attributed to the presence of halogen substituents in their

structures which may lead to similar intermolecular interactions in the solid state structures of the three compounds. This is in addition to the existing hydrocarbon contacts. N...O and $\pi\cdots\pi$ interactions play an important role in the packing of all three compounds (see Chapter 3).

2,6-dimethylphenylthioamide (**17**) and 2-chloro-6-methylphenylthioamide (**18**) have the same intermolecular interactions (N-H...S, C-H...S hydrogen bonds and C-H... π intermolecular interactions). Apart from these similar hydrocarbon interactions, chloro-methyl interchange also plays a role in the isomorphism of these two structures. 2,6-difluorophenylthioamide (**15**) is not isomorphous with the structures of **17** and **18**.

Isomorphism is not uncommon in aromatic compounds with chlorine and methyl group as substituents. This phenomenon is also observed in number of structures in literature, for example the 2,4,6-trichloro and 2,4,6-trimethyl phenylacetamides [Nyburg et al., 1987; Upadhaya et al., 2002]. The two compounds crystallize in the monoclinic space group *Pn* with 2 molecules in the unit cell [cell parameters, 8.224(3) 8.200(4), 8.237(3), $\beta = 113.01(5)$ and 8.538(4), 7.966(3) 8.295(4), $\beta = 113.63(6)$ respectively]. The calculated powder patterns are similar with peaks in approximately the same 2θ positions. Compounds **2a**, **4a**, **17**, **18** and 2,4,6-trichloro and 2,4,6-trimethyl phenylacetamides shows the validity of chloro-methyl

exchange as proposed by Kitaigorodskii [1973] and discussed by Edwards *et. al.*, [2001].

Isomorphism in the third set of compounds [2,6-diisopropylphenylformamide (**6**) and 2,6-diisopropylphenylthioamide (**20**)] is possibly due to the overall size of the molecules as well as the major interactions that determine the packing of molecules in the crystals. The isopropyl groups in both compounds presumably occupy a large volume, making the overall molecule volume large, and as such create a void in which one can easily replace an oxygen atom with a sulfur atom without changing the overall structure of the compounds.¹ Other than the volume, both molecules have similar substituents and are therefore bound to have similar regions of intermolecular interactions. The two compounds have in common N-H...O/S hydrogen bonds and C-H... π intermolecular interactions as the major interactions governing the packing of molecules in the crystal.

An example from literature in which volume is important for isomorphism is the case of the isomorphous *trans*-2'-methylbenzanilide and *trans*-2',6'-methylbenzanilide [Azumaya *et. al.*, 1994] both of which crystallize in the orthorhombic space group *Pbca*. One of the compounds is mono-substituted at the aryl ring with a methyl group in the '2' position, while the other is disubstituted with two methyl groups in the '2' and '6'

¹ The main comparison here is between the sizes of the molecules relative to the sizes of the oxygen and sulphur atoms.

positions of the aryl ring. Therefore this is a case where one methyl group replaces a hydrogen atom (difference in volume, about 24 Å³ for Me compared to 2 Å³ for a hydrogen atom), but because the molecule is big enough when one methyl group is removed from the molecule the eventual structural pattern is not significantly affected.

A correlation exists between contacts and unit cell parameters between crystals that are isomorphous. For isomorphism between **1a**, **2a** and **4a** similar halogen interactions as well as hydrocarbon interactions seem to play a vital role. The same applies for the structures of **17** and **18**. Disorder of the substituents in positions 2 and 6 on the aryl ring of **4a** and **18** seem also plays a role. The disorder allows for formation of contacts that are similar to the counterpart isomorphous compounds. For compounds **6** and **20** the overall size of the molecule seem to be vital. The large size of the molecules is due to the isopropyl substituents in positions 2 and 6 of the aryl rings. These two groups are involved in important C-H... π interactions in both compounds and also serve the purpose of creating a “void” into which the thioamide moiety of compound **20** can fit (also might be the reason for *trans* conformation) just like the formamide moiety of **6** can.

5.5.2 Cocrystallization

The three sets of cocrystals in this project have been created from isomorphous compounds and from non-isomorphous compounds. Cocrystals **22** and **23** were synthesized from non-isomorphous compounds (2,6-dichlorophenylformamide (**2a**) and 2,6-dimethylphenylformamide (**3**), and 2,6-dichlorophenylthioamide **16** and 2,6-dimethylphenylthioamide **17** respectively). The two sets of compounds have chlorine and methyl groups as substituents on the aryl ring. The presence of the two groups allows disorder of the whole molecule in the resulting cocrystal.

It is however noted that the cocrystal of compound **2a** and **3** adopts the structure of 2,6-dichlorophenylformamide. More evidence was seen in the stoichiometric studies of a mixture of the two compounds (see Figure 5.4) where the structure of compound **2a** was adopted in all cocrystals of compounds **2a** and **3** irrespective of the stoichiometry. It is therefore possible that the cocrystallization of **2a** and **3** to give **22** could be chloro-directed.

The structure of cocrystal **23** is totally different from those of the starting materials (2,6-dichlorophenylthioamide **16** and 2,6-dimethylphenylthioamide **17**). It adopts a *cis* conformation different from the *trans* conformations adopted by the starting materials and most of the

***N*-aryl -formamides and -thioamides**

other thioamides synthesized in this project. One noticeable feature about this compound is the size of the torsion angle defined by C(2)-C(1)-N(1)-C(7). The angle is 81.7° in cocrystal **23** only smaller than that of 2,6-dibromophenylformamide **5** (82.7°) and slightly larger than that of 2,6-diisopropylphenylformamide **6** [78.9(2)°] and 2,6-diisopropylphenylthioamide **20** [80.7(3)°]. 2,6-diisopropylphenylthioamide (**20**) and cocrystal **23** are the only thioamide structures that adopt a *trans* conformation in the solid state.

Cocrystal **24** may be considered as a hybrid of 2,6-diisopropylphenylformamide **6** and 2,6-diisopropylphenylthioamide **20**. It is synthesized from two isomorphous compounds and is in itself isomorphous to the starting material.

It has been shown that the main factors contributing to isomorphism of the above discussed aryl -formamides and -thioamides include the effect of disorder and intermolecular interactions where structures have similar regions of halogen interactions and hydrocarbon interactions, effect of substituents e.g. chloro-methyl substituents as well as isomorphism between molecules i.e. great similarity between molecules and not crystals. Cocrystallization can occur between non-isomorphous structures as well as between isomorphous structures. The resulting cocrystals can adopt the structure of one of the starting materials as in cocrystal **22**, of

***N*-aryl -formamides and -thioamides**

none of the starting materials as in cocrystal **23**, or of both of the starting materials as in cocrystal **24**.

6. An in-depth look at the nature of hydrogen bonds and weak intermolecular interactions in compounds 1 – 21

6.1 Introduction

The study of hydrogen bonds and weak intermolecular interactions has often involved the use of theoretical and computational calculations, experimental data from single crystals or powdered samples etc. In this chapter a more in-depth analysis of hydrogen bonds and weak intermolecular interactions is undertaken. Other crystallographic details were given in chapter 3. Our aim was to combine such methods (single crystal data, powder XRD data and theoretical calculations) to fully understand the nature of intermolecular interactions in disubstituted arylformamides and arylthioamides. The approach therefore was to study all the intermolecular interactions involved in the crystal packing of all the formamides and thioamides reported in this work. It was hoped that a clear distinction between the hydrogen bonding patterns and the energies related to the emerging patterns for the compounds in question would become evident. Emphasis was put on the strength of these interactions as well as the structural patterns that arise from them using methods such as the one proposed by Etter [1990] in which interactions are characterized based on predefined motifs like ribbons, tapes and loops *etc.* (see discussion in Chapter 1).

This study involved experimental data from X-ray studies as well as computational calculations on lattice energies and molecule-to-molecule energies of the most important interactions in the crystal structures. N-

***N*-aryl formamides and thioamides**

H...O=C in formamides and N-H...S=C hydrogen bonds are the dominant interaction in formamides and thioamides, respectively. A number of other weak interactions are also observed and these too contribute in one way or another to the overall packing of molecules in the crystals of these compounds. The presence of these weak interactions is, however, largely dependent on the type of substituent on the aryl ring. Some common intermolecular interactions besides N-H...O and N-H...S hydrogen bonds include (listed in no particular order), bonds involving halogen atoms (X...O, X...X, X...H, X = halogen) and C-H...O, C-H...S, Y-H... π (Y = C, N or O) and π ... π intermolecular interactions. Their contribution to the overall packing of the crystal can be stabilizing or destabilizing as we shall see later in this Chapter. We start by discussing the general motifs formed by the N-H...O and N-H...S hydrogen bonds and use them as a basis to discuss other intermolecular interactions and the general motifs or graph set patterns they generate and then try to identify the common motif in compounds **1** to **24**. We will also look at the energy contributions of the various interactions in an attempt to establish the most significant ones.

6.2 N-H...O hydrogen bonds in arylformamides

The N-H...O hydrogen bond is one of the most important intermolecular interactions that determine the primary molecular-packing modes of all formamides discussed in this thesis. The characterization of this hydrogen bond has been done following methods of previous studies of the hydrogen bond (see Chapter 1, section 1.3.4). The N-H...O=C

***N*-aryl formamides and thioamides**

hydrogen bond of all the formamides that we synthesized are characterized by the N...O distance, the C=O...N and the C-N...O angles and how these parameters relate to certain motifs. The data related to these parameters for compounds **1** – **14** is presented in Table 6.1. A short comparison will be made to some related structures from literature.

6.2.1 The main packing modes and motifs formed by the N-H...O hydrogen bond in compounds 1 – 14

For the sake of clarity it is important to emphasise that two different groups of compounds are present in compounds **1** to **14**: 2,6-disubstituted formamides and formamides with substitutions in other positions. It is noted that four distinct categories of different hydrogen bonding motifs arise from these two groups. These motifs depend, to some extent, on the type of substituent on the aryl ring (especially for the 2,6 substituted ones) and more on the position of the substituents on the aryl ring. Figure 6.1(a) – (d) is a representation of the four different categories of N-H...O hydrogen bonding motifs generated by compounds **1** – **14**.

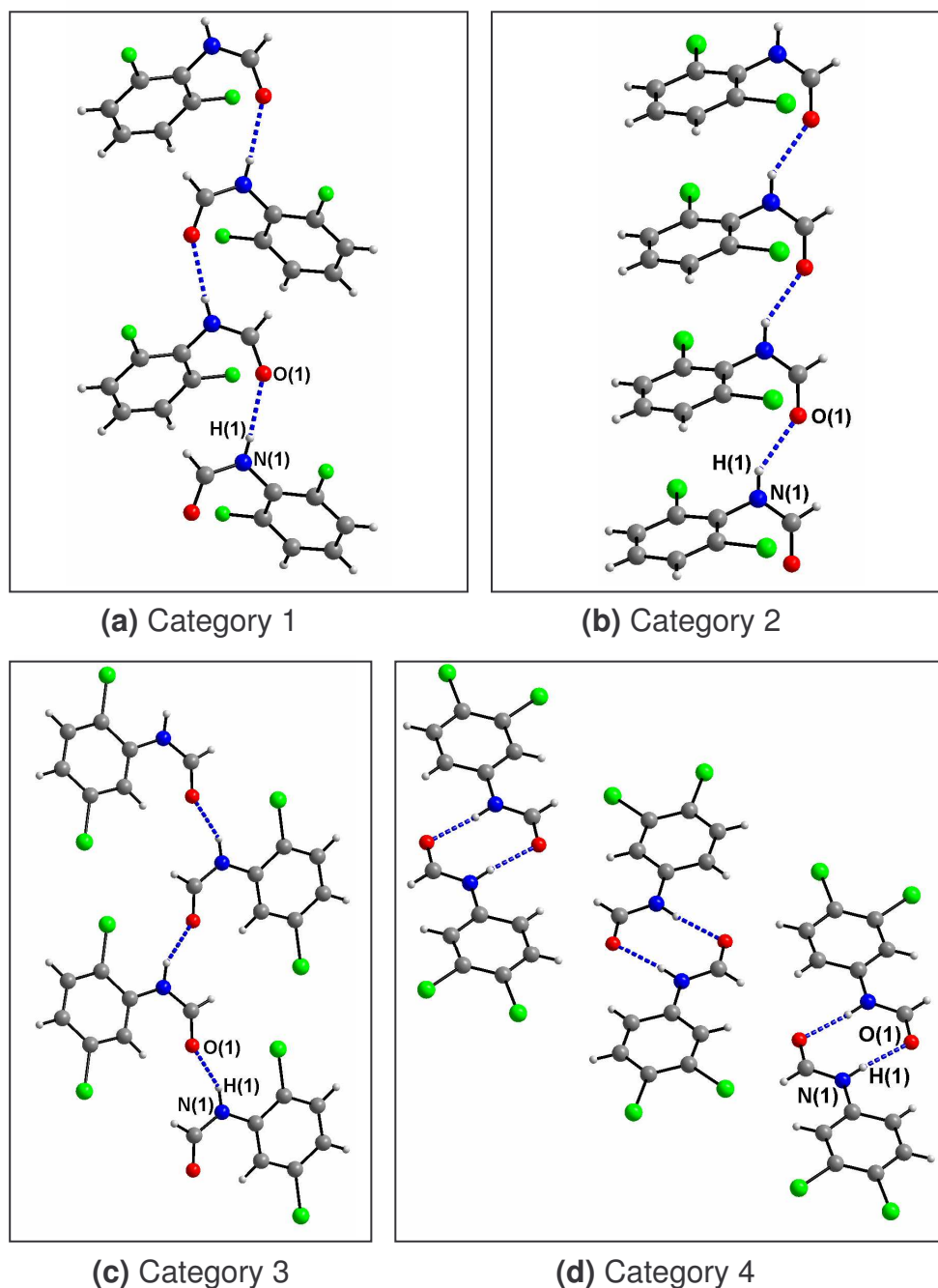


Figure 6.1: The four different categories generated by the N-H...O hydrogen bonds of arylformamides **1** – **14**. (a) Category 1 Spirals of N-H...O hydrogen bonded chains in 2,6-difluorophenylformamide **1a**, (b) Category 2, stacks of hydrogen bonded chains in 2,6-dichlorophenylformamide **2a**, (c) Category 3, sheets of N-H...O hydrogen bonded chains in 2,5-dichlorophenylformamide **9** and (d) Category 4, N-H...O hydrogen bonded dimers of 3,4-dichlorophenylformamide **13**.

***N*-aryl formamides and thioamides**

Category 1 is generated by N-H...O hydrogen bonded formamide molecules forming chains in which the molecules are facing alternate directions. The molecules along the chains are related either by a glide plane or a 2_1 -screw axis. The example used in this category is that of 2,6-difluorophenylformamide **1a**.

Category 2 is also generated by N-H...O hydrogen bonded molecules forming chains in which the formamide molecules are stacked parallel to one another along the shortest crystallographic axis, usually about 4 Å long, of the unit cell. The molecules along the chains of this category are related by unit cell translation. The example used for this category is that of the high temperature phase of 2,6-dichlorophenylformamide, **2b**.

Category 3 has molecules connected by N-H...O hydrogen bonds form sheets. The sheets are sometimes planar and sometimes corrugated depending on the dihedral angle between adjacent molecules along hydrogen bonded chains. The sheets are in-turn layered and have an inter-sheet distance of approximately 3.5 Å – 4.1 Å. Most of the molecules that belong to this category are without a substituent in the 6 position of the aryl ring and the example used in Figure 6.1 is that of 2,5-dichlorophenylformamide. Either a glide plane or a 2_1 -screw axis relates molecules along the hydrogen-bonded sheets.

Category 4 is represented by 3,4-dichlorophenylformamide (**13**) and phenylformamide (**21**). This type of motif formed by **13** possibly arises as a

***N*-aryl formamides and thioamides**

result of the *cis* conformation that the compound adopts. The *cis* conformation exposes the amino hydrogen making it easy for dimers to form. This type of conformation is rather rare amongst the disubstituted formamides but is found and is thought to be more stable in most simple formamides such as dimethylformamide. Compound **21**, has a packing pattern similar to that of **13**, but contains both *cis* and *trans* conformers resulting in hydrogen bonded tetramers (see the last Chapter 3, section 3.4).

6.2.2 Factors determining the molecular packing modes of compounds 1 – 14

Table 6.1 summarises the following important hydrogen bonding parameters of compounds **1 – 14**:

1. The preferred N-H...O=C geometry as described by N...O distance and C=O...N, C-N...O and N-H...O angles,
2. a categorization of the resulting hydrogen bonding motifs depending on the type of molecule to molecule relationship (glide, screw axis of translation) along the N-H...O hydrogen-bonded chain.

N-aryl formamides and thioamides

Table 6.1: N-H...O=C geometry of N-disubstituted arylformamides (compounds 1 – 14)

Compound	Space group	Dist. (Å) N...O	Angle (°) C=O...N	Angle (°) C-N...O	Angle (°) N-H...O	Hydrogen bonding symmetry element axis	Dihedral angle between adjacent N-H...O hydrogen bonded molecules
Category 1							
1a	<i>Pbca</i>	2.84	145	113	170	Glide on 8.50 Å axis	N/A – molecule not planar
2a	<i>Pbca</i>	2.87	146	114	171	Glide on 8.60 Å axis	
4a	<i>Pbca</i>	2.88	144	121	163	Glide on 8.51 Å axis	
6	<i>P2₁/c</i>	2.94	146	124	170	Screw axis on 8.86 Å axis	
Category 2							
1b	<i>P2₁</i>	2.81	150	97	156	Translation on 4.46 Å axis	N/A – molecule not planar.
2b	<i>P2₁/n</i>	2.78	148	93	142	Translation on 4.35 Å axis	
3	<i>P2₁2₁2₁</i>	2.85	151	97	154	Translation on 4.50 Å axis	
4b	<i>P2₁/c</i>	2.79	146	91	140	Translation on 4.32 Å axis	
5	<i>P2₁2₁2₁</i>	2.81	145	90	121	Translation on 4.33 Å axis	
12	<i>P2₁/c</i>	2.87	156	102	157	Translation on 4.64 Å axis	
Category 3							
7	<i>P2₁/n</i>	2.89	141	93	148	Glide diagonally across the <i>ac</i> plane	13.9
8	<i>P2₁/c</i>	2.92	134	89	142	Screw axis on 15.07 Å axis	53.4
		2.87	132	90	145		
9	<i>P2₁</i>	2.87	140	93	137	Screw axis diagonally across the <i>ac</i> plane	26.5
10	<i>P2₁2₁2₁</i>	3.00	104	84	144	Screw axis down the <i>b</i> axis	52.4
14	<i>P2₁/n</i>	2.80	134	100	162	Glide diagonally across the <i>ac</i> plane	1.8
Category 4							
13	<i>P2₁/c</i>	2.91	118	118	174	dimers	
21	<i>C2/c</i>	2.84	112	117	176	tetramers	
		2.82	152	116	178		

An analysis of hydrogen bond geometry of compounds **1** – **14** shows that the occurrence of the different motifs is evenly distributed between translation, 2_1 -screw axis and glide motifs. The geometry of the N-H...O=C angle in glide and 2_1 axis motifs (Table 6.1) vary considerably and depends on the nature of the aryl ring. The size of the substituents on the ring affects the tilt of the molecules with respect to either the glide plane or the 2_1 -screw axis. 2,6-difluoro **1a**, 2,6-dichloro **2a** and 2-chloro-6-methyl **4a** -phenylformamides (glide motif) and 2,6-diisopropylphenylformamide **6** (2_1 screw axis motif) belong to category 1. These compounds have a linear N-H...O angle ranging between 160 and 175°. The angles compare well to the secondary amides analysed by Leiserowitz *et. al.* [1978] (motif 3b in their paper is equivalent to category 1 in this thesis). In Category 1 compounds, contact between the disubstituted aryl rings of N-H...O hydrogen bonded arylformamides is avoided as exemplified by 2,6-difluorophenylformamide in Figure 6.1a. Compounds in this category form N-H...O hydrogen bonded chains that can be described by the graph set C(4).

2,6-dichloro **2b**, 2,6-dimethyl **3**, 2-chloro-6-methyl **4b**, 2,6-dibromo **5** and 5-chloro-2-methyl **12** -phenylformamides belong to Category 2. The aryl rings are separated by the same distance as the shortest axis of the unit cell; about 4 Å. The N-H...O hydrogen bond angle in this motif type is clearly non linear and is smaller compared to the one in Category 1 compounds. This motif is not very common amongst acetamides and only seems to be adopted mostly by structures with either chlorine atoms or

methyl groups as substituent on the aryl ring. This is in agreement with the argument put forward by a number of authors [Cohen *et. al.*, 1970, 1972, 1973; Desiraju *et. al.*, 1986] of a strong influence by chlorine atom to give cell axes of about 4 Å. Examples of such structures from literature are tabulated in Chapter 1 (Table 1.2c). In this category N-H...O hydrogen bond chains are also described by the C(4) graph set, but also can result in $R_4^2(8)$ secondary graph set when the C(4) chains are connected through C-H...O interactions.

2,4-dichloro **7**, 2,4-dibromo **8**, 2,5-dichloro **9**, 2,5-dibromo **10** and 3,5-dichloro **14** -phenylformamides belong to Category 3 in which N-H...O hydrogen bonded chains similar to β -pleated sheets in proteins are formed [Zeller *et. Al.*, 2005 and references therein]. Some examples were given in section 1.3.4 of chapter 1.

The C=O...N angle seems to be similar for all 2,6-disubstituted formamides. This angle is approximately 145° and slightly larger in 2,6-difluorophenylformamide **1b**, 2,6-dimethylphenylformamide **3** and 5-chloro-2-methylphenylformamide **12**. **1b**, **3** and **12** have strong C-F... π (3.4 Å) for **1b** and C-H... π (2.9 for **3** and 2.8 Å for **12**) interactions through the fluorine and methyl substituents on the aryl ring. This could possibly be the cause for the relatively large C=O...N angle as the aryl rings have to adjust themselves to allow for the formation of the π interactions thereby making the N...O interaction slightly longer and the C=O...N wider. This

wider C=O...N angle is also observed in *N*-Formyl-4-bromo-2,6-difluoroaniline [Ferguson *et. al.*, 1998] which has a short axis of about 4.6 Å and a possible C-F... π interaction (about 3.6 Å long). Amongst category 3 compounds there is a spread in the value of this angle with that of 2,5-dibromophenylformamide **10** being the smallest 103°.

The C-N...O and the N-H...O angles are directly proportional. For category 1 compounds N-H...O and C-N...O angles are relatively large with N-H...O tending towards linearity when compared to category 2 compounds. The C-N...O angle decreases in size for category 2 and 3 compounds where most of them are just slightly more than 90°. The decrease in the size of C-N...O angle in category 2 compounds is most likely induced by the necessity to avoid too short intermolecular contacts between H(7) and the aryl ring along the hydrogen-bond. In category 3 the angle is smaller since adjacent molecules are forced further apart in the formation of N-H...O hydrogen bond. This has also been observed in *N*-methylbenzamide [Leiserowitz and Tuval, 1978]. For category 2 compounds there is some repulsion between the aryl rings and therefore the rings are often slightly displaced from each other (because of π electrons) along the hydrogen bond chain hence a relatively short N...O distance, a probable cause of the decrease in C=O...N and C-N...O angles.

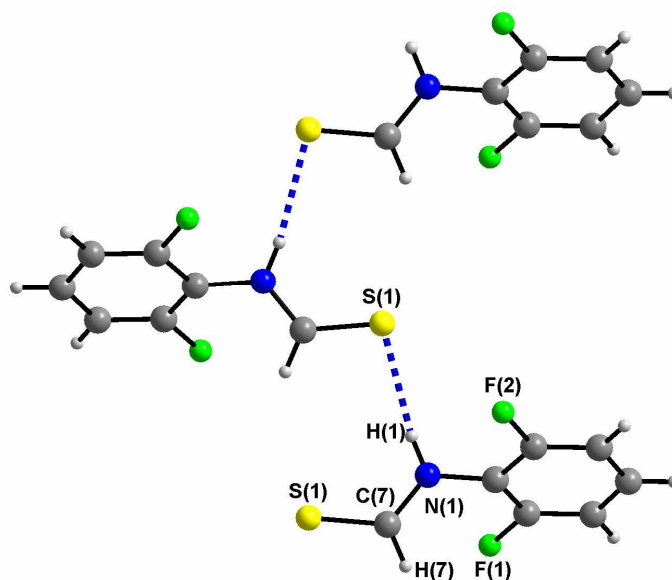
6.3 The N-H...S hydrogen bond

In this thesis only six sulphur analogues of the arylformamides were synthesised. We therefore use the crystallographic data of the six compounds to analyse the geometric characteristics of the N-H...S=C hydrogen bond. Parameters like the N...S hydrogen bond distance, the N-H...S, C-N...S and C=S...N angles will be used in the analysis of this hydrogen bond. This group of compounds comprise a new category, category 5.

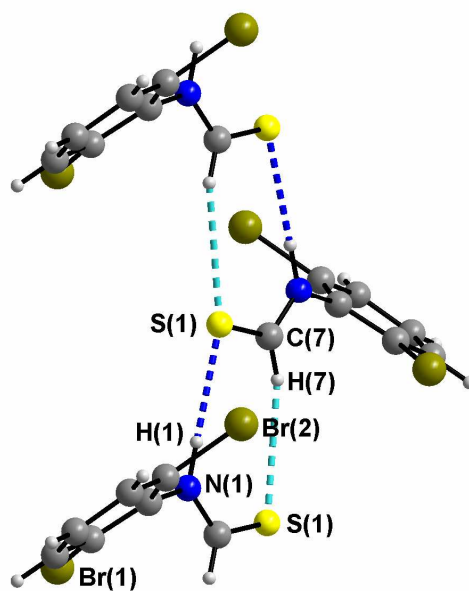
6.3.1 Molecular packing mode and the hydrogen bond geometry of arylthioamides 15 – 20

All the arylthioamides discussed adopt a *cis* conformation with the exception of 2,6-diisopropylphenylthioamide, which retains the *trans* conformation of the formamide analogue. There is only one major N-H...S hydrogen-bonding motif that arises from this set of compounds. The N-H...S hydrogen-bonded chains are composed of molecules that are related either by a 2_1 -screw axis or a glide plane but all can be described by C(4) graph set. The C(4) chains can occur alone as in 2,6-difluorophenylthioamide **15** or parallel with C-H...S interactions to result in ribbons described by $R_2^2(7)$ graph set (see Figure 6.2). 2,6-difluorophenylthioamide **15** and to some extent 2,6-dichlorophenylthioamide **16** do not form ribbons due to the fact the H(7) - S(1) [or C(7) - S(1)] distance is too long to allow for a C-H...S interaction

to form. Molecules along the N-H...S interaction in (a) the chains and in (b) the ribbons form spirals almost similar to the ones formed by category 1 arylformamides.



(a)



(b)

Figure 6.2: The two different groups generated by the N-H...S hydrogen bonds of compounds **15** – **20**. (a) Chains of N-H...S hydrogen bonded

chains in 2,6-difluorophenylthioamide, (b) Chains of N-H...S hydrogen bonded chains in 2,6-dibromophenylformamide combined with C-H...S hydrogen bonds leading to ribbons.

Table 6.2 below details the geometric parameters of the N-H...S=C hydrogen bond. Compounds **15** – **20** have nearly linear N-H...S angles and similar N...S distances. The linearity of this angle may be attributed to the *cis* conformation that the compounds adopt. In this type of conformation, the donor and acceptor atoms have no steric interference from the aryl rings hence allowing for a more linear interaction. This trend is very common in most compounds that have this type of hydrogen bonding [Allen et. al., 1997].

Table 6.2: N-H...S=C geometry of *N*-disubstituted arylthioamides (compounds **15** – **20**, Category 5).

Compound	Space group	Dist (Å) N...S	Dist (Å) C...S	Angle (°) C-N...S	Angle (°) C=S...N	Angle (°) N-H...S	Angle *
15	<i>Pbca</i>	3.37	3.92	124	102	172	53
16	<i>P2₁/c</i>	3.50	3.82	116	94	176	54
17	<i>C2/c</i>	3.46	3.80	119	98	177	64
18	<i>C2/c</i>	3.43	3.79	119	99	177	60
19	<i>P2₁/c</i>	3.47	3.81	118	99	177	63
20	<i>P2₁/c</i>	3.32	-	128	126	167	81

* = C(7)-N(1)-C(1)-C(2)

The N...S distance is relatively short in 2,6-difluorophenylformamide while the C-N...S and C=S...N angles are larger when compared to compounds **16**, **17**, **18** and **19**. The C(7)-N(1)-C(1)-C(2) torsion angle (the twist of thioamide moiety with respect to the aryl ring) is

small [52.5°] in **15** and increases as the substituents in the 2 and 6 positions increase in size (volume) in compounds **17**, **18** and **19** by between 7 and 10°. The difference is even bigger in the case of 2,6-diisopropylphenylthioamide **20** (*trans* conformation) by as much as 28°. This torsion angle is what makes the distances between H(7) and S(1) in compounds **15** and **16** longer (more than 3.0 Å). No C(7)-H(7)...S(1) interactions are formed in **15** and **16**. This probably also affects the C-N...S and C=S...N angles in 2,6-difluorophenylformamide. The C(7)-N(1)-C(1)-C(2) torsion angle in 2,6-dichlorophenylthioamide **16** is closer to that of 2,6-difluorophenylthioamide; the distance between H(7) and S(1) is slightly shorter than that of 2,6-difluorophenylthioamide. 2,6-diisopropylphenylthioamide **20** adopts a *trans* conformation similar to the formamides discussed in the previous chapter and is isomorphous to its formamide analogue.

6.4 The C-H...O and C-H...S hydrogen bonds in arylformamides 1 to 21

The discussion below is of all the other important interactions which support the N-H...O and the N-H...S interactions in the overall stability of crystals. Their geometries are only rather generalised for all the compounds and our aim is to show their significance in the whole crystal.

The C-H...O interaction is another important contributor to the stability of crystals in arylformamides. This type of hydrogen bond appears

at least once in most of the arylformamides that are discussed (it is expected in any organic compound containing an oxygen atom). In all compounds this hydrogen bond is involved in one or two of two ways; (i) along or parallel to the N-H...O hydrogen bond chain and (ii) perpendicular to the N-H...O hydrogen bond and therefore involved in linking adjacent N-H...O hydrogen bonded chains.

Our aim was to study the behaviour of this interaction in the arylformamides that were synthesised looking at the type of motifs they generate and also at the geometry of the interaction. The convention for the representation of lengths (C...O) and angle (C-H...O) is followed in terms of the geometry of the bond. The compounds are grouped using the categorisation that was used in relating the N-H...O hydrogen bonds in the previous section (Table 6.1). C...O distances are in range of 3.100 – 3.755 Å and C-H...O angle between 108 and 175° well within what is reported in literature (3 - 4 Å and 90 - 180°) [Taylor and Kennard, 1982]. Both the C...O and O...H distances correlate in a linear fashion with the C-H...O angle (see Figure 6.3) and the N-H...O angle. As the C...O or the O...H distances increase, the C-H...O and N-H...O angles increase.

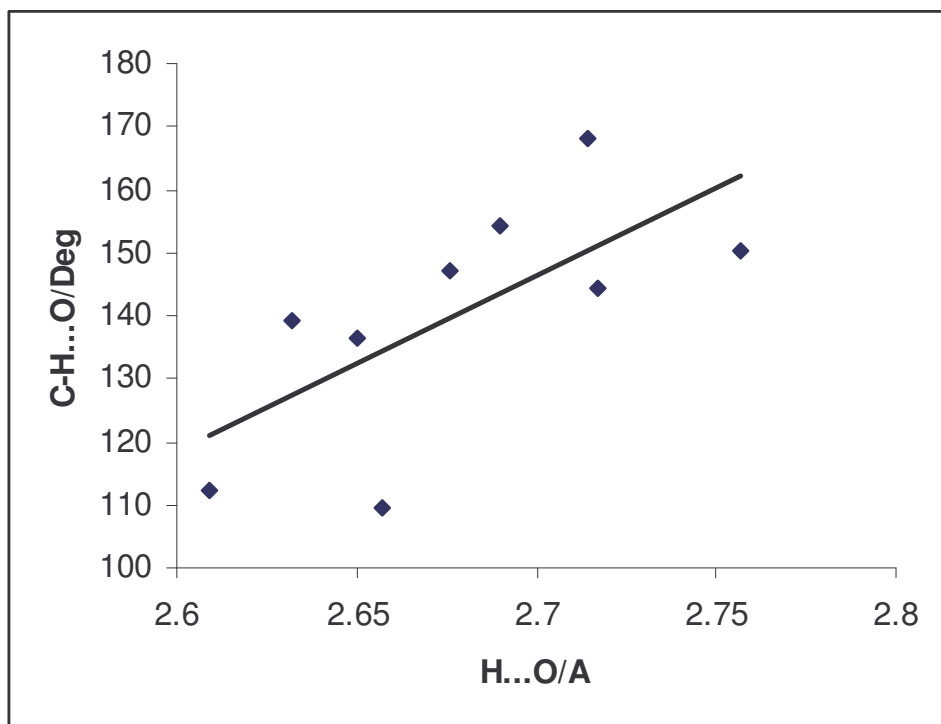


Figure 6.3: A scatter plot showing the correlation between the C-H...O angle and H...O distances for C-H...O hydrogen bonds in disubstituted aryl formamides (**1 – 14**). Only those whose H...O distances are below 2.75 Å have been used ($C...O < 3.55$, see Table 6.3).

Some of the C-H...O angles especially those involving H(4) look suspicious as they deviate a lot from 180°. The dipole-monopole and dipole-dipole contribution to the electrostatic energy is a maximum at C-H...O angle of 180° and reduces as this angle becomes smaller [Desiraju, 1996]. However the ones listed on Table 6.3 seem to play a vital role in the structures of the compounds. H(4)...O(1) links up N-H...O hydrogen bonded chains in some category 1 and 2 compounds. H(7)...O(1) supports and occurs along N-H...O hydrogen bond chains resulting in catemers or in rings connecting adjacent hydrogen bond chains.

Table 6.3: C-H...O geometry of N-disubstituted arylformamides (Categories 1 and 2)

Compound & Space group		Dist. (Å) C...O	Angle (°) C-H...O	Competing interactions
Category 1				
1a <i>Pbca</i>	C(4)-H(4)...O(1)	3.525	141	
	C(3)-H(3)...O(1)	3.425	145	
2a <i>Pbca</i>	non	-	-	Cl...H
4a <i>Pbca</i>	C(4)-H(4)...O(1)	3.679	168	
	C(8)-H(8c)...O(1)	3.559	144	
6 <i>P2₁/c</i>	non	-	-	C-H... π and π ... π
Category 2				
1b <i>P2₁/c</i>	C(4)-H(4)...O(1)	3.460	151	
	C(7)-H(7)...O(1)	3.248	169	
2b <i>P2₁/n</i>	non	-	-	Cl...H
3 <i>P2₁2₁2₁</i>	C(4)-H(4)...O(1)	3.551	154	
	C(7)-H(7)...O(1)	3.288	169	
4b <i>P2₁/c</i>	C(7)-H(7)...O(1)	3.409	139	
	C(8)-H(8c)...O(1)	3.626	175	
5 <i>P2₁2₁2₁</i>	C(4)-H(4)...O(1)	3.103	111	
	C(7)-H(7)...O(1)	3.380	136	
12 <i>P2₁/c</i>	C(7)-H(7)...O(1)	3.755	174	
Category 3 and 4				
7 <i>P2₁/n</i>	non	-	-	Cl...H
8 <i>P2₁/c</i>	non	-	-	Br...O
9 <i>P2₁</i>	Non	-	-	Cl...Cl
10 <i>P2₁2₁2₁</i>	C(7)-H(7)...O(1)	3.158	120	
14 <i>P2₁/n</i>	non	-	-	π ... π
13 <i>P2₁/c</i>	non	-	-	
21	non	-	-	

Two major motifs are generated by the C-H...O hydrogen bond as illustrated in Figure 6.4. In one motif catemers described by the $R_2^1(5)$ graph set are formed (blue dashed lines in Figure 6.4). This motif is common in most of the formamides (amongst all category 1, 2 and 3 compounds (**1b**, **3**, **4b**, **5**, **10** and **12**) and is analogous to that formed in β -sheets reported in literature [Zeller *et. al.*, 2005 and references therein; Lee *et. al.*, 2003].

The second motif formed by C-H...O interactions is generated by a combination of 2 motifs described by C(4) and D(2) graph sets. These results in rings described by $R_2^2(6)$ and $R_2^2(4)$ secondary graph sets (see Figure 6.4). This motif is common in category 2 compounds and is prominent in compound **4b** and **12** but can also be found in compounds **1b**, **2b**, **3** and **5** with longer N...O and H...O.

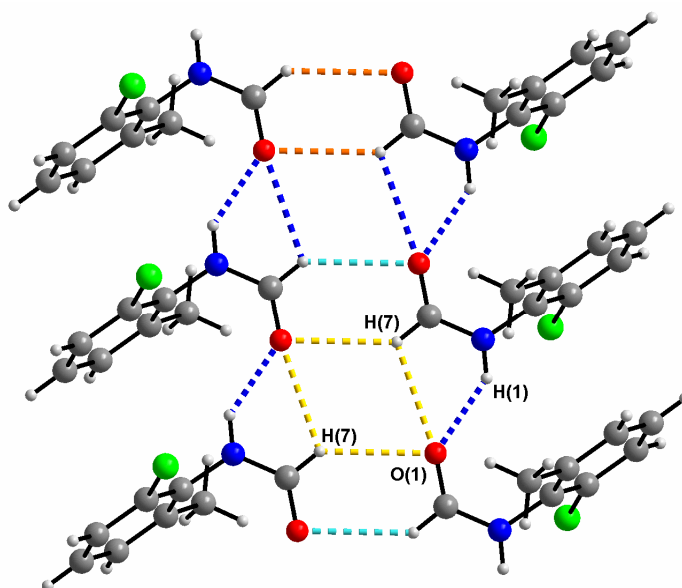


Figure 6.4: Hydrogen bonding motifs generated by C-H...O interactions in 2-chloro-6-methylphenylformamide. (i) $R_2^1(5)$ catemers which involve the N-H...O hydrogen bonds (indicated in blue dashed lines) (ii) interactions linking formamide molecules from adjacent N-H...O hydrogen bonded chains into dimers (indicated in orange dashed lines) forming rings described by $R_2^2(6)$ graph set notation and three and (iii) interactions linking up the C-H...O hydrogen bonded dimers (indicated in gold dashed lines) forming rings described by $R_2^2(4)$. The two motifs occur either separately like in most category 1 and 3 compounds or together as shown here in Figure 6.4 like in some category 2 compounds.

The C-H...O interaction seems to be stronger in most category 2 compounds and is therefore important especially in linking adjacent N-H...O hydrogen bonded chains. N-Formyl-4-bromo-2,6-difluoroaniline [Ferguson *et. al.*, 1998] has its N-H...O hydrogen bonded chains linked up by C-H...O interactions to form rings. However these are different from the ones we observe in the formamides discussed in this thesis (see Figure 6.5).

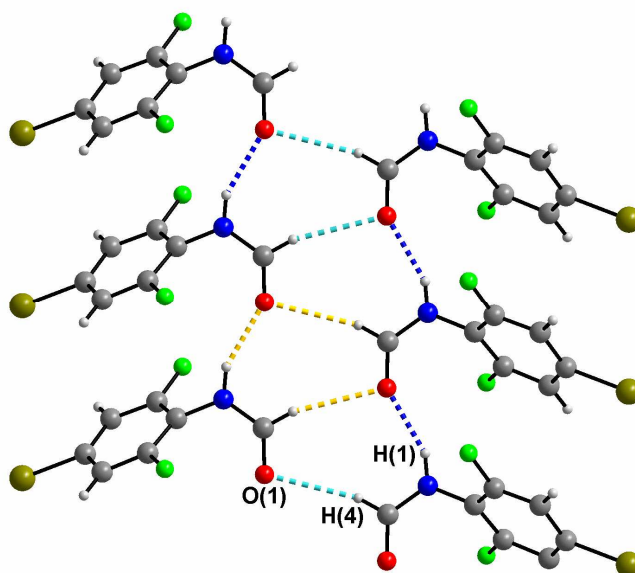


Figure 6.5: Adjacent N-H...O hydrogen bond (in blue dashed lines) chains in N-Formyl-4-bromo-2,6-difluoroaniline described by C(4) graph sets are linked up by C-H...O hydrogen bonds (in light blue dashed lines) described by D(2) graph sets resulting in secondary rings described by $R_3^2(8)$ graph set (in gold dashed lines).

The sulphur analogues (compounds **15** – **19**) of the 2,6-disubstituted arylformamides (compounds **1** to **6**) have a different variety of intermolecular interactions. Since the N-H...S hydrogen bond is generally considered weak other interactions become more important and the C-H...S interaction is one of them.

The geometric parameters for the C-H...S hydrogen bond are given in Table 6.4. As a result of the larger size of the sulphur atom compared to the oxygen atom, it can have more than one contact to H atoms that are close to sum of van der Waals radii of S and H atoms. The important C-H...S interactions are those involving H(7) which together with N-H...S contribute to the formation of rings described by $R_2^2(7)$ graph set (see Figure 6.6) which extends into infinite ribbons (compounds **16** – **19**). Then there are other weaker ones (like the one that involves C(4)-H(4)) which support $\pi\cdots\pi$ interactions in linking up adjacent ribbons or C(4) chains. Compound **20** retains the *trans* conformation of the analogous formamide and has no significant C-H...S interactions.

The geometry of this hydrogen bond in the arylthioamides is rather similar and compare quite well with those in literature. The C-H...S angle increases with the decrease of the C...S distance in a similar fashion as C...O does for C-H...O interactions. The C-H...S angle ranges from 146 - 163° (see Table 6.4).

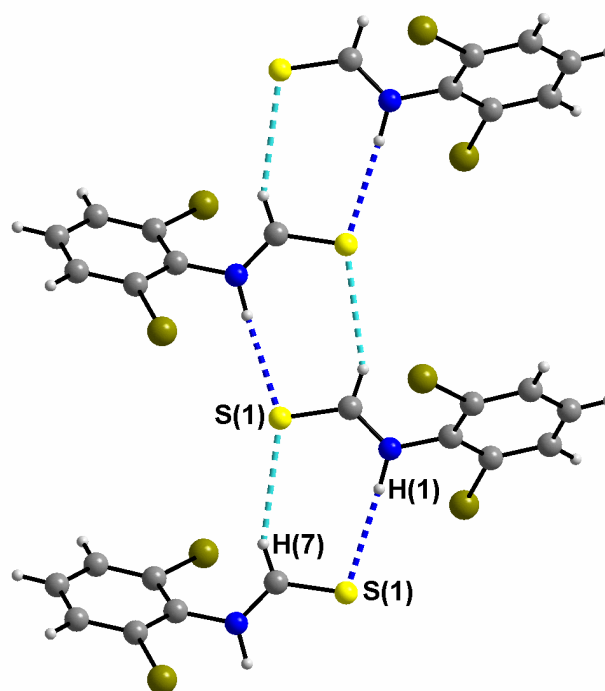


Figure 6.6: Hydrogen bonded ribbons of 2,6-dibromophenylthioamide. The light blue dashed lines indicate the C-H...S interactions while the blue dashed line indicate the N-H...S hydrogen bonds.

Table 6.4: Geometric parameters for the C-H...S hydrogen bond for compounds **15** to **20**.

Compound		Dist (Å) C...S	Angle (°) C-H...S	Angle (°) C=S...H
15	S1...H7	3.776	163	100
16	S1...H7	3.820	146	99
17	S1...H7	3.806	155	104
18	S1...H7	3.788	153	106
19	S1...H7	3.770	154	106
20	non	-	-	-

6.5 Halogen bonding in compounds 1 to 20

2,6-dimethylphenylformamide **3**, 2,6-diisopropylphenylformamide **6**, 2,6-dimethylphenylthioamide **17**, 2,6-diisopropylphenylthioamide **20** and phenylformamide **21** do not have halogen substituents. The rest of the compounds have at least one halogen interaction from a variety that are observed in the packing of most these compounds; these include, X...H, X...O, X...X and X... π (X = F, Cl or Br). There are no F...F interactions in any of the fluoro-substituted formamide or thioamides (compounds **1a**, **1b** and **15**). In these three fluorinated compounds, C-H...F interactions become more important. In other compounds interaction involving a halogen atom and an oxygen atom (Cl...O and Br...O as in compounds **2a**, **9** and **10**) are also observed despite the presence of direct Cl...Cl or Br...Br interactions. In **16** a S...X interaction is observed. Most of the halogen contacts cannot be considered strong since they are slightly longer than the sum of the van der Waals radii of the interacting atoms. They therefore only make a small contribution to the lattice energy of these compounds.

The low temperature form 2,6-dichlorophenylformamide **2a** has the shortest Cl...Cl distance (by 0.03 Å shorter than the sum of the van der Waals radii of Cl atoms) of all chloro substituted compounds. 2,6-dibromophenylformamide **5** has the shortest Br...Br contact (0.13 Å shorter than the sum of the van der Waals radii of Br atoms) of the bromo-substituted formamides and thioamides. An attempt to establish the

important types of halogen interactions in all the various categories is made.

6.5.1 *Geometry of X...X interactions in compounds 1 – 20*

Table 6.5 lists the X...X bond distances and angles for halogenated compounds that have this halogen bond. The distances include those that are 0.2 Å longer than the sum of van der Waals radii of the halogens. The geometric orientation for halogen...halogen interactions in halogen-substituted formamides and thioamides varies and seems to be similar for compounds in the same N-H...O hydrogen bonding categories discussed above. Category 1 and 2 compounds prefer an orientation in which (for definition of θ_1 and θ_2 see Chapter 1) θ_1 is unequal to θ_2 (one angle is closer to 90° while the other tends towards 180° or L-shaped). 2,6-dichlorophenylthioamide **16** however has a second halogen-to-halogen interaction in which θ_1 and θ_2 are equal and linear (close to 180° or close-packing) and represents the only thioamide that shows some evidence of halogen...halogen interactions (see Table 6.5 for geometric values and Figure 6.8).

For category 3 compounds, 2,4-dichlorophenylformamide **7** does not have any halogen-to-halogen interactions. 2,4-dibromophenylformamide **8** has Br...Br interactions that have the same θ_1 and θ_2 angles. 2,5-dichlorophenyl formamide **9** and 2,5-dibromophenylformamide **10** each have two halogen-to-halogen

interactions. θ_1 and θ_2 in 2,5-dichlorophenyl formamide **9** are equal for each of the two interactions. In 2,5-dibromophenylformamide **10** the two angles are different in each of the two Cl...Cl interactions. In 3,5-dichlorophenylformamide **14** the two angles are close but not equal. An illustration of the two interactions in compounds **9**, **10** and **12** is given in Figure 6.7.

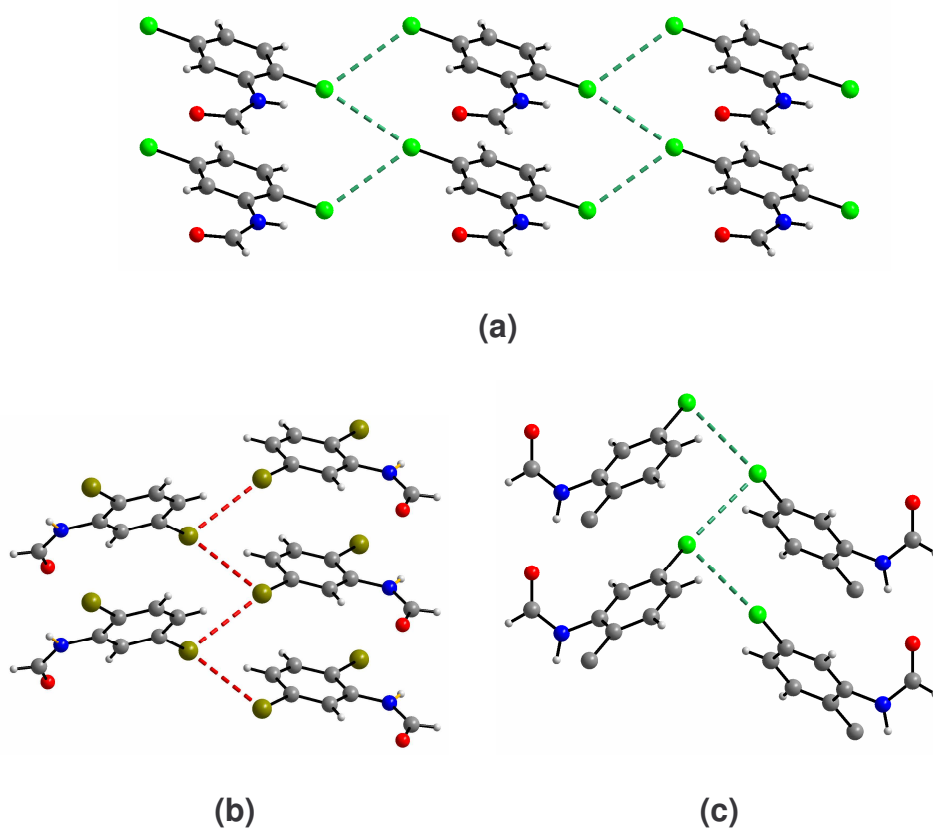
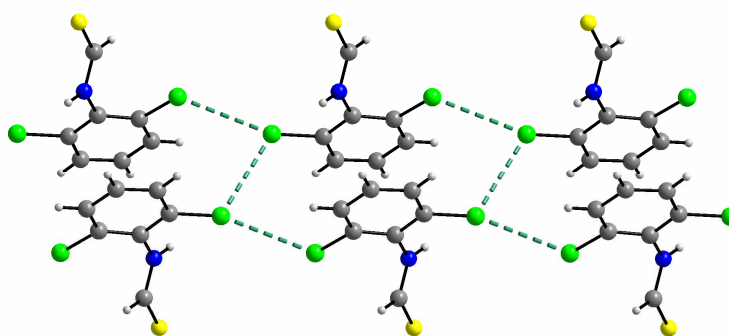


Figure 6.7: Diagram showing X...X interactions in (a) 2,5-dichlorophenyl formamide **9**, (b) 2,5-dibromophenylformamide **10** and (c) 5-chloro-2-methylphenylformamide **12**.

Table 6.5: Geometric parameters for halogen...halogen interactions in halogen substituted formamides and thioamides (see section 1.3.3.4)

Compound	Short axis (Å)	Space group	Distance X...X (Å)	Angle C-X...X (θ_1 & θ_2) In ($^\circ$)
2a	8.604	<i>Pbca</i>	3.642	171 & 117
2b	4.354	<i>P2₁/n</i>	3.490	164 & 93
5	4.317	<i>P2₁2₁2₁</i>	3.571	165 & 100
8	4.021	<i>P2₁/c</i>	3.869	123 & 123
9	8.652	<i>P2₁</i>	3.604 3.545	123 & 122 156 & 155
10	4.0133.968	<i>P2₁2₁2₁</i>	3.783 3.783	155 & 129 155 & 129
12	4.644	<i>P2₁/c</i>	3.551 3.551	167 & 99 167 & 99
14	8.016	<i>P2₁/n</i>	3.665	145 & 139
16	7.873	<i>P2₁/c</i>	3.658 3.591	159 & 102 122 & 122

**Figure 6.8:** The two Cl...Cl interactions in 2,6-dichlorophenylthioamide.

All the noncentrosymmetric compounds (**5** *P2₁2₁2₁*, **9** *P2₁* and **10** *P2₁2₁2₁*) have the L-shaped halogen...halogen structure since this structure generally occurs across 2_1 screw axis or glide plane [Saha *et. al.*, 2006]. The close packing which occurs across inversion centre is observed in the other compounds. The L-shaped interhalogen interaction is favoured amongst most of the formamides and thioamides discussed due to greater polarizability of Cl and Br atoms.

6.6 Influence of C-H... π , C-X... π and π ... π interactions in compounds 1 to 21

6.6.1 C-H... π and C-F... π

Table 6.6: Geometric parameters for C-H... π , C-F... π and C-Cl... π interactions in compounds 1 - 21

Compound & space group	Bond	H...Cg (Å)	C... Cg (Å)	<C-H... Cg (°)
1a, <i>Pbca</i>	C(7)-H(7)...Cg	3.137	3.657	117
1b, <i>P2₁</i>	C(6)-F(2)...Cg	3.433	3.757	93
2a, <i>Pbca</i>	C(7)-H(7)...Cg	3.175	3.753	122
3, <i>P2₁2₁2₁</i>	C(8)-H(8)...Cg	2.931	3.692	137
4a, <i>Pbca</i>	C(7)-H(7)...Cg	2.974	3.589	124
6, <i>P2₁/c</i>	C(7)-H(7)...Cg	2.893	3.768	157
	C(10)-H(10)...Cg	2.768	3.569	141
12, <i>P2₁/c</i>	C(8)-H(8) ...Cg	2.784	3.609	145
16, <i>P2₁/c</i>	C(6)-Cl(2)...Cg	3.545	4.124	97
17, <i>C2/c</i>	C(9)-H(9A) ...Cg	2.847	3.647	141
18, <i>C2/c</i>	C(8)-H(8B) ...Cg	3.008	3.679	128
20, <i>P2₁/c</i>	C(7)-H(7)...Cg	2.748	3.637	160
	C(10)-H(10)...Cg	3.256	3.740	113
21, <i>C2/c</i>	C(3)-H(3) ...Cg(1)	3.106	3.798	131
	C(6)-H(6) ...Cg(1)	3.330	4.111	141
	C(7)-H(7) ...Cg(1)	3.085	3.873	142

Table 6.6 gives some geometric parameters for compounds that have C-H... π , C-Cl... π and C-F... π intermolecular interactions. The most common atom that participates in a C-H... π interaction is C(7) [H(7)] but this is only true when H(7) is not involved in other interactions; especially in C-H...O interactions as in compounds **3**, **17** and **12**. The interactions that involve C(7)-H(7) help to stabilize the N-H...O hydrogen bonded chains and are therefore in the same direction as N-H...O hydrogen bonded chains as shown in Figure 6.9.

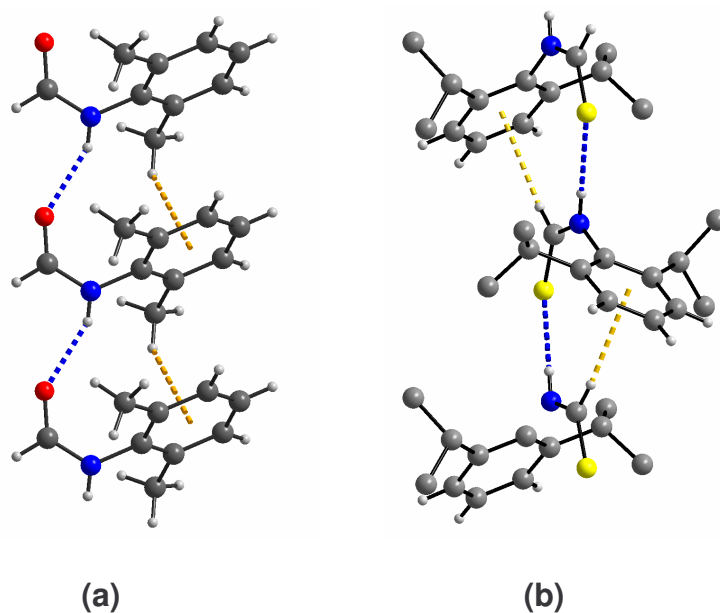


Figure 6.9: Hydrogen bond chains in (a) 2,6-dimethylphenylformamide and (b) 2,6-diisopropylphenylthioamide showing the C-H... π interactions. In (a) the methyl group acts as a donor while in (b) C(7)-H(7) is involved.

Category 2 compounds with methyl substituents have a C-H... π interaction in the structure. Category 2 that do not have methyl substituents on the aryl ring use alternative donor atoms forming non-conventional C-H... π interactions. In 2,6-difluorophenylformamide **1b**, F interacts with a aryl ring to form C-F... π interactions. This interaction has been observed in other fluorinated aromatic compounds and is known to be stabilizing [Vangala *et. al.*, 2002 and references therein]. Phenylformamide uses H(7) and two aromatic protons H(3) and H(6) to form C-H... π interactions between the layered sheets of N-H...O hydrogen bonded tetramers (see Figure 6.10) making them, together with π ... π interactions, important.

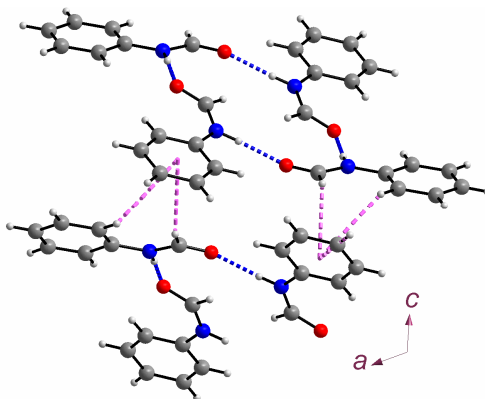


Figure 6.10: Hydrogen bonded tetramers in phenylformamide supported by C-H... π interactions.

The H...*C_g* length is observed to be comparatively short when the aryl ring is electron rich as in compounds **3**, **4**, **6**, **12**, **17** and **18** (all have methyl or isopropyl groups as substituents on the aryl ring making C-H... π more favourable. This is consistent with the nature of C-H... π interaction [Madhavi, 1997; Nishio, 2004] and ranges between 2.7 – 3.0 Å.

6.6.2 $\pi\cdots\pi$ interactions**Table 6.7:** Geometric parameters for $\pi\cdots\pi$ interactions in compounds **1** - **21** (α = the angle between the planes through each of the interacting rings)

<i>Compound</i>	<i>Cg...Cg (Å)</i>	α (°)	<i>Closest \perp dist. (Å)</i>
1a	3.903	0.00	3.484
2a	3.668	0.00	3.437
4a	3.675	0.00	
8	4.987	0.00	3.487
	3.595	0.00	3.496
9	3.725	0.02	3.666
10	3.537	0.00	3.532
14	3.763	0.00	3.429
	3.694	0.00	3.452
15	4.262	2.68	3.270
	4.262	2.68	3.331
16	4.986	0.02	3.487
	3.595	0.02	3.496
18	3.676	0.00	3.618
19	3.537	0.00	3.532
21	4.278	0.03	3.586

Table 6.7 gives geometric parameters for all compounds with $\pi\cdots\pi$ interactions. This interaction seems to be vital and is present in all category 1 compounds as well as all the thioamides (with the exception of **20**). Most of the halogen substituted category 2 compounds do not have this interaction. Most category 3 have $\pi\cdots\pi$ interaction. Most of the $\pi\cdots\pi$ interactions act as links between N-H...O hydrogen-bonded chains in category 1 compounds (see Figure 6.11a) and between planar or corrugated sheets in category 3 and 4 compounds (Figure 6.11c) as well as in phenylformamide **21** and the arylthioamides (Figure 6.11b).

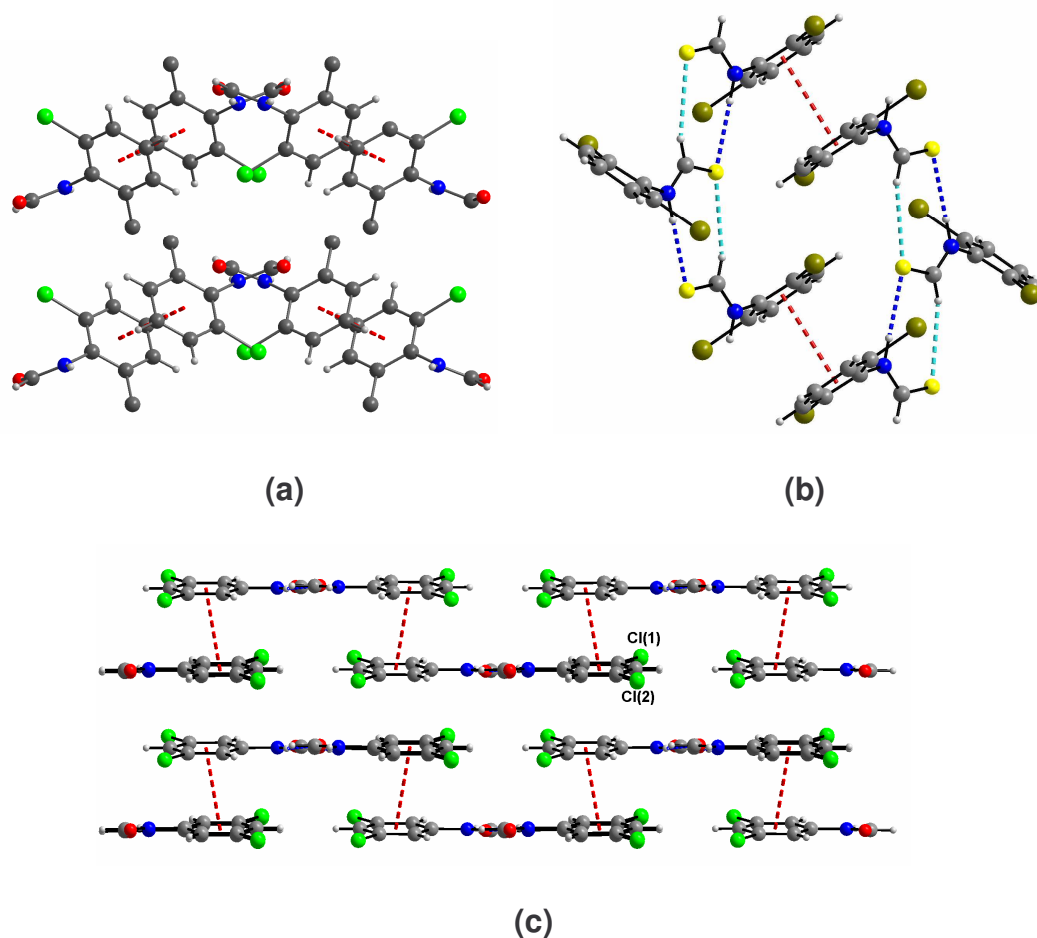


Figure 6.11: $\pi\cdots\pi$ interactions in (a) category 1 compounds and (b) arylthioamides linking up N-H...O and N-H...S hydrogen bond chains, and (c) in category 4 compounds, linking up sheets of N-H...O hydrogen bond chains.

The three different types of $\pi\cdots\pi$ interactions, the edge-to-face ($\alpha = 90^\circ$), face-to-face ($\alpha = 0^\circ$) and the tilt angle interacting rings ($10 \leq \alpha \leq 75^\circ$) are observed for compounds **1** to **21**. However the stronger and predominant type is the face-to-face interaction.

According to the literature, most aromatic interactions, including aromatic side chains in proteins show a preference of face-to-face

geometry with an average separation (Cg...Cg) of 3.4 - 6.5 Å [Nishio, 2004]. C-H... π and π ... π interactions in related disubstituted acetamides and formamides from the literature display similar geometries. Both interactions play a major role in the crystal packing of compounds especially when they occur in cooperativity with other interactions such as the N-H...O hydrogen bond, the C-H...O/S and the halogen...halogen intermolecular interactions.

6.7 Discussion

The results and analysis of crystal packing of the arylformamides and arylthioamides have shown that four different categories of N-H...O hydrogen bond motifs from arylformamides and one N-H...S hydrogen bond motif are formed from thioamides. The preferred N-H... O hydrogen-bond geometry for category 1 is such that the N-H...O angle is linear. Category 2 compounds have the shortest N...O distances comparatively but with a less linear N-H...O hydrogen bond angle. 3,4-dichlorophenylformamide and phenylformamide (category 4) have the most linear N-H...O angle. All N-H...S hydrogen bond angles are also linear and have very short N...S distances.

The C-H...O and C-H...S play a supporting role in the compounds that have them. In most formamides, they serve as supports for N-H...O hydrogen bonds and as link between N-H...O/S hydrogen bond chains.

Nearly all halogenated arylformamides have the short 4 Å axis. It has been shown that chlorine atoms of neighbouring molecules in the crystal lattice come close within a distance of about 4.2 Å. [Gnanaguru et al., 1985]. This steers the structures of these compounds to the 4 Å axis structure (more so in the category 3 and 4 compounds). The exceptions are **1a**, **2a**, **13** and **14** and all the aryl thioamides. This short axis is not seen in the arylthioamides probably due to the *cis* conformation that the compounds form. This conformation only allows for a spiral type of N-H...S hydrogen bond chain in which adjacent molecules are related by a glide or 2_1 screw axis and these form approximately '8 Å axis' just like category 1 compounds. As expected no F...F interactions are observed in the fluoro-substituted **1a** and **1b**. This is because F...F interactions do not have any additional stabilizing role in close packing unlike the other halogen-halogen interactions [Desiraju and Parthasarathy, 1989]. Instead because of the strongly dipolar character between fluorine and hydrogen C-H...F interactions are formed in these two compounds. The other halogens form L-shaped X...X and close-packing X...X interactions as well as X...O and X...H intermolecular interactions (X = halogen).

In the absence of strong interhalogen bonds, C-H... π and π ... π interactions contribute to the stability of crystals. C-H... π in most cases supports the N-H...O hydrogen bonds in these structures whereas the π ... π interaction links up adjacent N-H...O and N-H...S hydrogen bond chains or ribbons in aryl -formamides and thioamides. These are some of the

interactions that contribute to the formation of crystals of these compounds. In the section we look at how they each contribute towards the formation of the crystal lattices.

All these interactions contribute to the stability of the crystals. Their importance individually is not easy to establish but cooperatively each has a role to play in the crystal. The N-H...O/S C-H...O/S, are present in most of the twenty four compounds. These are supported either by C-H... π , π ... π and halogen contacts depending on the category of N-H...O/S hydrogen bond and the support is mainly in linking up adjacent C(4) chains or whatever ribbon types formed. To investigate which ones are more important in the stability of the crystal the next section outlines results from lattice energy calculations.

6.8 Results from lattice energy calculations

The ZipOpec module of the OPIX program suite [Gavezzotti., 2003] was used to estimate lattice energies by summation of potential energies of interactions between atom pairs described by the UNI force field, (see Chapter 1) [Filippini and Gavezzotti, 1993]. The categories used to classify the N-H...O (N-H...S in thioamides) hydrogen bonds in the previous section will once again be used in this discussion. The variety of intermolecular interactions observed in the different categories all contribute differently and we list only the most common and the ones that

contribute most to the stability of crystals. All five different categories have certain favourable intermolecular interactions supporting the crystal lattices.

Our goal was to first identify all interactions on the basis of experimental X-ray diffraction data (using programs like *MERCURY* and *PLATON*). Calculations of lattice energies of the crystals were then carried out and the two sources of information used to assess and gain insight into the nature of weak intermolecular interactions in the crystal lattices of arylformamides and thioamides. We shall first outline the major interactions (based on the strength) in each category and use the energy calculations to determine which of the interactions contribute most to the stabilization of the crystals. For compounds with disorder the total lattice energies cannot be considered accurate because the extra stabilization due to the entropy of disorder has been ignored. However the contributions of individual interaction are considered to be a good approximation and will be used in this discussion.

6.8.1 Category 1: [C(4) spirals in Figure 6.1a]

The compounds in this category are listed in Table 6.8. The major interactions of the 4 compounds above are, the N-H...O hydrogen bond, C-H...O, Cl...O, C-Cl...H, Cl...Cl and π ... π .

Table 6.8: Most stabilizing molecule-to-molecule interactions in compounds **1a**, **2a**, **4a** and **6** [Category 1, (4) spirals].

Structure (ΔH given in kJ/mol)	Symmetry operator between molecules	Energy/kJmol ⁻¹ †	Interactions relating molecules
1a ΔH (sub) = -91.28	-0.5+x, y, 1.5-z	-35.2	N-H...O
	2-x, 1-y, 1-z	-29.9	π ... π
	1.5-x, -0.5+y, z	-9.1	H...F
2a ΔH (sub) = -103.51	-0.5+x, y, 0.5-z	-39.8	N-H...O
	-x, 1-y, -z	-29.8	π ... π
	-x, 0.5+y, 0.5-z	-8.9	Cl...Cl
4a¹ (Cl...O) ΔH (sub) = -96.71	0.5+x, y, 0.5-z	-41.5	N-H...O
	-x, 1-y, -z	-28.5	π ... π
	-x, -0.5+y, 0.5-z	-8.7	Cl...Cl
4a (C-H...O) ΔH (sub) = -101.93	0.5+x, y, 0.5-z	-39.8	N-H...O
	-x, 1-y, -z	-30.1	π ... π
	0.5-x, -0.5+y, z	-8.2	Cl...Cl
6 ΔH (sub) = -107.98	-x, 0.5+y, 0.5-z	-43.2	N-H...O
	-x, 1-y, -z	-25.5	C-H... π
	x, 0.5-y, -0.5+z	-11.6	π ... π

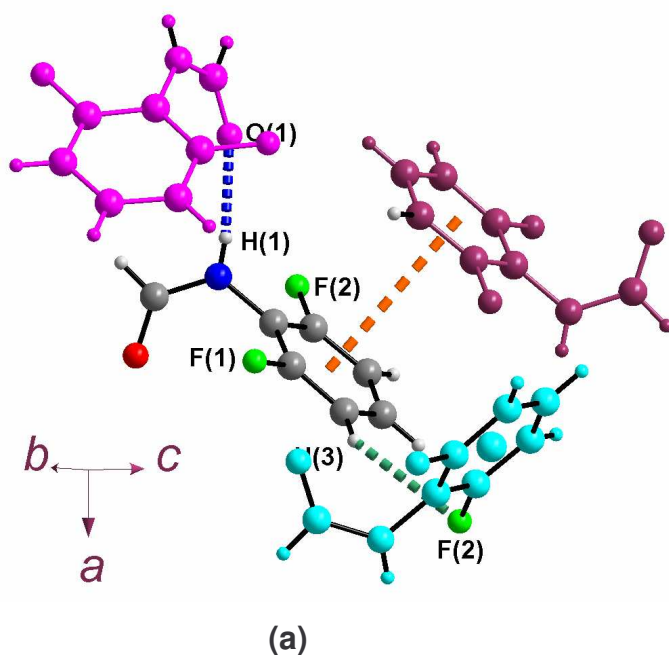
Table 6.8 above summarises the energies between molecules that are related by the listed interactions in each of the compounds. Analysis of the compounds revealed that interactions that bring molecules close through the N-H...O hydrogen bond contributed the most energy towards stabilization of the crystals. π ... π interactions are next in line except for compound **6** where C-H... π seems to contribute more to the crystal packing than the π ... π interaction. In compound **1** C-H...F interactions were found to play an important role in the stability of the crystal especially since there are no F...F interactions. The difference in polarity of hydrogen

† Crystal energy calculations done using OPiX.

¹ Separate calculations have been done for the two conformations of compound **4** and have been indicated by whether the calculation was done on conformation allowing the Cl...O interaction or on the one allowing the C-H...O interaction.

and fluorine atoms may be the reason for C-H...F interactions formation as opposed to F...F interactions [Thallapally and Nangia, 2001 and references therein]. Similar interactions (C-H...Cl) in compound **2a** however aid in the formation of Cl...Cl interactions.

The lattice energy of the compounds increases with the increase in mass of the molecule, -91.28 kJ/mol for compound **1a** and -107.98 kJ/mol for compound **6**. The arrangement of three or four molecules around a central molecule that contributes most to the stability of the structures of compounds **1a** and **2a** is given in Figure 6.12.



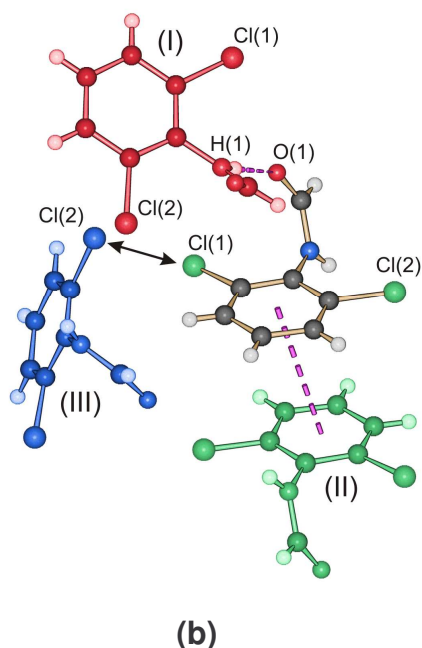


Figure 6.12: The arrangement of the three molecules around a central molecule (highlighted in purple colour) contributing most to the stability of structure (a) **1a**; molecules involved in N(1)-H(1)...O(1) hydrogen bonding (-0.5+x, y, 0.5-z; -35.2 kJ/mol); molecules involved in the π ... π interaction (2-x, 1-y, 1-z; -29.9 kJ/mol) and molecules involved in the C(6)-F(2)...H(3) interaction (1.5-x, -0.5+y, z; -9.1 kJ/mol). (b) **2a**; (I) molecules involved in hydrogen bonding (-0.5+x, y, 0.5-z; -39.8 kJ/mol); (II) molecules involved in the π ... π interaction (-x, 1-y, -z; -29.8 kJ/mol); (III) molecules involved in the Cl...Cl interaction (-x, 0.5+y, 0.5-z; -8.9 kJ/mol).

6.8.2 Category 2: [C(4) stacks in Figure 6.1b]

Category 2 compounds have N-H...O hydrogen bond, Cl...Cl, Br...Br, C-H... π , Cl...O and C-H...O interactions as the major interactions.

Table 6.9: Most stabilizing molecule-to-molecule interactions in compounds **1b**, **2b**, **4b**, **3**, **5** and **12**. [Category 2 stacks]

Structure (ΔH given in kJ/mol)	Symmetry operator between molecules	Energy/kJmol ⁻¹	Interactions relating molecules
1b $\Delta H(\text{sub}) = -89.87$	-1+x, y, z	-36.9	N-H...O
	1-x, -0.5+y, 2-z	-12.6	H...F
	1-x, -0.5+y, 1-z	-12.4	C-F... π
2b $\Delta H(\text{sub}) = -96.02$	-1+x, y, z	-42.1	N-H...O
	2-x, 2-y, 2-z	-11.7	π ... π
	-x, -0.5+y, 0.5-z	-8.9	Cl...Cl
4b (Cl...O) $\Delta H(\text{sub}) = -94.87$	x, -1+y, z	-43.6	N-H...O
	x, 1+y, z	-9.8	C-H ...O
	0.5+x, 1.5-y, z	-9.2	C-H...Cl
4b (C-H...O) $\Delta H(\text{sub}) = -97.21$	x, -1+y, z	-43.7	N-H...O
	-0.5+x, 0.5-y, z	-11.5	C-H ...O
	0.5-x, -0.5+y, 1-z	-9.9	C-H...Cl
3 $\Delta H(\text{sub}) = -97.40$	-1+x, y, z	-44.0	N-H...O
	-x, 0.5+y, 0.5-z	-10.1	C-H...O
	-0.5+x, 1.5-y, -z	-10.0	C-H... π
5 $\Delta H(\text{sub}) = -90.48$	-1+x, y, z	-40.0	N-H...O and N-H... π
	-0.5-x, 1-y, -0.5+z	-9.5	C-H...O
	0.5-x, 1-y, -0.5+z	-8.1	Br...Br
12 $\Delta H(\text{sub}) = -104.96$	x, -1+y, z	-45.6	N-H...O and C-H... π
	-x, -y, 1-z	-15.7	C-H...O
	-x, -0.5+y, 1.5-z	-8.1	Cl...Cl

Table 6.9 outlines the major interactions plus the energies they contribute to the packing in the crystals of these compounds. The π ... π interaction is not common in this set of compounds with exception of compound **2b** and even then, the two molecules involved in this interaction experience a lower energy relative to the ones in category 1 compounds. The highest energy is for the interaction between molecules related by N-H...O hydrogen bonds of each of the compounds and seems to be slightly

stronger than those of the corresponding interactions in category 1. The other important interactions in this category include halogen bonds (Cl...Cl and Br...Br for 2,6-dichlorophenylformamide **2b** and 2,6-dibromophenylformamide **5** respectively), C-H... π and C-H...O interactions, which on average contribute equally to the stability of the crystal. Figures 6.13, 6.14 and 6.15 give the arrangement of molecules around a central molecule indicating the interactions involved relative to the listed energies; 6.13 shows interactions for halogenated category 2 and 6.14 shows interactions around a central molecule of 2,6-dimethylphenylformamide.

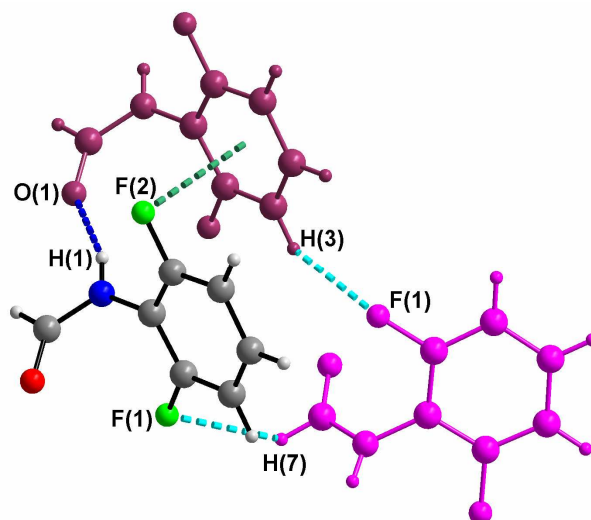


Figure 6.13: The arrangement of the three molecules contributing most to the stability of 2,6-difluorophenylformamide **1a**; molecules involved in N-H...O hydrogen bonding (1-x, y, z; -36.9 kJ/mol) [indicated by blue dashed lines]; molecules involved in a C-F... π interaction (1-x, y, z; -12.4 kJ/mol) [indicated by green dashed lines]; and molecules close enough to each other such that a fluorine atom is interacting with a hydrogen atom, C-

F...H interaction ($-x, \frac{1}{2}+y, -z$; -12.6 kJ/mol) [indicated by light blue dashed lines].

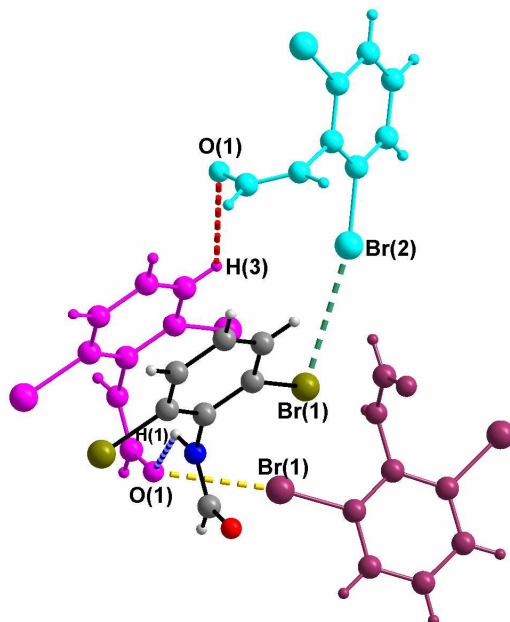


Figure 6.14: The arrangement of the four molecules contributing most to the stability of 2,6-dibromophenylformamide **5**; (I) molecules involved in N-H...O hydrogen bonding ($1-x, y, z$; -40.0 kJ/mol) [indicated by blue dashed lines]; (II) molecules involved in C-H...O hydrogen bond ($-1/2-x, 1-y, -1/2+z$; -9.5 kJ/mol) [indicated by red dashed lines]; (III) molecules connected through Br...Br interaction ($1/2-x, 1-y, \frac{1}{2}+z$; -8.1 kJ/mol) [indicated by sky-blue dashed lines].

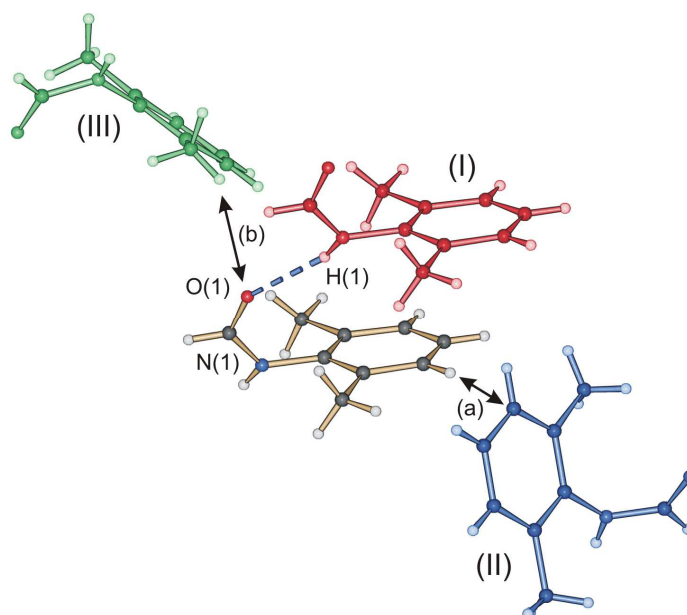


Figure 6.15: The arrangement of the three molecules contributing most to the stability of 2,6-dimethylphenylformamide **3**; (I) molecules involved in hydrogen bonding ($-1+x, y, z$; -44.0 kJ/mol); (II) molecules possibly involved in a edge-to-face C-H... π interaction as indicated with arrow (a) ($-0.5+x, 1.5-y, z$; -10.0 kJ/mol); (III) molecules orientated such that the methyl group of one molecule is pointing towards the carbonyl oxygen [indicated by arrow (b)] of the central molecule ($-x, 0.5+y, 0.5-z$; -10.1 kJ/mol).

6.8.3 Comparison of compounds 1-, 2- and 4- a and b

2,6-difluorophenylformamide **1a**, 2,6-dichlorophenylformamide **2a** and 2-chloro-6-methylphenylformamide **4a** (category 1) have larger lattice energy values when compared to **1b**, **2b** and **4b** (category 2) see Tables 6.8 and 6.9. Both sets of compounds have N-H...O hydrogen bond as the

major interaction contributing to the stability of the crystals. The energy between molecules related by this interaction is however higher in **1b**, **2b** and **4b** than in **1a**, **2a** and **4a**. The $\pi\cdots\pi$ interaction is the second major interaction in all **a** compounds. Only **2b** has this interaction in category 2 compounds but has a small value energetically (-29.8 in **2a** vs -11.7 kJ/mol in **2b**) when compared to **1a**, **2a** and **4a**. So these interactions become less important as the compounds change from **1a**, **2a** and **4a** to form **1b**, **2b** and **4b**. The difference in lattice energies in the two categories could therefore be as a result of larger value $\pi\cdots\pi$ interactions in category 1 which is absent or smaller in value in category 2 compounds. Other interactions collectively contribute on average the same (between 8 and 13 kJ/mol) to the stability of crystals of each compound in both categories. However there is a trend in order of magnitude of the listed energies in categories 1 and 2.

6.8.4 Category 3 and 4: [Sheets, dimers and tetramers]

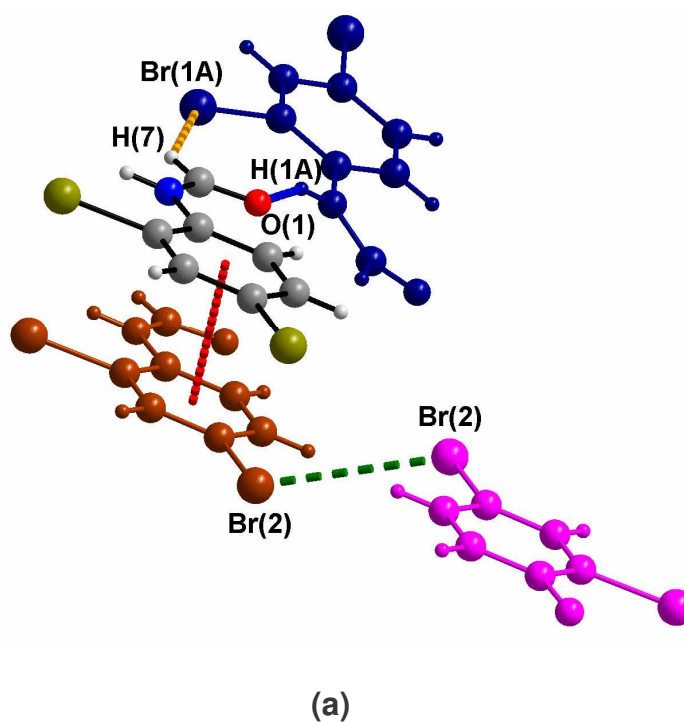
Categories 3 and 4 molecules are planar and as such behave differently from categories 1 and 2 in terms of the intermolecular interactions that they possess.

Table 6.10: Most stabilizing molecule-to-molecule interactions in compounds **7**, **8**, **9**, **10**, **13** and **14**. [Category 3 sheets]

Structure (ΔH in kJ/mol)	Symmetry operator between molecules	Energy kJmol ⁻¹	Interactions relating molecules
7 ΔH (sub) = -105.19	-1+x, y, z	-38.1	N-H...O and C-Cl... π
	-0.5+x, 0.5-y, 0.5+z	-20.3	C-H...O
	-0.5+x, 0.5-y, -0.5+z	-10.8	C-H...Cl
8 ΔH (sub) = -215.54 for 2 molecules in assym. unit	x, -1+y, z	-40.2	π ... π
	x, 0.5-y, -0.5+z	-32.4	N-H...O
	x, -1+y, 1+z	-15.2	C-H...Br
9 ΔH (sub) = -106.74	-1+x, y, z	-39.4	π ... π
	-x, 0.5+y, -z	-20.0	N-H...O
	1-x, -0.5+y, -z	-13.1	Cl...Cl
10 ΔH (sub) = -101.67	-1+x, y, z	-40.7	π ... π
	1-x, -0.5+y, 1.5-z	-12.3	N-H...O
	-1+x, -1+y, z	-11.9	Br...O
13 ΔH (sub) = -110.87	1-x, -y, 2-z	-38.9	N-H...O & C-H...O
	1-x, -y, 1-z	-36.1	π ... π
	2-x, -y, 1-z	-25.9	π ... π
	x, y, -1+z	-17.4	Cl...C(7)
	x, 0.5-y, -0.5+z	-12.3	Cl(1)...H(5)
14 ΔH (sub) = -102.62	1-x, 2-y, -z	-41.8	π ... π
	-x, 2-y, -z	-36.4	π ... π
	-0.5+x, 1.5-y, -0.5+z	-21.8	N-H...O & C-H...O
	1-x, 2-y, 1-z	-9.8	Cl...C(7)
	-1+x, y, -1+z	-7.7	Cl...Cl

Energies related to interactions common to compounds from categories 3 and 4 are listed in Table 6.10. In crystal structures of compounds in category 3 (compounds **8**, **9**, **10** and **14**) the energy contribution of molecules related by π ... π interactions seem to be greater in magnitude than that contributed by N-H...O hydrogen bond related molecules. This is probably due to the fact that N-H...O hydrogen bonds form planar sheets in which adjacent molecules are further apart in the

alternate arrangement along the N-H...O hydrogen bond chain. This then leaves interactions like π ... π , C-H... π , X...O, X...H and C-H...O to link up the hydrogen bonded sheets. It seems like it's the π ... π interactions that holds these sheets more effectively. Figure 6.16 shows arrangements of four molecules showing interactions that contribute most to the stability of crystals in some category 3 compounds. 2,4-dibromophenylformamide **8** and 3,5-dichlorophenylformamide **14** are used as example.



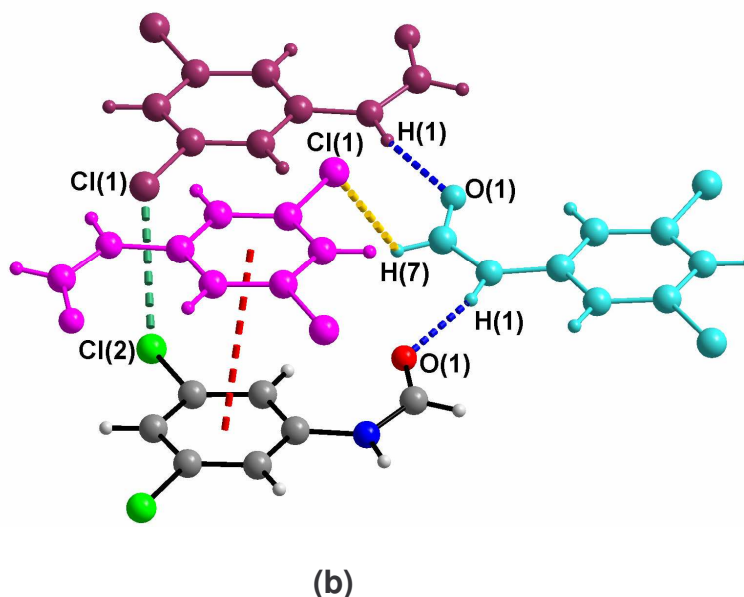


Figure 6.16: The arrangement of the three molecules contributing most to the stability of (a) 2,5-dibromophenylformamide **8**; molecules involved in hydrogen bonding ($x, \frac{1}{2}-y, -1/2+z$; -32.35 kJ/mol); molecules possibly involved in a face-to-face $\pi\cdots\pi$ interaction as indicated with a red dashed line ($x, 1+y, z$; -40.2 kJ/mol); (b) 3,5-dichlorophenylformamide **14**; molecules involved in hydrogen bonding ($-1/2+x, 1\frac{1}{2}-y, -1/2+z$; -21.80 kJ/mol); molecules involved in $\pi\cdots\pi$ interactions ($1-x, 2-y, -z$; -41.80; $-x, 2-y, -z$; -36.44 kJ/mol); and molecules involved in Cl...H interactions ($1-x, 2-y, 1-z$; -9.8 kJ/mol).

The situation is different in category 4 (where dimers of N-H...O hydrogen bonded molecules are formed) and interactions involving N-H...O hydrogen bonded molecules and those of $\pi\cdots\pi$ interactions contribute about the same and the most in stabilizing the crystal structure. Other interactions such as Cl...H also contribute substantially to the overall lattice energy.

6.8.5 Arylthioamides 15 to 20 [Category 5]

A variety of interactions play a role in stabilizing the crystals of these compounds 15 to 20.

Table 6.11: Most stabilizing molecule-to-molecule interactions in compounds 15 and 20. [Category 5]

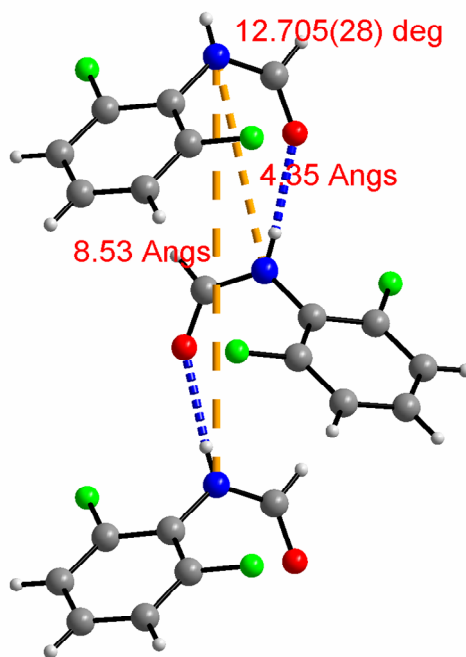
Structure (ΔH is given in kJ/mol)	Symmetry operator between molecules	Energy/kJmol ⁻¹	Interactions related to the symmetry operators
15 ΔH (sub) = -93.13	1-x, -y, 1-z	-23.76	$\pi \dots \pi$
	1.5-x, -0.5+y, z	-23.1	N-H...S
	0.5-x, -0.5+y, z	-16.76	
16 ΔH (sub) = -107.71	2-x, 1-y, -z	-37.42	$\pi \dots \pi$
	1-x, 1-y, -z	-35.4	$\pi \dots \pi$
	x, 0.5-y, -0.5+z	-25.98	N-H...S
	2-x, -0.5+y, 0.5-z	-8.7	C-H(3)...S
	1+x, y, 1+z		Cl...Cl
17 ΔH (sub) = -97.97	0.5-x, 1.5-y, -z	-32.1	$\pi \dots \pi$
	0.5-x, 0.5+y, 0.5-z	-26.03	N-H...S
	x, 1-y, -0.5+z	-6.07	C-H(9b)...S
18 ΔH (sub) = -149.09	1.5-x, 0.5-y, 1-z	-52.3	$\pi \dots \pi$ & C-H(8b)... π
	2-x, 1-y, 1-z	-49.7	$\pi \dots \pi$
	1.5-x, -0.5+y, 0.5-z	-29.8	N-H...S
	2-x, -y, 1-z	-21.2	$\pi \dots \pi$
	2-x, y, 0.5-z	-17.96	C-H...S
19 ΔH (sub) = -106.51	1-x, 1-y, 2-z	-37.6	$\pi \dots \pi$
	-x, -0.5+y, 1.5-z	-27.0	N-H...S
	1-x, 2-y, 2-z	-16.35	$\pi \dots \pi$
	1-x, -0.5+y, 1.5-z	-11.5	C-H...S
	-1+x, y, z	-11.2	S...H(5)
20 ΔH (sub) = -108.38	1-x, -0.5+y, 1.5-z	-45.5	N-H...S & C-H(8b)... π
	1-x, -y, 1-z	-24.4	$\pi \dots \pi$

In this set of compounds the $\pi \dots \pi$ interaction again makes the largest energy contribution to the packing of molecules in the crystal. The

magnitude of the interactions between molecules that are related by this interaction is higher than that between molecules that are joined through an N-H...S hydrogen bond. Generally the magnitude of these interactions (π ... π interactions) in the thioamides is the same as that of N-H...O interactions in crystals of 2,6 disubstituted arylformamides. 2,6-diisopropylphenylthioamide **20** behaves in a similar manner to its formamide analogue **6**. The two are isomorphous hence have similar hydrogen bonding patterns.

The π ... π interactions plays a major role in the structures of 2,6-difluorophenylthioamide **15**, 2,6-dichlorophenylthioamide **16**, 2,6-dimethylphenylthioamide **17**, 2-chloro-6-methylphenylthioamide **18** and 2,6-dibromophenylthioamide **19**. All of these compounds adopt a *cis* conformation which gives rise to a different hydrogen bonding pattern as compared to the 2,6-disubstituted arylformamides. The arylthioamide molecules are arranged in an alternate fashion thereby aligning the aryl rings of molecules along adjacent hydrogen bonded ribbons for π ... π interactions. The distance between adjacent amide groups along a N-H...S hydrogen bond with *cis* conformation is short (see figure 6.17). The *trans* conformation in formamides results in a distance (N...N distance between alternate molecules along N-H...O hydrogen bond = 8.53 Å) larger than that in thioamides with a *cis* conformations (N...N distance between alternate molecules along N-H...S hydrogen bond = 8.11 Å). For this reason aryl rings from adjacent hydrogen bond chains in the

thioamides are much closer and contribute more towards the stability of the crystal as compared to the weaker N-H...S hydrogen bond.



(I)

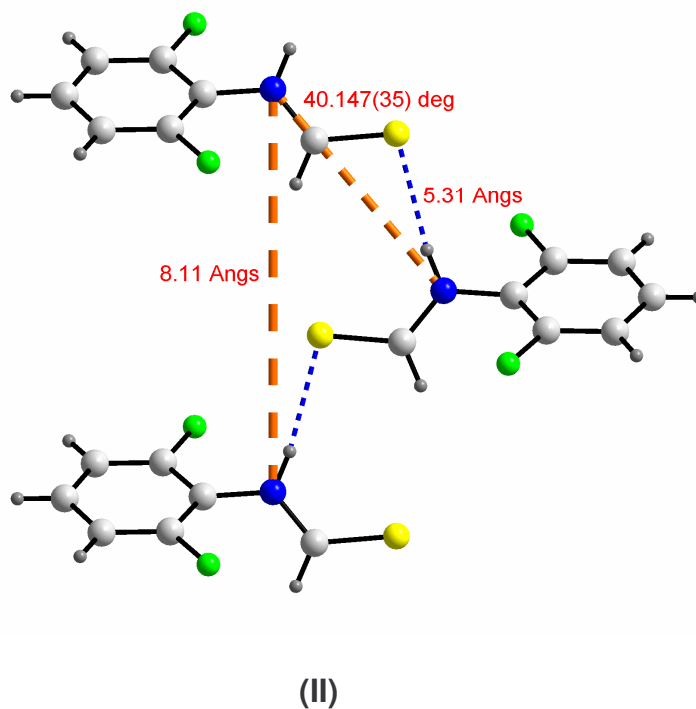


Figure 6.17: The distance and general angle between adjacent and alternate molecules along hydrogen bonded chains in (I) 2,6-difluorophenylformamide **1a** and (II) 2,6-difluorophenylthioamide **15**.

6.9 Conclusion

Generally three most important interactions in each of the 24 crystals structures of all formamides and thioamides discussed in this thesis have, combined, been found to contribute more than half the total lattice energy. Whereas N-H...O contributes more towards crystal stabilization in categories 1 and 2 compounds, the π ... π interaction contributes more in categories 3 and 5. These results seem to be dependent on the conformation that these compounds adopt. 2,6-disubstituted phenylformamides have the formamide moiety out of the

plane of the aryl ring and adopt a *trans* conformation in which the N-H...O hydrogen bond is favoured.

The other group of formamides with substitutions in other positions on the aryl ring have a planar conformation and forms N-H...O hydrogen bonded sheets. This sets up the molecules for easy $\pi\cdots\pi$ interactions and therefore making this interaction favourable in these structures.

The thioamides on the other hand adopt a *cis* conformation and in doing so the $\pi\cdots\pi$ interactions become more important compared to N-H...S interaction in the stabilization of the crystals.

3,4-dichlorophenylformamide **13** adopts a *cis* conformation and forms hydrogen bonded dimers. Phenylformamide **21** has two molecules in the asymmetric unit which adopt a *cis* and *trans* each forming hydrogen bonded tetramers. In both structures the $\pi\cdots\pi$ interaction is important in the stabilization of the crystals.

7. Conclusions

7.1 Introduction

Studies on crystal structures, polymorphism, isomorphism, cocrystallization and theoretical lattice energy calculations have been done using a variety of methods such as DSC measurements, powder X-ray diffraction, single crystal X-ray diffraction, nuclear magnetic resonance and theoretical calculations of lattice energies of crystals using Gavezzottis' OPIX program suite. Some new findings that arose from this study include;

- The thermal phase transitions and the second phases of 2,6-difluorophenylformamide **1b**, 2,6-dichlorophenylformamide **2b** and 2-chloro-6-methylphenylformamide **4b**. The hydrogen bonding patterns in the second phases of these formamides is different from the initial phases but similar to the initial phases of other formamides (2,6-dimethylphenylformamide **3** and 2,6-dibromophenylformamide **5**). Phase transitions were observed for 2,4-dibromophenylformamide **8** and 3,4-dichlorophenylformamide **13**. It was not possible to isolate the second polymorphs of **8** and **13** to support the observation from DSC results.

- The formation of cocrystal **22** (from 2,6-dichlorophenylformamide **2a** and 2,6-dimethylphenylformamide **3**), cocrystal **23** (from 2,6-dichlorophenylthioamide **16** and 2,6-dimethylphenylthioamide **17**) and cocrystal **24** (from 2,6-diisopropylphenylformamide **6** and 2,6-diisopropylphenylformamide **20**).
- The structure of 1:1 *cis:trans* phenylformamide **21** was elucidated. The structure of phenylformamide has not been reported despite the amount of interest in it by many scientists. In the structure of this compound, two molecules are found in the asymmetric unit. The two *cis* and *trans* phenylformamide molecules form N-H...O hydrogen bonded tetramers, whereas only dimers have been reported from theoretical and spectroscopic studies done on this compound.

7.2 Conformations and hydrogen bonding patterns

The crystal structures of all formamides and thioamides discussed in this thesis exhibited at least two conformations, either *cis* or *trans*, where the amide group was either in the plane of the aryl ring or twisted out of the plane by about 50 - 80°. This allowed for more than one hydrogen-bond motif to be

***N*-aryl -formamides and -thioamides**

adopted. The *cis* and *trans* conformations in the formamides allowed for the formation of four distinct motifs referred to as categories 1, 2, 3 and 4 here. Five thioamides adopted a *cis* conformation resulting in a different motif (category 5). The categories are based on the type hydrogen bonding chains formed of which each has its somewhat unique properties. It is notable that in all cases NMR evidence shows that there is a mixture of the *cis* and *trans* conformations in solution.

The C=O double bond and the N-H bond allows for the formations of chains described by C(4) graph set in category one and two compounds and a $R_2^2(6)$ ring in the one and only category three compound (only one other formamide, 2-methylphenylformamide is known to adopt a *cis* conformation). The C(4) chains may either be twisted or spiralled (as in category 1 compounds) or stacked or parallel (as in category 2 compounds). Certain intermolecular interactions play important roles in the stabilization of crystals of compounds in particular categories. Category 3 and 4 compounds form chains described by C(4) graph set notation except for 3,4-dichlorophenylformamide which forms hydrogen bonded dimers (and also adopts a *cis* conformation) described by a $R_2^2(8)$ graph set. Adjacent C(4) chains in 5-chloro-6-methylphenylformamide are joined together by C-H...O interactions resulting in rings described by $R_2^2(6)$ and $R_2^2(4)$ secondary graph set notations. The thioamides **15** and **20** form C(4) chains. The C(4) chains

are joined through C-H...S interactions to form (for **16**, **17**, **18** and **19**) ribbons described by $R_2^2(7)$ graph set notation. The ribbons are connected to each other by $\pi\cdots\pi$ or C-H... π intermolecular interactions between molecules related by inversion centers.

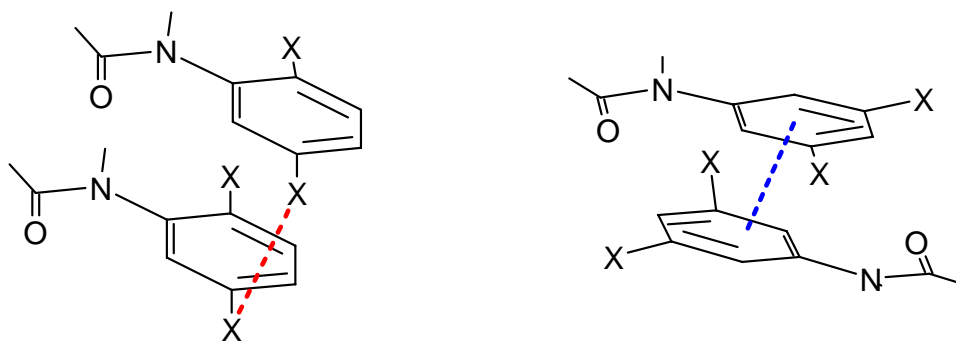
7.3 Major interactions in the crystal structures of the formamides and thioamides

The N-H...O hydrogen bonded chains in category 1 links molecules facing alternate directions that are related by a glide plane or a 2_1 -screw axis. Category 2 is generated when the molecules along the N-H...O hydrogen bond are stacked and related by unit cell translation. $\pi\cdots\pi$ interactions play an important role in category 1 compounds. C-H...O and halogen contacts such as C-H... π , C-H...Cl, Cl...Cl, C-H...F and Cl...O are the other intermolecular interactions that contribute much to the stabilization of the crystals in this category. Interestingly category 2 compounds lacked the $\pi\cdots\pi$ interactions despite the stacking of the aryl rings which might seem to be promoted by such interactions. In these structures, C-H...O, C-H... π , C-H...Cl, Cl...Cl, C-H...F, Cl/Br...O, and Br...Br interactions become important.

Category 3 compounds can further be sub-categorized. We have the 2,4-, the 2,5- and the 3,5- disubstituted arylformamides. Some of the $\pi\cdots\pi$

***N*-aryl -formamides and -thioamides**

interactions in the structures from this category are rather weak (longer *Cg...Cg* distances > 5.0 Å). An apparent explanation for this observation could have something to do with the arrangement of molecules along hydrogen bonded sheets. In the 2,4- and 2,5- disubstituted formamides, molecules that would have been involved in a $\pi\cdots\pi$ interaction face the same direction along the N-H...O hydrogen bonded sheets leaving the halogen substituents (Cl and Br) on the aryl ring aligned (or in close proximity). The alignment of the halogen substituents is such that only the rare V-type X...X interaction can be favored. These two factors could be the main cause for the relatively long *Cg...Cg* distances in the compounds. The 3,4- (category 4) and 3,5- disubstituted arylformamides on the other hand have N-H...O hydrogen bonded sheets whose molecules that are involved in $\pi\cdots\pi$ interactions are related by a center of inversion. In this way the halogen substituents are far apart and little interference between ring to ring interactions would be expected. The two chloro- compounds do not even have Cl...Cl interactions (see illustration in Figure 7.1). Its not easy to tell whether the positions of the substituents on the aryl ring play a role in this observation, but it is notable from the results of lattice energy calculations that the $\pi\cdots\pi$ interactions play a major role in the stabilization of the crystals of compounds from category 3.



X = Cl or Br

Figure 7.1: The arrangement of aligned molecules between hydrogen bonded sheets in (a) 2,5-disubstituted arylformamide and (b) 3,5-disubstituted arylformamide. The distance between the centers of the aryl rings is slightly shorter in (b) about 3.78 Å than in (a) between 3.83 and 4.02 Å.

For the thioamides N-H...S hydrogen bonds and $\pi\cdots\pi$ intermolecular interactions seem to be the most important. The $\pi\cdots\pi$ interaction is observed in the structure of every compound except for 2,6-dimethylphenylthioamide **17**. This compound however has a C-H... π interaction that serves the same purpose as $\pi\cdots\pi$ in the others. A look at the dihedral angles between the plane of the aryl ring and the thioamide moiety shows that, this angle is slightly larger in two thioamides: 2,6-dimethylphenylthioamide **17** (63.9°) and 2,6-diisopropylphenylthioamide **20** (80.7° *trans* isomer). The twist in this angle together with the presence of methyl groups in these two compounds could

be the reason for the absence of $\pi\cdots\pi$ interactions in compound **17** and only weak $\pi\cdots\pi$ interaction in compound **20**.

7.4 Isomorphism

From our results we have seen that a number of chemically distinct aryl formamides and thioamides exhibit isomorphous crystal structures depending on different conditions. There are only two sets of compounds that are isomorphous; the first set of compounds contained chlorine and methyl groups as substituents on the aryl ring, while the second set of compounds differed in one core atom of the molecule i.e. oxygen vs. sulfur atom.

From the first set of compounds there is an orientational disorder observed in Cl-Me in one of the isomorphous compounds. The known reason for disorder between these two groups of atoms is related to their sizes. It is known that because of the similarity in sizes of Cl and Me groups they can often be easily interchanged in molecules without changing the crystal structures of compounds (see Chapter 1). Other than the sizes of substituents, corresponding intermolecular interactions need to be a near match in their pattern and distance. Despite the substitution of a Cl group with a Me group in 2-chloro-6-methylphenylformamide (**4a**), the Cl-Me disorder in the compound still allows for Cl...Cl contact formation, apart from N-H...O hydrogen bonds, $\pi\cdots\pi$ and Cl...O interactions which 2,6-

***N*-aryl -formamides and -thioamides**

dichlorophenylformamide (**2a**) also have. Similar regions of halogen interactions and hydrocarbon interactions (as in **2a** and **4a**) are observed in 2,6-difluorophenylformamide (**1a**). And so its not only the Cl...Cl interactions that steer isomorphism between the three (**1a**, **2a** and **4a**) but a sum of the halogen and hydrocarbon interactions. 2,6-dimethylphenylthioamide (**17**) and 2-chloro-6-methylphenylthioamide (**18**) also have common intermolecular interactions (N-H...S, C-H...S and C-H... π hydrogen bonds and π ... π intermolecular interactions) apart from Cl...Cl interactions in compound **18**. This Cl...Cl contact is however about 0.18 Å longer than the sum of van der Waals radii of Cl. Its presence is as such a consequence of the overall structure of the compound. Thus the pair of isomorphous compounds have at least similar regions of intermolecular interactions (see Figures 5.3a and b).

2,6-diisopropylphenylformamide **6** and 2,6-diisopropylphenylthioamide **20** have similar major interactions that determine the packing of molecules in the crystals and can therefore be easily isomorphous. The isopropyl groups in both compounds presumably the biggest contributors to isomorphism in that they create a void in which one can easily replace an oxygen atom with a sulfur atom without changing much the overall structure of the compounds. The two compounds have in common N-H...O/S and C-H... π hydrogen bonds and π ... π intermolecular interactions as the major interactions governing the packing of molecules in the crystal.

7.5 Cocrystallization

Three cocrystals were discussed in this thesis, one generated from isomorphous compounds (**24**) and the others from two non-isomorphous compounds (**22** and **23**). Cocrystal **24** may be considered as a hybrid of the two starting compounds used to synthesize it, 2,6-diisopropylphenylformamide **6** and 2,6-diisopropylphenylthioamide **20**.

Cocrystals **22** (a 1:1 mixture of 2,6-dichlorophenylformamide and 2,6-dimethylphenylformamide) and **23** (a 1:1 mixture of 2,6-dichlorophenylthioamide and 2,6-dimethylphenylthioamide) are perfect examples in which the property of similar volumes of substituents (chlorine group and methyl group) is exploited. This property allows for the chloro and methyl groups to interchange in such a way that the two are disordered in the same positions on a compound. Interestingly cocrystal **22** was even found to be isomorphous to 2-chloro-6-methylphenylformamide **4a** (and **2a**). The fact that the cocrystal and 2-chloro-6-methylphenylformamide adopt the structure of 2,6-dichlorophenylformamide and not that of 2,6-dimethylphenylformamide could be an indication that both the halogen interactions and the hydrocarbon interactions play a significant part in the formation of these structures.

A different situation is observed for cocrystal **23**. The starting compounds adopt *cis* conformations while the resulting solid mixture adopts a *trans* conformation and crystallizes in the space group *Pbca*. We believe that the torsion angle defined by C(2)-C(1)-N(1)-C(7) could have something to do with difference in conformations of the starting materials and the product. The angle is 81.7° in cocrystal **23**, 82.7° in 2,6-dibromophenylformamide **5**, 78.9° in 2,6-diisopropylphenylformamide **6** and 80.7° in 2,6-diisopropylphenylthioamide **20**. We attribute the size of this angle in compounds **6** and **20** to the presence of intramolecular C-H... π interactions on either sides of the formamide and thioamide moieties of the two compounds. For compound **5** it can be attributed to the volume of bromine atom coupled with a possible N-H... π interaction. There is however no clear reason for the large size of the torsion angle in cocrystal **23** but a C-H... π interaction could be a contributing factor.

For all structures discussed in this thesis we took three interactions that contributed the most to the stability of crystals and these were found to contribute in total more than half the total lattice energy in each of the structures. Whereas N-H...O contributes more towards packing in category 1 and 2 compounds, the π ... π interaction contributes more in some category 3, category 4 and category 5 compounds. The thioamides adopt a *cis* conformation and because the N-H...S interaction is generally weak, these

***N*-aryl -formamides and -thioamides**

compounds depend more on $\pi\cdots\pi$ interactions for better stability in their crystals. 3,4-dichlorophenylformamide **13** adopts a *cis* conformation and forms hydrogen bonded dimers whereas phenylformamide **21** has two molecules (*cis* and *trans*) in the asymmetric unit forms tetramers. For these two compounds both the N-H...O and $\pi\cdots\pi$ interactions contribute about the same towards the stability of crystals.

7.6 Polymorphism and phase transitions

In this study five compounds showed phase transitions from their DSC traces but we were only able to isolate and structurally characterize the second polymorphs of three of these. The phase transitions adopted common patterns which are characterized by having first order structural phase transitions. Comparison of the structures of 2,6-dichlorophenylformamide (**2a** and **2b**) and 2-chloro-6-methylphenylformamide (**4a** and **4b**) reveals that there is an apparent steering effect of the chloro substituent in the low temperature polymorphs. The phase transformation of **2a** involves rotation of the aryl group, leaving the N-H...O hydrogen bonding chain intact. This transformation is probably entropically driven, and reverts back to the low temperature form in large part because of the stabilizing $\pi\cdots\pi$ interactions. For 2-chloro-6-methylphenylformamide, no reverse phase change is observed and is probably inhibited by intermolecular C-H...O interactions present in the

***N*-aryl -formamides and -thioamides**

high temperature polymorph of this compound but not present in the high temperature polymorph of 2,6-dichlorophenylformamide. The results discussed above (DSC, powder XRD and single crystal XRD) suggest that the low temperature forms are the thermodynamically stable forms at room temperature while the high temperature forms are kinetically driven and stable at high temperatures.

We have shown three interactions for each polymorph that contributes most to stabilization of the crystals. The two sets of energies follow the same trend that is outlined above for 2,6-dichlorophenylformamide and 2-chloro-6-methylphenylformamide. **1a** has a higher lattice energy which could have resulted partly from the $\pi \dots \pi$ interaction (not present in **1b**). **1b** does not seem to revert to **1a** an indication of stability of **1b** at room temperature. Lattice energy calculations indicate that **1a** is more stable by 1.4 kJ/mol and is probably the thermodynamic polymorph. We still do not know the exact conditions for the crystallization of **1b** but our suspicion is that it is somehow influenced by the presence of 2,6-difluorophenylthioamide in the crystallization solution.

References

A

- Aakeröy, C. B.; Evans, T. A.; Seddon, K. R.; Pálincó, I.; *New J. Chem.*, **23**, 1999, 145.
- Aakeröy, C. B.; Debra, J. S.; *CrystEngComm.*, **7**, 2005, 439.
- Aakeröy, C. B.; Desper, J.; Scott, B. M. T.; *Chem. Comm.*, 2006, 1445.
- Andreev, Y. U. G.; Lundström, T.; *J. Appl. Cryst.*; **28**, 1995, 534.
- Andreev, Y. U. G.; Macglashan, G. S.; Bruce, P. G.; *Phys. Rev. B***55**, 1997, 12011.
- Addadi, L.; Lahav, M.; *Pure Appl. Chem.*, **51**, 1979, 1269.
- Adams, H.; Bernard, Jr. P. L.; Eggleston, D. S.; Haltiwanger, R. C.; Harris, K. D. M.; Hembury, G. A.; Hunter, C. A.; Livingstone, D. J.; Kariuki, B. M.; McCabe, J. F.; *Chem. Comm.*, 2001, 1500.
- Allen, F. H.; Bird, C. M.; Rowland, R. S.; Raithby, P. R.; *Acta. Cryst.*, **B53**, 1997, 680.
- Allen, F. H.; Bird, C. M.; Rowland, R. S.; Raithby, P. R.; *Acta. Cryst.*, **B53**, 1997, 696.
- Amabilino, D. B.; Stoddart, J. F.; *Chem. Mater*, **6**, 1994, 1159.
- Andreeti, G. D.; Cavalca, L.; Domiano, P.; Musatti, A.; *Acta. Cryst.*, **B24**, 1968, 1195.
- Aoyama, T.; Matsuoka, O.; Nakagawa, N.; *Chem. Phys. Lett.*, **67**, 1979, 508.
- Atkins, P. W., in "Physical Chemistry", 4th. Ed., Richard Clay Ltd, Suffolk (Great Britain), 1998, pp. 654-655.
- Aullón, G.; Bellamy, D.; Brammer, L.; Bruton, E. A.; Sherwood, P.; *Chem. Comm.*, 1998, 653.
- Azumaya, I.; Yamaguchi, K.; Kagechika, H.; Saito, S.; *J. Pharm. Soc. Jpn.*, **114**, 1994, 414.
- Azumaya, I.; Okamoto, I.; Nakayama, S.; Tanatani, A.; Yamaguchi, K.; Shudo, K.; Kagechika, H.; *Tetrahedron*, **55**, 1999, 11237.
- Azumaya, I.; Okamoto, I.; Takayanagi, H.; *Anal. Sci.*, **19**, 2003, x3.

B

- Bar, I.; Bernstein, J.; *Tetrahedron*, **43**, 1987, 1299.
- Bain, A. D.; Hazendouk, P.; Couture, P.; *Can. J. Chem.*, **77**, 1999, 1340.
- Bennet, A. J.; Wang, Q.-P.; Slebocka-Tilk, H.; Somayaji, V.; Brown, R. S.; *J. Am. Chem. Soc.*, **112**, 1990, 6383.
- Blessing, R. H.; *J. Am. Chem. Soc.*, **105**, 1983, 2776.

N-aryl -formamides and -thioamides

- Beyer, T.; Day, G. M.; Price, S. L.; *J. Am. Chem. Soc.*, **123**, 2001, 5086.
- Beyer, T.; Price, S. L.; *J. Phys. Chem.* **B104**, 2000, 2647.
- Bernstein, J.; Enger, Y. M.; Hagler, A. T.; *J. Chem. Phys.*, **75**, 1981, 2346.
- Bernstein, J.; Etter, M. C.; McDonald, J.; *Acta. Cryst.*, **B46**, 1990, 256.
- Bernstein, J.; in *"Polymorphism in Organic Compounds"* Oxford, Claredon Press, 2002.
- Bernstein, J.; Davis, R. E.; Shimoni, L.; Chang, N-L.; *Angew. Chem. Int. Ed. Engl.*, **34**, 1995, 1555.
- Blagden, N.; Davey, J. R.; *Cryst. Growth & Des.*, **3**, 2003, 873.
- Boldyreva, E. V.; Shakhtshneider, T. P.; Vasilchenko, M. A.; Ahsbahs, H.; Uchtmann, H.; *Acta. Cryst.*, **A51**, 2000, 299.
- Boldyreva, E. V.; Kivikoski, J.; Howard, J. A. K.; *Acta. Cryst.*, **B53**, 1997^a, 394.
- Boldyreva, E. V.; Kivikoski, J.; Howard, J. A. K.; *Acta. Cryst.*, **B53**, 1997^b, 405.
- Bondi A.; *J. Phys. Chem.*, **68**, 1964, 441.
- Bosch, E.; Barnes, C. L.; *Cryst. Growth & Des.*, **2**, 2002, 299.
- Botoshansky, M.; Ellern, A.; Gasper, N.; Henck, J. -O.; Herbstein, F. H.; *Acta Cryst.*, **B54**, 1998, 277.
- Boeyens, J. C. A.; Denner, L.; Evans, D. G.; *J. Cryst. Spect. Res.*, **18**, 1988, 175.
- Bourn, A. J. R.; Randall, E. W.; *Mol. Phys.*, **8**, 1964, 567.
- Braga, D.; Grepioni, F.; *Chem. Soc. Rev.*, **29**, 2000, 229.
- Braga, D.; Desiraju, G. R.; Miller, J. S.; Guy Orpen, A.; Price, S. L.; *CrystEngComm.*, **4**, 2002, 500.
- Brader, M. L.; Sukumar, M.; Pekar, A. H.; McLellan, D. S.; Chance, R. E.; Flora, D. B.; Cox, A. L.; Irwin, L.; Myers, S. R.; *Nature Biotechnology*, **20**, 2002, 800.
- Brammer, L.; Bruton, E. A.; Sherwood, P.; *Cryst. Growth & Des.*, **1**, 2001, 277.
- Brown, R. F. C.; Radom, L.; Sternhell, S.; Rae, I. D.; *Can. J. Chem.*, **46**, 1968, 2577.
- Bruker SAINT+. Version 6.02 (includes XPREP and SADABS), 1999, Bruker AXS Inc., Madison, Wisconsin, USA.

C

- Camilleri, P.; Kirby, A. J.; Lewis, R.; Sanders, J. K. M.; *Chem. Comm.*, 1988, 1537.
- Caira, M. R.; Robbertse, Y.; Bergh, J. J.; Song, M. N.; De Villiers, M. M.; *J. Pharm. Sci.*, **92**, 2003, 2519.

N-aryl -formamides and -thioamides

Choudhury, A. R.; Urs, U. K.; Guru Row, T. N.; Nagarajan, K.; *J. Mol. Struct.*, **605**, 2002, 71.

Childs, S. L.; Chyal, L. J.; Dunlap, J. T.; Smolenskaya, V. N.; Stahly, B. C.; Stahly, G. P.; *J. Am. Chem. Soc.*, **126**, 2004, 13335.

Csöreg, I.; Brehmer, T.; Bombicz, P.; Weber, E.; *Crystal Engineering*, **4**, 2001, 343.

Crowley, K. J.; Zografi, G.; *J. Pharm. Sci.*, **91**, 2002, 492.

Czugler, M.; *CrystEngComm.*, **6**, 2004, 494.

D

Das, D.; Jetti, R. K. R.; Boese, R.; Desiraju, G. R.; *Cryst. Growth & Des.*, **3**, 2003, 675.

Day, G. M.; Motherwell, W. D. S.; Ammon, H. L.; Boerrigter, S. X. M.; Della Valle, R. G.; Venuti, E.; Dzyabchenko, A.; Dunitz, J. D.; Schweizer, B.; van Eijck, B. P.; Erk, P.; Facelli, J. C.; Bazterra, V. E.; Ferraro, M. B.; Hofmann, D. W. M.; Leusen, F. J. J.; Liang, C.; Pantelides, C. C.; Karamertzanis, P. G.; Price, S. L.; Lewis, T. C.; Nowell, H.; Torrisi, A.; Scheraga, H. A.; Arnautova, Y. A.; Schmidt, M. U.; Verwer, P.; *Acta. Cryst.*, **B61**, 2005, 511.

David, W. I. F.; Shankland, K.; McCusker, L. M.; *J. Appl. Cryst.* **36**, 2003, 169.

David, W. I. F.; Shankland, K.; Shankland, N.; *Chem. Comm.*, 1998, 931.

de Armas, H. N.; Peeters, O. M.; Blaton, N. M.; De Ranter, C. J.; Marill, L. X.; *Acta. Cryst.*, **C57**, 2001, 86.

Dey, A.; Desiraju, G. R.; *CrystEngComm.*, **8**, 2006, 477.

Dey, A.; Jetti, R. K. R.; Boese, R.; Desiraju, G. R.; *CrystEngComm.*, **5**, 2003, 248.

Dougill, M. W.; Jeffrey, G. A.; *Acta. Cryst.*, **6**, 1953, 831.

Desiraju, G. R.; *Angew. Chem. In. Ed. Engl.*, **34**, 1995, 2311.

Desiraju, G. R.; *Acc. Chem. Res.*, **35**, 2002, 565.

Desiraju, G. R.; *Acc. Chem. Res.*, **24**, 1991, 290.

Desiraju, G. R.; *Acc. Chem. Res.*, **29**, 1996, 441.

Desiraju, G. R.; Parthasarathy, R.; *J. Am. Chem. Soc.*, **111**, 1989, 8725.

Desiraju, G. R.; in *“Crystal Engineering: The Design of Organic Solids. Material Science Monographs”*. 54, Elsevier, Amsterdam, 1989.

Desiraju, G. R.; Sharma, C. V. K.; in *“The Crystal as a Supramolecular Entity”* (Ed.: G. R. Desiraju, Wiley, New York, 1996 Ch. 2, pp. 31261.

Desiraju, G. R.; Steiner, T.; in *“The Weak Hydrogen Bonds: In Structural Chemistry and Biology”* Oxford University Press, Oxford, New York, 1999.

N-aryl -formamides and -thioamides

Dickinson, J. A.; Hockridge, M. R.; Robertson, E. V.; Simons, J. P.; *J. Phys. Chem.*, **A103**, 1999, 6938.

Doerksen, R. J.; Chen, B.; Liu, D.; Tew, G. N.; DeGrado, W. F.; Klein, M. L., *Chem. Eur. J.*; **10**, 2004, 5008.

Drakenberg, T.; Forsén, S.; *J. Phys. Chem.*, **74**, 1970, 1.

Ducharme, Y.; Wuest, J. D.; *J. Org. Chem.*, **53**, 1988, 5787.

Dunitz, J. D.; *Acta. Cryst.*, **B51**, 1995, 619.

Dunitz, J. D.; Taylor, R.; *Chem. Eur. J.*, **3**, 1997, 89.

Dzuibek, K. F.; Katruziak, A.; *Z. Kristallogr.*, **219**, 2004, 1.

E

Edwards, M. R.; Jones, W.; Motherwell, W. D. S.; Shields, G. P.; *Mol. Cryst. Liq. Cryst.*, **356**, 2001, 337.

Etter, M. C.; *J. Chem.* **25**, 1985, 312.

Etter, M. C.; Baures, P. W., J.; *Am. Chem. Soc.*, **110**, 1988, 639.

Etter, M. C.; Panunto, T. W.; *J. Am. Chem. Soc.*, **110**, 1988, 5896.

Etter, M. C.; Reutzler, S. M.; *J. Am. Chem. Soc.*, **113**, 1991, 2586.

Etter, M. C.; Frankenbach.; *Chem. Mater.*, **1**, 1989, 10.

Etter, M. C.; *Acc. Chem. Res.*, **23**, 1990, 120.

Etter, M. C.; Urbaiiczek-Lipkowska, Z.; Jahn, D. A.; Frye, J. S.; *J. Am. Chem. Soc.*, **108**, 1986, 5871.

F

Fábián, L.; Kálmán, A., *Acta. Cryst.*; **B55**, 1999, 1099.

Fábián, L.; Kálmán, A., *Acta. Cryst.*; **B60**, 2004, 547.

Fábián, L.; Kálmán, A.; Argay, G.; *Acta. Cryst.*, **B49**, 1993, 1039.

Ferguson, G.; Low, J. N.; Penner, G. H.; Wardell, J. L.; *Acta. Cryst.*, **C54**, 1998, 1974.

Fernandes, M. A.; Levendis, D. C.; Schoening, F. R. L.; *Acta Cryst.*, **B60**, 2004, 300.

Filippini, G.; Gavezzotti, A., *Acta Cryst.*; **B49**, 1993, 868.

Florian, J.; Leszczynski, J.; Johnson, B.; *J. Mol. Struct.*, **349**, 1995, 421.

Florian, J.; Johnson, B. G.; *J. Phys. Chem.*, **99**, 1995, 5899.

Fogarasi, G.; Szalay, P. G.; *J. Phys. Chem. A*, **101**, 1997, 1400.

Frisch, M. J.; Trucks, G. W.; Schlegel, H. B.; Scuseria, G. E.; Robb, M. A.; Cheeseman, J. R.; Zakrzewski, V. G.; Montgomery, Jr., J. A.; Stratmann, R. E.; Burant, J. C.; Dapprich, S.; Millam, J. M.; Daniels, A. D.; Kudin, K. N.; Strain, M. C.; Farkas, O.; Tomasi, J.; Barone, V.; Cossi, M.; Cammi, R.; Mennucci, B.; Pomelli, C.; Adamo, C.; Clifford, S.; Ochterski, J.; Petersson, G. A.; Ayala, P. Y.; Cui, Q.; Morokuma, K.; Malick, D. K.; Rabuck, A. D.; Raghavachari, K.; Foresman, J. B.; Cioslowski, J.; Ortiz, J. V.; Stefanov, B. B.; Liu, G.; Liashenko, A.; Piskorz, P.; Komaromi, I.; Gomperts, R.; Martin, R. L.; Fox, D. J.; Keith, T.; Al-Laham, M. A.; Peng, C. Y.; Nanayakkara, A.; Gonzalez, C.; Challacombe, M.; Gill, P. M. W.; Johnson, B.; Chen, W.; Wong, M. W.; Andres, J. L.; Gonzalez, C.; Head-Gordon, M.; Replogle, E. S.; Pople, J. A., *Gaussian 98*, Revision A.7, Gaussian, Inc., Pittsburgh PA, 1998.

G

Gasparro, F. P.; Kolodny, N. H.; *J. Chem. Educ.*, **54**, 1977, 258.

Gavezzotti, A.; *J. Am. Chem. Soc.*, **105**, 1983, 5220.

Gavezzotti, A.; *J. Am. Chem. Soc.*, **107**, 1985, 962.

Gavezzotti, A.; Filippini, G.; *J. Phys. Chem.*, **98**, 1994, 4831.

Gavezzotti, A.; Filippini, G.; *J. Am. Chem. Soc.*, **117**, 2000, 12299.

Gavezzotti, A.; Filippini, G.; Kroon, J.; van Eijck, B. P.; Klewinghaus, P., *Chem. Eur. J.*, **3**, 1997, 893.

Gavezzotti, A.; *J. Phys. Chem. B.*, **106**, 2002, 4145.

Gavezzotti, A.; *J. Phys. Chem. B.*, **107**, 2003, 2344.

Gavezzotti, A.; *CrystEngComm*, **4**, 2002, 343.

Gavezzotti, A.; *CrystEngComm*, **5**, 2003, 429.

Gavezzotti, A.; *CrystEngComm*, **5**, 2003, 439.

Gavezzotti, A.; OPIX, *A computer program package for the calculation of intermolecular interactions and crystal energies*, University of Milano, 2003.

Glasstone, S.; *Trans. Faraday Soc.*, **33**, 1937, 200.

Gnanaguru, K.; Ramasubbu, N.; Venkatesan, K.; Ramamurthy, V.; *J. Org. Chem.*, **50**, 1985, 2337.

Gowda, B.T.; Paulus, H.; Fuess, H.; *Z. Naturforsch. A: Phys. Sci.*, **55**, 2000, 791.

Gonnade, G. R.; Bhadbhade, M. M.; Shashidhar, M. S.; Sanki, A. K.; *Chem. Comm.*, 2005, 5870.

Green, B. S.; Lahav, M.; Rabinovich, D.; *Acc. Chem. Res.*, **12**, 1979, 191.

Grell, J.; Bernstein, J.; Tinhofer, G.; *Acta Cryst.*, **B55**, 1999, 1030.

N-aryl -formamides and -thioamides

Grell, J.; Bernstein, J.; Tinhofer, G.; *Acta. Cryst.*, **B56**, 2000, 166.

Grossel, M. C.; Cheetham, A. K.; Hope, D. A. O.; Weston, S. C.; *J. Org. Chem.*, **58**, 1993, 6654.

Groke, D.; Heger, G.; Schweiss, P.; Weiss, A.; *Z. Kristallogr.*, **209**, 1994, 448.

Gu, Y.; Kar, T.; Scheiner, S.; *J. Am. Chem. Soc.*, **121**, 1999, 9411.

H

Hamilton, W. C.; Ibers, J. A.; in *"Hydrogen bonding in solids"*, W. A. Benjamin Inc.: New York, 1968, pp 19-21.

Hans, B.; Tran, T. H.; Slouki, B.; Schodel, H.; Artus, G.; Herdtweck, E.; Herrmann, W. A.; *Liebigs. Ann.*, 1996, 403.

Hanson, J. R.; Hitchcock, P. B.; Rodriguez-Medina, I. C.; *J. Chem. Res.*, 2004, 664.

Haisa, M.; Kashino, S.; Kawaii, R.; Maeda, H.; *Acta. Cryst.*, **B32**, 1976, 1283.

Haisa, M.; Kashino, S.; Maeda, H.; *Acta. Cryst.*, **B30**, 1974, 2510.

Haisa, M.; Kashino, S.; Ueno, T.; Shinozaki, N.; Matsuzaki, Y.; *Acta. Cryst.*, **B36**, 1980, 2306.

Haisa, M.; Kashino, S.; Matsuzaki, Y.; Hawaii, R.; Kunitomi, K.; *Acta Cryst.*, **B33**, 1977, 2449.

Hashizume, D.; Miki, N.; Yamazaki, T.; Aoyagi, Y.; Arisato, T.; Uchiyama, H.; Endo, T.; Yasuia, M.; Iwasaki, F.; *Acta Cryst.*, **B59**, 2003, 404.

Herbstein, E H.; *J. Mol. Struct.*, **374**, 1996, 111.

Ho, S. Y.; Lai, C. S.; Tiekink, E. R. T.; *Acta. Cryst.*, **E59**, 2003, o1155.

Hoeg-Jensen, T.; Olsen T. E.; Holm, A.; *J. Org. Chem.*, **59**, 1994, 1257.

Holden, J. R.; Du, Z.; Ammon, H. L.; *J. Comput. Chem.*, **14**, 1993, 422.

Hostettler, M.; Birkedal, H.; Gardon, M.; Chapuis, G.; Schwarzenbach, D.; Bonin, M.; *Acta. Cryst.*, **B55**, 1999, 448.

Hunter, C. A.; Sanders, J. K. M.; *J. Am. Chem. Soc.*, **112**, 1990, 5525.

J

Jeffrey, G. A.; Rubble, J. R.; McMullan, R. K.; DeFrees, J. D.; Pople, J. A.; *Acta Cryst.*, **B37**, 1981, 1885.

Jeffrey, G. A.; in *"An introduction to hydrogen bonding"*, New York: Oxford University Press, 1997.

***N*-aryl -formamides and -thioamides**

Jeffrey, G. A.; Saenger, W.; in *"Hydrogen Bonding in Biological Structures"*; Springer, Berlin, 1994.

Jiang, L.; Lai, L.; *J. Biol. Chem.*, **40**, 2002, 37732.

Johansson, A.; Kollman, P.; Rothenberg, S.; McKelvey, J.; *J. Am. Chem. Soc.*, **96**, 1974, 3794.

Jones, W.; Theocharis, C. R.; Thomas, J. M.; Desiraju, G. R.; *Chem. Comm.*, 1983, 1443.

Jones, W.; Ramdas, S.; Theocharis, C. R.; Thomas, J. M.; Thomas, N. W.; *J. Phys. Chem.*, **85**, 1981, 2594.

Johnson, S. W.; Eckert, J.; Barthes, M.; McMullan, R. K.; Muller, M.; *J. Phys. Chem.*, **99**, 1995, 16253.

Jorgensen, W. L.; Severance, D. L.; *J. Am. Chem. Soc.*, **112**, 1990, 4168.

Juranić, N.; Macura, S.; Prendergast, F. G.; *Protein Science*, **12**, 2003, 2633.

K

Kálmán, A.; Párkányi, L.; Argay, Gy.; *Acta Cryst.*, **B49**, 1993, 1039.

Katrusiak, A.; *Acta Cryst.*, **B56**, 2000, 872.

Kaftory, M.; Botoshansky, M.; Shteiman, V.; *Acta. Cryst.*, **B57**, 2001, 791.

Kessler, H.; *Angew. Chem. Int. Ed.*, **9**, 1970, 219.

Keller, E. *SCHAKAL92, A Program for the Graphic Representation of Molecular and Crystallographic Models*, University of Freiburg, 1993.

Kitaigorodskii, A. I.; in *"Molecular Crystals and Molecules"*, Academic Press: London, 1973.

Kobko, N.; Danneberg, J. J.; *J. Phys. Chem.*, **107**, 2003, 6688.

Kubicki, M.; *Acta Cryst.*, **B60**, 2004, 333.

Kuleshova, L. N.; Zorkii, P. M.; *Acta. Cryst.*, **B36**, 1980, 2113.

L

LaPlanche, L. A.; Rogers, M. T.; *J. Amer. Chem. Soc.*, **86**, 1964, 337.

Lauvergat, D.; Hiberty, P. C.; *J. Am. Chem. Soc.*, **119**, 1997, 9487.

Lee, K. M.; Chang, H-C.; Jiang, J-C.; Chen, J. C. C.; Kao, H-E.; Lin, S. H.; Lin, I. J. B.; *J. Am. Chem. Soc.*, **125**, 2003, 12358.

Leiserowitz, L.; Tuval, M.; *Acta. Cryst.*, **B34**, 1978, 1230-1245.

N-aryl -formamides and -thioamides

- Leiserowitz, L.; Schmidt, G. M. J.; *Acta. Cryst.*, **18**, 1965, 1058.
- Leiserowitz, L.; Hagler, A. T.; *Proc. R. Soc. London*, **A388**, 1983, 133.
- Leser, J.; Rabinovich, D.; *Acta. Cryst.*, **B34**, 1978, 2272.
- Lieberman, H. F.; Davey, R. J.; Newsham, D. M. T.; *Chem. Mater.*, **12**, 2000, 490.
- Linden, A.; Gündüs, M. G.; Şimşek, R.; Şafak, C.; *Acta. Cryst.*, **C62**, 2006, o227.
- Lommerse, J. P. M.; Stone, A. J.; Taylor, R.; Allen, F. H.; *J. Am. Chem. Soc.*, **118**, 1996, 3108.
- Lommerse, J. P. M.; Motherwell, W. D. S.; Ammon, H. L.; Dunitz, J. D.; Gavezzotti, A.; Schweitzer, B.; van Eijck, Hofmann, D. W. M.; Leusen, F. J. J.; Mooij, W. T. M.; Price, S. L.; Schmidt, M. U.; Verwer, P.; Williams, D. E.; *Acta. Cryst.*, **B56**, 2002, 697.

M

- Madhavi, N. N. L.; Katz, A. M.; Carrell, H. L.; Nangia, A.; Desiraju, G. R.; *Chem. Comm.*, 1997, 1953.
- Maeda, H.; Kamijo, N.; Fukui, K.; *Cryst. Struct. Commun.*, **5**, 1976, 129.
- Manea, V. P.; Wilson, K. J.; Cable, J. R.; *J. Am. Chem. Soc.*, **119**, 1997, 2033.
- Mahalakshmi, L.; Upadhyaya, V.; Guru Row, T. N.; *Acta Cryst.*, **E58**, 2002, o946.
- Maierov, V. N.; Crispen, G. M.; *J. Mol. Biol.*, **235**, 1994, 625.
- McGregor, P. A.; Allan, D. R.; Parsons, S.; Pulham, C. R.; *J. Pharm. Sci.*, **91**, 2002, 1308.
- McCrone, W. C.; in "Polymorphism in Physics and Chemistry of the Organic Solid State" Eds. D. Fox, M. M. Labes, A. Weissenberg, Interscience: New York, 1965; vol. II, 726.
- Milner-White, E. J.; *Protein Sci.*, **6**, 1997, 2477.
- Minton, J.; Jani, Y.; Grosso, A.; *Pharm. J.*, **273**, 2004, 422.
- Moisan, S.; Dannenberg, J. J.; *J. Phys. Chem. B.*, **107**, 2003, 12842.
- Moulton, B.; Zaworotko, M. J.; *Chem. Rev.*, **101**, 2001, 1629.
- Motherwell, W. D. S.; Ammon, H. L.; Dunitz, J. D.; Dzyabchenko, A.; Erk, P.; Gavezzotti, A.; Hofmann, D. W. M.; Leusen, F. J. J.; Lommerse, J. P. M.; Mooij, W. T. M.; Price, S. L.; Scheraga, H. A.; Schweizer, B.; Schmidt, M. U.; van Eijck, B. P.; Verwer, P.; Williams, D. E.; *Acta. Cryst.*, **B58**, 2002, 647.
- Murray, J. S.; Paulsen, K.; Politzer, P.; *Proc. Indian Acad. Sci. (Chem. Sci.)*, **118**, 1994, 3108.

N

- Navon, O.; Bernstein, J.; Khodorkovsky, V.; *Angew. Chem. Int. Ed. Engl.*, **36**, 1997, 601.
- Nagarajan, V.; Paulus, H.; Weiden, N.; Weiss, A.; *J. Chem. Soc., Faraday Trans. 2*, **82**, 1986, 1499.
- Nassimbeni, L. R.; Weber, H. S. E.; Skobridis, K.; *Cryst. Growth & Des.*, **4**, 2004, 85.
- Neuheuser, T.; Hess, B. A.; Reutel, C.; Weber, R.; *J. Phys. Chem.*, **98**, 1994, 6459.
- Neumann, Jr. R. C.; Jones, V.; *J. Am. Chem. Soc.*, **90**, 1968.
- Nicholas, G.; Frampton, C. S.; *J. Pharm. Sci.*, **87**, 1998, 684.
- Nishio, M.; *CrystEngComm*, **6**, 2004, 130.
- Nishio, M.; Umezawa, Y.; Hirota, M.; Takeuchi, Y.; *Tetrahedron*, **51**, 1995, 8701.
- Novoa, J. J.; Whangbo, M.-H.; *J. Am. Chem. Soc.*, **113**, 1991, 9017.
- Nyburg, S. C.; Fawcett, J. K.; Szymanski, J. T.; *Acta Cryst.*, **C43**, 1987, 2452.

O

- Oberlander, E. A.; Tebby, J. C.; *ARKIVOC*, **1**, 2000, 340.
- Omondi, B.; Fernandes, M. A.; Layh, M.; Levendis, D. C.; Mkwizu, T.; Look, J.; *CrystEngComm.*, **7**, 2005, 690.
- Olenik, B.; Boese, R.; Sustmann, R.; *Cryst. Growth & Des.*, **3**, 2003, 175.
- Oshrit, N.; Bernstein, J.; Khodorkovsky, V.; *Angew. Chem. Int. Ed. Engl.*, **36**, 1997, 601.
- Oswald, L. D. H.; Allan, D. R.; McGregor, P. A.; Motherwell, W. D. S.; Parsons, S.; Pulham, C. R.; *Acta. Cryst.*, **B58**, 2002, 1057.
- Ottersen, T. J.; *J. Mol. Struct.*, **26**, 1975, 365.
- Ouvrard, C.; Le Questel, J.-Y.; Berthelot, M.; Laurence, C.; *Acta Cryst.*, **B59**, 2003 512.

P

- Palmer, R. A.; Puddle, N.; Lisgarten, J. N.; *Acta. Cryst.*, **C49**, 1993, 1777.
- Panunto, T. W.; Urbaiiczuk-Lipkowska, Z.; Johnson, R.; Etter, M. C.; *J. Am. Chem. Soc.*, **109**, 1987, 7786.

N-aryl -formamides and -thioamides

Pauling, L.; in *"The Nature of the Chemical Bond"*, New York: Cornell University Press, 1939.

Pauling L.; in *"The Nature of the Chemical Bond"*, 3rd ed.; Cornell University Press: Ithaca, 1960; p549.

Pedireddi, V. R.; Reddy, D. S.; Goud, B. S.; Craig, D. C.; Rae, A. D.; Desiraju, G. R.; *J. Chem. Soc. Perkin Trans. 2*, 1994, 2353.

Peters, D.; Peters, J.; *J. Mol. Struct.*, **68**, 1980, 255.

Petrov, K. A.; Andreev, L. N.; *Russ. Chem. Rev.*, **38**, 1969, 21.

Pliego, Jr. J. R.; Riveros, J. M.; *Phys. Chem. Chem. Phys.*, **4**, 2002, 1622.

Pimentel, G. C.; McClellan, A. L.; in *"The Hydrogen Bond"*, W. H. Freeman, San Francisco, 1960.

Portalone, G.; Colapietro, M.; *J. Chem. Cryst.*, **34**, 2004, 609.

Prasanna, M. D.; Guru Row, T.N.; *Cryst. Eng.*, **3**, 2000, 135.

Prasanna, M.D.; Guru, Row, T.N.; *J. Mol. Struct.*, **562**, 2001, 55.

Prasanna, M.D.; Guru, Row, T.N.; *J. Mol. Struct.*, **559**, 2001, 255.

Price, S. L.; *CrystEngComm.*, **61**, 2004, 344.

Price, S. L.; Stone, A. J.; Lucas, J.; Rowland, R. S.; Thornley, A. E.; *J. Am. Chem. Soc.* 1994, **116**, 4910.

Q

Quintanilla-Licea, R.; Colunga-Valladares, J. F.; Caballero-Quintero, A.; Rodríguez-Padilla, C.; Tamez-Guerra, R.; Gómez-Flores, R.; Waksman, N.; *Molecules*, **7**, 2002, 662.

Quiñonero, D.; Frontera, A.; Capó, M.; Ballester, P.; Suñer, G. A.; Garau, C.; Deyà, P. M.; *New J. Chem.*, **25**, 2001, 259.

R

Rahman, A.; van der Helm, D.; *Acta. Cryst.*, **B36**, 1980, 2444.

Ramamurthy, V.; Venkatesa, K.; *Chem. Rev.*, 1987, 433.

Ramasubbu, N.; Parthasarathy, R.; Murray-Rust, P.; *Aust. J. Chem.*, 1986, **39**, 4308.

Ramasubbu, N.; Parthasarathy, R.; Murray-Rust, P.; *J. Am. Chem. Soc.*, **108**, 1986, 4308.

N-aryl -formamides and -thioamides

Remenar, J. F.; Morissette, S. L.; Peterson, M. L.; Moulton, B.; MacPhee, J. M.; Guzmán, H. R.; Almarson, Ö.; *J. Am. Chem. Soc.*, **125**, 2003, 8456.

Roberts, D. S., US Patent 4 973 597, 6-7.

Rowland, R. S.; *Amer. Cryst. Assoc. Abstracts*, **23**, 1995, 63.

Rutherford, J. S.; *Acta. Chim. Hun.*, **134**, 1997, 395.

S

Saenger, W.; in *"Principles of Nucleic Acid Structure"*, Berlin: Springer, 1984.

Sakaki, S.; Kato, K.; Miyazaki, T.; Musashi, Y.; Ohkubo, K.; Ihara, H.; Hirayama, C.; *J. Chem. Soc., Faraday Trans.*, **89**, 1993, 659–664.

Sakurai, T.; Sundaralingam, M.; Jeffrey, G. A.; *Acta Cryst.*, **16**, 1963, 354.

Salazar, L.; Espada, M.; Sanz, D.; Claramunt, R. M.; Elguero, J.; Garcia-Granda, S.; Diaz, M. R.; Gomez-Beltran, F.; *J. Chem. Soc. Perkin. Trans 2*, 1993, 377.

Sarma, J. A. R. P.; Desiraju, G. R.; *J. Chem. Soc., Perkin Trans.*, **2**, 1985, 1905.

Scheiner, S.; Wang, L.; *Protein Sci.*, **115**, 1993, 1958.

Schmidt G. M. J.; *Pure Appl. Chem.*, **27**, 1971, 647.

Shankland, K.; David, W. I. F.; Csoka, T.; McBride, L.; *Int. J. Pharm.*, **165**, 1998, 117.

Shankland, N.; David, W. I. F.; Shankland, K.; Kennedy, A. R.; Frampton, C. S.; Florence, A. J.; *Chem. Comm.* 2001, 2204.

Shaw, A. J.; Gescher, A.; Mraz, J.; *Int. J. LeprOther Mycobact. Dis.*, **53**, 1985, 587.

Sheldrick, G. M.; *SADABS*, 1996, University of Göttingen, Germany.

Siddall, III, T. H.; Steart, W. E.; Marston, A. L.; *J. Phys. Chem.*, **72**, 1988, 2135.

Siddall, III, T. H.; Stewart, W. E.; Knight, F. D.; *J. Phys. Chem.*, **74**, 1970, 3580.

Sikorski, A.; Krzymiński, K.; Niziolek, A.; Błażejowski, J.; *Acta. Cryst.*, **C61**, 2005, o690.

Sponer, J.; Hobza, P.; *J. Phys. Chem. A*, **2000**, *104*, 4592.

Steiner, T.; *Cryst. Rev.*, **9**, 2003, 177.

Steiner, T.; *Chem. Commun.*, 1997, 727.

Steiner, T.; *Acta. Crst.* **C54**, 1998, 1121.

Steiner, T.; *Cryst. Rev.*, **6**, 1996, 1.

Steiner, T.; *Angew. Chem. Int. Ed.*, **41**, 2002, 48.

N-aryl -formamides and -thioamides

Steiner, T.; *J. Phys. Chem A*, **102**, 1998, 7041-7052.

Steiner, T.; Majerz, I.; Wilson, C. C.; *Angew, Chem., Int. Ed. Engl.*, **40**, 2001, 2651.

Steiner, T.; Starikov, B.; Amado, A. M.; Teixeira-Dias, J. J. C.; *J. Chem. Soc. Perkin. Trans.*, 1995, 1321.

Steiner, T.; Saenger, W.; *Acta, Cryst.*, **B34**, 1998, 450.

Stewart, W. E.; Siddall, T. H.; *Chem. Rev.*, **70**, 1970, 517.

Suhai, S.; *J. Phys. Chem.*, **100**, 1996, 3950.

Sutor, D. J.; *Nature*, **68**, 1962, 195.

Sutor, D. J.; *J. Chem. Soc.*, 1963, 1105.

T

Takagi, T.; Tanaka, A.; Matsuo, S.; Maezaki, H.; Tani, M.; Fujiwara, H.; Sasaki, Y.; *J. Chem. Soc., Perkin Trans. 2*, 1987, 1015.

Takahashi, H.; Umezawa, Y.; Tsuboyama, S.; Uzawa, J.; Nishio, M.; *Tetrahedron*, **55**, 1999, 10047.

Tam, C. N.; Cowan, J. A.; Schultz, A. J.; Young, Jr. V. G.; Trouw, F. R.; Sykes, A. G.; *J. Phys. Chem.*, **B107**, 2003, 7601.

Tan, T. F.; Han, J.; Pang, M. L.; Song, H. B.; Ma, Y. X.; Meng, J. B.; *Cryst. Growth Des.*, **6**, 2006, 1186.

Taylor, R.; Kennard, O.; *J. Am. Chem. Soc.*, **104**, 1982, 5063.

Taylor, R.; Kennard, O.; Versichel, W.; *Acta Cryst.*, **B39**, 1983, 133.

Taylor, R.; Kennard, O.; Versichel, W.; *J. Am Chem. Soc.*, **105**, 1983, 5761.

Taylor, R.; Kennard, O.; Versichel, W.; *J. Am Chem. Soc.*, **106**, 1984, 244.

Taylor, R.; Kennard, O.; Versichel, W.; *Acta Cryst.*, **B40**, 1984, 280.

Thallapally P. K. And A. Nangia, *CrystEngComm.*, **27**, 2001, 248.

Theocharis, C. R.; Desiraju, G. R.; Jones, W.; *J. Am. Chem. Soc.*, **106**, 1984, 3606.

Trask, A. V.; Motherwell, W. D. S.; Jones, W.; *Chem. Commun.*, 2004, 890.

Trask, A. V.; Shan, N.; Motherwell, W. D. S.; Jones, W.; Feng, S.; Tan, R. B. H.; Carpenter, K. J.; *Chem Commun.*, 2005, 880.

Truter, M. R.; *Acta. Cryst.*, **22**, 1967, 556.

N-aryl -formamides and -thioamides

Tsiaousis, D.; Munn, R. W.; Smith, P. J.; Popelier, P. L. A.; *Chemical Physics*, **305**, 2004, 317.

U

Ugi I.; Fetzer U.; Ehozer U.; Knuffer H.; Offermason K.; *Angew Chemie. Int. Ed.*, **4**, 1965, 472.

Upadhyaya, V.; Mahalakshmi, L.; Row, T.N.G.; *Acta Cryst.*, **E58**, 2002, o997.

Usman, A.; Abdul, I.; Satar, S.; Kadir, M. A.; Yamin, B. M.; Fun, H.; *Acta. Cryst.*, **E58**, 2002, o656.

V

van de Streek, J.; Motherwell, W. D. S.; *J. Appl. Cryst.*, **38**, 2005, 694.

Vangala, V. R.; Nangia, A.; Lynch, V. M.; *Chem. Comm.*, 2002, 1304.

Vargas, R.; Garza, J.; Friesner, R. A.; Stern, H.; Hay, B. P.; Dixon, D. A.; *J. Phys. Chem A*, **105**, 2001, 4963.

Venkataramaiah, T. H.; Plapp, B. R.; *J. Biol. Chem.*, **278**, 2003, 36699.

Venkataramanan, B.; Saifudin, M-A.; Jagadise, V. J.; Suresh, V.; *CrystEngComm.*, **6**, 2004, 284-289.

Verwer, P.; Leusen, F. J. J.; *Rev. Comput. Chem.* **12**, 1998, 327.

Vishweshwar, P.; Nangia, A.; Lynch, V. M.; *Chem. Comm.*, 2001, 179.

W

Walsh, R. D. B.; Bradner, M. W.; Fleischman, S.; Morales, L. A.; Moulton, B.; Rodríguez-Hornedo, N.; Zaworotko, M. J.; *Chem. Commun.*, 2003, 186.

Wasserman, H. J.; Ryan, R. R.; Layne, S. P.; *Acta Cryst.*, **C41**, 1985, 783.

Watson, J. D.; Crick, F. H. C.; *Nature*, **171**, 1953, 737.

Weissbuch, I.; Popovitz-biro, R.; Lahav, M.; Leiserowitz, L.; *Acta Cryst.*, **B51**, 1995, 115.

Wells, A. F.; in *"Structural Inorganic Chemistry"*; Clarendon Press: Oxford, 1962, pp 294-315.

N-aryl -formamides and -thioamides

- Wiberg, K. B.; Rablen, P. R.; *J. Am. Chem. Soc.*, **117**, 1995, 2201.
- Wiberg, K. B.; Breneman, C. M.; *J. Am. Chem. Soc.*, **114**, 1992, 831.
- Wiberg, K. B.; Laith, K. E.; *J. Am. Chem. Soc.*, **109**, 1987, 5935.
- Wiberg, K. B.; Hadad, C. M.; Rablen, P. R.; Cioslowski, J.; *J. Am. Chem. Soc.*, **114**, 1992, 8644.
- Williams, D. E.; Houpt, D. J.; *Acta. Cryst.*, **B42**, 1986, 286.
- Willock, D. J.; Price, S. L.; Leslie, M.; Catlow, C. R. A.; *J. Comput. Chem.*, **16**, 1995, 628.
- Williams, D.E.; *PCK83, Quantum Chemistry Program Exchange Program no. 548, Indiana University, Bloomington, IN. (1983).*
- Williams, D. E.; *Acta Cryst.*, **A52**, 1996, 326.
- Williams, D. E.; *Acta Cryst.*, **A28**, 1972, 629.
- Williams, D. E.; *Acta Cryst.*, **A29**, 1973, 408.
- Williams, D. E.; *J. Comput. Chem.*, **7**, 1994, 719.
- Williams, D. E.; MPA/MPG, Molecular Packing Analysis & Molecular Packing Graphics. Chemistry Department, University of Louisville, Louisville, KY 40292, USA. (1996b).
- Williams, D. E.; PDM97, Potential-Derived Multipoles. Chemistry Department, University of Louisville, Louisville, KY 40292, USA. (1997).
- Wilson, C. C.; *Acta. Cryst.*, **B57**, 2001, 435.
- Wojcik, M. J.; Hirakawa, A. Y.; Tsuboi, M.; Kato, S.; Morokuma, K.; *Chem. Phys. Lett.*, **143**, 1988, 450.
- Young, R. A.; *The Rietveld Method*, International Union of Crystallography, Oxford University Press, Nueva York, 1993.

Z

- Zeller, M.; Wilcox, R. J.; Snyder III, R. J.; Seibel II, H. A.; Takas, N. J.; Hunter, A. D.; *J. Chem. Cryst.*, **35**, 2005, 723.

A1: Final refinement calculations for compounds 1a - 20.

Compound	1a	1b	2a	2b	3
Empirical formula	C ₇ H ₅ F ₂ N O	C ₇ H ₅ F ₂ N O	C ₇ H ₅ Cl ₂ N O	C ₇ H ₅ Cl ₂ N O	C ₉ H ₁₁ N O
Formula weight	157.12	157.12	190.04	190.02	149.2
Temperature (K)	293(2)	293(2)	293(2)	293(2)	293(2)
Radiation/ λ , (Å)	0.71073	0.71073	0.71073	0.71073	0.71073
Crystal system/space group	Orthorhombic/ <i>Pbca</i>	Monoclinic/ <i>P2₁</i>	Orthorhombic/ <i>Pbca</i>	Monoclinic/ <i>P2₁/n</i>	Orthorhombic/ <i>P2₁2₁2₁</i>
Unit cell dimensions					
a, (Å)	8.5031(15)	4.468(5)	8.6036(10)	4.3539(8)	4.5023(4)
b, (Å)	11.387(2)	8.486(5)	12.7431(15)	13.406(3)	8.5886(8)
c, (Å)	14.075(3)	8.881(5)	14.4016(16)	14.073(3)	21.297(2)
α, β, γ (°)	90, 90, 90	90, 100.698(5), 90	90, 90, 90	90, 92.616(4), 90	90, 90, 90
Volume (Å ³)	1578.9(3)	330.9(5)	1578.9(3)	820.5(3)	823.53(14)
Z	8	2	8	4	4
Density (Mg/m ³)	1.532	1.577	1.599	1.538	1.203
μ (mm ⁻¹)	0.140	0.144	0.756	0.727	0.079
<i>F</i> (000)	640	160	768	384	320
Approx. crystal size (mm)	0.50 x 0.16 x 0.10	0.35 x 0.09 x 0.04	0.50 x 0.30 x 0.20	0.83 x 0.47 x 0.40	0.48 x 0.36 x 0.36
Theta range for data collection (°)	2.89 to 28.32	2.33 to 28.00	2.83 to 28.00	2.10 to 28.30	1.91 to 25.50
Index ranges, <i>h, k, l</i>	-10/11, -11/15, -18/18	-5/5, -11/11, -11/11	-11/11, -16/15, -19/16	-5/5, -17/17, -18/14	-5/5, -8/10, -25/24
Reflections collected	8554	8166	10023	5389	6763
Independent reflections	1689 [R(int) = 0.0391]	843 [R(int) = 0.0674]	1895 [R(int) = 0.0282]	2020 [R(int) = 0.0259]	943 [R(int) = 0.0238]
Completeness to theta = 28.30	99.50%	99.90%	99.50%	99.10%	99.80%
Absorption correction	none	none	Semi empirical from equiv.	Semi empirical from equiv.	none
Max. and Min. transmission	0.9761 and 0.9332	0.9943 and 0.9512	0.8635 and 0.7037	0.7597 and 0.5836	0.9721 and 0.9631
Refinement method	Full matrix least sqs. on <i>F</i> ²	Full matrix least sqs. on <i>F</i> ²	Full matrix least sqs. on <i>F</i> ²	Full matrix least sqs. on <i>F</i> ²	Full matrix least sqs. on <i>F</i> ²
Data/restraints/parameters	1689 / 0 / 105	843 / 0 / 104	1895 / 0 / 104	2020 / 0 / 104	943 / 0 / 106
Goodness of fit on <i>F</i> ²	0.736	1.100	1.005	0.974	0.664
Final R indices [<i>I</i> >2sigma(<i>I</i>)]	R1 = 0.0388, wR2 = 0.1266	R1 = 0.0343, wR2 = 0.0708	R1 = 0.0423, wR2 = 0.0990	R1 = 0.0485, wR2 = 0.1443	R1 = 0.0310, wR2 = 0.1001
R indices all data	R1 = 0.0803, wR2 = 0.1733	R1 = 0.0481, wR2 = 0.0767	R1 = 0.0583, wR2 = 0.1070	R1 = 0.0646, wR2 = 0.1573	R1 = 0.0348, wR2 = 0.1074
Largest diff. peak and hole	0.181 and -0.119 e.Å ⁻³	0.223 and -0.242 e.Å ⁻³	0.286 and -0.615 e.Å ⁻³	0.336 and -0.440 e.Å ⁻³	0.109 and -0.111 e.Å ⁻³
Absolute structure parameter for 3		10(10)			

A2

Compound	4a	4b	5	6	7
Empirical formula	C ₈ H ₈ Cl N O	C ₈ H ₈ Cl N O	C ₇ H ₅ Br ₂ N O	C ₁₃ H ₁₉ N O	C ₉ H ₅ Cl ₂ N O
Formula weight	169.61	169.61	278.94	205.29	190.02
Temperature (K)	173(2)	173(2)	293(2)	293(2)	293(2)
Radiation/ λ , (Å)	0.71073	0.71073	0.71073	0.71073	0.71073
Crystal system/space group	Orthorhombic/ <i>Pbca</i>	Monoclinic/ <i>P2₁/a</i>	Orthorhombic/ <i>P2₁2₁2₁</i>	Monoclinic/ <i>P2₁/c</i>	Monoclinic/ <i>P2₁/n</i>
Unit cell dimensions					
a, (Å)	8.4446(2)	13.498(3)	4.315(10)	9.0343(14)	3.839(3)
b, (Å)	12.9028(3)	4.3186(10)	13.976(3)	8.8580(13)	27.90(2)
c, (Å)	14.4186(3)	14.938(3)	14.325(3)	16.001(2)	7.424(6)
α, β, γ (°)	90, 90, 90	90, 111.365(4), 90	90, 90, 90	90, 104.896(3), 90	90, 97.690(14), 90
Volume (Å ⁻³)	1571.04(6)	810.4(3)	864.0(3)	1237.5(3)	823.53(14)
Z	8	4	4	4	4
Density (Mg/m ³)	1.434	1.389	2.145	1.102	1.601
μ (mm ⁻¹)	0.421	0.408	9.323	0.069	0.757
<i>F</i> (000)	704	352	528	448	384
Approx. crystal size (mm)	0.35 x 0.32 x 0.20	0.60 x 0.24 x 0.08	0.56 x 0.08 x 0.08	0.40 x 0.26 x 0.20	0.36 x 0.20 x 0.10
Theta range for data collection (°)	2.83 to 27.99	1.46 to 28.00	2.04 to 28.00	2.63 to 26.00	1.46 to 25.54
Index ranges, <i>h, k, l</i>	-11/11, -17/15, -12/19	-15/17, -5/5, -18/19	-5/5, -15/18, -18/16	-11/9, -10/10, -19/19	-4/4, -33/31, -5/8
Reflections collected	11245	9940	5753	6779	3497
Independent reflections	1894 [R(int) = 0.0198]	1951 [R(int) = 0.0174]	2074 [R(int) = 0.0456]	2423 [R(int) = 0.0285]	1300 [R(int) = 0.0274]
Completeness to theta = 28.30	100.00%	99.4%	100.00%	99.8%	88.0%
Absorption correction	none	none	Semi empirical from equiv.	Semi empirical from equiv.	Multi-scan
Max. and Min. transmission	0.9205 and 0.8666	0.9681 and 0.7919	1.4326 and 0.9878	0.9863 and 0.9729	0.9281 and 0.7723
Refinement method	Full matrix least sqs. on F ²	Full matrix least sqs. on F ²	Full matrix least sqs. on F ²	Full matrix least sqs. on F ²	Full-matrix least sqs. on F ²
Data/restraints/parameters	1894 / 4 / 105	1951 / 31 / 123	2074 / 0 / 100	2423 / 0 / 146	1300 / 0 / 104
Goodness of fit on F ²	1.060	1.053	0.994	1.043	1.054
Final R indices [$>2\sigma(I)$]	R1 = 0.0405, wR2 = 0.1049	R1 = 0.0395, wR2 = 0.1021	R1 = 0.0418, wR2 = 0.0748	R1 = 0.0451, wR2 = 0.1079	R1 = 0.0492, wR2 = 0.1233
R indices all data	R1 = 0.0454, wR2 = 0.1086	R1 = 0.0506, wR2 = 0.1111	R1 = 0.0935, wR2 = 0.0875	R1 = 0.0777, wR2 = 0.1219	R1 = 0.0567, wR2 = 0.1268
Largest diff. peak and hole	0.378 and -0.633 e.Å ⁻³	0.265 and -0.210 e.Å ⁻³	0.415 and -0.382 e.Å ⁻³	0.144 and -0.133 e.Å ⁻³	0.346 and -0.270 e.Å ⁻³

Absolute structure parameter for 5

0.00(2)

A3

Compound	8	9	10	12	13
Empirical formula	C ₇ H ₅ Br ₂ N O	C ₇ H ₅ Cl ₂ N O	C ₇ H ₅ Br ₂ N O	C ₈ H ₈ Cl N O	C ₇ H ₅ Cl ₂ N O
Formula weight	278.94	190.02	278.94	169.60	190.02
Temperature (K)	293(2)	293(2)	293(2)	293(2)	293(2)
Radiation/ λ , (Å)	0.71073	0.71073	0.71073	0.71073	0.71073
Crystal system/space group	Monoclinic/ <i>P</i> 2 ₁ / <i>c</i>	Monoclinic/ <i>P</i> 2 ₁	Orthorhombic/ <i>P</i> 2 ₁ 2 ₁ 2 ₁	Monoclinic/ <i>P</i> 2 ₁ / <i>c</i>	Monoclinic/ <i>P</i> 2 ₁ / <i>c</i>
Unit cell dimensions					
a, (Å)	27.774(2)	3.9695(3)	4.0133(3)	6.0732(14)	9.489(3)
b, (Å)	4.0206(4)	8.6600(6)	7.0428(4)	4.6444(11)	12.393(4)
c, (Å)	15.0667(13)	11.3277(9)	28.895(3)	28.439(7)	6.705(2)
α, β, γ (°)	90, 98.313(5), 90	90, 91.151(6), 90	90, 90, 90	90, 93.905(4), 90	90, 100.721(7), 90
Volume (Å ³)	1664.8(3)	389.32(5)	816.70(10)	800.3(3)	774.7(5)
Z	8	2	4	4	4
Density (Mg/m ³)	2.226	1.621	2.269	1.408	1.629
μ (mm ⁻¹)	9.676	0.768	9.862	0.413	0.770
<i>F</i> (000)	1056	192	528	352	384
Approx. crystal size (mm)	0.50 x 0.07 x 0.05	0.64 x 0.36 x 0.08	0.26 x 0.18 x 0.10	0.36 x 0.10 x 0.06	0.26 x 0.24 x 0.07
Theta range for data collection (°)	0.74 to 28.00	1.80 to 28.27	1.41 to 28.00	1.44 to 28.00	2.18 to 27.99
Index ranges, <i>h, k, l</i>	-36/36, -2/5, -19/19	-5/5, -11/7, -14/14	-4/5, -9/9, -20/37	-5/8, -6/5, -37/36	-12/11, -16/16, -8/7
Reflections collected	7429	2533	3580	4730	5093
Independent reflections	3760 [R(int) = 0.0273]	1364 [R(int) = 0.079]	1753 [R(int) = 0.0253]	1987 [R(int) = 0.0500]	1857 [R(int) = 0.0293]
Completeness to theta = 28.30	93.3%	98.20%	93.9%	99.20%	99.1%
Absorption correction	Multi-scan	Multi-scan	none	none	Multi-scan
Max. and Min. transmission	0.6433 and 0.0855	0.9411 and 0.6392	0.4388 and 0.1836	0.9756 and 0.8654	0.9481 and 0.8249
Refinement method	Full matrix least sqs. on <i>F</i> ²	Full matrix least sqs. on <i>F</i> ²	Full matrix least sqs. on <i>F</i> ²	Full matrix least sqs. on <i>F</i> ²	Full matrix least sqs. on <i>F</i> ²
Data/restraints/parameters	3760 / 0 / 199	1364 / 1 / 100	1753 / 0 / 100	1897 / 0 / 105	1857 / 0 / 100
Goodness of fit on <i>F</i> ²	1.038	0.981	1.135	0.818	1.086
Final R indices [<i>I</i> >2sigma(<i>I</i>)]	R1 = 0.0386, wR2 = 0.0798	R1 = 0.0455, wR2 = 0.0627	R1 = 0.0415, wR2 = 0.0816	R1 = 0.0518, wR2 = 0.1304	R1 = 0.0838, wR2 = 0.2649
R indices all data	R1 = 0.0668, wR2 = 0.0889	R1 = 0.0477, wR2 = 0.1326	R1 = 0.0589, wR2 = 0.1016	R1 = 0.1152, wR2 = 0.1623	R1 = 0.1097, wR2 = 0.2815
Largest diff. peak and hole	0.388 and - 0.823 e.Å ⁻³	0.375 and - 0.246 e.Å ⁻³	0.585 and -0.804 e.Å ⁻³	0.257 and -0.255 e.Å ⁻³	0.987 and -0.394 e.Å ⁻³
Absolute structure parameter for 9 = -0.06(6) and for 10 = -0.04(4)					

A4

Compound	14	15	16	17	18
Empirical formula	C ₇ H ₅ Cl ₂ N O	C ₇ H ₅ F ₂ N S	C ₇ H ₅ Cl ₂ N S	C ₉ H ₁₁ N S	C ₈ H ₈ Cl N S
Formula weight	190.02	173.18	206.08	165.25	185.66
Temperature (K)	293(2)	173(2)	293(2)	293(2)	293(2)
Radiation/ λ , (Å)	0.71073	0.71073	0.71073	0.71073	0.71073
Crystal system/space group	Monoclinic/ <i>P2₁/n</i>	Orthorhombic/ <i>Pbca</i>	Monoclinic/ <i>P2₁/c</i>	Monoclinic/ <i>C2/c</i>	Monoclinic/ <i>C2/c</i>
Unit cell dimensions					
a, (Å)	7.371(2)	10.346(5)	7.873(2)	14.555(3)	14.367(5)
b, (Å)	14.787(5)	8.119(5)	15.643(4)	8.0597(16)	8.022(5)
c, (Å)	8.016(3)	17.883(5)	7.991(2)	16.133(3)	16.068(5)
α, β, γ (°)	90, 110.143(6), 90	90, 90, 90	90, 117.336(5), 90	90, 101.422(10), 90	90, 100.920(5), 90
Volume (Å ³)	820.3(5)	1502.2(12)	874.3(3)	1855.1(6)	1818.3(14)
Z	4	8	4	8	8
Density (Mg/m ³)	1.539	1.532	1.566	1.183	1.356
μ (mm ⁻¹)	0.727	0.393	0.911	0.285	0.584
<i>F</i> (000)	384	704	416	704	768
Approx. crystal size (mm)	0.44 x 0.20 x 0.18	0.38 x 0.24 x 0.14	0.30 x 0.18 x 0.14	0.47 x 0.20 x 0.06	0.47 x 0.20 x 0.06
Theta range for data collection (°)	2.76 to 26.99	2.28 to 27.99	2.60 to 25.99	2.58 to 28.30	2.58 to 28.27
Index ranges, <i>h, k, l</i>	-7/9, -18/15, -10/10	-13/13, -8/10, -20/23	-7/9, -18/19, -9/9	-19/11, -10/10, -20/21	-19/18, -10/10, -21/19
Reflections collected	4917	15097	5126	6342	15916
Independent reflections	1782 [R(int) = 0.0297]	1815 [R(int) = 0.0939]	1715 [R(int) = 0.0243]	2294 [R(int) = 0.0580]	2249 [R(int) = 0.0305]
Completeness to theta = 28.30	99.40%	100.00%	100.00%	99.7%	99.9%
Absorption correction	none	none	none	none	Semi-empirical from equiv
Max. and Min. transmission	0.8802 and 0.7402	0.9470 and 0.8650	0.8831 and 0.7717	0.9831 and 0.8775	0.9658 and 0.7710
Refinement method	Full matrix least sqs. on <i>F</i> ²	Full matrix least sqs. on <i>F</i> ²	Full matrix least sqs. on <i>F</i> ²	Full matrix least sqs. on <i>F</i> ²	Full matrix least sqs. on <i>F</i> ²
Data/restraints/parameters	1782 / 0 / 104	1815 / 0 / 104	1715 / 0 / 105	2294 / 0 / 105	2249 / 26 / 106
Goodness of fit on <i>F</i> ²	1.020	0.936	1.014	0.894	1.034
Final R indices [<i>I</i> > 2 σ (<i>I</i>)]	R1 = 0.0419, wR2 = 0.1033	R1 = 0.0410, wR2 = 0.1138	R1 = 0.0265, wR2 = 0.0643	R1 = 0.0475, wR2 = 0.1129	R1 = 0.0428, wR2 = 0.1195
R indices all data	R1 = 0.0781, wR2 = 0.1174	R1 = 0.0962, wR2 = 0.1422	R1 = 0.0404, wR2 = 0.0679	R1 = 0.1144, wR2 = 0.1321	R1 = 0.0539, wR2 = 0.1282
Largest diff. peak and hole	0.258 and -0.234 e.Å ⁻³	0.276 and -0.357 e.Å ⁻³	0.218 and -0.192 e.Å ⁻³	0.353 and -0.230 e.Å ⁻³	0.462 and -0.429 e.Å ⁻³

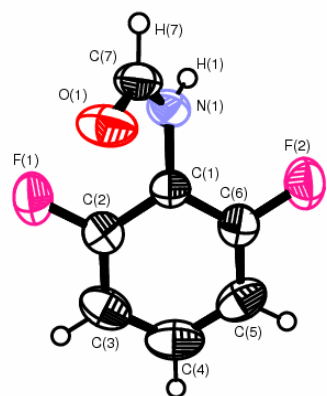
A5

Compound	19	20	21	22
Empirical formula	C ₇ H ₅ Br ₂ N S	C ₁₃ H ₁₉ N S	C ₇ H ₇ N O	C ₈ H ₈ Cl N O
Formula weight	295.00	221.35	121.14	169.61
Temperature (K)	293(2)	293(2)	173(2)	293(2)
Radiation/ λ , (Å)	0.71073	0.71073	0.71073	0.71073
Crystal system/space group	Monoclinic/ <i>P2₁/c</i>	Monoclinic/ <i>P2₁/c</i>	Monoclinic/ <i>C2/c</i>	Orthorhombic/ <i>Pbca</i>
Unit cell dimensions				
a, (Å)	7.9801(5)	9.023(5)	31.177(3)	8.5073(12)
b, (Å)	8.0314(5)	9.367(5)	6.1229(5)	13.093(2)
c, (Å)	14.5984(9)	16.269(5)	14.3335(12)	14.448(2)
α, β, γ (°)	90, 99.884(10), 90	90, 101.453(5), 90	90, 113.771(2), 90	90, 90, 90
Volume (Å ³)	921.74(10)	1347.7(11)	2504.1(4)	1609.3(4)
Z	4	4	16	8
Density (Mg/m ³)	2.126	1.091	1.285	1.400
μ (mm ⁻¹)	8.955	0.212	0.088	0.411
<i>F</i> (000)	560	480	1024	704
Approx. crystal size (mm)	0.38 x 0.20 x 0.04	0.36 x 0.14 x 0.12	0.53 x 0.20 x 0.14	0.23 x 0.18 x 0.08
Theta range for data collection (°)	2.59 to 28.34	2.30 to 28.00	1.43 to 28.17	2.82 to 25.00
Index ranges, <i>h, k, l</i>	-10/10, -10/10, -19/18	-10/11, -12/12, -21/17	-41/41, -6/8, -19/19	-3/10, -15/15, -16/17
Reflections collected	6720	8422	8010	7505
Independent reflections	2281 [R(int) = 0.0427]	3248 [R(int) = 0.1029]	3062 [R(int) = 0.0275]	1413[R(int) = 0.0418]
Completeness to theta = 28.30	99.3%	99.8%	99.9%	99.6%
Absorption correction	Semi empirical from equiv.	none	none	Semi empirical from equiv.
Max. and Min. transmission	0.7159 and 0.1320	0.9751 and 0.9277	0.9879 and 0.9551	0.9681 and 0.7918
Refinement method	Full matrix least sqs. on F ²	Full matrix least sqs. on F ²	Full matrix least sqs. on F ²	Full matrix least sqs. on F ²
Data/restraints/parameters	2281 / 0 / 104	3248 / 0 / 144	3062 / 0 / 163	1413 / 38 / 108
Goodness of fit on F ²	1.098	0.817	1.024	1.106
Final R indices [<i>I</i> >2sigma(<i>I</i>)]	R1 = 0.0462, wR2 = 0.1254	R1 = 0.0594, wR2 = 0.1602	R1 = 0.0421, wR2 = 0.1030	R1 = 0.0469, wR2 = 0.1108
R indices all data	R1 = 0.0683, wR2 = 0.1350	R1 = 0.1366, wR2 = 0.2141	R1 = 0.0708, wR2 = 0.1189	R1 = 0.0821, wR2 = 0.1318
Largest diff. peak and hole	1.128 and -0.505 e.Å ⁻³	0.238 and - 0.326 e.Å ⁻³	0.201 and -0.186 e.Å ⁻³	0.175 and -0.203 e.Å ⁻³

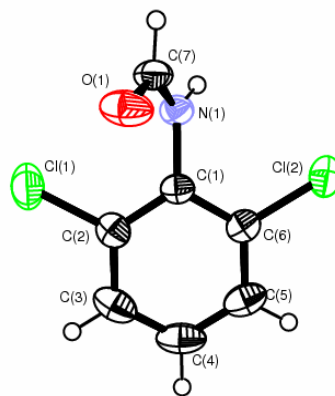
A6

Compound	23	24
Empirical formula	C ₉ H ₁₁ Cl ₂ N ₂ S ₂	C ₁₃ H ₁₉ N ₁ O ₁ S ₁
Formula weight	149.2	211.69
Temperature (K)	123(2)	173(2)
Radiation/ λ , (Å)	0.71073	0.71073
Crystal system/space group	Orthorhombic/ <i>Pbca</i>	Monoclinic/ <i>P2₁/c</i>
Unit cell dimensions		
a, (Å)	9.208(5)	9.022(5)
b, (Å)	13.142(5)	9.003(5)
c, (Å)	14.617(5)	16.005(5)
α, β, γ (°)	90, 90, 90	90, 103.170(5), 90
Volume (Å ³)	1768.8(13)	1768.8(13)
Z	8	4
Density (Mg/m ³)	2.120	1.111
μ (mm ⁻¹)	1.162	0.140
<i>F</i> (000)	1160	460.7
Approx. crystal size (mm)	0.37 x 0.17 x 0.14	0.43 x 0.18 x 0.14
Theta range for data collection (°)	2.79 to 27.98	2.32 to 28.35
Index ranges, <i>h, k, l</i>	-11/12, -17/17, -19/17	-8/11, -11/11, -21/20
Reflections collected	21156	15602
Independent reflections	2133 [R(int) = 0.0637]	3122 [R(int) = 0.0948]
Completeness to theta = 28.30	99.80%	99.20%
Absorption correction	none	none
Max. and Min. transmission	0.9721 and 0.9631	0.9443 and 0.8421
Refinement method	Full matrix least sqs. on F ²	Full matrix least sqs. on F ²
Data/restraints/parameters	2133 / 26 / 112	3122 / 4 / 145
Goodness of fit on F ²	0.951	1.033
Final R indices [<i>I</i> >2sigma(<i>I</i>)]	R1 = 0.0407, wR2 = 0.1202	R1 = 0.0522, wR2 = 0.1438
R indices all data	R1 = 0.0493, wR2 = 0.1272	R1 = 0.0943, wR2 = 0.1568
Largest diff. peak and hole	0.433 and -0.285 eÅ ⁻³	0.320 and -0.281 eÅ ⁻³

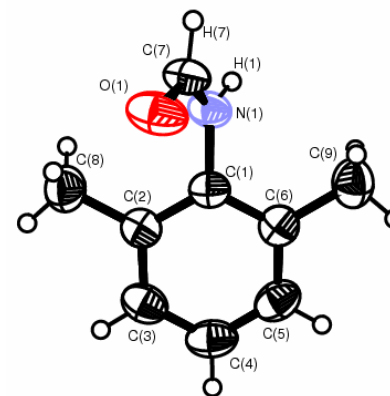
B1: ORTEP diagrams and crystal data for compounds 1 – 24.



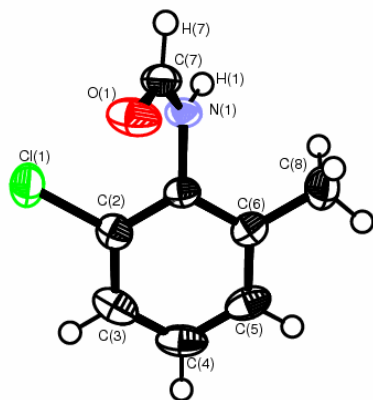
1a and 1b



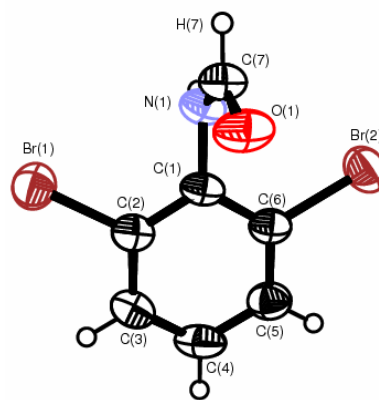
2a and 2b



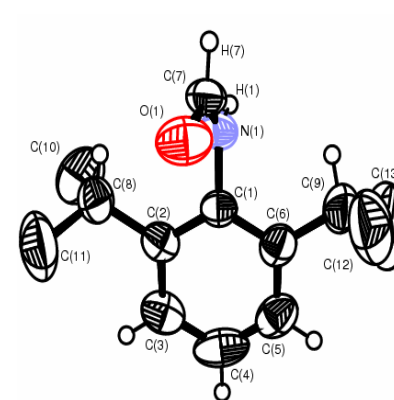
3



4a and 4b

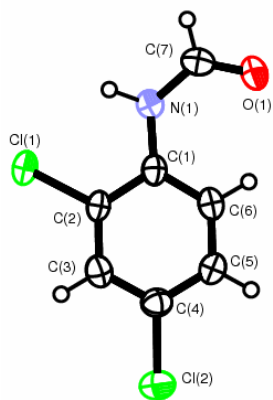


5

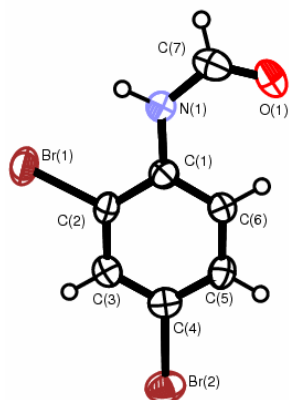


6

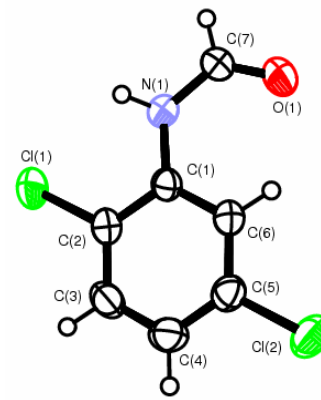
B2



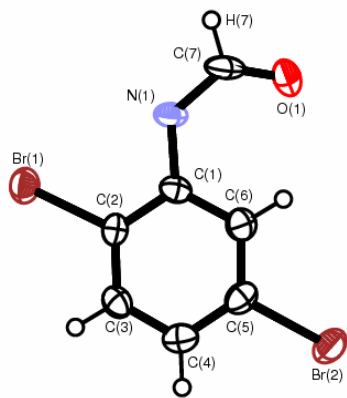
7



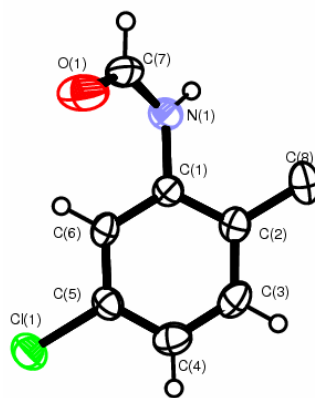
8



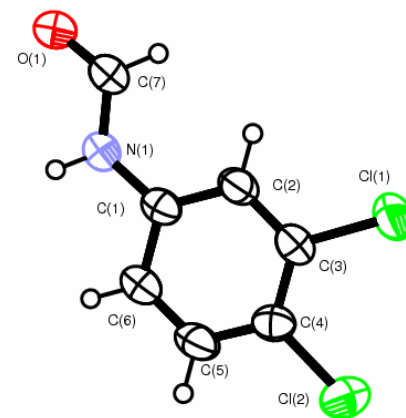
9



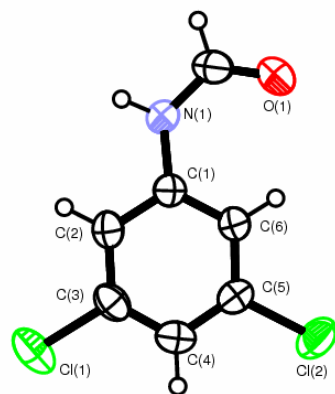
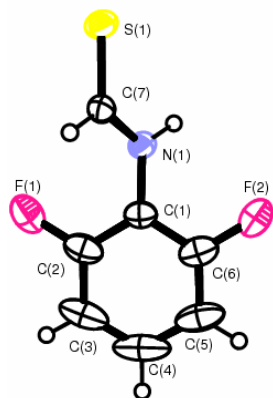
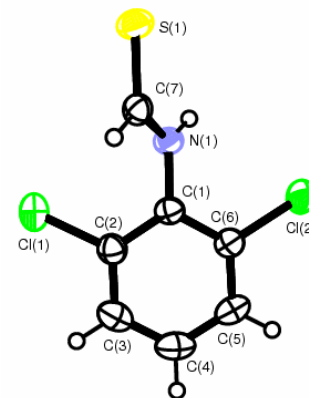
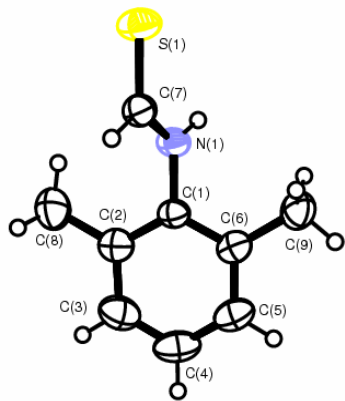
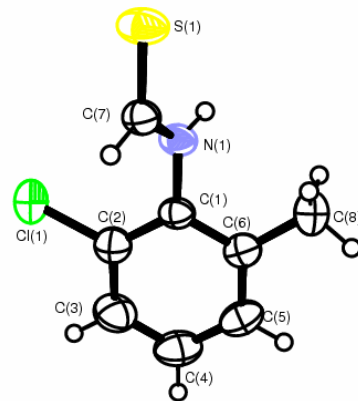
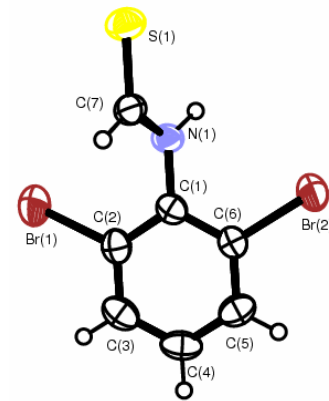
10

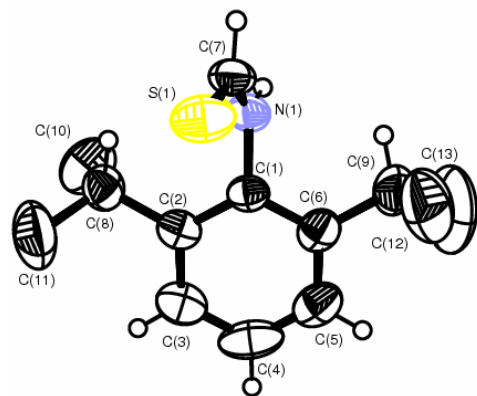


12

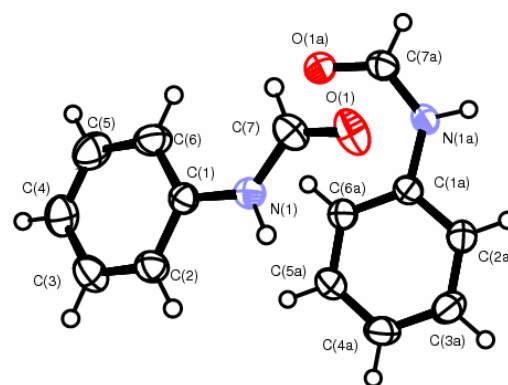


13

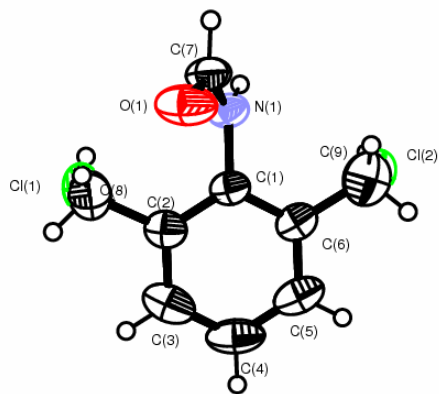
B3**14****15****16****17****18****19**



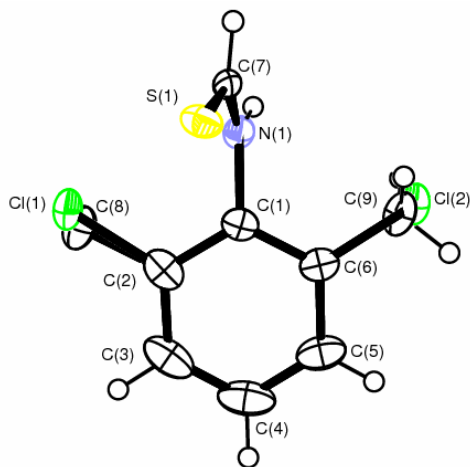
20



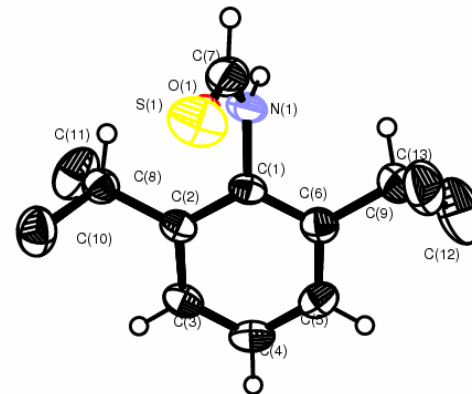
21



22

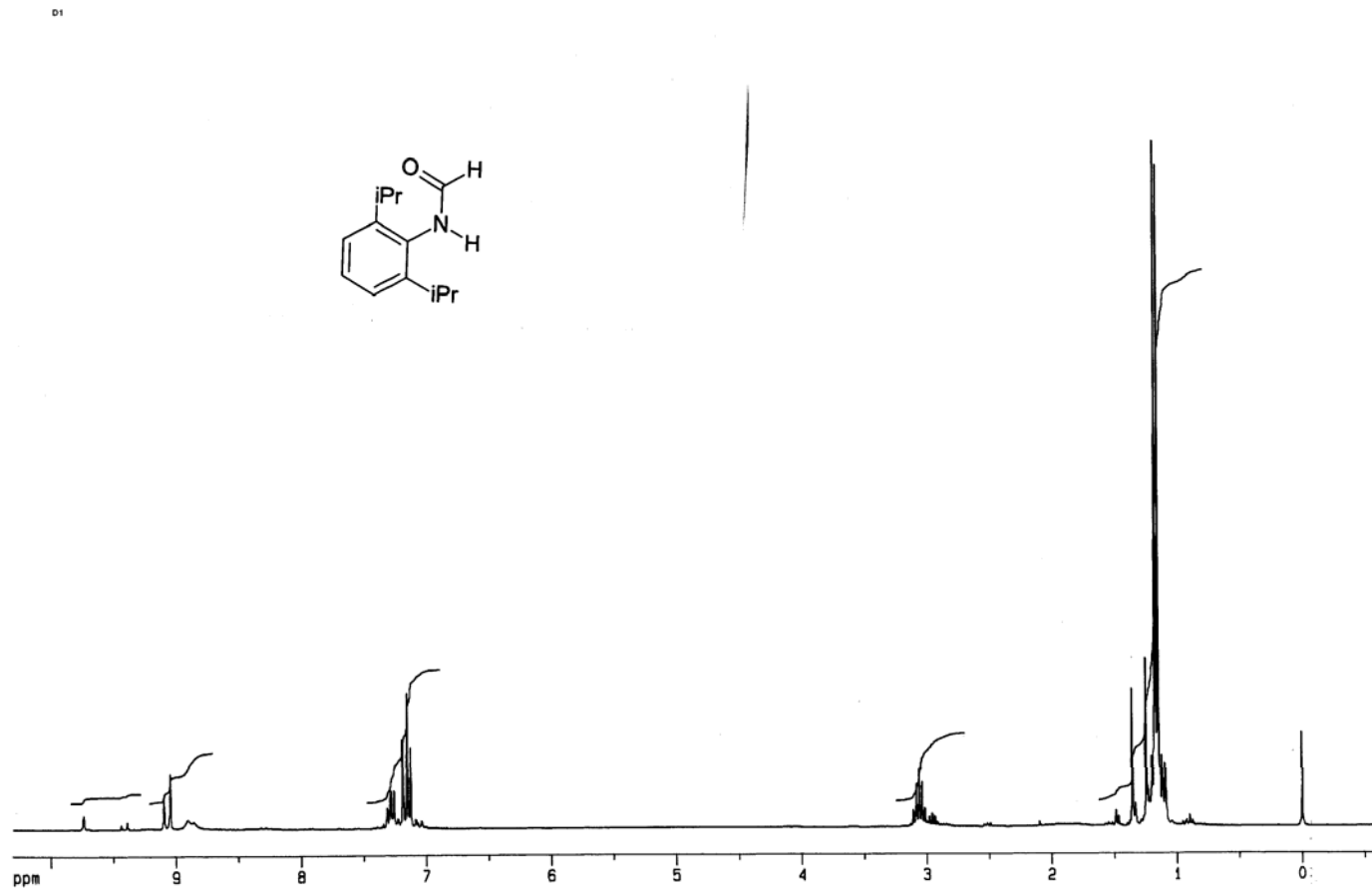


23

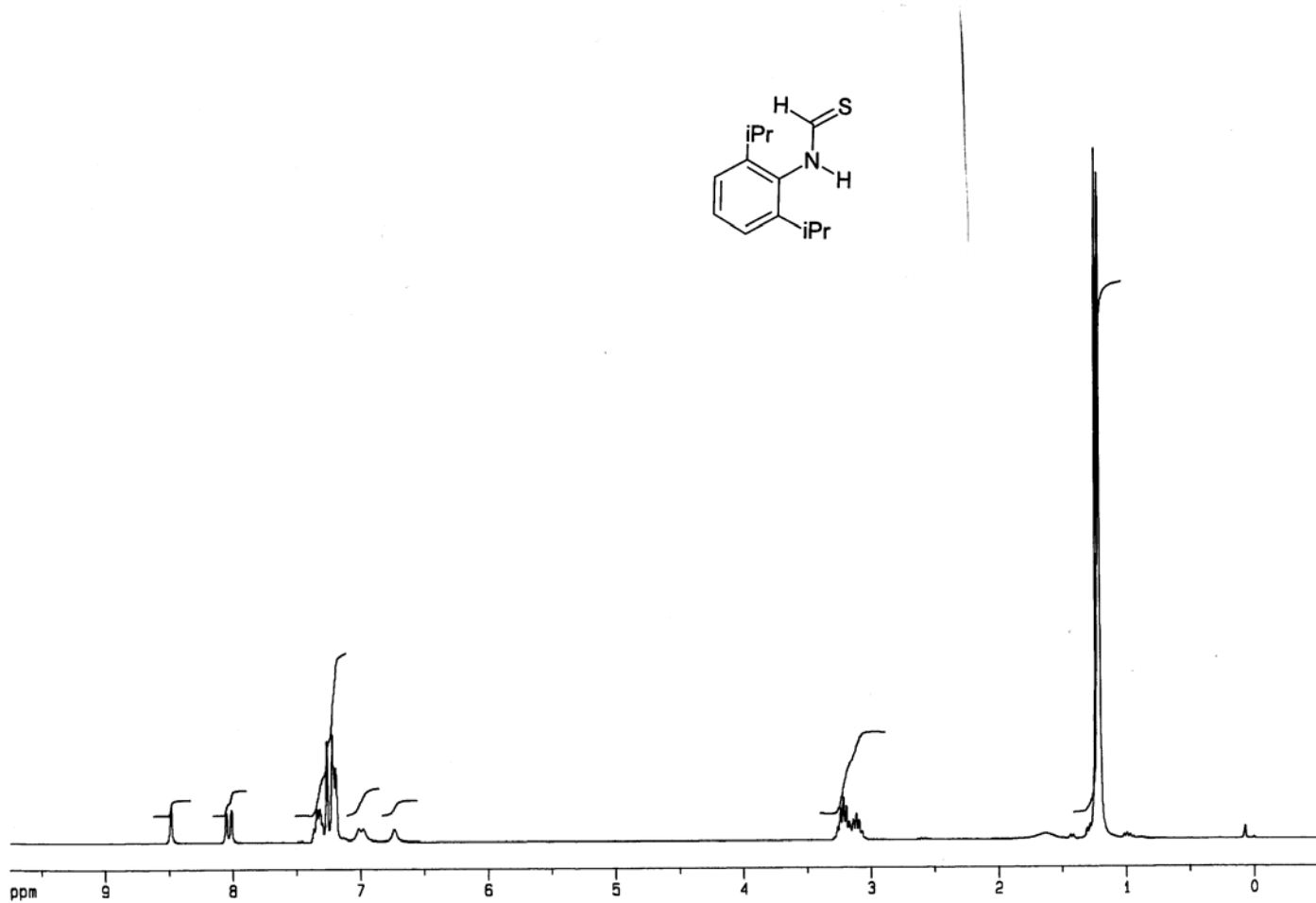
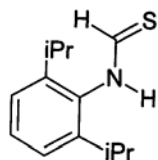


24

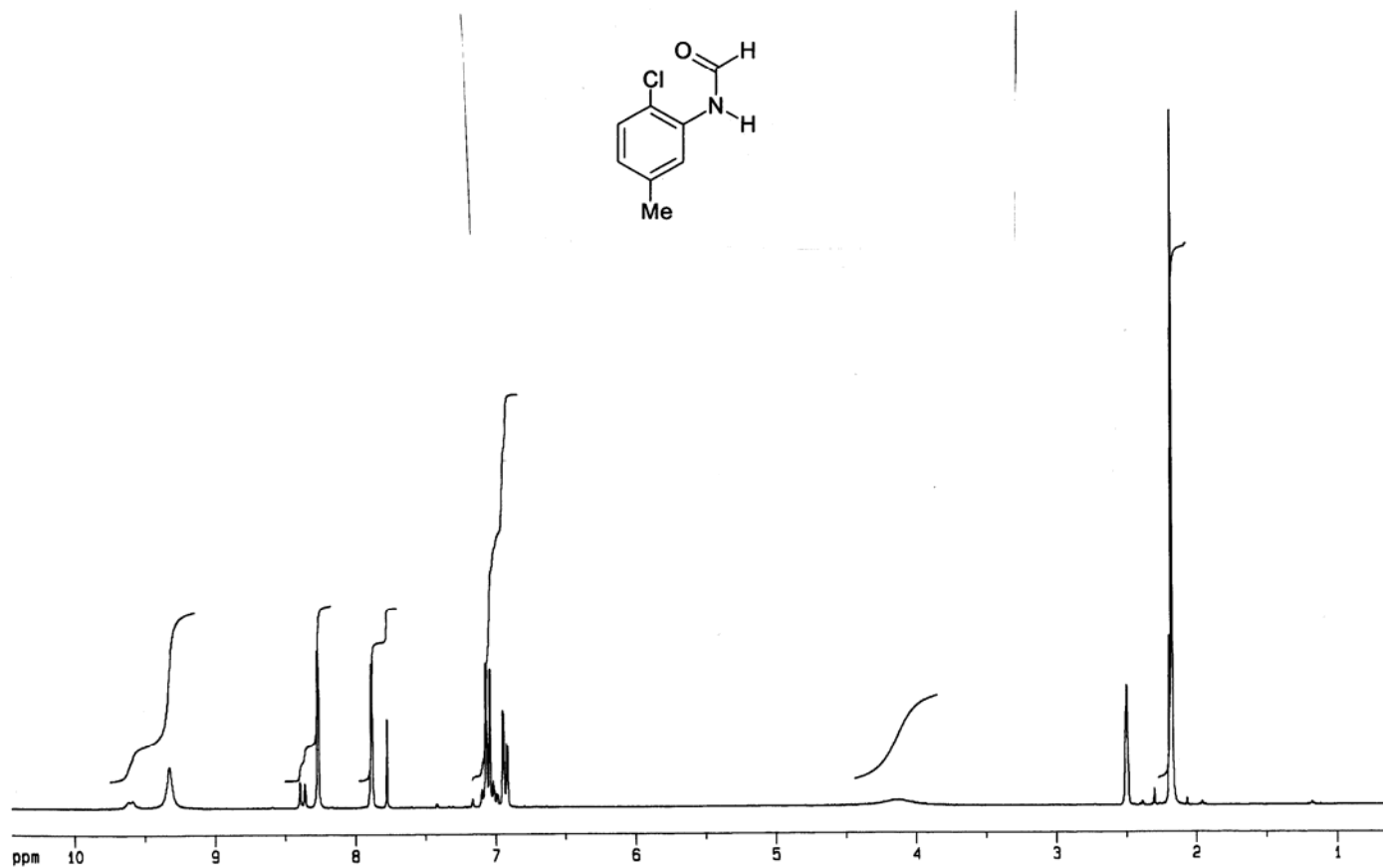
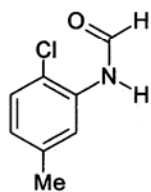
C1 NMR for 2,6-Diisopropylphenylformamide (6) in CDCl₃



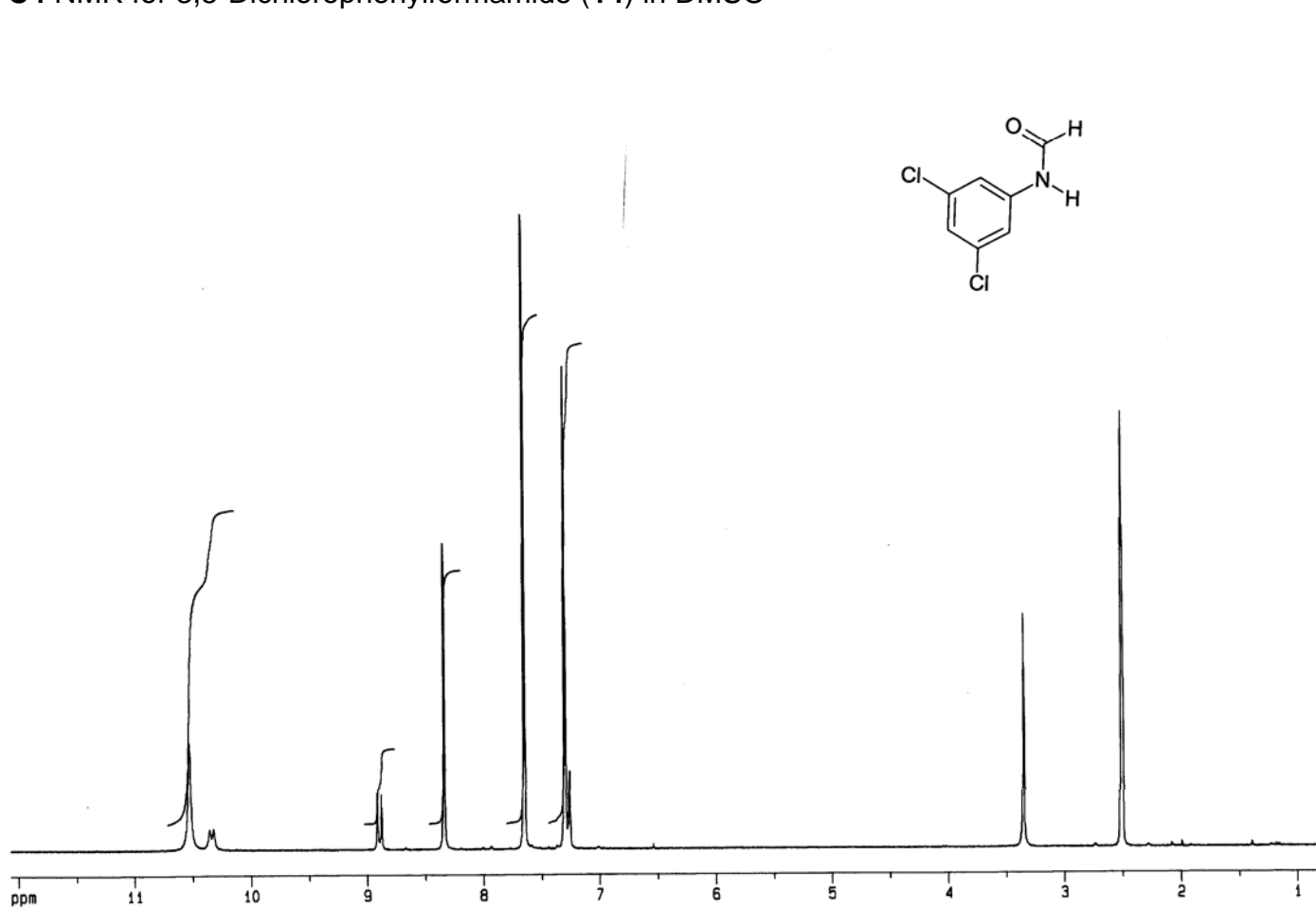
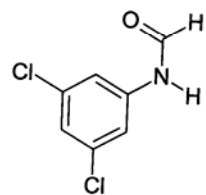
C2 NMR for 2,6-Diisopropylphenylthioamide (**20**) in CDCl₃



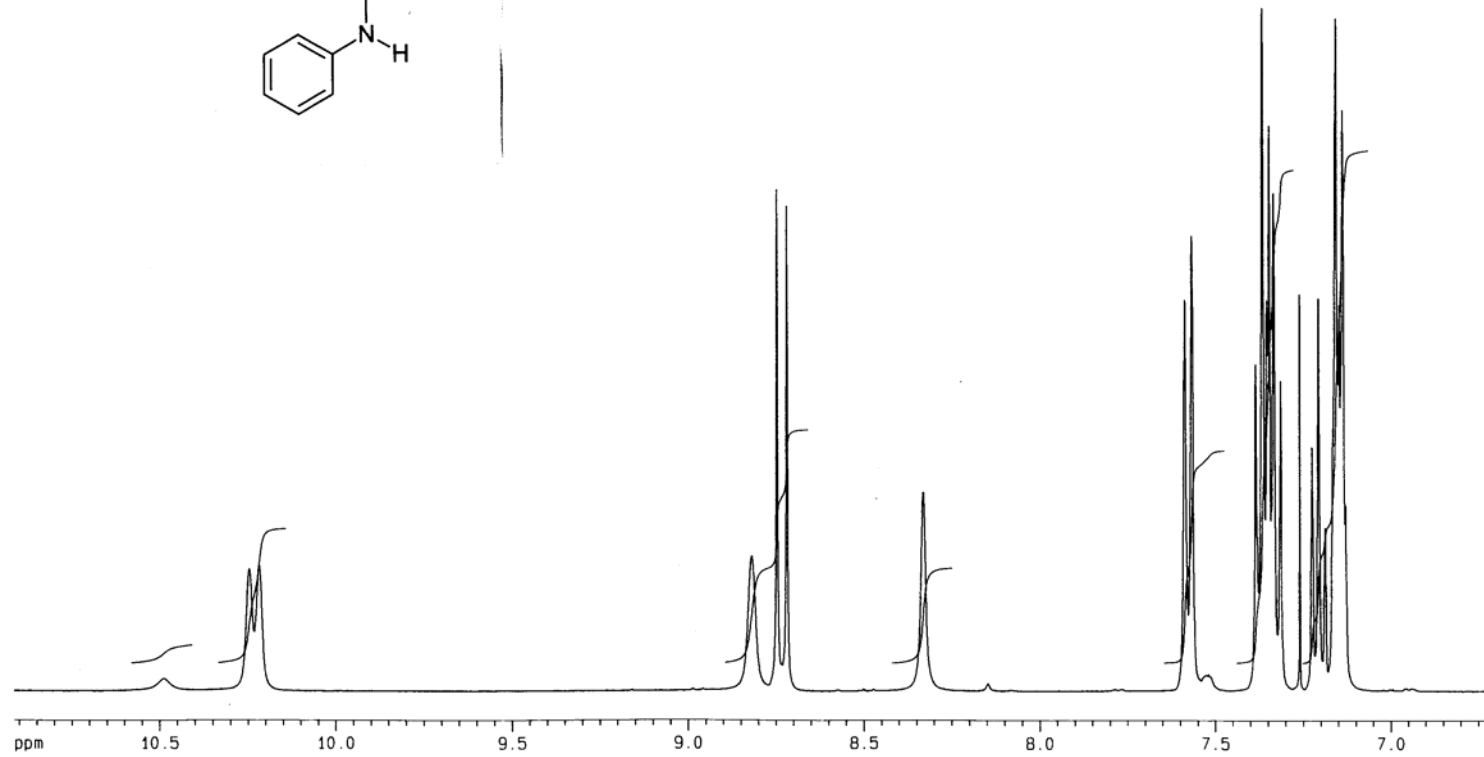
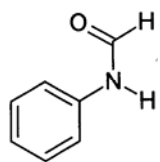
C3 NMR for 2-chloro-5-methylphenylformamide (12) in DMSO



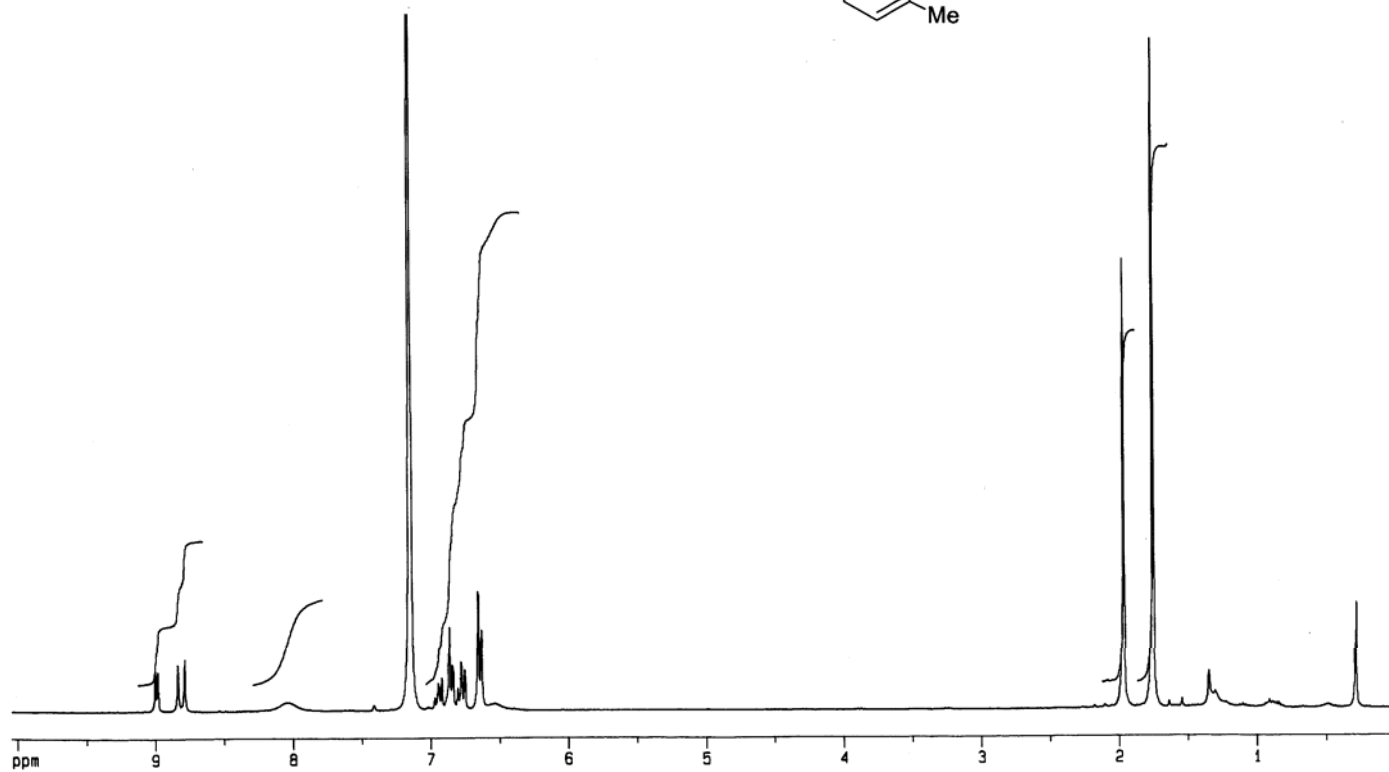
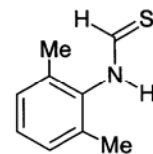
C4 NMR for 3,5-Dichlorophenylformamide (**14**) in DMSO



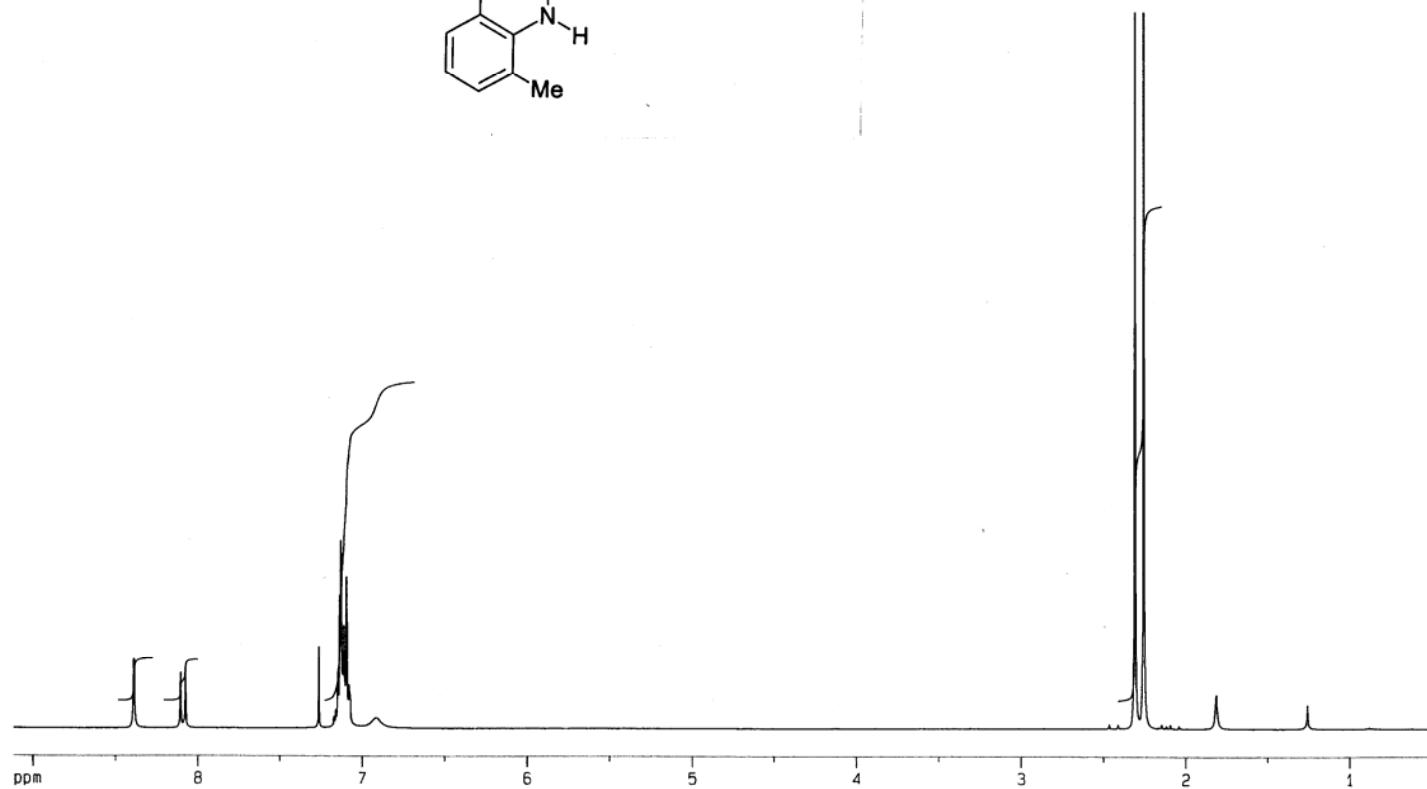
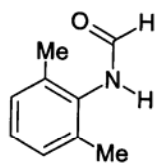
C5 NMR for Phenylformamide (**21**) in CDCl₃



C6 NMR for 2,6-Dimethylphenylthioamide (**3**) in C₆D₆



C7 NMR for 2,6-Dimethylphenylformamide (**3**) in C₆D₆



D1

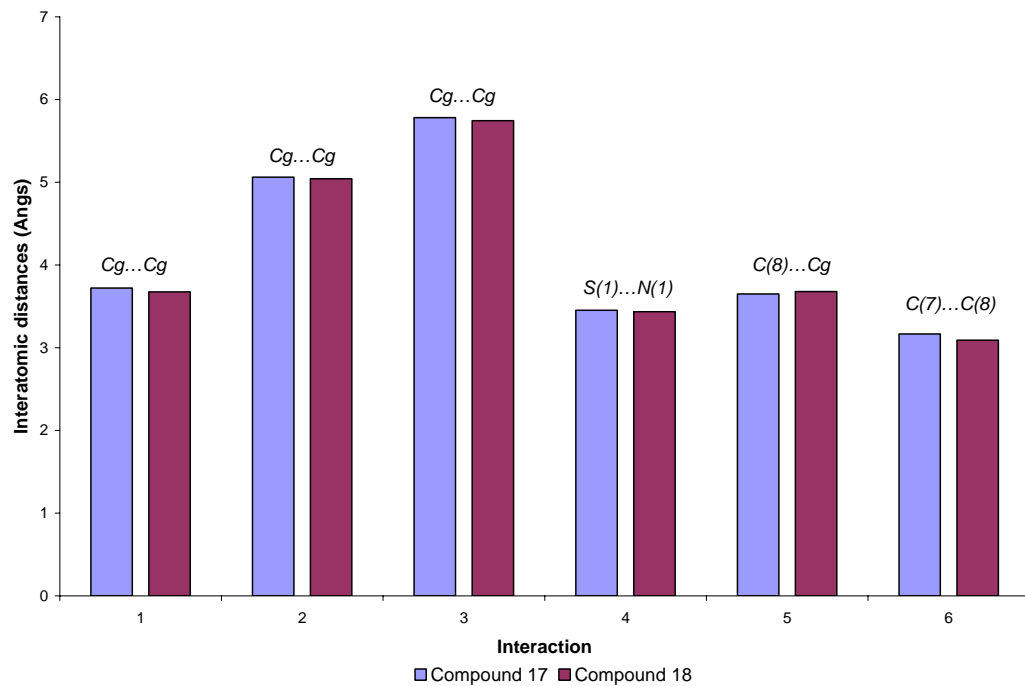
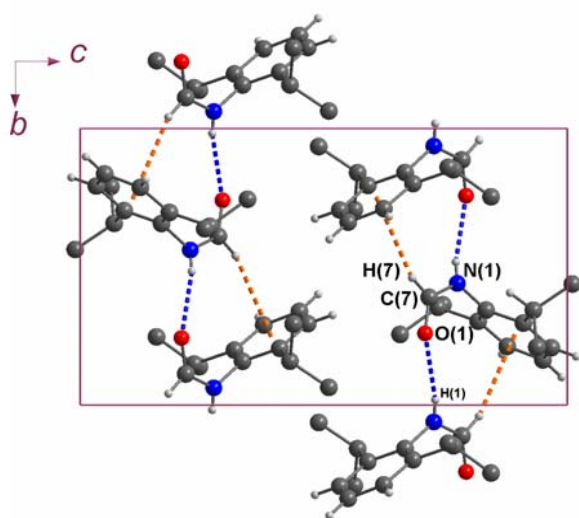
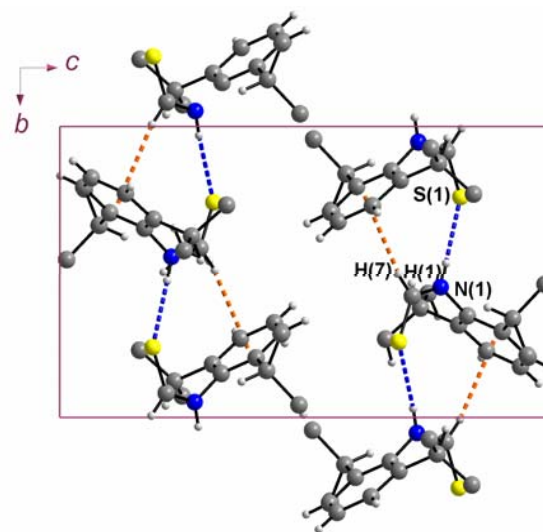


Figure 5.3b: Bar graph comparing isostructural compounds; a comparison of the closest non-bonding distances of 2,6-dimethylphenylthioamide and 2-chloro-6-methylphenylthioamide.

D2



(a)



(b)

Figure 5.6: Hydrogen bonding pattern in (a) 2,6-diisopropylphenylformamide **6** and (b) 2,6-diisopropylphenylthioamide **20**